Satellite Image Atlas
of Glaciers of the World

EUROPE

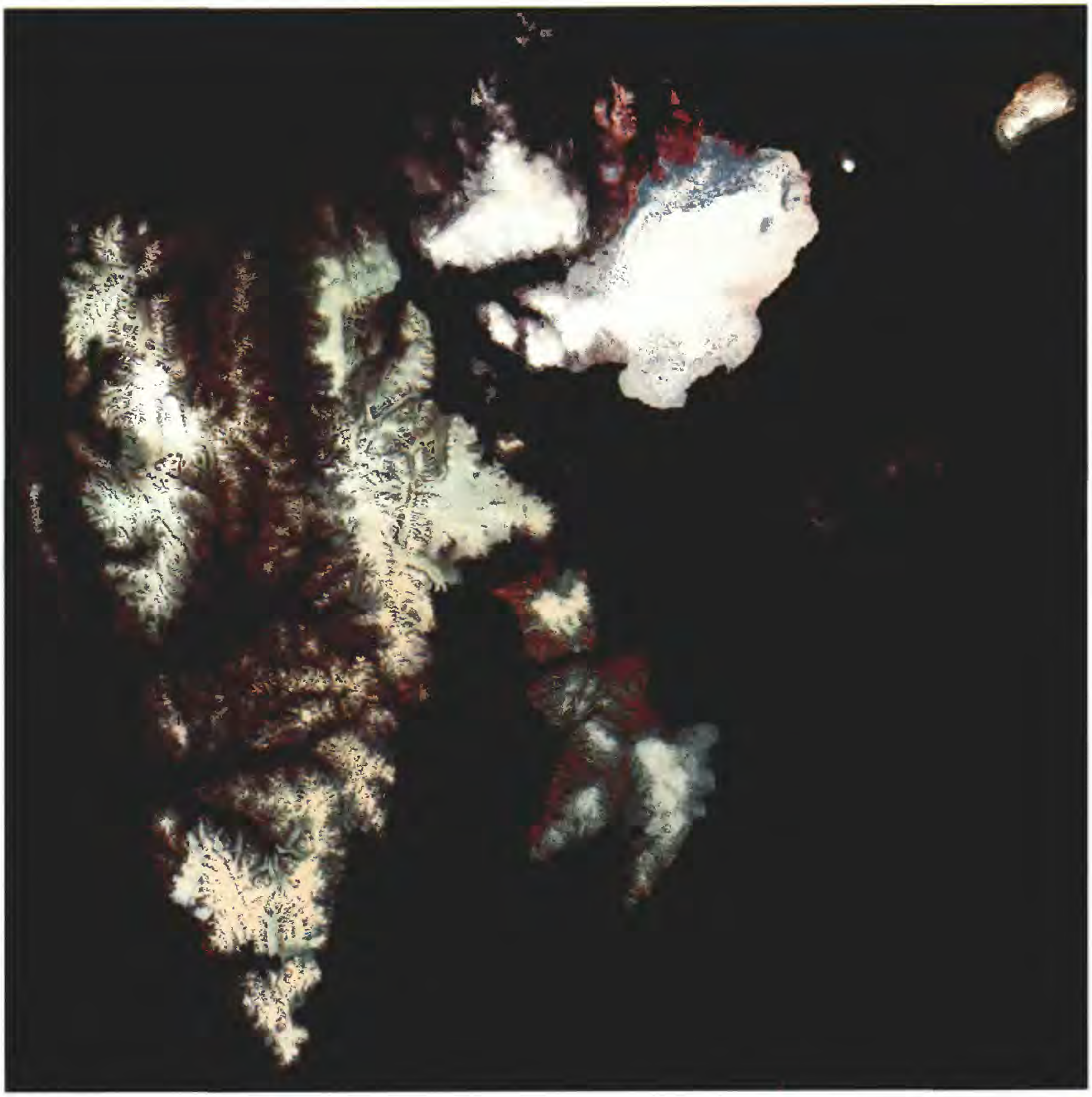

United States Geological Survey
Professional Paper 1386–E

Cover: Landsat false-color image mosaic of Svalbard, Norway, a heavily glacierized archipelago situated about 900 kilometers north of the Norwegian mainland. Mosaic compiled by Fjellanger Widerøe A-S. See page E142.

GLACIERS OF EUROPE—

E–1. GLACIERS OF THE ALPS
THE AUSTRIAN ALPS
By HELMUT ROTT
THE SWISS ALPS
By KARL E. SCHERLER
THE FRENCH ALPS
By LOUIS REYNAUD
THE ITALIAN ALPS
By ROSSANA SERANDREI BARBERO *and* GIORGIO ZANON
E–2. GLACIERS OF THE PYRENEES, SPAIN AND FRANCE
By DAVID SERRAT *and* JOSEP VENTURA
E–3. GLACIERS OF NORWAY
By GUNNAR ØSTREM *and* NILS HAAKENSEN
E–4. GLACIERS OF SWEDEN
By VALTER SCHYTT
E–5. GLACIERS OF SVALBARD, NORWAY
By OLAV LIESTØL
E–6. GLACIERS OF JAN MAYEN, NORWAY
By OLAV ORHEIM

SATELLITE IMAGE ATLAS OF GLACIERS OF THE WORLD

Edited by RICHARD S. WILLIAMS, Jr., *and* JANE G. FERRIGNO

U.S. GEOLOGICAL SURVEY PROFESSIONAL PAPER 1386–E

Landsat images, in conjunction with other data, have been used to map the extent of glaciers, update glacier inventories, determine changes in mass balance, and produce runoff estimates for hydroelectric power production

UNITED STATES GOVERNMENT PRINTING OFFICE, WASHINGTON: 1993

U.S. DEPARTMENT OF THE INTERIOR

BRUCE BABBITT, ***Secretary***

U.S. GEOLOGICAL SURVEY

Robert M. Hirsch, ***Acting Director***

Technical editing by John M. Watson

Design and illustrations by Lynn Hulett

Library of Congress Cataloging in Publication Data

(Revised for vol. E)
Satellite image atlas of glaciers of the world.
(U.S. Geological Survey professional paper ; 1386)
Two fold. col. maps in pocket in v. B.
Includes bibliographical references.
Contents: — B. Antarctica / by Charles Swithinbank ; with sections on The "dry valleys" of Victoria Land, by Trevor J. Chinn, [and] Landsat images of Antarctica, by Richard S. Williams, Jr., and Jane G. Ferrigno — E. Glaciers of Europe — G. Glaciers of the Middle East and Africa.
Supt. of Docs. no.: I 19.16:1386–B, etc.
1. Glaciers—Remote sensing. I. Williams, Richard S. II. Ferrigno, Jane G. III. Series.
GB2401.72.R42S28 1988 551.3'12 87–600497

For sale by the U.S. Geological Survey, Map Distribution,
Box 25425, MS 306, Federal Center,
Denver, CO 80225

Foreword

On 23 July 1972, the first Earth Resources Technology Satellite (ERTS 1 or Landsat 1) was successfully placed in orbit. The success of Landsat inaugurated a new era in satisfying mankind's desire to better understand the dynamic world upon which we live. Space-based observations have now become an essential means for monitoring global change.

The short- and long-term cumulative effects of processes that cause significant changes on the Earth's surface can be documented and studied by repetitive Landsat images. Such images provide a permanent historical record of the surface of our planet; they also make possible comparative two-dimensional measurements of change over time. This Professional Paper demonstrates the importance of the application of Landsat images to global studies by using them to determine the current distribution of glaciers on our planet. As images become available from future satellites, the new data will be used to document global changes in glacier extent by reference to the image record of the 1970's.

Although many geological processes take centuries or even millenia to produce obvious changes on the Earth's surface, other geological phenomena, such as glaciers and volcanoes, cause noticeable changes over shorter periods. Some of these phenomena can have a worldwide impact and often are interrelated. Explosive volcanic eruptions can produce dramatic effects on the global climate. Natural or culturally induced processes can cause global climatic cooling or warming. Glaciers respond to such warming or cooling periods by decreasing or increasing in size, thereby causing sea level to rise or fall.

As our understanding of the interrelationship of global processes improves and our ability to assess changes caused by these processes develops further, we will learn how to use indicators of global change, such as glacier variation, to more wisely manage the use of our finite land and water resources. This Professional Paper is an excellent example of the way in which we can use technology to provide needed earth-science information about our planet. The international collaboration represented by this report is also an excellent model for the kind of cooperation that scientists will increasingly find necessary in the future in order to solve important earth-science problems on a global basis.

Dallas L. Peck

Dallas L. Peck
Director,
U.S. Geological Survey

Preface

This chapter, consisting of six independently authored subchapters, including one subchapter, Glaciers of the Alps, that has four independently authored sections, is the fourth to be released in U.S. Geological Survey Professional Paper 1386, Satellite Image Atlas of Glaciers of the World, a series of 11 chapters. In each chapter, remotely sensed images, primarily from the Landsat 1, 2, and 3 series of spacecraft, are used to study the glacierized regions of our planet and monitor glacier changes. Landsat images, acquired primarily during the middle to late 1970's, were used by an international team of glaciologists and other scientists to study various geographic areas or discuss glaciological topics. In each geographic area the present areal distribution of glaciers was compared, where possible, with historical information about their past extent. The atlas provides an accurate regional inventory of the areal extent of glacier ice on our planet during the 1970's as part of a growing international scientific effort to measure global environmental change on the Earth's surface.

The Alps of Austria, Switzerland, France, and Italy have a total area covered by glaciers of 542, 1,342, 350, and 608 square kilometers, respectively. Landsat multispectral scanner (MSS) images have been used in this area to map the extent of snow and ice areas, update glacier inventories, correlate changes in snowline elevation to glacier mass balance, and with digital processing to monitor individual glaciers to calibrate snowmelt models used to produce runoff estimates for hydroelectric power production.

The 41 glaciers in the Pyrenees (Spain and France), covering a total area of 8.10 square kilometers, have all receded since the mid-19th century, although some minor advances took place in the late 1950's. The small size of Pyrenean glaciers precludes the use of Landsat MSS images for monitoring glacier variations.

Norway has 1,627 glaciers that total 2,595 square kilometers in area; these glaciers, most commonly ice caps, outlet, cirque, and valley glaciers, have been receding since about 1750. Landsat images are used to evaluate suspended sediment in lakes and fjords and to monitor the transient snowline as a measure of approximate net mass balance.

Sweden has a total area of 314 square kilometers covered by glaciers, one of which (Storglaciären, in Swedish Lapland) is the subject of the longest continuous series of mass-balance measurements in the world, initiated in 1945–46. Landsat MSS images have only limited application because of spatial resolution considerations and the small size of Sweden's glaciers.

Svalbard, Norway, an archipelago in the North Atlantic Ocean, has more than 2,100 glaciers that cover 36,591 square kilometers, or 59 percent of the total area of the islands; Landsat images have been used to monitor fluctuations in the equilibrium line and glacier termini and to revise maps.

Jan Mayen, Norway, has 113 square kilometers, or 30 percent of its area, covered by an ice cap and the 20 named outlet glaciers that surmount the active Beerenberg stratovolcano. Satellite monitoring of fluctuations of outlet glaciers would be useful, but persistent cloud cover has limited the acquisition of cloud-free Landsat images.

Richard S. Williams, Jr.

Jane G. Ferrigno

Editors

About this Volume

U.S. Geological Survey Professional Paper 1386, Satellite Image Atlas of Glaciers of the World, contains 11 chapters designated by the letters A through K. Chapter A is a general chapter containing introductory material and a discussion of the physical characteristics, classification, and global distribution of glaciers. The next nine chapters, B through J, are arranged geographically and present glaciological information from Landsat and other sources of data on each of the geographic areas. Chapter B covers Antarctica; Chapter C, Greenland; Chapter D, Iceland; Chapter E, Continental Europe (except for the European part of the former Soviet Union), including the Alps, the Pyrenees, Norway, Sweden, Svalbard (Norway), and Jan Mayen (Norway); Chapter F, Asia, including the European part of the former Soviet Union, China (P.R.C.), India, Nepal, Afghanistan, and Pakistan; Chapter G, Turkey, Iran, and Africa; Chapter H, Irian Jaya (Indonesia) and New Zealand; Chapter I, South America; and Chapter J, North America. The final chapter, K, is a topically oriented chapter that presents related glaciological topics.

The realization that one element of the Earth's cryosphere, its glaciers, was amenable to global inventorying and monitoring with Landsat images led to the decision, in late 1979, to prepare this Professional Paper, in which Landsat 1, 2, and 3 multispectral scanner (MSS) and Landsat 2 and 3 return beam vidicon (RBV) images would be used to inventory the areal occurrence of glacier ice on our planet within the boundaries of the spacecraft's coverage (between about 81° north and south latitudes). Through identification and analysis of optimum Landsat images of the glacierized areas of the Earth during the first decade of the Landsat era, a global benchmark could be established for determining the areal extent of glaciers during a relatively narrow time interval (1972 to 1982). This global "snapshot" of glacier extent could then be used for comparative analysis with previously published maps and aerial photographs and with new maps, satellite images, and aerial photographs to determine the areal fluctuation of glaciers in response to natural or culturally induced changes in the Earth's climate.

To accomplish this objective, the editors selected optimum Landsat images of each of the glacierized regions of our planet from the Landsat image data base at the EROS Data Center in Sioux Falls, S. Dak., although some images were also obtained from the Landsat image archives maintained by the Canada Centre for Remote Sensing, Ottawa, Ontario, Canada, and by the European Space Agency in Kiruna, Sweden, and Fucino, Italy. Between 1979 and 1981, these optimum images were distributed to an international team of more than 50 scientists who agreed to author a section of the Professional Paper concerning either a geographic area or a glaciological topic. In addition to analyzing images of a specific geographic area, each author was also asked to summarize up-to-date information about the glaciers within the area and to compare their present areal distribution with historical information (for example, from published maps, reports, and photographs) about their past extent. Completion of this atlas will provide an accurate regional inventory of the areal extent of glaciers on our planet during the 1970's.

Richard S. Williams, Jr.
Jane G. Ferrigno
Editors

CONTENTS

	Page
Foreword	III
Preface	V
About this volume	VI
E–1. Glaciers of the Alps	
The Austrian Alps, by Helmut Rott	E6
The Swiss Alps, by Karl E. Scherler	E14
The French Alps, by Louis Reynaud	E23
The Italian Alps, by Rossana Serandrei Barbero and Giorgio Zanon	E37
E–2. Glaciers of the Pyrenees, Spain and France, by David Serrat and Josep Ventura	E49
E–3. Glaciers of Norway, by Gunnar Østrem and Nils Haakensen	E63
E–4. Glaciers of Sweden, by Valter Schytt	E111
E–5. Glaciers of Svalbard, Norway, by Olav Liestøl	E127
E–6. Glaciers of Jan Mayen, Norway, by Olav Orheim	E153

Glaciers of Europe—

GLACIERS OF THE ALPS

THE AUSTRIAN ALPS
By HELMUT ROTT

THE SWISS ALPS
By KARL E. SCHERLER

THE FRENCH ALPS
By LOUIS REYNAUD

THE ITALIAN ALPS
By ROSSANA SERANDREI BARBERO *and* GIORGIO ZANON

SATELLITE IMAGE ATLAS OF GLACIERS OF THE WORLD

Edited by RICHARD S. WILLIAMS, Jr., *and* JANE G. FERRIGNO

U.S. GEOLOGICAL SURVEY PROFESSIONAL PAPER 1386-E-1

The Alps of Austria, Switzerland, France, and Italy have a total area covered by glaciers of 542, 1,342, 350, and 608 square kilometers, respectively

CONTENTS

Page

Introduction ---------- E1

FIGURE 1. Landsat image mosaic of the Alps at 1:600,000 scale ---------- 2
2. Index map to the optimum Landsat 1, 2, and 3 images of the glaciers of the Alps ---------- 5

TABLE 1. Optimum Landsat 1, 2, and 3 images of glaciers of the Alps ---------- 4

The Austrian Alps, by Helmut Rott ---------- 6

Abstract ---------- 6
Introduction ---------- 6

FIGURE 3. Sketch map of the Eastern Alps showing the main glacierized mountain groups and the drainage basins ---------- 7

TABLE 2. Main glacierized mountain groups in the Eastern Alps of Italy and Austria ---------- 7

Climatic conditions ---------- 6
Occurrence of glaciers ---------- 7

TABLE 3. The largest glaciers of the Austrian Alps ---------- 8

Observations and mapping of glaciers ---------- 8
Historic studies ---------- 8
Modern studies ---------- 10

FIGURE 4. Painting of the Dorferkees (Hohe Tauern group) in 1840 near its maximum extent ---------- 9
5. Photograph of the terminus of the Dorferkees on 5 October 1965 from the same point of view as figure 4 ---------- 9
6. Graph showing mean specific mass balance and mean altitude of the equilibrium line of Hintereisferner (Ötztaler Alpen) from the budget years 1952–53 to 1988–89 ---------- 10

Satellite imagery ---------- 11

FIGURE 7. Part of a Landsat 2 MSS image of the Eastern Alps taken on 15 August 1980 (band 6; Path 207, Row 27) ---------- 11
8. Enlargement of part of a Landsat 1 MSS image taken on 13 August 1972 (1021–09380, band 7; Path 208, Row 27) ---------- 12
9. Enlargement at approximately 1:250,000 scale of part of a Landsat 5 TM image over the Ötztaler Alpen group taken on 30 September 1985 (bands 1, 2, 3; Path 193, Row 27) ---------- 13

Selected references ---------- 13

The Swiss Alps, by Karl E. Scherler ---------- 14

Abstract ---------- 14
Introduction ---------- 14

FIGURE 10. Map showing glacier distribution in Switzerland ---------- 15

TABLE 4. The largest glaciers in Switzerland ---------- 15

Observations of glaciers ---------- 14
Mapping of glaciers ---------- 16
Satellite imagery ---------- 17

FIGURE 11. Landsat 2 MSS false-color composite image of the western part of the Swiss Alps on 16 September 1978 (21333–09210; Path 210, Row 28) ---------- 18
12. Landsat 2 MSS image of the eastern part of the Swiss Alps on 4 September 1980 (band 7; Path 209, Row 27) ---------- 19

13. Enlargement of part of figure 11 showing the Aletschgletscher and surrounding area ---- E20
14. A Landeskarte der Schweiz sheet at 1:200,000 scale showing the same region as in figure 13 ---- 21

Acknowledgment ---- 22
References cited ---- 22

The French Alps, by Louis Reynaud ---- 23

Abstract ---- 23
Introduction ---- 23

FIGURE 15. Map showing the distribution of glaciers in the French Alps compiled from 1:25,000-scale Institut Géographique National maps ---- 24
16. Landsat 1 MSS image mosaic of the French Alps showing the Mont Blanc, the Grandes Rousses, and the Pelvoux areas without clouds ---- 27

TABLE 5. The main groups of glaciers of the French Alps ---- 25

Satellite images of glaciers of the French Alps ---- 26

FIGURE 17. Enlarged sections of the Landsat image mosaic of the French Alps ---- 28

The history of glacier variations in the French Alps ---- 26

FIGURE 18. Graph showing variation in length of four glaciers on the north side of Mount Blanc from 1870 to 1984 ---- 31

Mass-balance measurements in the French Alps ---- 30

FIGURES 19–20. Graphs showing accumulated balance variations versus time for:
19. Glacier de Sarennes ---- 33
20. Glacier de Gébroulaz from 1908 to 1950 and a comparison of the accumulated variations with the Glacier de Sarennes and Aletschgletscher ---- 34

TABLE 6. Mass-balance measurements on glaciers in the French Alps ---- 32

Aerial and terrestrial photogrammetric surveys in Alpine glaciological studies ---- 35
References cited ---- 36

The Italian Alps, by Rossana Serandrei Barbero and Giorgio Zanon ---- 37

Abstract ---- 37
Introduction ---- 37

FIGURE 21. Sketch map of the main glacierized mountain areas in the Italian Alps ---- 38

Location and distribution ---- 37

TABLE 7. The largest glaciers in the Italian Alps ---- 39

Italian glaciological research ---- 39

TABLE 8. Examples of large-scale maps of Italian glaciers published by the Consiglio Nazionale delle Ricerche, Comitato Glaciologico Italiano, Turin ---- 40

Glacier surveys by satellite remote sensing ---- 41

FIGURE 22. Landsat 2 MSS image (21333–09210, band 6; 16 September 1978; Path 210, Row 28) showing part of the Monte Bianco (*A*) and the Monte Rosa (*B*) mountain groups ---- 41
23. Landsat 1 MSS false-color composite image (1021–09383; 13 August 1972; Path 208, Row 28) showing part of the central Italian Alps ---- 42

24. Landsat 1 MSS image (band 7; 26 October 1975; Path 207, Row 28) showing the eastern Italian Alps between the Alpi Venoste and the Alpi Carniche ---------- E43

TABLE 9. Total surface area and snow-covered surface area of selected glaciers as derived from Landsat MSS images acquired on 13 September 1975 (20234–09320; Path 209, Row 28), 28 August 1978 (21314–09142; Path 209, Row 28), and 4 September 1980 (Path 209, Row 28) ---------- 44

FIGURE 25. Digitally processed Landsat 2 MSS image (2 September 1980; Path 207, Row 27) of part of the eastern Italian Alps ---------- 45

26. Digitally processed Landsat 3 false-color MSS image (6 September 1981; Path 207, Row 27) of part of the eastern Italian Alps ---------- 46

27. Digitally processed Landsat 4 image (40389–09272; 9 August 1983; Path 192, Row 27, approximately equivalent to Landsats 1–3 Path 207, Row 27) of part of the eastern Italian Alps ---------- 47

References cited ---------- 48

GLACIERS OF EUROPE—

GLACIERS OF THE ALPS

Introduction

The Alps are a complex system of mountain ranges in south-central Europe that extend about 1,000 km in a crescent shape along Italy's common border with Yugoslavia, Austria, Switzerland, and France. The southern flank of the Alpine chain is subdivided by Italian geographers into the Western, Central, and Eastern Alps. Other scientists, especially those from the regions along the northern slope of the Alps, subdivide the system into the Western and Eastern Alps by an imaginary line following the Rhine River from Bodensee (Lake of Constance) to Lake Como.

The Alps have summit elevations that reach a maximum of more than 4,800 m, as on Mont Blanc. The major glacierized areas are situated along the crest of the mountain chain. The largest glaciers are often at the highest elevations, especially where comparatively level areas exist above the snowline. Numerous smaller glaciers are, however, scattered throughout the Alps.

Far fewer glaciers are found on the southern flanks than on the northern slopes of the Alps because of seasonal weather patterns and greater intensity of solar radiation on the south. Humid, moisture-laden winds tend to blow from westerly and northwesterly directions in the winter. More southerly winds predominate in the spring and autumn. Southward-facing slopes receive greater amounts of solar radiation throughout the year. Orographic effects complicate the situation. More precipitation falls in the external ranges than in the interior ones because rain shadows related to the prevailing seasonal winds are created by the presence of these outer mountains. The firnline follows the precipitation pattern. The maximum altitude for the firnline is lower in the external, more humid massifs and higher in the interior ranges. Therefore, maximum precipitation on northern slopes, greatest ablation on southern ones, location of mountain range, and elevation and configuration of the terrain govern the distribution of glaciers throughout the Alps.

The Alps are composed of numerous principal mountain ranges, many subsidiary ranges, and several smaller groups. Several ranges cross international boundary lines and are known by different names in the bordering countries. The massif called Mont Blanc in France is Monte Bianca in Italy, and the chain called Alpi Venoste in Italy becomes Ötztaler Alpen in Austria. Sometimes the same name is spelled differently in bordering countries. The Alpes Maritimes in France are the Alpi Marittime in Italy.

In this subchapter, the glaciers of the Alps are discussed geographically by country. To solve the problem that arises because different names describe a single geographic place or feature, an editorial decision was made to use the geographic names approved by the United States Board on Geographic Names for each country in each of the four divisions of the section. The authorities used for reference were the gazetteers approved by the United States Board on Geographic Names, as follows:

Austria, Gazetteer No. 66, 1962; Switzerland, Preliminary Gazetteer, 1950; France, Gazetteer No. 83, 1964; and Italy and associated areas, Gazetteer No. 23, 1956.

Various terms are used for glaciers throughout the Alps. "Gletscher" is commonly used in the German-speaking region of the Western Alps. In the German-speaking region of the Eastern Alps, "Ferner" and "Kees" are used. "Glacier" is used in the French Alps and "ghiacciaio" in the western Italian Alps. "Vedret" or "vedretta" is used in the eastern Italian Alps.

Glaciological studies have been carried out in the Alps since the 1800's. Some areas have been studied intensively, others only moderately. Early glaciological studies were conducted with labor- and time-intensive fieldwork. Aerial photographic surveys are now commonly used to supplement ground studies. Recently, other remote sensing techniques, such as satellite imagery, have been explored to see what the data can contribute to glaciological studies of the Alps. The four divisions of this section of Chapter E describe some of the applications of Landsat imagery, although constraints imposed by the spatial resolution of the multispectral scanner (MSS) image limit the use of Landsat to the largest glaciers in the Alps.

Landsat imagery of the Alps has been acquired since 1972. Although the Alps are frequently cloud covered, enough Landsat data had been collected by 1982 that the Georg Westermann Company was able to produce an almost cloud-free image mosaic of the entire Alps area by using portions of 50 images. The images selected were acquired during the summer months (June through August), so areas of snow and ice are strikingly evident (fig. 1).

Initially, all the Landsat data were acquired and archived by the United States. Starting in 1975, the European Space Agency's receiving station in Fucino, Italy, also began acquiring and archiving the data. Landsat images of the Alps are frequently cloud covered, but some optimum imagery has been archived by the United States and is listed in table 1. Also listed are the best images archived by the European Space Agency that are known to the authors or editors. The coverage of the optimum imagery is shown in figure 2.

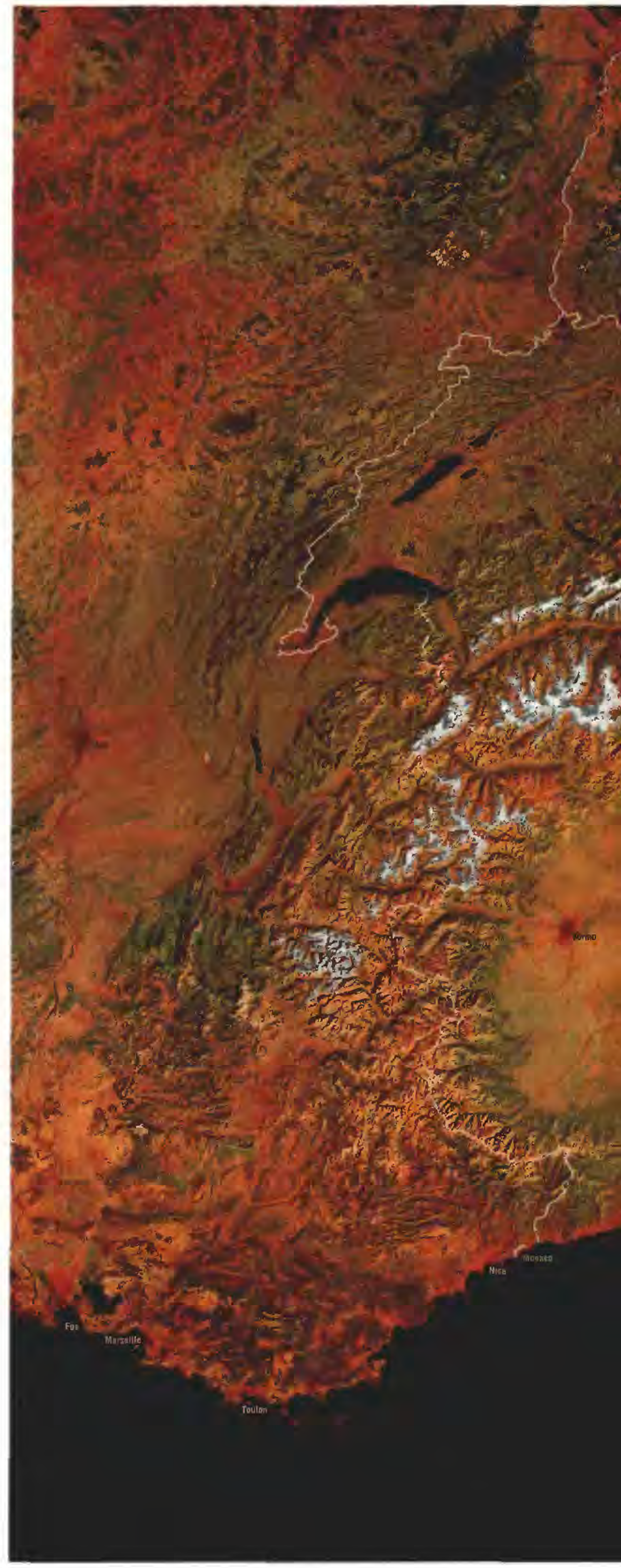

Figure 1.—*Landsat image mosaic of the Alps at 1:3,300,000 scale. The mosaic was produced by the Georg Westermann Company, Braunschweig, Germany. Parts of 50 Landsat images were used.*

TABLE 1.—*Optimum Landsat 1, 2, and 3 images of glaciers of the Alps*

[The Landsat imagery evaluated for this chapter is archived primarily at the EROS Data Center, Sioux Falls, S. Dak. It is likely that better imagery of this area is archived by the European Space Agency, but, because of the difficulty determining what imagery is available and evaluating it for glaciological purposes, only those images known to the authors or editors have been listed. Two optimum Landsat thematic mapper images are included at the end of the table to provide better coverage of the glacierized areas of the Eastern Alps]

Path-Row	Nominal scene center (lat-long)	Landsat identification number	Date	Solar elevation angle (in degrees)	Code (see fig. 2)	Cloud cover (in percent)	Remarks
206–27	047°20′N. 013°52′E.	2231–09142	10 Sep 75	41	◑	20	Hohe Tauern and Dachstein areas, Austria
206–28	045°55′N. 013°17′E.	2231–09144	10 Sep 75	42	◑	30	Alpi Carniche, Italy, Julian Alps, Yugoslavia
207–27	047°20′N. 012°26′E.	2934–08573	13 Aug 77	44	◑	50	Zillertaler Alpen, Hohe Tauern, Austria; Alpi Breonie, Aurine, Italy; archived by European Space Agency, Frascati, Italy
207–28	045°55′N. 011°51′E.	—	26 Oct 75	25	◕	10	Alpi Dolomitiche, Italy; archived by European Space Agency, Frascati, Italy
208–27	047°20′N. 011°00′E.	1021–09380	13 Aug 72	50	◑	20	Ötztaler, Stubaier Alpen, Austria; Alpi Venoste, Brenonie, Italy
208–28	045°55′N. 010°25′E.	1021–09383	13 Aug 72	51	◑	30	Rhätische Alpen, Switzerland/ Alpi Retiche, Italy
209–27	047°20′N. 009°34′E.	1076–09440	7 Oct 72	33	●	0	Rhätische Alpen, Switzerland and Austria
209–27	047°20′N. 009°34′E.	—	4 Sep 80	—	●	0	Rhätische Alpen, Switzerland and Austria; archived by European Space Agency, Frascati, Italy
209–28	045°55′N. 008°59′E.	2234–09320	13 Sep 75	41	●	0	Switzerland/Italy border from Monte Rosa to the Gruppo del Bernina
209–29	044°30′N. 008°25′E.	2234–09322	13 Sep 75	42	●	0	Mont Clapier area in the Alpes Maritimes (Alpi Marittime), France and Italy
210–27	047°20′N. 008°08′E.	—	3 Aug 76	48	●	0	Berner Alpen, Switzerland; archived by European Space Agency, Frascati, Italy
210–28	045°55′N 007°33′E	2217–09374	27 Aug 75	46	◑	50	Berner Alpen, Switzerland
210–28	045°55′N. 007°33′E.	—	16 Sep 78	—	●	0	Alpi Pennine, Switzerland and Italy; Alpes de Savoie, France and Italy; archived by European Space Agency, Frascati, Italy
210–29	044°30′N. 006°59′E.	2955–09143	3 Sep 77	40	◑	50	Alpes Cottiennes (Alpi Cozie) and Alpes Maritimes (Alpi Marittime), France and Italy; archived by European Space Agency, Frascati, Italy
211–27	047°20′N. 006°42′E.	1078–09553	9 Oct 72	33	◑	60	Berner Alpen, Switzerland
211–28	045°55′N. 006°07′E.	1078–09555	9 Oct 72	34	◑	60	Orographic clouds on the Vanoise glaciers and some on the Mont Blanc glaciers; Alpes Grées (Alpi Graie) and Alpes de Savoie, France and Italy

TABLE 1.—*Optimum Landsat 1, 2, and 3 images of glaciers of the Alps*—Continued

Path-Row	Nominal scene center (lat-long)	Landsat identification number	Date	Solar elevation angle (in degrees)	Code (see fig. 2)	Cloud cover (in percent)	Remarks
211–29	044°30′N. 005°33′E.	1078–09562	9 Oct 72	35	●	0	Glacierized areas of Grandes Rousses and Mont Pelvoux are cloud free; Alpes du Dauphiné
211–29	044°30′N. 005°33′E.	2254–09434	3 Oct 75	—	●	0	The best image of Mont Pelvoux area, France
			Optimum Landsat TM images				
192–27	047°27′N. 012°33′E.	—	7 Sep 85	37	●	0	Zillertalen Alpen, Hohe Tauern, Austria
193–27	047°27′N. 011°00′E.	—	30 Sep 85	43	●	0	Ötztaler and Stubaier Alpen, Austria

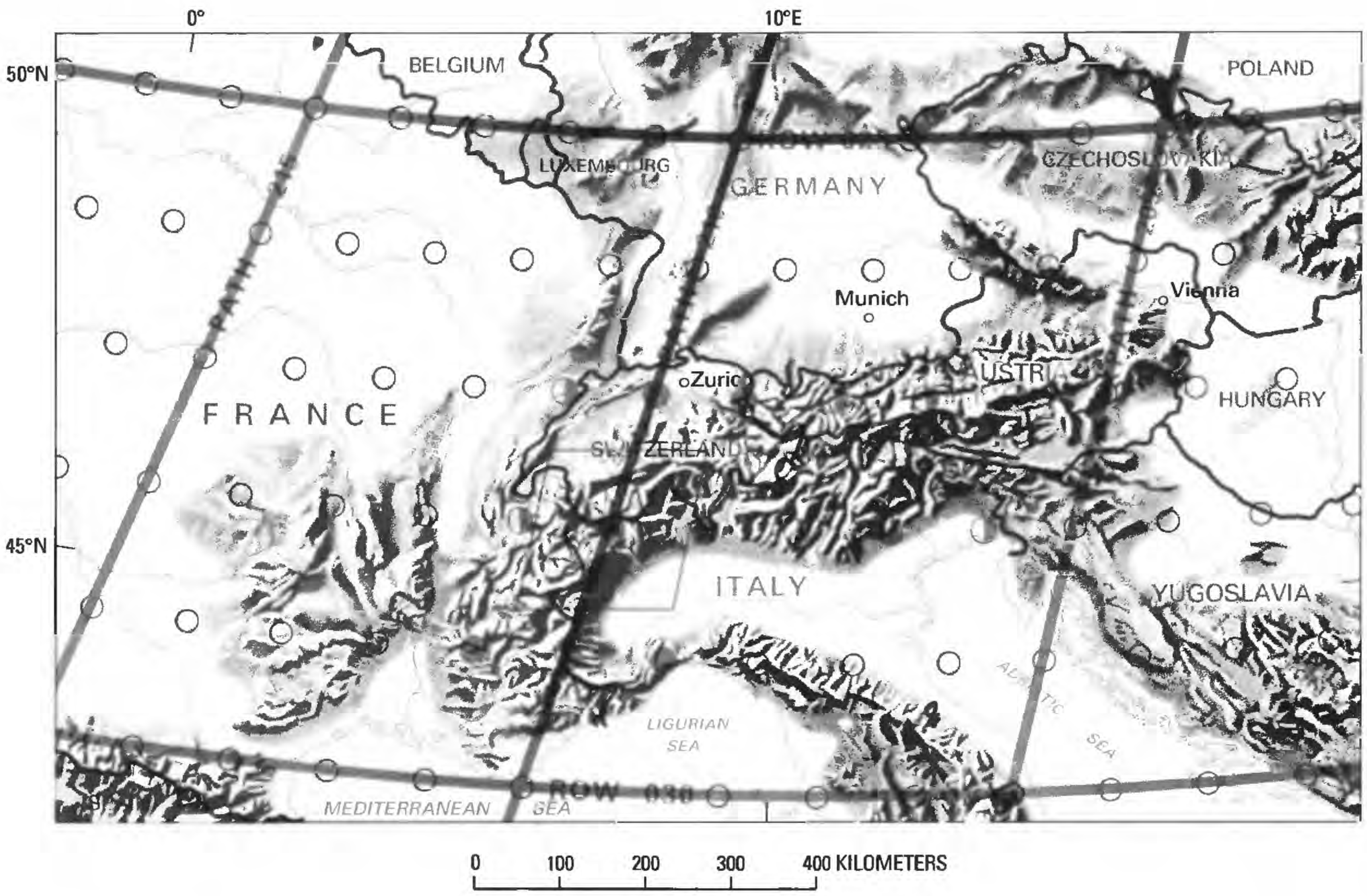

EXPLANATION OF SYMBOLS

Evaluation of image usability for glaciologic, geologic, and cartographic applications. Symbols defined as follows:

- Excellent image (0 to ≤5 percent cloud cover)
- Good image (>5 to ≤10 percent cloud cover)
- Fair to poor image (>10 to ≤100 percent cloud cover)
- Nominal scene center for a Landsat image outside the area of glaciers
- Approximate size of area encompassed by nominal Landsat MSS image

***Figure 2.**—Optimum Landsat 1, 2, and 3 images of the glaciers of the Alps. The vertical lines represent nominal paths. The rows (horizontal lines) have been established to indicate the latitude at which the imagery has been acquired.*

The Austrian Alps

By Helmut Rott [1]

Abstract

An overview is provided on the occurrence of the glaciers in the Eastern Alps of Austria and on the climatic conditions in this area. Historical documents on the glaciers have been available since the Middle Ages. Special glaciological observations and topographic surveys of individual glaciers were initiated as early as 1846. Recent data in an inventory based on aerial photographs taken in 1969 show 925 glaciers in the Austrian Alps with a total area of 542 square kilometers. Present research topics include studies of mass and energy balance, relations of glaciers and climate, physical glaciology, a complete inventory of the glaciers, and testing of remote sensing methods. The location of the glacier areas is shown on Landsat multispectral scanner images; the improved capabilities of the Landsat thematic mapper are illustrated with an example from the Ötztaler Alpen group.

Introduction

A line from Bodensee (Lake of Constance) along the Rhine River to Lake Como is usually taken as the division between the Eastern and the Western Alps. The main rivers and the major glacierized mountain groups of the Eastern Alps are shown in the sketch map of the region (fig. 3), and total areas for the glacierized regions are listed in table 2. Runoff from the northern region drains to the North Sea through the Rhine River. The eastern regions drain to the Black Sea through the Danube River from its tributaries, the Inn, Salzach, and Drava Rivers. The major glacier areas are distributed along the main east-west ridge of the drainage divide, which is composed of resistant igneous and metamorphic rocks. Summit elevations reach between 3,500 and 3,798 m in the Austrian Alps. The Nördliche Kalkalpen (Northern Calcareous Alps), which extend north of the line along the Inn and Salzach Rivers, reach summit heights just below 3,000 m and contain only a few small glaciers.

Climatic Conditions

The altitude of the equilibrium line (ELA) varies on East Alpine glaciers from about 2,600 to 3,100 m above mean sea level, depending on the geographic location and on slope orientation (Gross and others, 1977). Regional differences in the ELA are primarily related to the precipitation pattern. Orographic effects result in a decrease of precipitation from the northern and southern slopes to the inner Alpine zone. In the central part of the Ötztaler Alpen group, where sheltering is most effective, mean annual precipitation at glacier altitudes is about 1,500 mm. In the Hohe Tauern and Silvretta groups, which receive the majority of their precipitation from northerly and westerly winds, annual precipitation is about 50 percent higher, and the ELA is 200 to 300 m lower than in the Ötztaler Alpen. An important factor influencing the mass balance of the glaciers is the synoptic weather situation during the ablation period (Hoinkes, 1970).

[1]University of Innsbruck, Institute for Meteorology and Geophysics, Innrain 52, A–6020 Innsbruck, Austria.

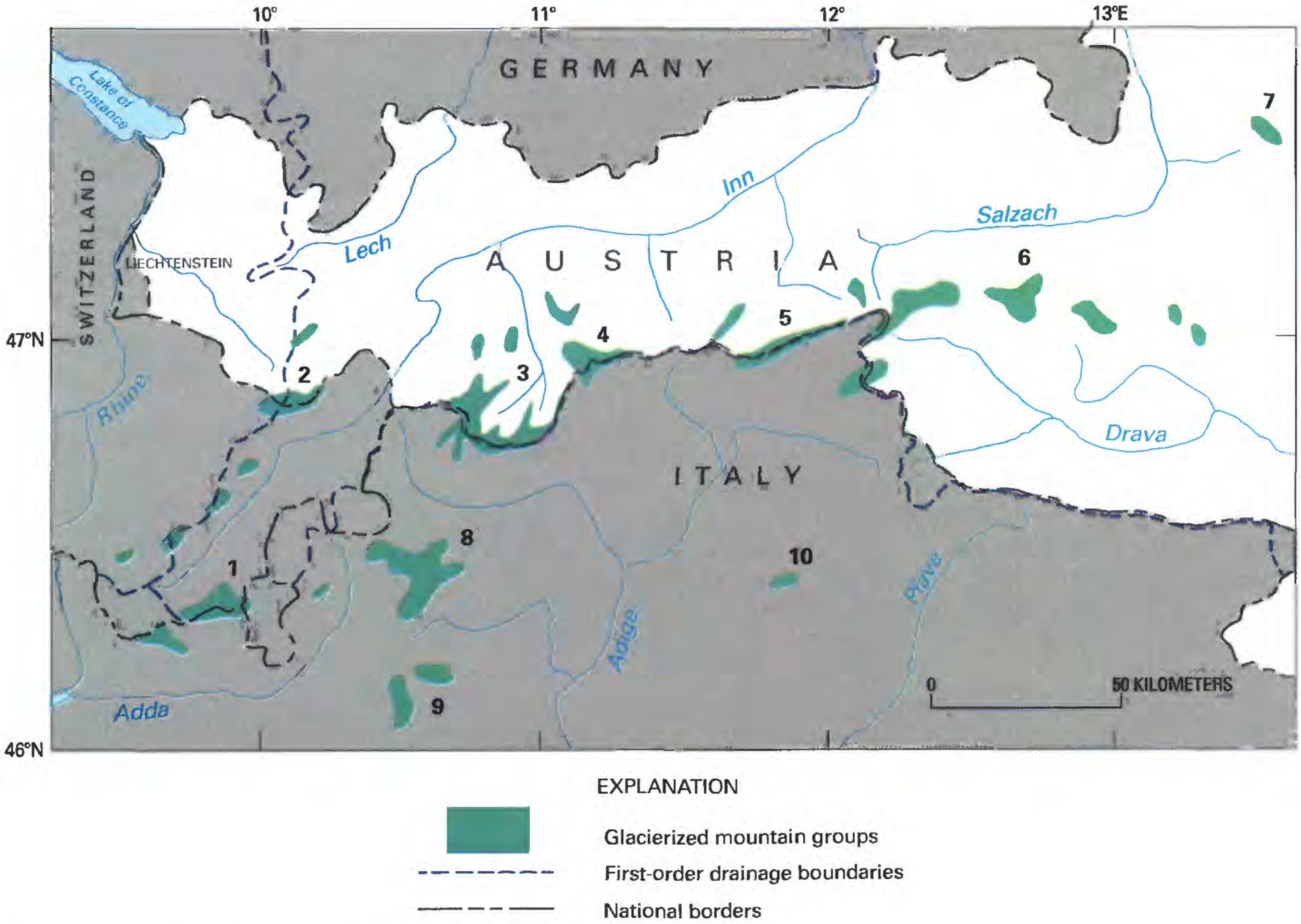

***Figure 3.**—The main glacierized mountain groups and the drainage basins of the Eastern Alps. The numbers refer to the mountain groups listed in table 2.*

TABLE 2.—*Main glacierized mountain groups in the Eastern Alps of Italy and Austria*

[The position of the mountain groups is shown in figure 3]

Number	Mountain group	Area (km^2) in Italy	Area (km^2) in Austria
1.......	Bernina-Disgrazia	42	
2.......	Silvretta		23
3.......	Ötztaler Alpen	40	174
4.......	Stubaier Alpen	14	61
5.......	Zillertaler Alpen	15	61
6.......	Hohe Tauern	13	206
7.......	Dachstein		6
8.......	Ortles-Cevedale	96	
9.......	Adamello-Presanella	53	
10.......	Alpi Dolomitiche	9	

Occurrence of Glaciers

Recent data on all Austrian glaciers are available in an inventory based on vertical aerial photographs taken in September and October 1969 (Patzelt, 1980). The Austrian Alps comprise 925 glaciers with a total area of 542 km^2; 5 glaciers are larger than 10 km^2. Current and historic data on the five largest glaciers are summarized in table 3. Twenty-five glaciers are larger than 4 km^2, but the majority are smaller than 1 km^2.

The largest glaciers cover mountain regions that have comparatively level areas above the snowline. These low-relief areas in the highlands

TABLE 3.—*The largest glaciers of the Austrian Alps*

[For 1969: I, area of the main glacier; II, area including tributary glaciers separated since 1850; —, no available data]

Glacier	Mountain group	Area (km^2) 1969 I	II	1925	1850	Altitude (1969) in meters above mean sea level Maximum	Minimum
Pasterzen Kees	Hohe Tauern	19.8	22.8	25.5	28.0	3,700	2,070
Gepatschferner	Ötztaler	17.7	17.7	19.6	22.1	3,517	2,063
Obersulzbach	Hohe Tauern	11.6	12.0	13.6	16.0	3,570	2,063
Gurgler Ferner	Ötztaler	11.1	12.9	—	16.8	3,420	2,270
Mittelberg Ferner ..	Ötztaler	10.9	14.2	17.5	18.6	3,530	2,250

are considered to be relic landforms from the Miocene Epoch, which ended about 5.3 m.y. ago. The accumulation of ice in these highland areas led to the formation of valley glaciers, with extended firn fields and ice tongues descending into narrow valleys. The maximum glacier length is 9.2 km (Pasterzen Kees in the Hohe Tauern). Many of the small glaciers are cirque, niche, and slope (ice apron) glaciers. A division of the glacier areas according to mountain groups is given in table 2. Several mountain groups containing small glaciers are not listed. Among these are the German Alps along the border with Austria, the largest glacier of which is the Schneeferner (0.4 km^2), near the meteorological observatory on the Zugspitze.

Observations and Mapping of Glaciers

HISTORIC STUDIES

East Alpine glaciers are mentioned and described in historic documents dating back to the Middle Ages, with an increasing number of reports beginning about the year 1600, when a major advance of the glaciers occurred. The early documents usually reported observations about individual glaciers, such as the Vernagtferner in the Ötztaler Alpen, the surges of which dammed a lake and caused outburst floods (jökulhlaups) in the years around 1600, 1680, 1773, and 1845 (Hoinkes, 1969). The first comprehensive studies of the East Alpine glaciers became possible with the availability of topographic maps produced from the second topographic survey of Austria, which also included most of the East Alpine glacier regions south of the main drainage divide. Maps at a scale of 1:28,800 were published during the period 1807 to 1834. After 1845, an increasing number of special glaciological observations were carried out, including mapping of individual glaciers and ice-velocity measurements. Some of the earliest observations are attributed to H. and A. Schlagintweit, C. Sonklar, and J. Payer. The first complete inventory of the East Alpine glaciers was published by Richter (1888). It was based on the original 1:25,000-scale maps of the third Austrian topographic survey carried out from 1871 to 1873. During the last two decades of the 19th century, many glacier investigations were initiated, some of which have been continued up to the present. Of special note are the first photogrammetric survey carried out of a glacier (Vernagtferner, Ötztaler Alpen) in 1887 and the drilling operations through Hintereisferner (Ötztaler Alpen) in the years between 1899 and 1909.

Historical documents and other published observations reveal similar periods of advance and retreat for East and West Alpine glaciers during the past 400 years. After a glacier maximum in the early 17th century, the glaciers remained in a fairly advanced position, with only small variations for the next 250 years. Most East Alpine glaciers reached another maximum at 1770 to 1780 and again around 1850. Since that time

Figure 4.—The Dorferkees (Hohe Tauern group) in 1840 near its maximum extent. Watercolor painting by Thomas Ender, from the Erzherzog Johann collection.

Figure 5.—The terminus of the Dorferkees on 5 October 1965 from the same point of view as figure 4. The dashed lines mark the glacier's extent in 1850. Photograph by Gernot Patzelt.

glaciers receded until about 1965, although the recession has been interrupted by small readvances between 1890 and 1920. In the period 1977 to 1982, between 50 and 70 percent of the approximately 100 Austrian glaciers, which are observed annually, were advancing; the annual average advance amounted only to a few meters. Due to warm summers and reduced snowfall on the glaciers, most of the advances stopped in the mid-1980's. In 1988, about 80 percent of the Austrian glaciers retreated.

Figures 4 and 5 exemplify historical glacier variation. Figure 4 shows a painting by Thomas Ender of the Dorferkees (Hohe Tauern) in 1840 near its maximum extent. The detail shown on the glacier is most remarkable. A modern photograph taken on 5 October 1965 (fig. 5) shows the glacier from nearly the same position. It documents a 2.5-km retreat of the glacier terminus (Patzelt, 1973) when compared with Ender's painting. The glacier area has decreased from a maximum of 6.9 km^2 in the 19th century to 4.6 km^2 in 1969.

MODERN STUDIES

A complete bibliography of the Austrian glaciers with more than 1,600 citations has been compiled for the Austrian glacier inventory (Patzelt, 1980). The inventory of all Austrian glaciers is based on a special aerial photographic survey conducted at the end of the ablation period in 1969, from which maps at scales of 1:10,000 to 1:15,000 were produced. The areas and altitude distributions of existing glaciers were mapped; in addition, the areas of the 1850 stage and, where possible, of the 1920 stage were evaluated from the positions of the moraines. The loss of total glacier area within Austria since the 1850 stage amounted to 40 percent, with 542 km^2 remaining in 1969 (Patzelt and Gross, personal commun.).

Many subjects of glaciological research have been investigated on East Alpine glaciers in the last decades. In Austria, glaciological research is conducted by a number of institutes, several of which are located at the University of Innsbruck. Several institutes in Germany, especially the Commission on Glaciology of the Bavarian Academy of Sciences, carry out investigations on the German glaciers and on a number of Austrian glaciers. The annual mass balance is investigated on several East Alpine glaciers. A long, continuous series of observations using the direct glaciological method, based on actual field measurements of the glacier, is available for Hintereisferner (since 1952–53) and Vernagtferner in the Ötztaler Alpen. Figure 6 shows the annual specific mass balance of Hintereisferner for the budget years 1952–53 to 1988–89 together with data on the ELA (Kuhn, 1981; Kuhn and others, 1985). The close relationship between ELA and mass balance is of particular interest for remote-sensing applications, as was discussed by Østrem (1975). Recent investigations are concerned with the development of remote-sensing methods for glacier studies. Airborne surveys with multispectral scanners (MSS) and synthetic aperture radar (SAR) have been carried out over glaciers in the Ötztaler Alpen (Rott and Domik, 1984; Rott and others, 1985).

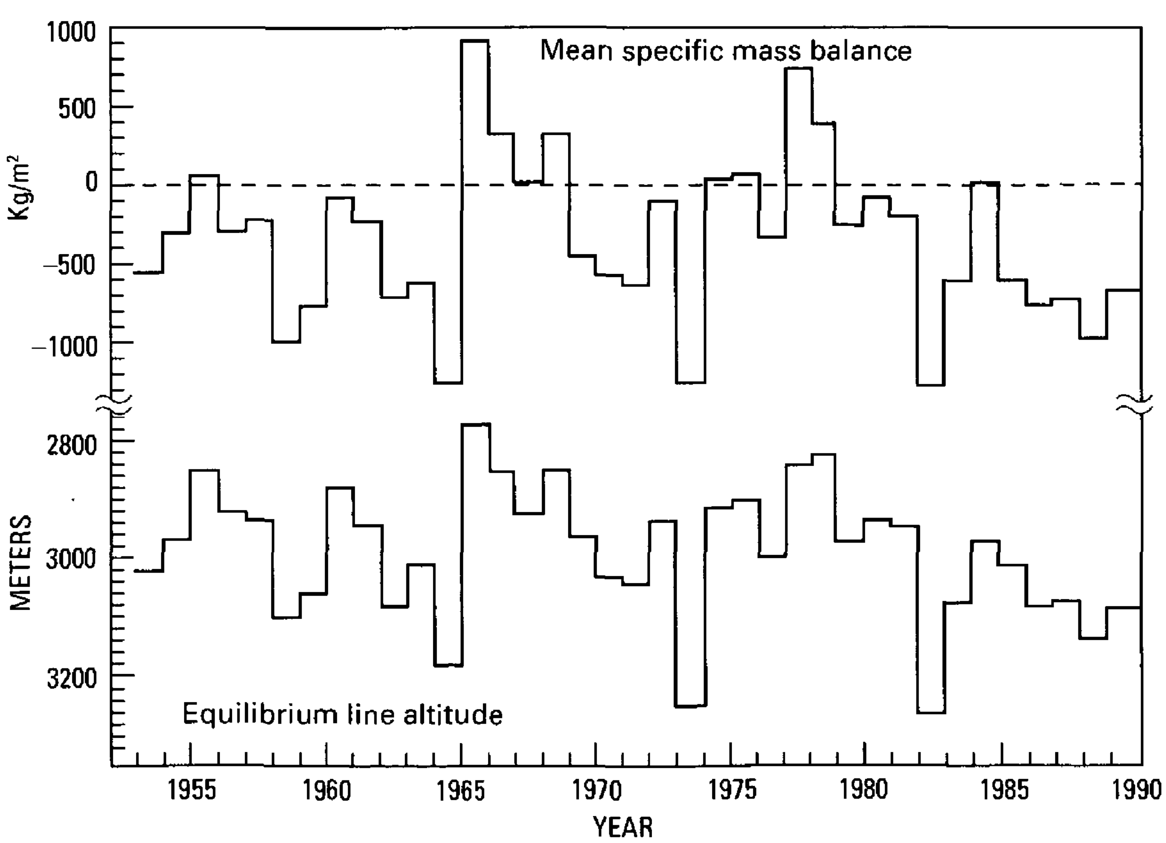

***Figure 6.**—Mean specific mass balance and mean altitude of the equilibrium line of Hintereisferner (Ötztaler Alpen) from the budget years 1952–53 to 1988–89.*

Satellite Imagery

Considering the size of the East Alpine glaciers, only high-resolution satellite sensors are of use for glaciological investigations. Sensors having the resolution of the Landsat MSS can be useful for mapping fast-changing phenomena such as the extent of the snow and ice areas on the glaciers (Rott, 1977). Landsat 4 and 5 thematic mapper (TM) and Landsat 3 return beam vidicon (RBV) images have pixel sizes of about 30 m, or nearly 3 times better than the pixel size of Landsat MSS images. Large Format Camera (LFC) photographs have a spatial resolution of 10 m or better. The new generation of sensors on Earth observation satellites or manned spacecraft that have higher surface resolution is useful for updating the inventories of the mountain glaciers and for mapping of snow and ice areas (Rott and Markl, 1989). Vertical aerial photographs are still needed for providing accurate maps of surface topography of the glaciers.

The Landsat MSS image in figure 7 shows a section of the Eastern Alps, from the Bavarian foothills on the north, to the Nördliche Kalkalpen and the glaciated Central Alps, and to the Alpi Dolomitiche in the south. The image includes the Zillertaler Alpen and Hohe Tauern groups.

Figure 7.— Part of a Landsat 2 MSS image of the Eastern Alps taken on 15 August 1980 (band 6; Path 207, Row 27). The numbers refer to the mountain groups listed in table 2. Landsat image from the European Space Agency, Frascati, Italy.

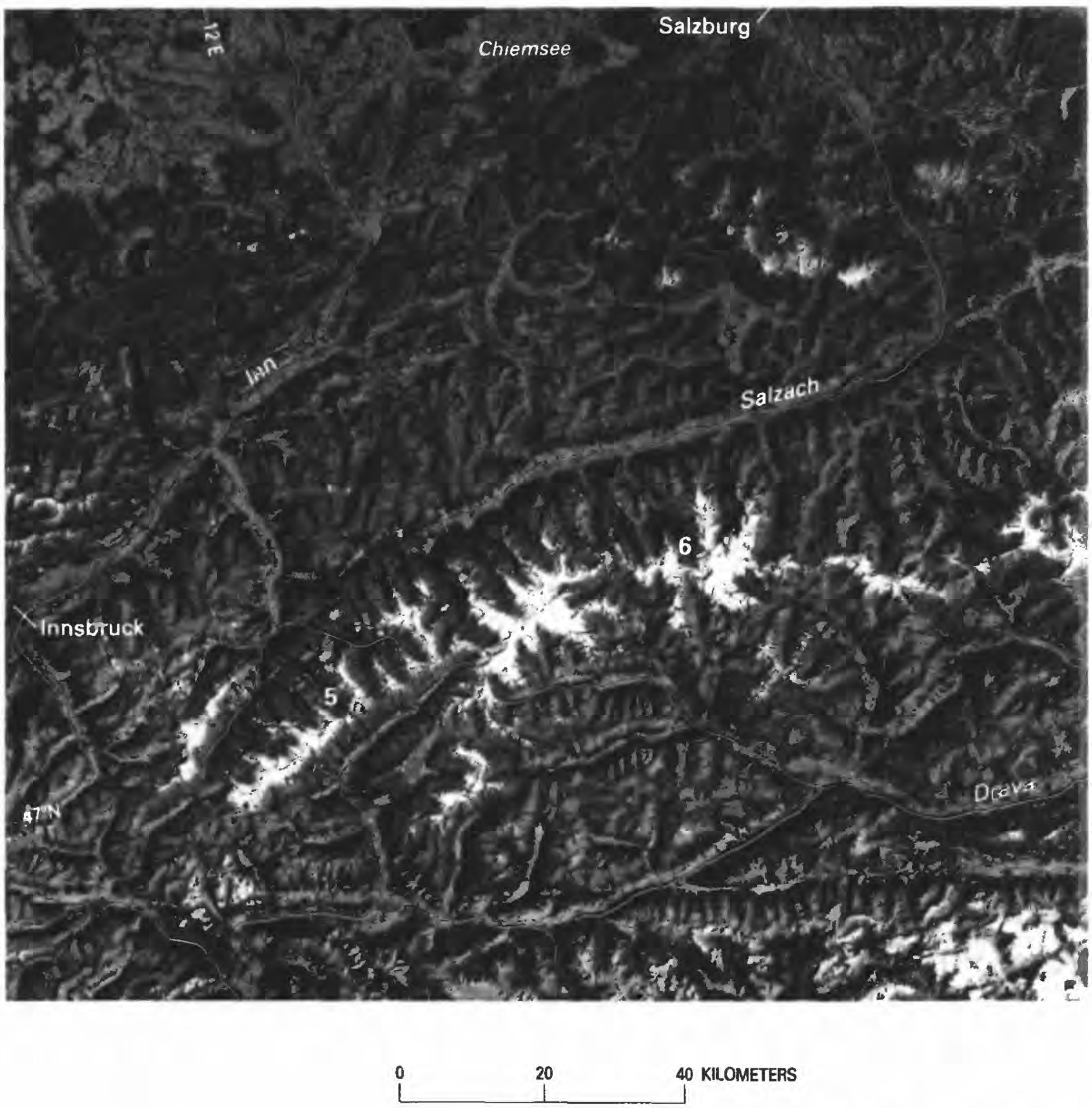

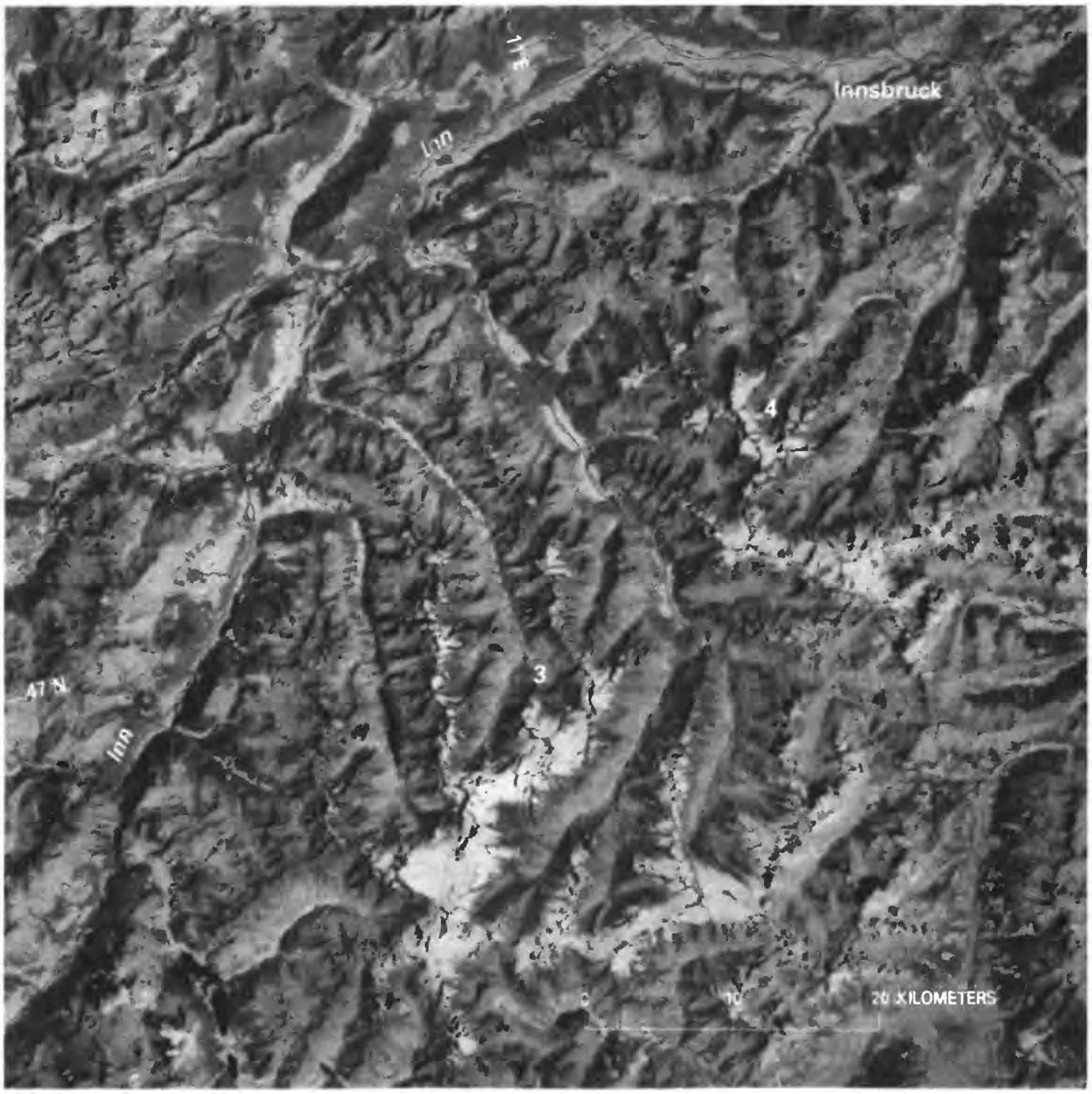

Figure 8 provides a view of the Ötztaler Alpen and Stubaier Alpen (table 2). Some scattered convective clouds are visible on both images, but the glacier regions are totally cloud free. In both figures only the lower parts of the glacier tongues are snow free. They cannot be easily distinguished from the surrounding terrain, which has a similar reflectivity in the near infrared. Both images clearly show the dendritic drainage network of the Alpine valleys that was formed by erosion during the Pleistocene Epoch. Figure 9 shows several glaciers of the Ötztaler Alpen group in a Landsat 5 TM image that was acquired on 30 September 1985, at the end of the ablation season. The main glaciers in the image are the Gepatschferner (17.7 km^2), the Vernagtferner (9.3 km^2), and the Hintereisferner (9.1 km^2). Because the mass balances of the glaciers were negative during the balance year 1 October 1984 to 30 September 1985, the equilibrium line was situated above the edge of the firn. The equilibrium line can be determined accurately from the TM image, because the firn from previous years shows significantly lower reflectivity than snow from the 1984–85 mass-balance season.

***Figure 8.**—Enlargement of part of a Landsat 1 MSS image taken on 13 August 1972 (1021–09380, band 7; Path 208, Row 27). The numbers refer to the mountain groups listed in table 2. Landsat image from the EROS Data Center, U.S. Geological Survey, Sioux Falls, S. Dak.*

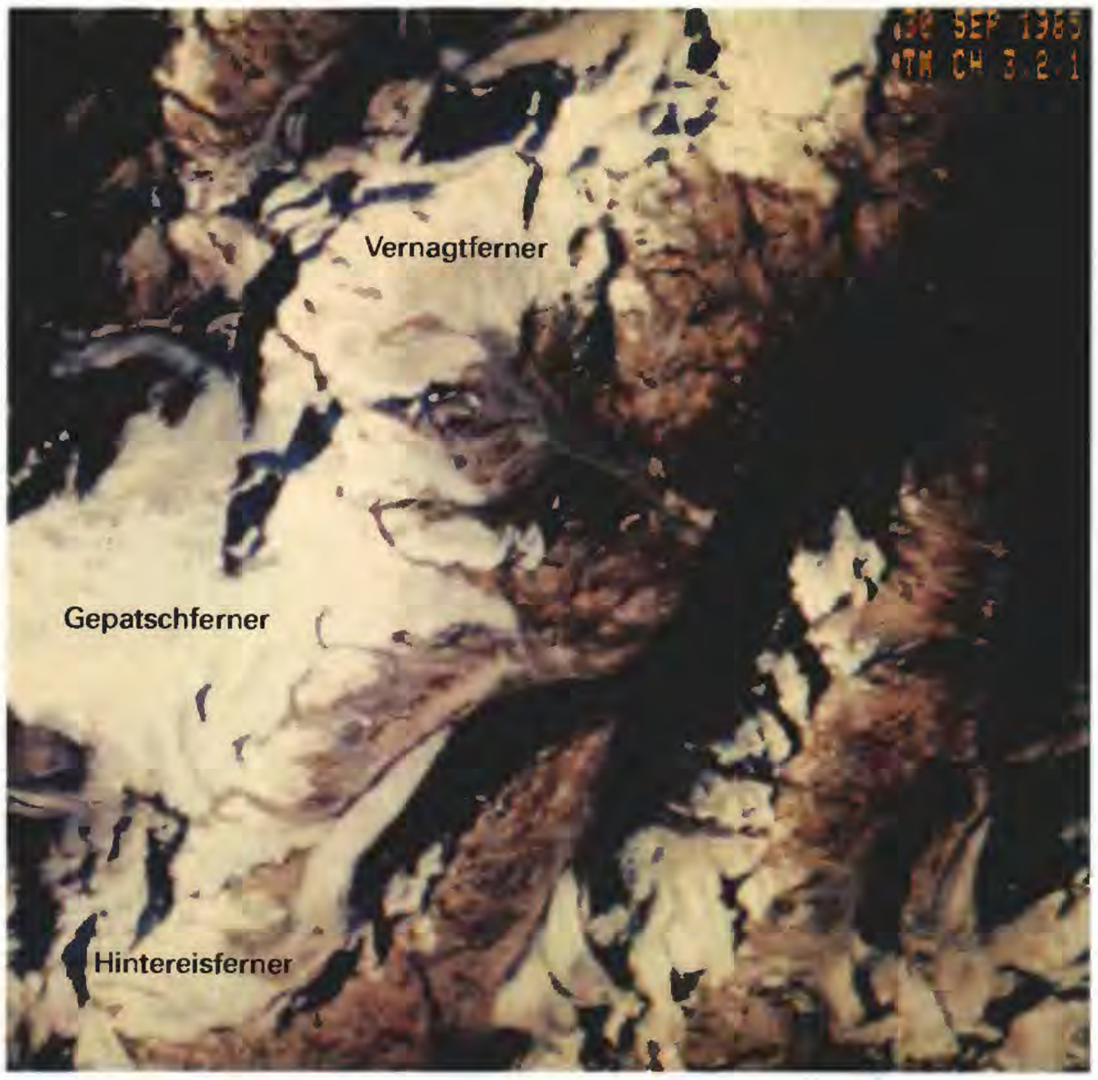

Figure 9.*—Enlargement at approximately 1:250,000 scale of part of a Landsat 5 TM image over the Ötztaler Alpen group taken on 30 September 1985 (bands 1, 2, 3; Path 193, Row 27). The main glaciers are Gepatschferner, Hintereisferner, and Vernagtferner. Landsat image from the European Space Agency, Frascati, Italy.*

Selected References

Escher-Vetter, H., 1985, Energy balance calculations from five years' meteorological records at Vernagtferner, Ötztal Alps: Zeitschrift für Gletscherkunde und Glazialgeologie, v. 21, p. 397–402.

Gross, G., 1987, Der Flächenverlust der Gletscher in Österreich 1850–1920–1969 [Areal losses of the glaciers in the Austrian Alps 1850–1920–1969]: Zeitschrift für Gletscherkunde und Glazialgeologie, v. 23, no. 2, p. 131–141.

Gross, G., Kerschner, H., and Patzelt, G., 1977, Methodische Untersuchungen über die Schneegrenze in alpinen Gletscher-gebieten [Systematic research on the snowline in Alpine glacier regions]: Zeitschrift für Gletscherkunde und Glazialgeologie, v. 12, no. 2, p. 223–251.

Hoinkes, H., 1969, Surges of the Vernagtferner in the Ötztal Alps since 1599: Canadian Journal of Earth Sciences, v. 6, no. 4, p. 853–861.

———1970, Methoden und Möglichkeiten von Massenhaus haltsstudien auf Gletschern. Ergebnisse der Messreihe Hintereisferner (Ötztaler Alpen) 1953–1968 [Techniques and feasibility of mass balance studies of glaciers. Results from measuring Hintereisferner (Ötztal Alps) 1953–1968]: Zeitschrift für Gletscherkunde und Glazialgeologie, v. 6, no. 1–2, p. 37–90.

Kuhn, M., 1981, Climate and glaciers, *in* Sea level, ice, and climatic change: International Association of Hydrological Sciences Publication No. 131, p. 3–20.

Kuhn, M., Markl, G., Kaser, G., Nickus, U., Obleitner, F., and Schneider, H., 1985, Fluctuations of climate and mass balance: Different responses of two adjacent glaciers: Zeitschrift für Gletscherkunde und Glazialgeologie, v. 21, p. 409–416.

Oerter, H., Reinwarth, O., Rufli, H., 1982, Core drilling through a temperate Alpine glacier (Vernagtferner, Ötztal Alps) in 1979: Zeitschrift für Gletscherkunde und Glazialgeologie, v. 18, no. 1, p. 1–11.

Østrem, G., 1975, ERTS data in glaciology—An effort to monitor glacier mass balance from satellite imagery: Journal of Glaciology, v. 15, no. 73, p. 403–415.

Patzelt, G., 1973, Die neuzeitlichen Gletscherschwankungen in der Venedigergruppe [Recent glacier variations in the Venedigergruppe] (Hohe Tauern, Ostalpen): Zeitschrift für Gletscherkunde und Glazialgeologie, v. 9, no. 1–2, p. 5–57.

———1980, The Austrian glacier inventory: Status and first results, *in* World Glacier Inventory: International Association of Hydrological Sciences–Association Internationale des Sciences Hydrologiques Publication No. 126, p. 181–183.

Richter, E., 1888, Die Gletscher der Ostalpen [The glaciers of the eastern alps]: Engelhorn, Stuttgart, 306 p.

Rott, H., 1977, Analyse der Schneeflachen auf Gletschern der Tiroler Zentral-alpen aus Landsat-Bildern [Analysis of snow areas on glaciers of the central alpine Tyrol using Landsat imagery]: Zeitschrift für Gletscherkunde und Glazialgeologie, v. 12, no. 1, p. 1–28.

Rott, H., and Domik, G., 1984, The SAR-580 experiment on snow and glaciers at the Austrian Test Site. Final report of the European SAR-580 Campaign: Ispra, Italy, v. 2 SA/I.04, E2.85.12, p. 217–231.

Rott, H., Domik, G., Mätzler, C., and Miller, H., 1985, Towards a SAR system for snow and land ice applications: Proceedings of Workshop on Thematic Applications of SAR Data, Frascati, Italy, September 1985, ESA SP–287, p. 29-39.

Rott, H., and Markl, G., 1989, Improved snow and glacier monitoring by the Landsat Thematic Mapper: Proceedings of Workshop on Landsat Thematic Mapper Applications, Frascati, Italy, December 1987, ESA SP–1102, p. 3–12.

The Swiss Alps

By Karl E. Scherler[2]

Abstract

According to a glacier inventory published in 1976, which is based on aerial photography of 1973, there are 1,828 glacier units in the Swiss Alps that cover a total area of 1,342 square kilometers. The Rhonegletscher, currently the ninth largest in the country, was one of the first to be studied in detail. Its surface has been surveyed repeatedly; velocity profiles were measured, and the fluctuations of its terminus were mapped and recorded from 1874 to 1914. Recent research on the glacier has included climatological, hydrological, and mass-balance studies. Glaciological research has been conducted on various other glaciers in Switzerland concerning glacier hydrology, glacier hazards, fluctuations of glacier termini, ice mechanics, ice cores, and mass balance. Good maps are available showing the extent of glaciers from the latter decades of the 19th century. More recently, the entire country has been mapped at scales of 1:25,000, 1:50,000, 1:100,000, 1:200,000, and 1:500,000. The 1:25,000-scale series very accurately represents the glaciers as well as locates supraglacial morainic debris and crevasses. The maps are revised every 6 years by use of aerial photogrammetric methods. The possibility of producing a glacier inventory by combining the topographic maps with Landsat digital and visual data is discussed.

Introduction

The Swiss Alpine mountain system, which encompasses two-thirds of the country, is divided into northern and southern chains by the deep west-southwest-east-northeast-trending tectonic trough occupied by the upper courses of the Rhône, Reuss, and Rhine River systems (fig. 10).

Moisture-bearing winds blow mostly from the westerly to northwesterly directions and produce precipitation on the windward northerly slopes of the northern chains. In spring and autumn, the situation is often reversed, with southerly winds causing heavy precipitation in the southern parts of the mountain chains. The large east-west valleys receive the least precipitation, because they are sheltered from both the north and the south. This pattern is especially marked in the Rhône River valley and its tributaries (Valais canton) and in the Engadine Valley of the Inn River.

The largest ice masses occur in the highest chains, the Alpi Pennine, Berner Alpen, Alpi Lepontine, and Rhätische Alpen (table 4; fig. 10). Numerous smaller glacier units of different types are dispersed throughout the remaining part of the Swiss Alps. According to Müller and others (1976a), 1,828 glacier units cover a total area of 1,342 km^2.

The elevations at which glaciers are found closely follow the precipitation pattern (Haeberli, 1983a). The median elevations of the glaciers in the dry Rhône basin are several hundred meters higher than those on the north slope or those which are exposed to the influence of the cyclonic storms passing south of the Alps (table 4, fig. 10). This difference is shown by Müller and others (1976a) and Müller and Scherler (1980).

Observations of Glaciers

Prior to the 18th century, man's attitude toward high mountains was one of fear and terror. Glaciers were mentioned in tales, when they

[2] Laboratory of Hydraulics, Hydrology, and Glaciology, Swiss Federal Institute of Technology (ETHZ), CH-8092 Zürich, Switzerland.

TABLE 4.—*The largest glaciers in Switzerland (from Müller and others, 1976a)*

[Glaciers are shown by number on figure 10]

Number	Glacier name	Drainage	Surface area (km^2)	Lowest elevation (m)	Median elevation (m)
1	Aletschgletscher	Rhône	86.8	1,520	3,140
2	Gornergletscher	Rhône	68.9	2,120	3,220
3	Fieschergletscher	Rhône	33.1	1,640	3,140
4	Unteraargletscher	Aar-Rhine	28.4	1,900	2,660
5	Ober Aletschgletscher	Rhône	21.7	2,180	2,920
6	Unterer Grindel-waldgletscher	Aar-Rhine	21.7	1,260	2,780
7	Findelengletscher	Rhône	19.1	2,320	3,300
8	Corbassière Glacier	Rhône	17.4	2,220	3,200
9	Rhonegletscher	Rhône	17.4	2,140	2,940
10	Vadret da Morteratsch	Inn-Danube	17.2	2,100	3,000
11	Triftgletscher	Aar-Rhine	17.1	1,720	2,900
12	Zmuttgletscher	Rhône	17.0	2,280	2,980

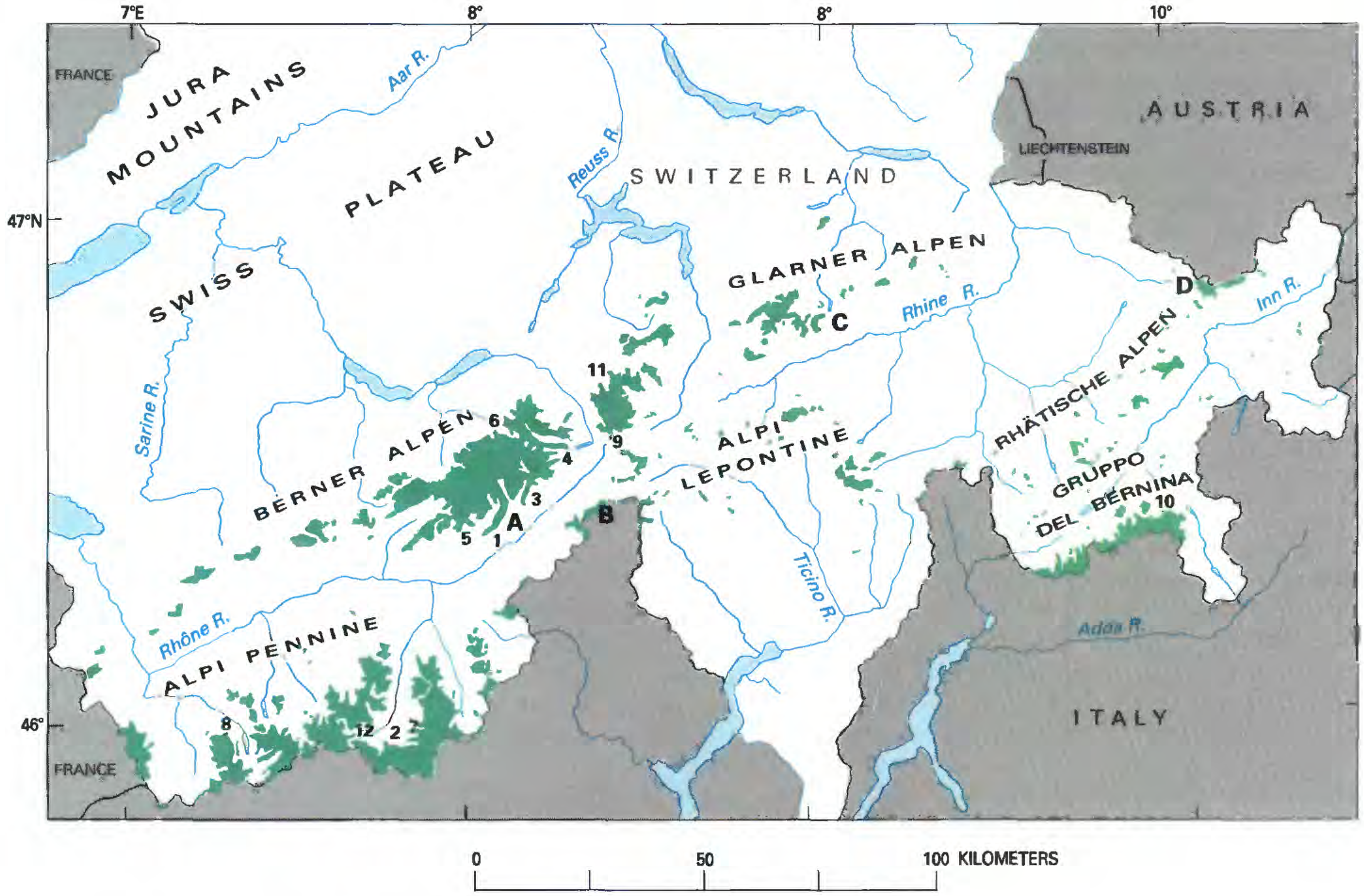

***Figure 10.**—Glacier distribution in Switzerland (after Müller and others, 1976a). Numbers refer to table 4; the location of the four glaciers where continuous mass-balance studies have been conducted is shown as follows: A, Aletschgletscher; B, Griesgletscher; C, Limmerngletscher; D, Silvrettagletscher.*

caused the sudden disappearance of fertile pastures under ice masses as a punishment for the sins committed by the mountain people. Ancient chronicles also told about ice avalanches and lake outbursts. In 1595, an outburst flood from a lake caused by the Giétro Glacier, Pennine Alps, caused 160 deaths; in 1597, an ice-and-snow avalanche from Hohmatten Glacier, Pennine Alps, caused 81 deaths.

Starting with the 18th century, this negative view changed to one of romantic enthusiasm, as is shown in poems by Albrecht von Haller and Jean-Jacques Rousseau. Then scientists turned their attention to glacial phenomena. Names of some of the pioneers in the field of glaciology were Scheuchzer, Venetz, Agassiz, and de Saussure.

The Rhonegletcher was one of the first Swiss glaciers to be observed in detail. Its surface was surveyed repeatedly, velocity profiles were measured, and the fluctuations of its terminus were mapped and recorded. This research was carried out continuously from 1874 to 1914 and published by the Swiss Academy of Sciences (Schweizerische Naturforschende Gesellschaft, 1916). Since 1880, fluctuations of the termini of a representative number of glaciers have been measured annually and published in the journal (Jahrbuch) of the Swiss Alpine Club (SAC) from 1891 to 1924, and in Die Alpen since 1925; Aellen (1985) gives a summary.

A good review of glacier research in Switzerland is given by the Swiss National Tourist Office (1981). During the 19th century, the most important tasks consisted of dealing with hazards related to glacier advances, glacier floods, and ice avalanches (Röthlisberger, 1981) and of starting long-term national as well as international glacier monitoring (Kasser, 1967, 1973; Müller, 1977; Haeberli, 1985; Haeberli and Müller, 1988). In the 20th century, intensive development of hydroelectric power schemes in heavily glacierized areas led to strong interaction between glaciology and hydraulic engineering. In recent years, concern for the quality of the environment has resulted in involvement in various fields of pure and applied ice research. Assessing glacier hazards in densely populated areas remains a task of vital importance (Haeberli, 1983b; Alean, 1985; Haeberli and others, 1989). Core drilling in cold firn and ice at 4,450 m above mean sea level on Colle Gnifetti, Monte Rosa, furnishes important information on the development of atmospheric composition (Oeschger and others, 1978; Haeberli and others, 1988; Wagenbach and others, 1988). Subglacial hydraulics and sliding processes at the beds of temperate valley glaciers are also intensely studied (Iken and Bindschadler, 1986). Continuous mass-balance measurements are being carried out on the Griesgletscher, Limmerngletscher, Plattalvagletscher, and Silvrettagletscher. The mass balance of the Aletschgletscher, the largest glacier in the Alps, is estimated by use of a hydrological model.

Glacier inventories were published by Jegerlehner (1902) and by Müller and others (1976a). The latter was based on aerial photographs taken near the end of the 1973 ablation season (Müller and others, 1976b), while the former consisted of measurements done on the 1:50,000-scale map sheets of the Siegfried Atlas (see following section), showing the state of the glaciers during the last two decades of the 19th century. Because different data bases were used in these two inventories, it is difficult to make comparisons.

Mapping of Glaciers

Topographical surveying of the Swiss Alps was carried out mainly by the Federal Topographical Survey Office, with the notable exception of the Meyer-Weisz Atlas of Switzerland (1796–1802), consisting of 16 sheets at an approximate scale of 1:108,000. During the first decades of the 19th century, the whole country was surveyed under the direction of General G.-H. Dufour. The survey was done at scales of 1:25,000 and 1:50,000, the latter for mountain regions. However, the Dufour Atlas was published at a scale of 1:100,000 only (1844–65). A revised version of the Dufour topographical survey was used as the basis for maps in the Siegfried Atlas, which was published in the years following 1870 at the larger scales. Therefore, good maps showing the extent of the glaciers in the last decades of the 19th century are available. All of these map sheets are in color, with contour intervals at 30 m (Grob, 1941). These two national atlases showed a remarkable degree of accuracy and were regarded as masterpieces of contemporary cartography at their time of publication.

As early as 1891, the Swiss Alpine Club requested the preparation of a uniform topographic atlas or set of topographic maps of Switzerland. The Siegfried Atlas had the serious disadvantage of using two different scales. In addition, the map sheets showed too strongly the individual mark of the responsible topographer and of the cantonal authorities who granted part of the financial support. Both of these factors influenced the scope and detail of the individual map sheets. A series of precision-leveling surveys, carried out during the period 1903 to 1925, and a new geodetic triangulation survey revealed serious errors both in elevations and positions of mapped features.

Therefore, in 1935, the Federal Assembly passed a law that was to form the basis of the New Topographical Atlas of Switzerland (Neue Landeskarte der Schweiz, now Landeskarte der Schweiz). The Atlas was published at scales of 1:25,000, 1:50,000, 1:100,000, 1:200,000, and 1:500,000, under the sole responsibility of the Federal Topographical Survey. The last sheet at the scale of 1:25,000 was published in 1979. At this scale, the glaciers are represented very accurately. The contour interval for high mountain regions is 20 m. Also shown are moraine cover and major crevasses. The maps are revised every 6 years by use of aerial photogrammetric methods. Therefore, the whole of Switzerland is periodically covered by high-quality vertical aerial photographs. Müller and others (1976b) provide a list of aerial photographs for all Swiss glaciers.

The Aletschgletscher was mapped at a scale of 1:10,000 by the Federal Topographical Survey and the Laboratory of Hydraulics, Hydrology, and Glaciology in 1957. This special topographic map shows the state of the Aletschgletcher, including detailed information on glaciological features such as crevasses and moraines.

Satellite Imagery

It is by no means easy to find optimum remotely sensed images of Swiss glaciers. The same applies to standard vertical aerial photographs. Glaciers should be photographed (or imaged) at the end of the ablation season, which may be any time between the end of August and the early part of October. The optimum time is very dependent on weather conditions, which are highly variable in the Swiss Alps. In addition, at the end of the ablation season, the solar elevation angle is already rather small, so deep shadows are produced on north and northwest slopes as Landsat passes over Switzerland during the morning hours. Thus, identification of the glaciers on the steep north slope of the Alps is difficult (figs. 11 and 12).

H.J. Gilgen, in his discussion in "Inventory of Glaciers" (this volume), shows that a preliminary glacier inventory can be prepared of an area on the basis of analysis of Landsat digital data recorded on computer-compatible tapes. So far, no attempt has been made to assess the glacier area of Switzerland from visual analysis of Landsat images. The assessment could be made, however, if the excellent maps that are available and enlargements of Landsat MSS images were used. Figures 13 and 14 show that it is possible to compile a simple glacier inventory on the basis of Landsat images and good topographic maps. The topographic base maps are important in assessing watershed areas and in estimating various altitudes in the regions encompassed by Landsat images.

***Figure 11.**—Landsat 2 MSS false-color composite image of the western part of the Swiss Alps on 16 September 1978 (21333–09210; Path 210, Row 28). The scale is approximately 1:1,000,000. Landsat image from the European Space Agency, Frascati, Italy.*

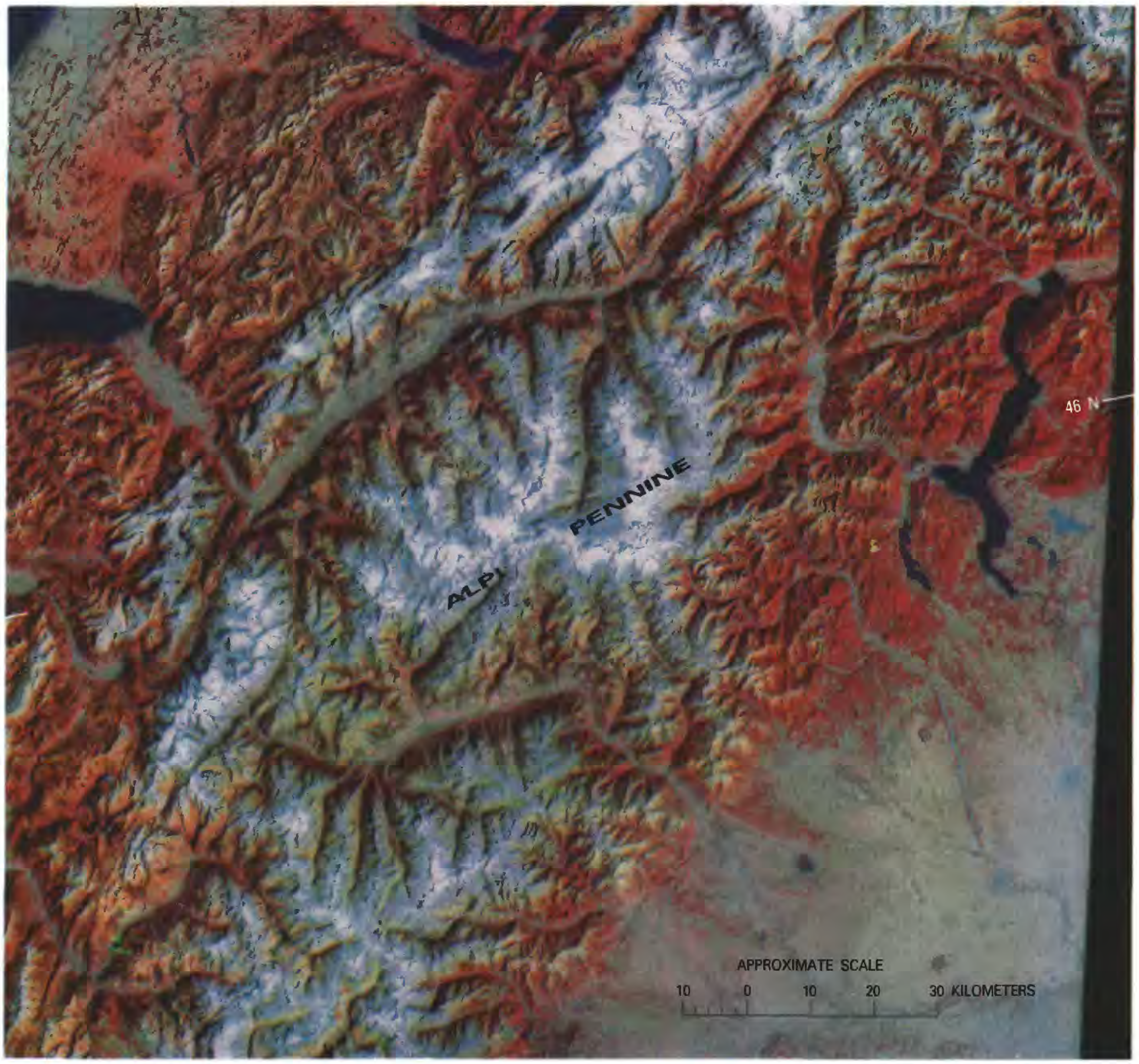

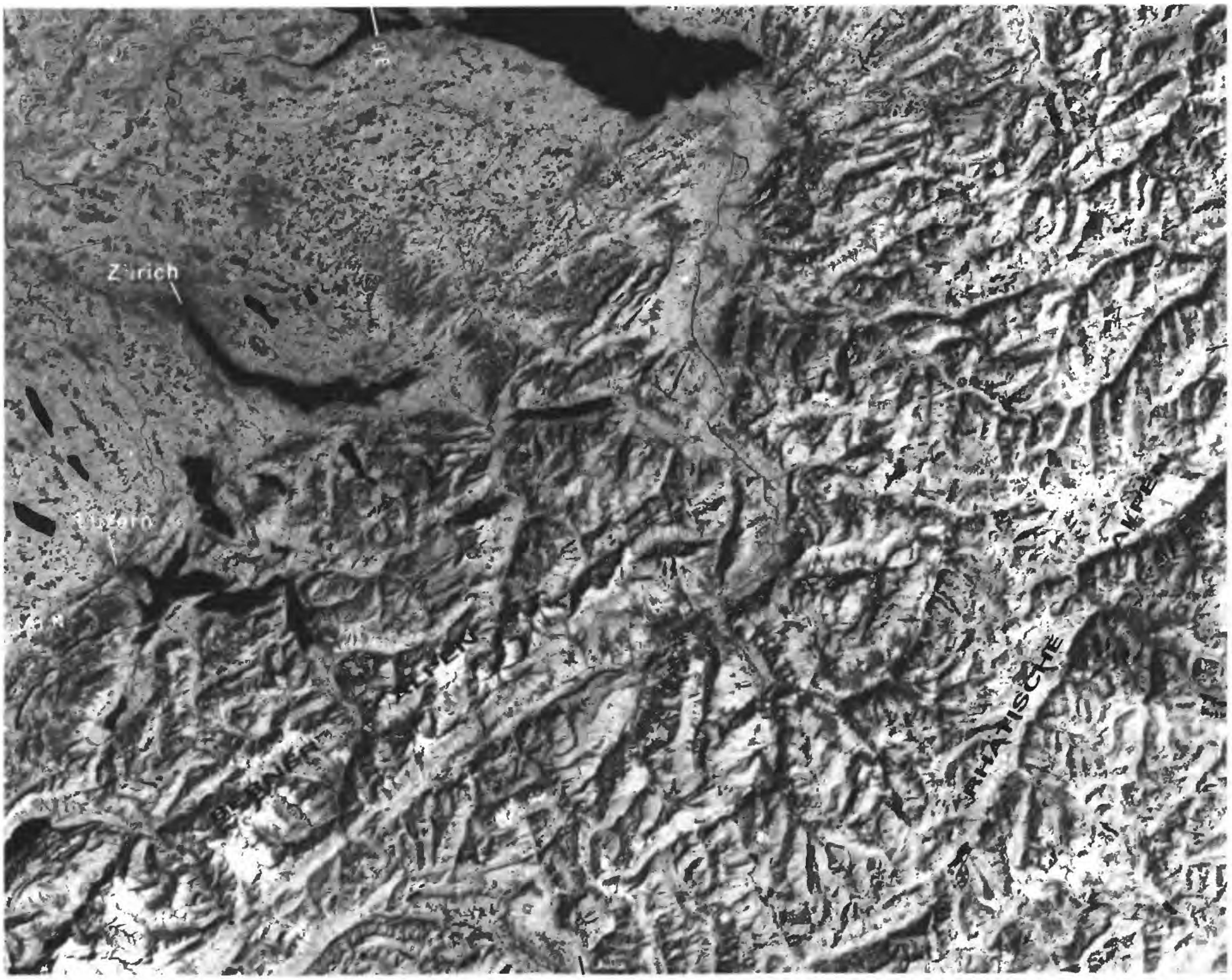

Figure 12.—*Landsat 2 MSS image of the eastern part of the Swiss Alps on 4 September 1980 (band 7; Path 209, Row 27). The scale is approximately 1:1,000,000. Landsat image from the European Space Agency, Frascati, Italy.*

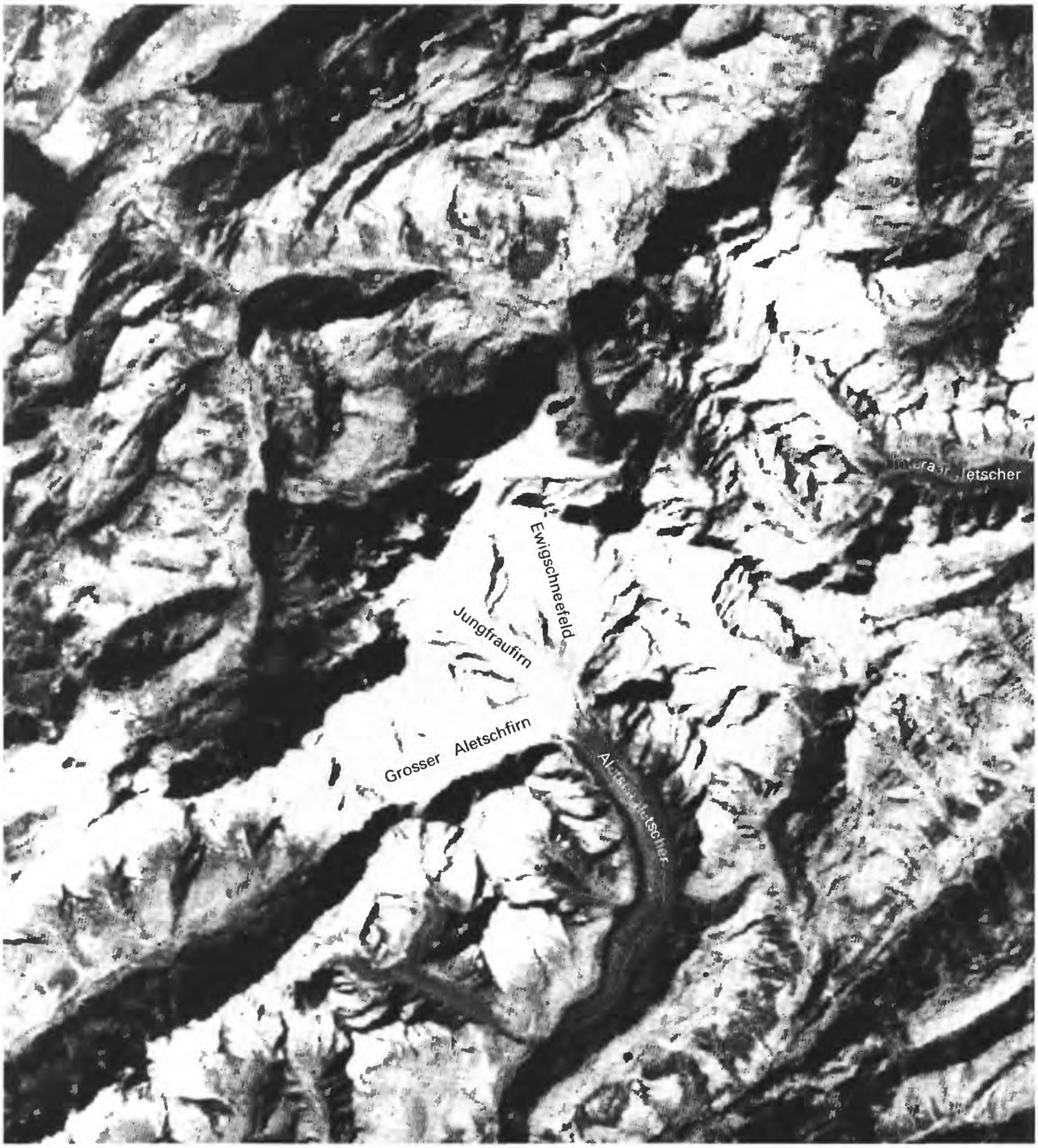

Figure 13.—*Enlargement of part of figure 11 to a scale of approximately 1:200,000 showing the Aletschgletscher and surrounding area.*

__Figure 14.__—A Landeskarte der Schweiz sheet at 1:200,000 scale showing the same region as in figure 13. Reproduced with permission of the Swiss Topographical Survey, dated 15 January 1982.

Acknowledgment

The editors thank Dr. Wilfried Haeberli, Swiss Federal Institute of Technology, who read the manuscript and made valuable contributions.

References Cited

Aellen, M., 1985, Les variations récentes des glaciers des Alpes Suisses [Recent variations of glaciers of the Swiss Alps]: Geografia Fisica e Dinamica Quaternaria, v. 8, no. 2, p. 73–82.

Alean, J., 1985, Ice avalanches: Some empirical information about their formation and reach: Journal of Glaciology, v. 31, no. 109, p. 324–333.

Grob, R., 1941, Geschichte der Schweizerischen Kartographie [History of Swiss mapping]: Bern, Kümmerly and Frey, 194 p.

Haeberli, W., 1983a, Permafrost-glacier relationships in the Swiss Alps—Today and in the past: Permafrost, Fourth International Conference, Fairbanks, Alaska, July 17–22, 1983, Proceedings, p. 415–420.

———1983b, Frequency and characteristics of glacier floods in the Swiss Alps: Annals of Glaciology, v. 4, p. 85–90.

———compiler, 1985, Fluctuations of glaciers 1975–1980, v. 4: Paris, International Association of Hydrological Sciences (IAHS) and United Nations Educational, Scientific, and Cultural Organization (UNESCO), 265 p., with 13 special topographic maps of glaciers.

Haeberli, W., Alean, J.-C., Müller, P., and Funk, M., 1989, Assessing risks from glacier hazards in high mountain regions: Some experiences in the Swiss Alps: Annals of Glaciology, v. 13, p. 96–102.

Haeberli, W., and Müller, P., compilers, 1988, Fluctuations of glaciers 1980–1985, v. 5: Zürich, IAHS/UNEP/UNESCO, 288 p., with 13 special topographic maps of glaciers.

Haeberli, W., Schmid, W., and Wagenbach, D., 1988, On the geometry, flow and age of firn and ice at the Colle Gnifetti core drilling site (Monte Rosa, Swiss Alps): Zeitschrift für Gletscherkunde und Glazialgeologie, v. 24, no. 1, p. 1–19.

Iken, A., and Bindschadler, R.A., 1986, Combined measurements of subglacial water pressure and surface velocity of Findelengletscher, Switzerland: Conclusions about drainage system and sliding mechanism: Journal of Glaciology, v. 32, no. 110, p. 101–119.

Jegerlehner, J., 1902, Die Schneegrenze in den Gletschergebieten der Schweiz [The snowline in the glacier region of Switzerland]: Beiträge zur Geophysik, v. 5, no. 3, p. 486–568.

Kasser, P., compiler, 1967, Fluctuations of glaciers 1959–1965, v. 1: Paris, International Association of Scientific Hydrology (IASH) and United Nations Educational, Scientific, and Cultural Organization (UNESCO), 52 p., with an additional 23 tables, 7 figures, and 1:25,000-scale photogrammetric map of Aletschgletscher.

———1973, Fluctuations of glaciers 1965–1970, v. 2: Paris, International Association of Hydrological Sciences (IAHS) and United Nations, Educational, Scientific, and Cultural Organization (UNESCO), 357 p., with 5 special topographic maps of glaciers.

Müller, F., 1977, Fluctuations of glaciers 1970–75, v. 3: Paris, International Association of Hydrological Sciences (IAHS) and United Nations Educational, Scientific, and Cultural Organization (UNESCO), 269 p., with 12 special topographic maps of glaciers.

Müller, F., Caflisch, T., and Müller, G., 1976a, Firn and Eis der Schweizer Alpen [Firn and ice in the Swiss Alps]: Glacier inventory: Zürich, Geographisches Institut ETH, Publication No. 57, 174 p.

———1976b, Firn and Eis der Schweizer Alpen [Firn and ice in the Swiss Alps]. Photoliste: Zürich, Geographisches Institut ETH, Publication No. 57a.

Müller, F., and Scherler, K., 1980, Some comments on the Swiss glacier inventory, *in* World Glacier Inventory Workshop: International Association of Hydrological Sciences-Association Internationale des Sciences Hydrologiques Publication No. 126, p. 185–194.

Oeschger, H., Schotterer, U., Stauffer, B., Haeberli, W., and Röthlisberger, H., 1978, First results from Alpine core drilling projects: Zeitschrift für Gletscherkunde und Glazialgeologie, v. 13, p. 193–208.

Röthlisberger, H., 1981, Eislawinen und Ausbrüche von Gletscherseen [Ice avalanches and outbursts from glacier lakes]: Jahrbuch der Schweizerischen Naturforschenden Gesellschaft 1978, p. 170–212.

Swiss National Tourist Office, eds., 1981, Switzerland and her glaciers: Bern, Kümmerly and Frey, 191 p.

Schweizerische Naturforschende Gesellschaft, 1916, Vermessungen am Rhonegletscher 1874–1915 [Measurements on the Rhône Glacier 1874–1915]: Basel, Georg & Co., 190 p.

Wagenbach, D., Munnich, K.O., Schotterer, U., and Oeschger, H., 1988, The anthropogenic impact on snow chemistry at Colle Gnifetti, Swiss Alps: Annals of Glaciology, v. 10, p. 183–187.

The French Alps

By Louis Reynaud[3]

Abstract

The glaciers of the French Alps are distributed in four main groups and have a total area of 350 square kilometers. The northernmost group, on the Mont Blanc massif, has a glacier area of 110 square kilometers, which includes Mer de Glace, which, with an area of 40 square kilometers, is the largest glacier in the Western Alps. Farther south, the Massif de la Vanoise contains 130 glaciers that have a total area of 85 square kilometers. The glaciers of the Grandes Rousses massif have a total area of 11 square kilometers. Lastly, the Massif du Pelvoux has a total glacier area of 120 square kilometers. Studies of glacier variations since 1600 A.D. have shown numerous fluctuations in glacier length. The glaciers on Mont Blanc that appear to show similar fluctuations in fact have different individual response times. Mass-balance measurements are presently being carried out on nine glaciers. The measurements on one of these glaciers, Glacier de Saint Sorlin, have been used to validate a linear statistical model for mass-balance variation. The model seems to give good results when extended over the entire region of French Alpine glaciers. New methods of mass-balance reconstructions by use of a continuity equation are discussed. Current satellite data have limited usefulness for glacier studies in the French Alps, with the exception of the method correlating changes in the elevation of snowline to changes in glacier mass balance.

Introduction

The French part of the Alps constitutes the western face of the chain, spanning the region between Lake Geneva and the Mediterranean Sea (fig. 15). Glaciers are distributed in four main groups from north to south over a distance of approximately 250 km (fig. 16 and table 5).

The summit regions in the French massifs are heavily dissected by erosion. At this end of the Alpine mountain chain, changes in elevation are large. In a distance of only 8 km from the summit of Mont Blanc to the channel of the Arve River there is 3,800 m of relief. Granite needles overlook deep-walled cirques, but the mean altitude of the massif is not very high. This low mean altitude explains why, although the summits are higher than in the central regions of the Alps, the glacier areas are in fact much smaller. Except for the extensive area of glaciers around the Mont Blanc massif, French glaciers are small or very small in size.

Precipitation in the French Alps is evenly distributed over all months of the year. However, there is a great variation with elevation and exposure. Chamonix, which is at the foot of Mont Blanc and has an elevation of 1,030 m, has 1,020 mm of annual precipitation, and the Col du Midi, at 3,500 m, has 3,100 mm, but near the summit, around 4,300 m, the annual precipitation is lower and reaches only 1,100 mm (Jouzel and others, 1984). At the edge of the Massif du Pelvoux, the valleys at an elevation of 1,000 m receive annually only 600 to 700 mm of precipitation. The precipitation is mostly due to a flow of maritime air from the west (Atlantic Ocean); circulation from the southeast (Mediterranean Sea) is less common. However, changes in the tracks of low-pressure disturbances during some years further accentuate the north-south differences of the mountain chain.

From Mont Blanc to Mont Pelvoux the snowline on the glaciers is between 2,750 m and 2,950 m, depending upon the exposure (2,800 m on

---

[3] Laboratory of Glaciology, Rue Molière, Domaine Universitaire, B.P. 96, 38402 St.-Martin d'Hères Cedex, France.

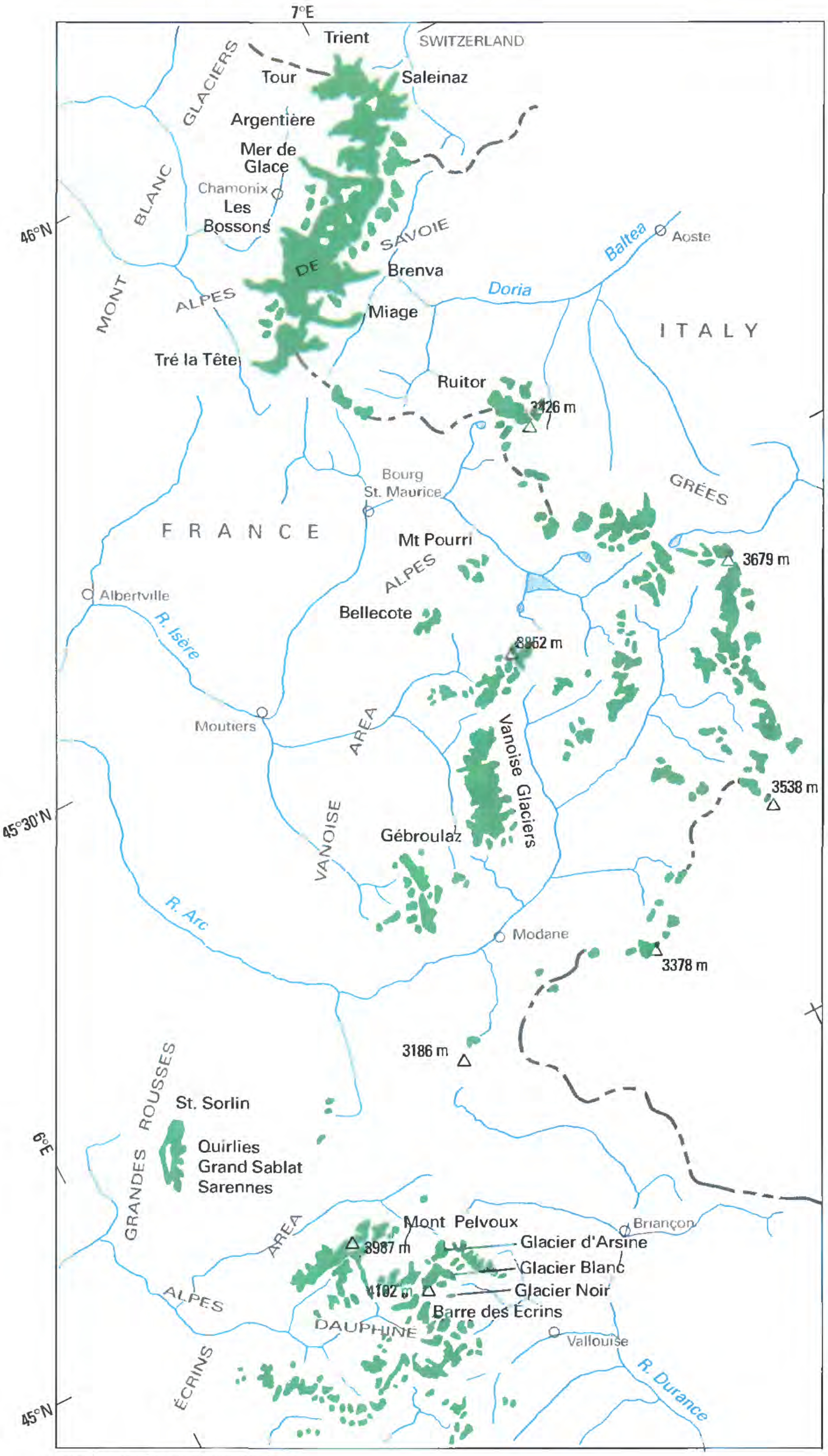

From Institut Géographique National
1:25,000-scale map series

0 25 KILOMETERS

Figure 15.—*Distribution of glaciers in the French Alps compiled from 1:25,000-scale Institut Géographique National maps (various dates). Glaciers in the Alpes Cottiennes and Maritimes are not included. Elevations are in meters.*

TABLE 5.—*The main groups of glaciers of the French Alps*

Alps	Massif	Glacier area (km^2)	Remarks
Savoie	Mont Blanc	110	Includes Mer de Glace, largest glacier in the Western Alps.
Grées	Vanoise	85	Source of the Arc and Isère Rivers.
Dauphiné	Grandes Rousses	11	Includes Glacier de Sarennes and Glacier de Saint-Sorlin.
	Pelvoux	120	Les Écrins area.
Cottiennes and Maritimes		4	Southern Alps, location of approximately 30 very small glaciers.
Total		330	

the northerly exposed Mer de Glace and 2,950 m on the Glacier Blanc, which faces south). Mont Blanc (4,807 m) is the only massif that has a large, relatively continuous area of glaciers. Mont Blanc accounts for 110 km^2 out of a total glacier area of 350 km^2 in the French Alps, and it includes the largest glacier in the Western Alps, the Mer de Glace, which has an area of 40 km^2.

To the south of the Mont Blanc massif is the Massif de la Vanoise; its highest elevation is Point de la Grande Casse, at 3,861 m. The massif contains about 130 glaciers that have a total glacierized area of 85 km^2.

The glaciers of the Grandes Rousses massif have a total area of 11 km^2. This massif includes Glacier de Sarennes and Glacier de Saint-Sorlin, which were mapped in detail in 1904.

Lastly, the Massif du Pelvoux, with its highest elevation, Barre des Écrins, at 4,102 m, is the most southerly glacial massif in the Alps (approximately 45° N. lat) and the second largest glacierized area in France at 120 km^2. To the south of the Massif du Pelvoux, the mean elevation of the chain declines sharply. Only about 30 small glaciers exist here, and their combined area is 4 km^2.

Previous work on glacier inventories of France document the substantial reduction in size of the French glaciers. Mougin (1925) published figures for the surface area of alpine glaciers at the end of the last century (1895) based on 1:80,000-scale maps and ground surveys. The areas given were 359 km^2 for the Savoie region and 159 km^2 for Dauphiné and Provence, or a total of 518 km^2 for the French Alps. Vivian (1975) conducted a systematic inventory between 1967 and 1971 of 919 glaciers of the Western Alps covering a total area of 568 km^2, of which 395 km^2 were in the French Alps. The inventory was conducted by use of completely revised cartography at 1:20,000 and 1:25,000 scale, fieldwork, and aerial photographic coverage from the Institut Géographique National's Photothèque.[4] An inventory has also been completed for the Temporary Technical Secretariat for the World Glacier Inventory (now part of the World Glacier Monitoring Service) by use of aerial photography and systematic field investigations.

[4] Institut Géographique National (IGN) Photothèque is located at 2 Avenue Pasteur, 94160 Saint Mandé, France.

Satellite Images of Glaciers of the French Alps

Only three Landsat images are required to cover the entire French Alps (see table 1, fig. 2). The Path 211, Row 28 nominal scene covers Mont Blanc and the Massif de la Vanoise; the Path 211, Row 29 nominal scene includes the Alpes du Dauphiné (Grande Rousses massif and Massif du Pelvoux); and the Path 209, Row 29 nominal scene encompasses the Alpes Maritimes.

The images of the French Alps noted in table 1 were taken in September or October with the Sun at an angle of 35° in elevation and 150° in azimuth, which roughly corresponds to about 0945 hours Universal, or Greenwich Mean Time. These circumstances allow for a good image of glaciers that are oriented to the south or southeast, but many glaciers that are to the north are hidden by shadows cast from the mountains (for example, Les Bossons in the Mont Blanc massif and Glacier Noir in the Massif du Pelvoux). Other glaciers are only partly visible, concealed by the very distinctive shadows of the nearest summits to the southeast.

Figures 16 and 17 illustrate the main groups of French glaciers shown on figure 15. Figure 17 shows enlarged sections from the two Landsat 1 multispectral scanner (MSS) images mosaicked in figure 16. The Mont Blanc, Grandes Rousses, and Pelvoux areas are practically cloud free, but most of the Vanoise glaciers are hidden by orographic clouds (figs. 16, 17). A light snowfall whitens the summits near the Italian border, to the east. The presence of snow or clouds makes it difficult to determine the areal extent of glaciers in the Alps.

Until 1983, no glaciological investigations had been done on the French Alps by use of satellite data. That is probably because of the recent availability of these data and the fact that the typical kind of information provided by such image data does not compare very well with conventional measuring methods that have been developed for these generally small, scattered glaciers and, therefore, does not meet the specific aims of the average glaciologist. In order for one to understand the potential future contribution of the satellite imagery to the glaciology of these areas, a brief historical description of glacier fluctuations and a survey of the objectives and methods of Alpine glaciology are needed.

The History of Glacier Variations in the French Alps

Through previous studies by Mougin (1934), Lliboutry (1964, 1965), and Le Roy Ladurie (1967), variations in the length of Alpine glaciers have been determined, beginning in about the year 1600. Earlier evidence is rare, but occasional documentation of previous glacier extent can be found in old books on geographic description and travel (Bourrit, 1787). Some local traditions mention a major glacier recession in the past (Vallot, 1900). The Chamonix glaciers on Mont Blanc reached one maximum position in about 1610, another about 1644, and the last and largest about 1664. The last of these was the greatest known advance in recorded history. After a major retreat there were other maxima in about 1720 and 1776, but the period of largest growth started about 1810 and reached its peak around 1818 to 1822. This peak was followed by a period of great shrinkage (for example, the Mer de Glace retreated 1,500 m), which continued until 1880. Recent information on fluctuations is given by Reynaud (1984).

To the casual observer, the fluctuations of the Mont Blanc glaciers may appear to be exactly synchronous, but annual measurements show that these fluctuations are not. Regular topographic surveys to measure the

Figure 16.*—Landsat 1 MSS image mosaic of the French Alps showing the Mont Blanc (A), the Grandes Rousses (C), and the Pelvoux (D) areas without clouds; the Vanoise area (B) is obscured by orographic clouds. Landsat images 1078–09555, band 7; 9 October 1972; Path 211, Row 28 and 1078–09562, band 7; 9 October 1972; Path 211, Row 229. The scale is approximately 1:1,000,000. Landsat images from the EROS Data Center, U.S. Geological Survey, Sioux Falls, S. Dak.* ▶

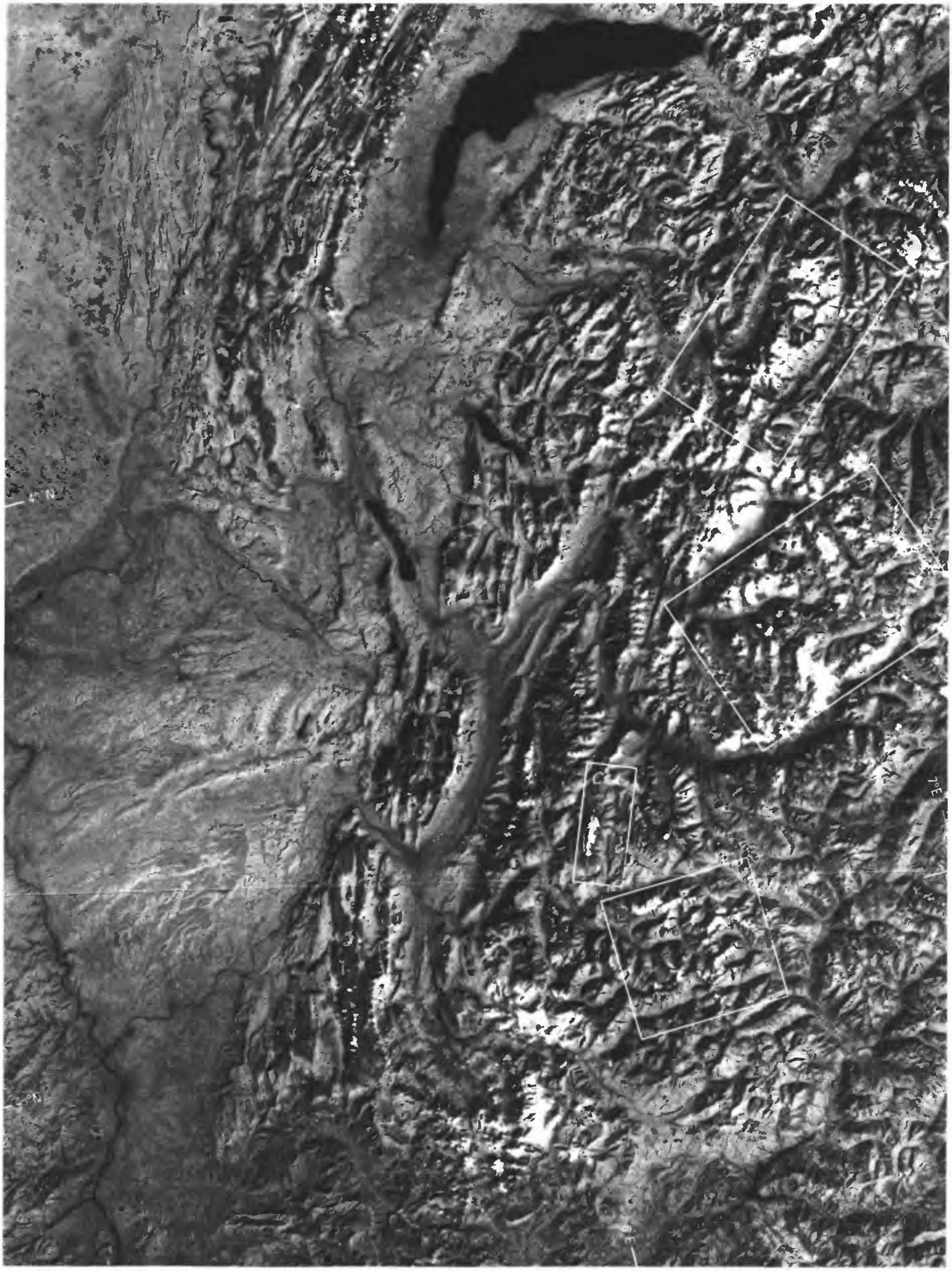

Figure 17.—Enlarged sections of the Landsat image mosaic of the French Alps (figure 16). The Mont Blanc area (A) and Vanoise area (B) are from Landsat image 1078–09555. The Grandes Rousses area (C) and Pelvoux area (D) are from Landsat image 1078–09562. On B, the glacier areas are shown in green to avoid confusion with cloudcover.

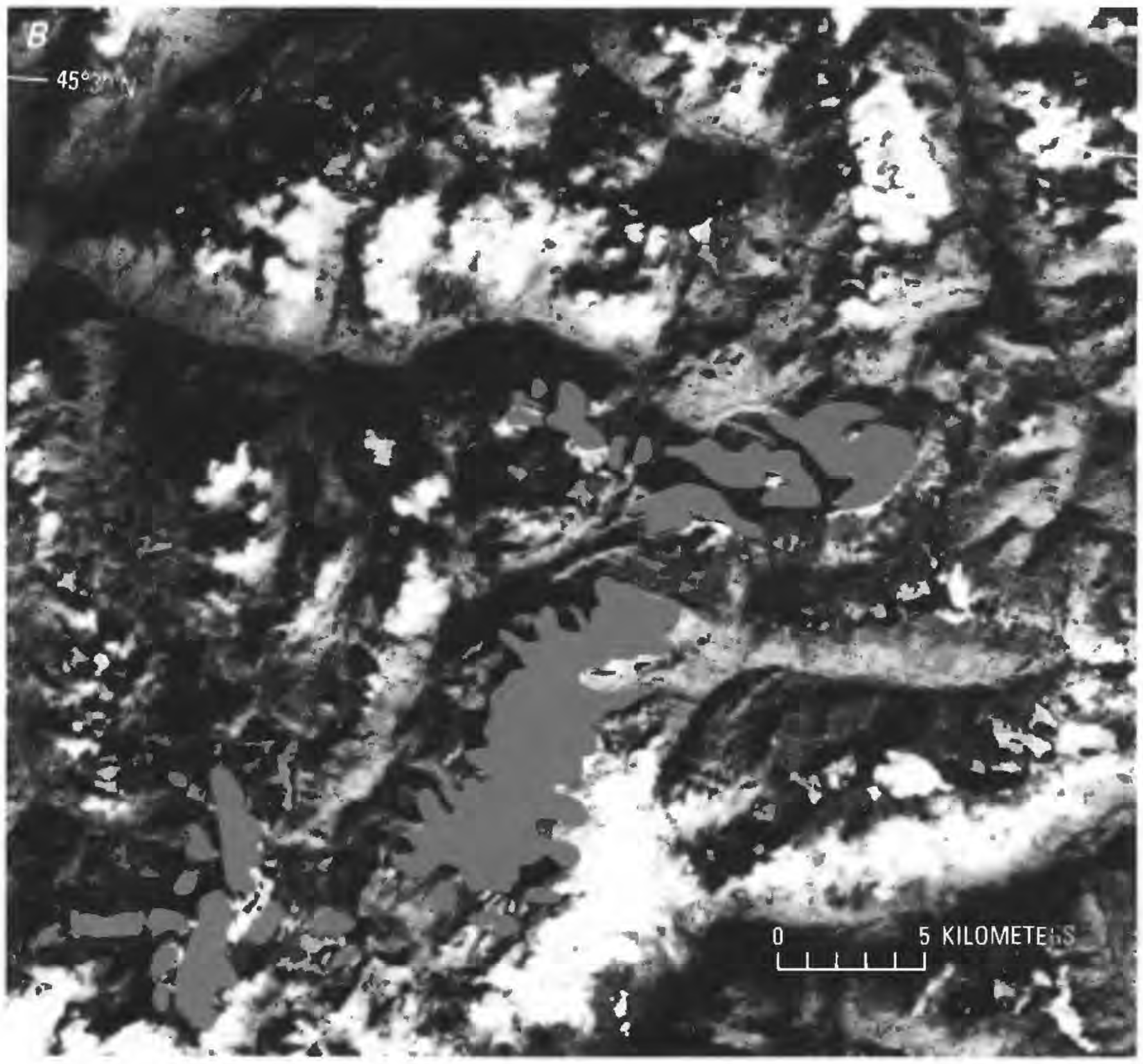
B
0
5 KILOMETERS

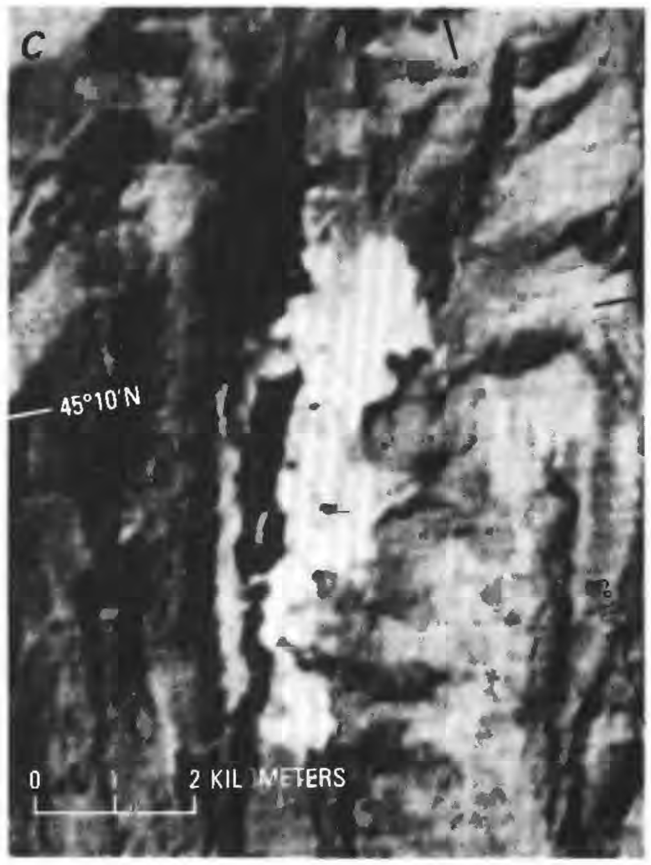
C
45°10'N
0
2

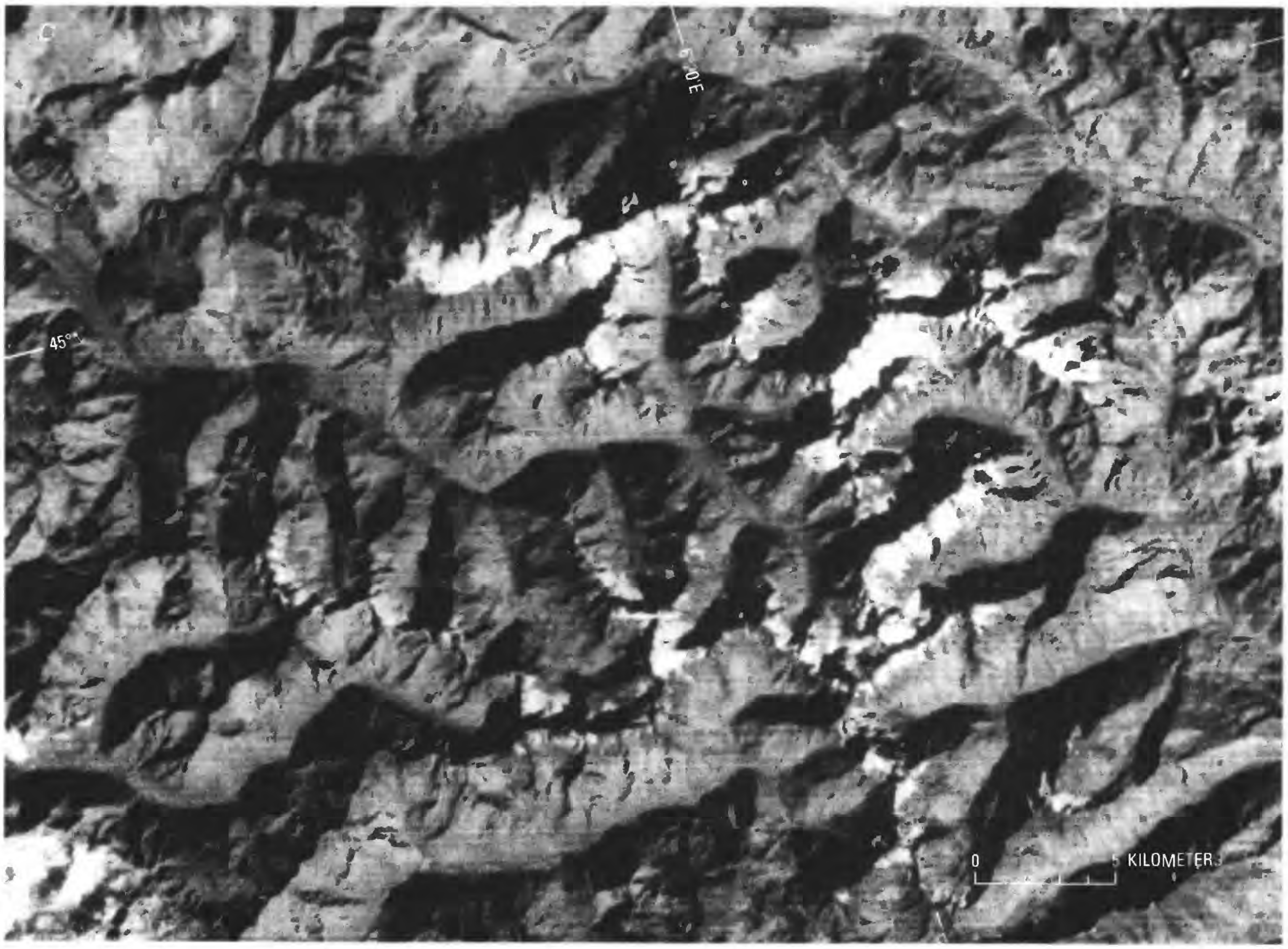
45°
0
5 KILOMETERS

advance of the Alpine glaciers were begun in the late 19th century. Annual measurements for slightly more than a century are now available for four large glaciers on the northern face of Mont Blanc (fig. 18). Three of these glaciers, Les Bossons, Glacier d'Argentière, and Mer de Glace, are in France, and one is in Switzerland, Trient Glacier. The four glaciers show similar fluctuations in length, with advances in 1890, 1920, and 1970 that alternate with recessions, including the period from 1940 to 1950, when there was a major retreat affecting all the glaciers in the Alps. Upon closer examination, these variations are not as close together as they first appear, because a time delay occurs between maxima on different glaciers. The starting dates of advance of the terminus during the three periods of expansion provide a more precise reference that can be plotted as shown in the lower part of figure 18. For each period, each of the glaciers has its own distinctive response time; Les Bossons reacts first, then Glacier d'Argentière and the Trient Glacier 4 to 7 years later, and the Mer de Glace is last, 11 to 15 years later.

Les Bossons is the only one whose terminus variation reflects small fluctuations which do not appear on longer glaciers (for example, the advances of Les Bossons in 1940) but which were also apparent on smaller glaciers in the French Alps. The length variations of the four Mont Blanc glaciers cannot therefore be taken to fully represent the fluctuation of the French Alpine glaciers, because the individual response time differs for each glacier. Nevertheless, the other glaciers do generally follow the fluctuations of Les Bossons, and even those of Glacier Blanc, the most southerly glacier studied in France.

What causes these fluctuations in glacier length? If the rate of nourishment is the cause, it is necessary to establish this regime for each glacier and learn how it operates over a complete massif.

Mass-Balance Measurements in the French Alps

At present, mass-balance measurements are being taken on nine glaciers in the French Alps (table 6). The only one of these glaciers for which direct measurements are being taken is Glacier de Sarennes on the Grandes Rousses massif, where mass-balance measurements were begun in 1948. This is the longest available series of mass-balance records in the Alps (those for the Aletschgletscher in Switzerland go back to 1923, but an indirect method is used, the hydrological method) and the second longest in all of Europe after the Swedish Storglaciären records, which were started in 1946 (see fig. 1 of "Glaciers of Sweden").

Glacier de Sarennes is a small cirque glacier that has an area of 0.87 km^2 that faces due south between 2,180 m and 3,300 m in altitude. It has been surveyed and photographed yearly since 1949 by the Centre d'Étude du Machinisme Agricole du Génie Rural des Eaux et Forêts (CEMAGREF)[5] in Grenoble (Valla, 1984), with accumulation and ablation recorded at five fixed points during every glaciological year (October to October) by the Ahlmann method.

At the northern end of the same massif (Grande Rousses) is Glacier de Saint-Sorlin, which has an area of 3 km^2. It faces north and extends from 2,650 m to 3,664 m, the altitude of the highest point of the massif. Mass-balance measurements conducted at 32 different points in the ablation zone since 1956 have been used to validate a linear statistical model (Lliboutry, 1974):

Figure 18.—Variation in length of four glaciers on the north side of Mont Blanc from 1870 to 1984. The lower portion of the figure plots the starting dates of advance of termini during three periods of expansion. ▶

[5] CEMAGREF is the French National Office of Waters and Forests. Photographic library established in 1975. The address is Domaine Universitaire, B.P. 76, 38402 St. Martin d'Hères Cedex, France.

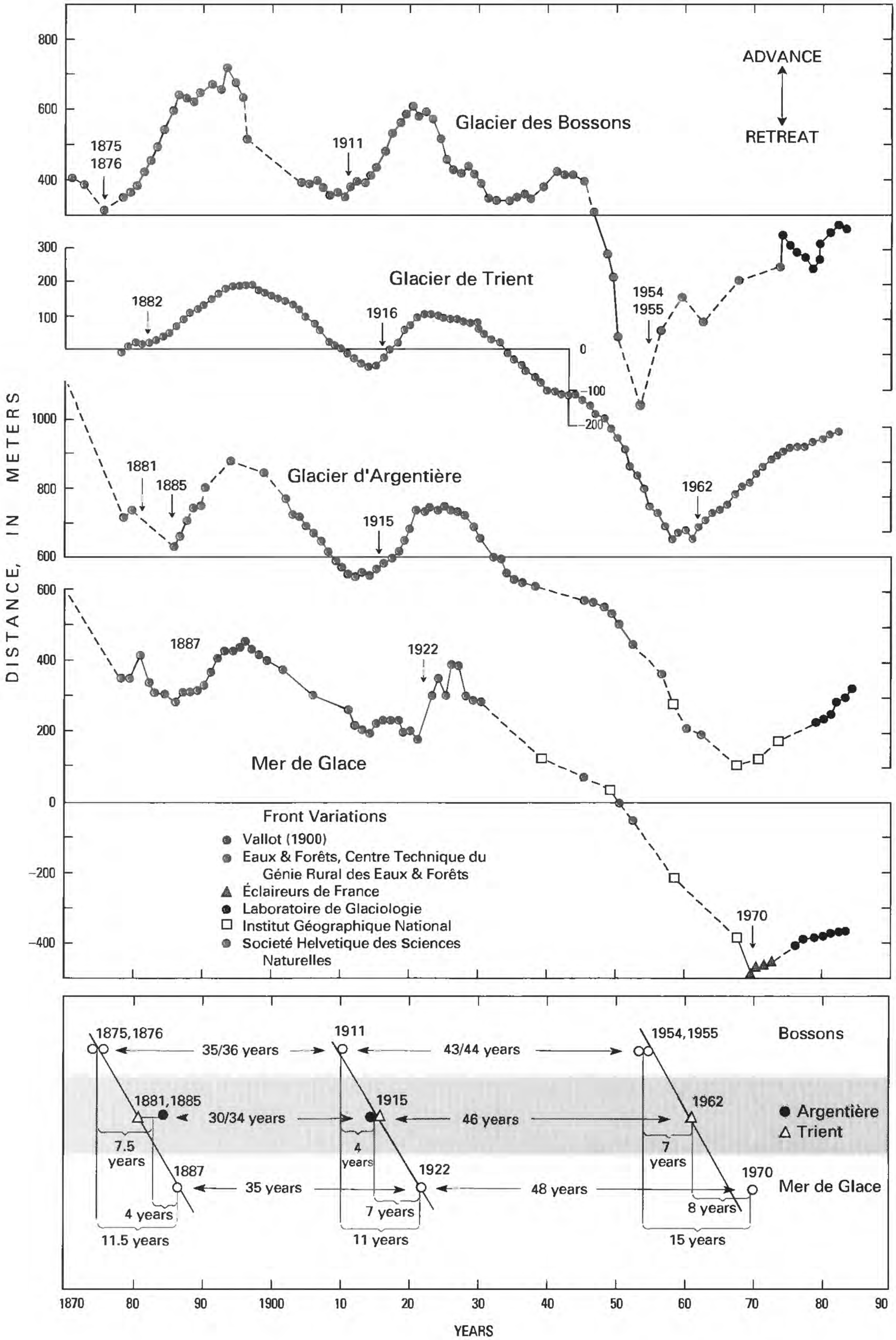

ADVANCE
RETREAT
Glacier des Bossons
Glacier de Trient
Glacier d'Argentière
Mer de Glace
DISTANCE, IN METERS
Front Variations
Vallot (1900)
Eaux & Forêts, Centre Technique du Génie Rural des Eaux & Forêts
Éclaireurs de France
Laboratoire de Glaciologie
Institut Géographique National
Societé Helvetique des Sciences Naturelles
1875, 1876
35/36 years
1911
43/44 years
1954, 1955
Bossons
1881, 1885
30/34 years
1915
46 years
1962
Argentière
Trient
7.5 years
4 years
7 years
1887
35 years
1922
48 years
1970
Mer de Glace
4 years
7 years
8 years
11.5 years
11 years
15 years
YEARS

TABLE 6.—*Mass-balance measurements on glaciers in the French Alps*

Alps	Massif	Glacier	Period of observation
Savoie	Mont Blanc	Glacier d'Argentière	1975–86
		Mer de Glace	1967–74, 1978–86
		Les Bossons	1975–76
Grées	Vanoise	Glacier de Gébroulaz	1907–50, 1978–86
Dauphiné	Grandes Rousses	Glacier de Saint-Sorlin	1956–86
		Glacier de Sarennes	1948–86
Dauphiné	Pelvoux	Glacier Blanc	1978–86
		Glacier Noir	1983–86
		Glacier d'Arsine	1969–70, 1985–86

$$b_{jt} = a_j + \mathrm{B}_t + \mathrm{E}_{jt}$$

where

b_{jt} is the mass balance measured at point j in year t,

a_j is a geographical parameter independent of the year,

B_t is a parameter linked to the year only, and not to the measurement point, and

E_{jt} is a centered random residue (20 cm of water for 16 years and 32 stakes).

This model has been extended to the whole glacier by Vallon and Leiva (1982) and tested on Glacier de Sarennes by using the 32 years of measurements, from 1949 to 1980 (Reynaud, 1983).

This linear statistical model of mass-balance variation has several advantages. First, it allows optimal processing of all the available data, in particular when series of measurements are incomplete (because stakes are missing or mass balance has not been measured for several consecutive years). Next, with this model, the annual mass-balance measurements can be limited to a few accessible ablation zones, without steep slopes, crevasses, or risk of avalanche, on which a dense network of stakes can be established and monitored yearly. This approach not only makes it easier to monitor a larger number of glaciers that are widely separate geographically (for example, Glacier de Gébroulaz in the Massif de la Vanoise and Glacier Blanc in the Massif du Pelvoux) but also enables mass-balance changes to be measured on large glaciers such as Glacier d'Argentière, Mer de Glace, and Les Bossons, which do not lend themselves very readily to conventional methods.

Lastly, the liner model has made it possible to obtain better objective knowledge of mass-balance variation in space and time on a glacier (Meier and Tangborn, 1965; Reynaud and others, 1986) and has made possible some studies of this variation near the equilibrium line (Hoinkes, 1970; Østrem, 1975). However, the relation obtained for mass balance versus altitude near the equilibrium line is only very roughly linear. The poor concordance is generally blamed on the altitude measurement, which is difficult to obtain. In fact, it must be acknowledged that the mass balance, too, is subject to much greater error than is usually admitted; the deviation from the linear model is 20 g/cm^2 averaged over 16 years for 32 stakes on the Glacier de Saint-Sorlin and 7 g/cm^2 averaged over 31 years for 5 stakes on the Glacier de Sarennes. These deviations should be attributed much more to the nature of the glacier surface than simply to measurement error. In other words, there is inevitable noise in this type of measurement, and our failure to recognize it still prevents us from determining the full significance of the fluctuations of glacier mass balances.

The comparison of mass balances of various alpine glaciers has shown that the linear-balance variation model, extended to a whole region, gives a good account of the balance fluctuations that were measured on 10 glaciers spread along the 500 km of the chain (Reynaud, 1980, 1983; Letréguilly, 1984).

The homogeneity of the balance fluctuations over a large area explains why the length variations seem to be caused by the same major factors in the nourishment. To enlarge the mass-balance series of Glacier de Sarennes, Martin (1978) did a reconstruction in which he used winter precipitations and summer temperatures from Lyon, 100 km from the glacier. This model of the balance fluctuations, which takes into account 77 percent of the variance for the survey period, gives a reconstruction of accumulated balance variations (B_t) since 1882 (fig. 19).

All the factors that are responsible for the advance around 1890 and 1920 can be found from this analysis, as well as the reason for the large recession beginning in 1940. The value of B_t during the period of 1940 to 1950 is generally 1 m of water less than the mean for the last century. In addition, during the last three decades, one can see some readvances around 1950 for the shorter glaciers and 1970 for the larger, although the accumulated balance variation only shows a steady state. This apparent balance is probably because of the reduced extent of the glaciers, for which a balance around the mean constitutes in fact an excess of nourishment. Therefore, the recent readvance of most of the alpine glaciers is caused by a return to conditions common from before 1940. In other words, the glacier is trying to regain the ground lost during the decade 1940 to 1950. Moreover, the less favorable weather pattern since 1977 should produce much larger advances in the near future.

Several additional long series of accumulated balance variations are needed to obtain a good understanding of glacier fluctuation and the climatic significance. Where ground observations in the past are lacking, one has to be satisfied with reconstructions such as those of the Glacier de Sarennes. Nevertheless, such reconstructions must be based on and confirmed by as many data as possible. Such work has been done on a section of the Glacier de Gébroulaz for the period between 1908 and 1950. The area selected is bounded by two cross profiles, where the velocities, levels, and thicknesses are known. Mass balances of this sector were computed by using the continuity equation (Reynaud and others, 1983, 1986). The values obtained in such a manner were compared to the Glacier de Sarennes reconstruction and to the hydrological values from the Aletschgletscher (fig. 20). These various series show a similar main

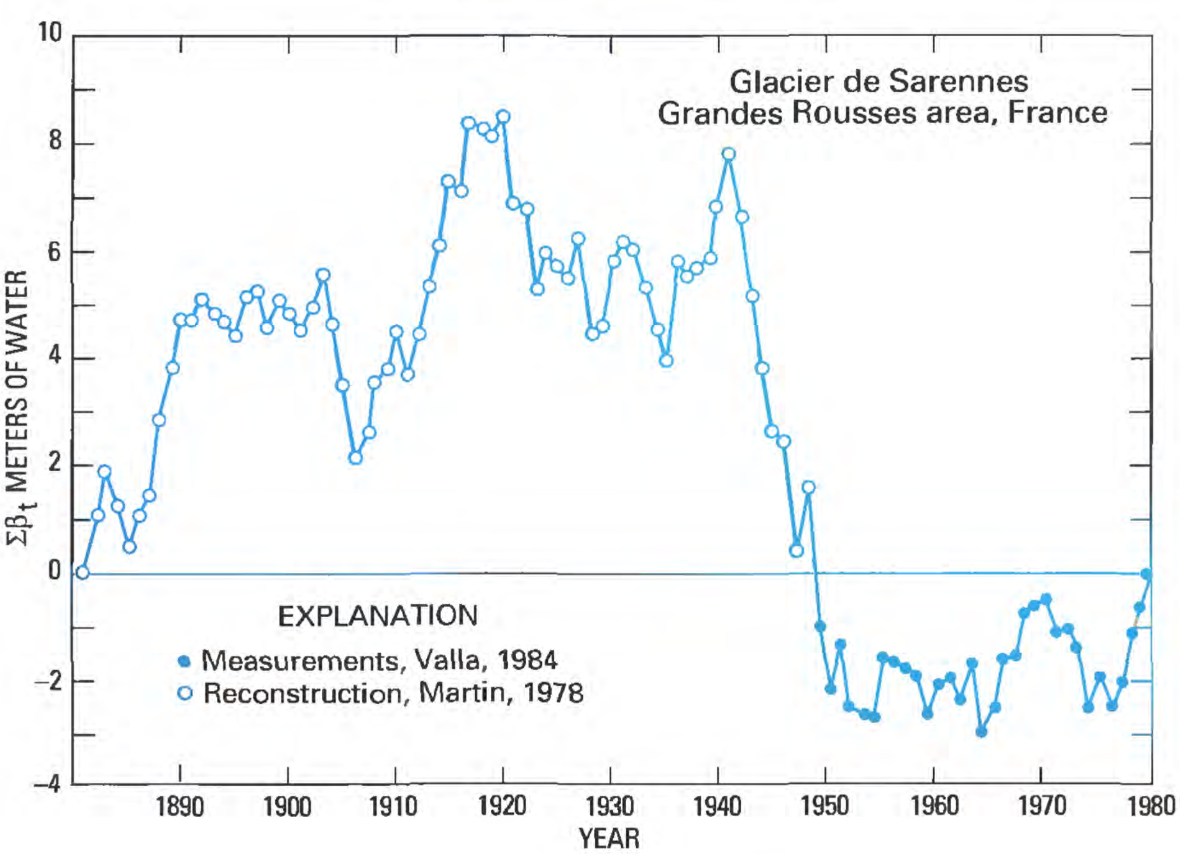

***Figure 19.**—Accumulated balance variations (B_t) versus time for Glacier de Sarennes. Ground measurements from Valla (1984); reconstruction of 1882 through 1948 from Martin (1978).*

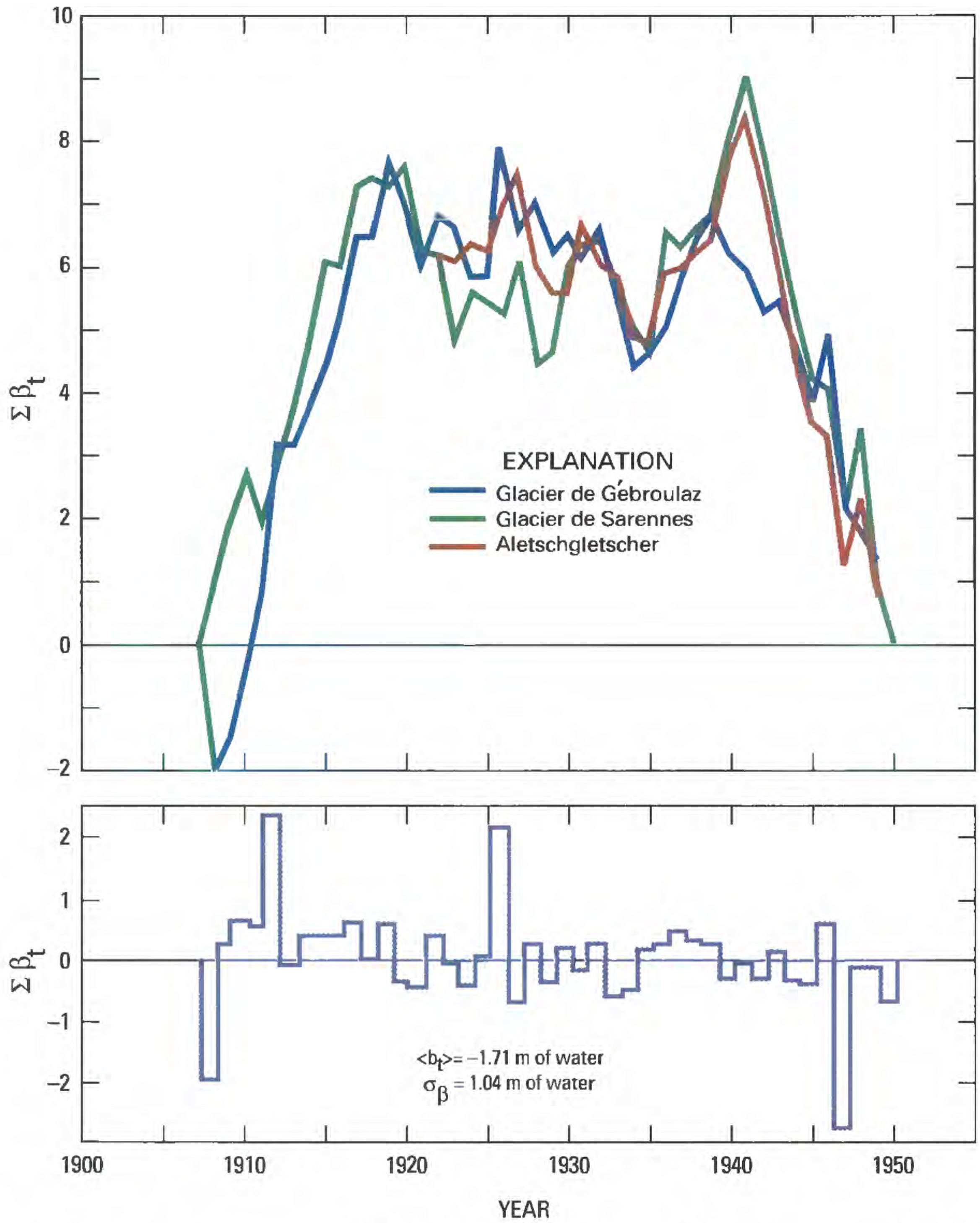

Figure 20.—Balance variations (B_t) versus time for Glacier de Gébroulaz from 1908 to 1950 and a comparison of the accumulated variations with the Glacier de Sarennes and Aletschgletscher (from Reynaud and others, 1986). Reproduced by courtesy of the International Glaciological Society from Journal of Glaciology, v. 32, no. 112, p. 452.

trend as well as accumulated balance variations of the same magnitude. This new way of computing mass balances gives us a means of producing a long series for several glaciers that have been surveyed repetitively on different cross profiles in the past, including a method of testing the accuracy of the reconstruction. In addition, it is a simpler alternative for mass-balance studies, because it only needs a survey of a sector of the glacier, when the bed topography is known.

The primary goal of glaciologists involved in glacier fluctuations is the establishment of an extended time series for many different glaciers in different geographic settings. The usual survey methods, such as direct ground measurements, require expensive equipment and are time consuming and labor intensive. For these reasons, there is great interest in the information that may be derived by indirect glaciological methods, such as aerial or satellite photogrammetry, and the kind of physical parameters that can be measured.

Aerial and Terrestrial Photogrammetric Surveys in Alpine Glaciological Studies

Aerial or terrestrial photogrammetry has been increasingly important during the past 30 years. As a result, a large set of aerial photographs is available for the Alpine glaciers. From these surveys, much glaciological information was derived and special analyses were done (Lliboutry and Reynaud, 1981; Vallon and Leiva, 1982). Aerial photogrammetry is very attractive, because it makes possible an instantaneous record of the shape of large surfaces. These data can be stored easily and retrieved for additional processing. Several national glacier services have changed their surveying methods following the recommendations of the first glacier mapping congress in Ottawa in 1965. Unfortunately, this method is very expensive, and, except for determination of area, the accuracy of conventional ground measurements is difficult to match. For example, it is well known that mass balances cannot be determined yearly by aerial photogrammetric methods but have to be spaced out in time, if we are to obtain relatively good precision on volumetric changes. In addition, successive annual aerial photogrammetric surveys do not give accurate surface velocities. Therefore, if the same financial support for glaciological studies were to be spent only on aerial surveys, there would result not only an information loss but also a hiatus in the extended time series of annual observation of glacier altitude, velocity, and mass-balance variation.

The same is true for satellite images, and, despite their real importance for regions not well mapped glaciologically, the images will not give any better information than aerial photogrammetry. One exception is where application of the linear variation of balance is used to relate the changes in elevation of the snowline to corresponding changes in glacier mass balance (Østrem, 1975). In this case the regional coverage by satellite images could be a significant advantage by allowing spatio-temporal distribution studies of mass balance over wide areas. In the French Alps, however, all but a few glaciers have such a small altitude range that they are entirely within the ablation zone or the accumulation zone, depending on the year.

In conclusion, regions like the French Alps are ill-suited to surveying by satellite sensors, because the glacierized areas are too fragmented and scattered (except in the Mont Blanc massif) and because they have been well studied by detailed ground and aerial methods (in situ measurement and regular aerial photography). However, satellite data may yet become useful for studying these types of glaciers as the quality of data recording and processing improves. In any event, such areas in the Alps are good testing areas for satellite glaciological surveys, because the results of indirect methods can be compared with data from the actual terrain.

References Cited

Bourrit, M.T., 1787, Nouvelle description des Alpes [A new description of the Alps]: Geneva, Chez Barde, Manget & Comp., 3 v., 838 p.

Hoinkes, H., 1970, Methoden und Möglichkeiten von Massenhaushatstudien auf Gletschern [Techniques and feasibility of mass-balance studies of glaciers]: Zeitschrift für Gletscherkunde und Glazialgeologie, v. 6, no. 1–2, p. 37–90.

Jouzel, J., and others, 1984, Chronologie d'un carottage de 20 m au col du Dome (Massif du Mt. Blanc) [Chronology of a core sample in the Col du Dome (Mt. Blanc area)]: La Houille Blanche, no. 6/7, p. 491–497.

Le Roy Ladurie, E., 1967, Histoire du climat depuis l'an Mil [History of the climate since the year 1000]: Paris, Flammarion, 381 p.

Letréguilly, A., 1984, Bilans de masse des Glaciers Alpins: Méthodes de mesures et repartition spatio-temporelle [Glacial mass balance of the Alpine glaciers: Methodology and spatio-temporal distribution]: unpublished Third Cycle thesis, University of Grenoble, September 1984.

Lliboutry, L., 1964, Traité de glaciologie [Treatise on glaciology], v. 1: Paris, Masson et Cie, 427 p.

———1965, Traité de glaciologie [Treatise on glaciology], v. 2: Paris, Masson et Cie, 611 p.

———1974, Multivariate statistical analysis of glacier annual balances: Journal of Glaciology, v. 13, no. 69, p. 371–392.

Lliboutry, L., and Reynaud, L., 1981, Global dynamics of a temperate valley glacier, Mer de Glace, and past velocities deduced from Forbes' bands: Journal of Glaciology, v. 27, no. 96, p. 207–226.

Martin, S., 1978, Analyse et reconstitution de la série de bilans annuels du glacier de Sarennes, sa relation avec les fluctuations du niveau de trois glaciers du massif du Mont-Blanc (Bossons, Argentière, Mer de Glace) [Analysis and reconstitution of the Sarennes Glacier annual mass balances, their relation to the altitude variations of three glaciers of the Mont Blanc massif (Bossons, Argentière, Mer de Glace)]: Zeitschrift für Gletscherkunde und Glazialgeologie, v. 13, no. 1–2, p. 127–153.

Meier, M.F., and Tangborn, W.V., 1965, Net budget and flow of South Cascade Glacier, Washington: Journal of Glaciology, v. 5, no. 41, p. 547–566.

Mougin, P., 1925, Études glaciologiques, tome 5 [Glaciological studies, v. 5]: Paris, Direction des Eaux et du Génie Rural, Imprimerie Nationale.

———1934, Études glaciologiques, tome 7 [Glaciological studies, v. 7]: Paris, Direction des Eaux et du Génie Rural, Imprimerie Nationale.

Østrem, G., 1975, ERTS data in glaciology—An effort to monitor glacier mass balance from satellite imagery: Journal of Glaciology, v. 15, no. 73, p. 403–415.

Reynaud, L., 1980, Can the linear balance model be extended to the whole Alps?, *in* World Glacier Inventory: International Association of Hydrological Sciences–Association International des Sciences Hydrologiques (IAHS–AISH) Publication No. 126, p. 273–284.

———1983, Recent fluctuations of Alpine glaciers and their meteorological causes: 1880–1980, *in* Street-Perrot, A., Beran, M., and Ratcliffe, R., eds., Variations in the global water budget: Dordrecht, D. Reidel Publishing Company, p. 197–205.

———1984, Mesures des fluctuations glaciaires dans les Alpes Françaises: Collecte des données et resultats [Measurements of glacial fluctuations in the French Alps: Collection of data and results]: La Houille Blanche, no. 6/7, p. 519–525.

Reynaud, L., Vallon, M., Carle, C., 1983, Analyse et synthèse des mesures glaciologiques effectuées sur le glacier de Gébroulaz, massif de la Vanoise [Analysis and synthesis of glaciological measurements made on the Gébroulaz Glacier, Vanoise massif]: Travaux scientifiques du Parc National de la Vanoise, v. 13, p. 9–29.

Reynaud, L., Vallon, M., and Letréguilly, A., 1986, Mass balance measurements: Problems and two new methods of determining variations: Journal of Glaciology, v. 32, no. 112, p. 446–454.

Valla, F., 1984, Bilan du Glacier de Sarennes: 1948–1983 [Glacial mass balance of Sarennes Glacier: 1948–1983]: La Houille Blanche, no. 6/7, p. 526–528.

Vallon, M., and Leiva, J.-C., 1982, Bilans de masse et fluctuations récentes du Glacier de Saint-Sorlin, Alpes Françaises [Mass balance and recent fluctuations of Saint-Sorlin Glacier, French Alps]: Zeitschrift für Gletscherkunde und Glazialgeologie, v. 17, no. 1–2, p. 143–167.

Vallot, J., 1900, Annales de l'Observatoire météorologique du Mont-Blanc, IV [Annals of the meteorological observatory of Mont-Blanc, IV]: Paris, Steinheil.

Vivian, R., 1975, Les glaciers des Alpes Occidentales [The glaciers of the Western Alps]: Grenoble, Allier, 513 p.

The Italian Alps

By Rossana Serandrei Barbero[6] *and* Giorgio Zanon[7]

Abstract

Research carried out by Italian glaciologists in support of the World Glacier Inventory project identified approximately 1,400 glaciers in the mountain groups of the Italian Alps. The total surface area of all glaciers, glacierets, and permanent snow fields in Italy with an area ≥5 hectares (~0.05 square kilometers) is 608 square kilometers. An earlier inventory of Italian glaciers, which was published in four volumes by the Comitato Glaciologico Italiano of the Consiglio Nazionale delle Ricerche showed a total glacier area of about 540 square kilometers, but this earlier inventory did not include glacierets and snow fields. Italian glaciers are primarily of the mountain type, especially the cirque variety, but alpine-type valley glaciers are frequent, and Scandinavian-type ice fields are also present. Scientific research on the glaciers of Italy began during the first quarter of the 20th century and included four efforts to accurately document the number and areal distribution of Italian glaciers. The most comprehensive was the work completed for the World Glacier Inventory project. The use of Landsat images to delineate glaciers and monitor their fluctuations in the Italian Alps has been limited because of the spatial resolution of the Landsat multispectral scanner sensor and the shadowing of glaciers in the high-relief Alps caused by the solar azimuth and elevation of the Landsat orbit. Nevertheless, digital image processing and enhancement techniques have been successful in the development of an operational tool for monitoring individual glaciers and variation in snow cover. This development is important for calibration of snowmelt models needed for runoff estimates in the production of hydroelectric power in small basins.

Introduction

The southern flank of the Alpine chain is generally subdivided by Italian geographers into the Western, Central, and Eastern Alps. Other scientists, especially those from regions encompassing the northern part of the Alps, only subdivide them into the Western and Eastern Alps. However, because of the arcuate east to west orientation of the Alps (fig. 21), this subdivision does not affect the distinctive features of its glaciers. It is the location of glaciers within or peripheral to the Alpine chain that is essential because of the strong relationship of glacier size and position to the source and propagation of masses of humid maritime air.

The maximum altitude of the firnline is, as a result, lower on the more external and humid massifs such as the Alpi Dolomitiche (Dolomites) and, to an even greater extent, the Alpi Carniche and Alpi Giulie, where it reaches its lowest altitudes in the Italian part of the Alpine chain. The firnline definitely rises in the more interior, drier mountain groups such as the Alpi Venoste, where the internal location is often accompanied by deep longitudinal valleys, frequent katabatic winds (fohn), and a continental-type precipitation regime, characterized by a winter minimum.

Location and Distribution

For the obvious reasons of general exposure and orography, the southern flank of the Alps has far fewer glaciers than the northern flank. The Monte Bianco and Bernina massifs and the Alpi Pennine and Alpi

[6] National Research Council (CNR), Institute for the Study of the Dynamics of Large Masses, S. Polo 1364, 30125 Venice, Italy.

[7] Department of Geography, University of Padua, Via del Santo 26, 35100 Padua, Italy.

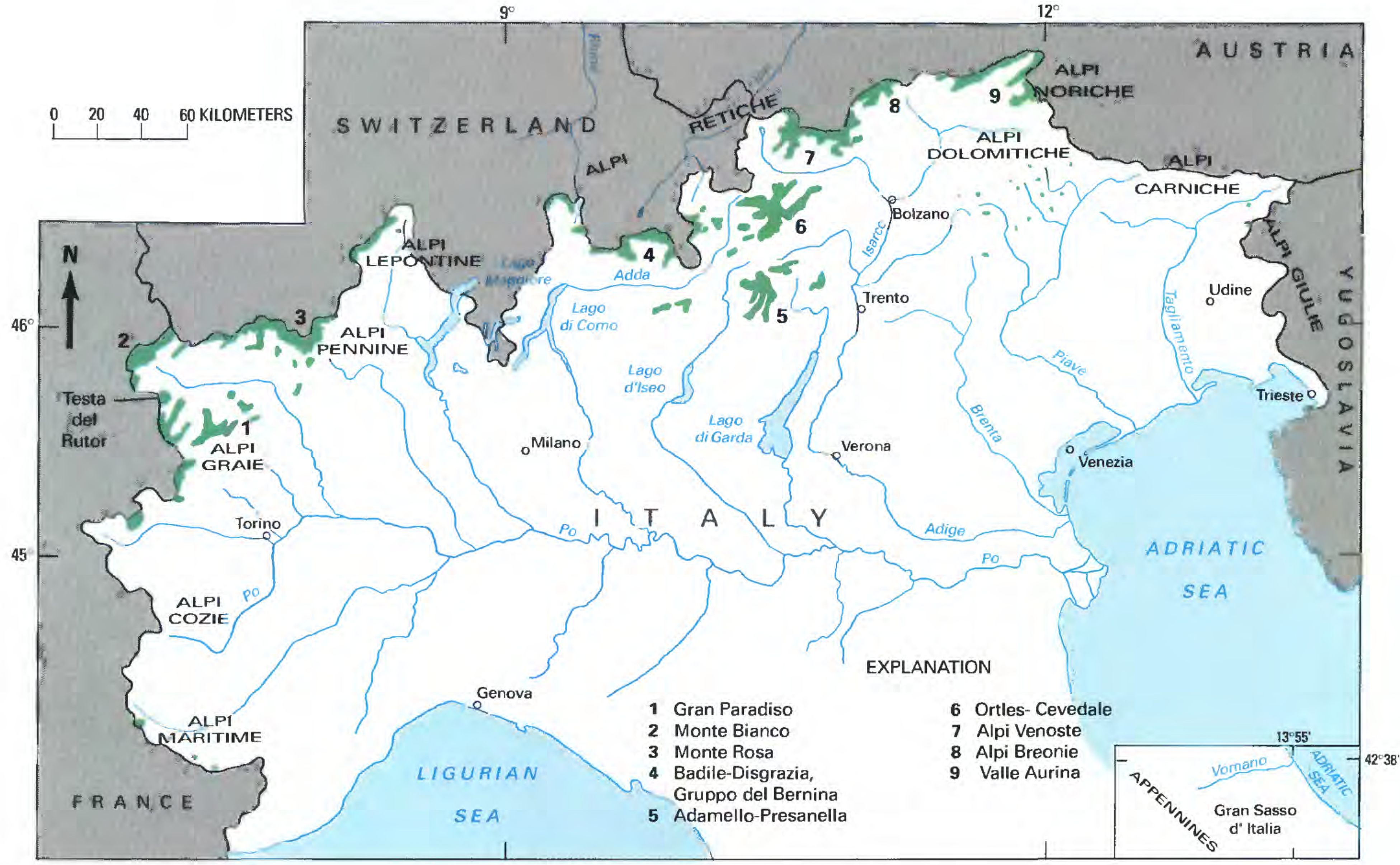

Figure 21.—The main glacierized mountain areas in the Italian Alps.

Venoste demonstrate this point. However, several mountains and ranges show important concentrations of glaciers, such as the Ortles-Cevedale, in the Alpi Retiche, which, according to the "Catasto dei Ghiacciai Italiani" of the Consiglio Nazionale delle Ricerche (1959; 1961a,b; 1962), includes 113 glaciers that have a total surface area of 105 km^2, and the Adamello-Presanella area, again in the Alpi Retiche, which has 89 glaciers covering 53 km^2.

The range of morphological types of the Italian glaciers is great, although mountain glaciers (especially cirque glaciers) predominate. Numerous alpine-type valley glaciers also are present, and they include some of the largest glaciers in the country. However, rather unusual types may be found, such as the Scandinavian-type ice field, which is found in the central part of the Gruppo del Adamello. The ice field is an almost flat plateau (Pian di Neve) from which outlet glaciers extend. On Monte Bianco, the great Ghiacciaio del Miage (Miage Glacier) has no real accumulation basin; rather, it is fed to a great extent by avalanches (Zanon 1980, 1985). Its tongue, about 10 km long, shows remarkable similarities to the avalanche glaciers of central Asia. Table 7 lists the largest glaciers in Italy.

Porro (1925) was the first scientist to make a systematic identification of the Italian glaciers. Two years later Porro and Labus (1927) prepared a 1:500,000-scale compilation that listed 774 glaciers. As a result of the International Geophysical Year research, the Consiglio Nazionale delle Ricerche (1959; 1961a,b; 1962) published a four-volume inventory of the glaciers of Italy ("Catasto dei Ghiacciai Italiani"). The inventory identified, plotted on 1:25,000-scale maps, and described 838 glaciers then existing in Italy and 190 others that had disappeared during the previous 50 years. Glacier distribution by region was as follows: Piedmont (and Valle d'Aosta), 322; Lombardy, 185; Tre Venezie, 330. Of these totals, 534 glaciers belonged to the Po basin, 255 to the Adige basin, and 48 to other basins. It should be noted that the isolated Ghiacciaio di Calderone, not included in the above categories, the southernmost glacier in Europe, lies in the Apennines (Gran Sasso d'Italia) of central Italy(fig. 21).

Between 1980 and 1986, Italian collaboration on the World Glacier Inventory project was concluded with the identification of 1,397 glaciers distributed as follows: Piedmont (and Valle d'Aosta), 531; Lombardy, 305; and Tre Venezie, 560. The total surface area of these glaciers is 608 km^2. The large difference in the number of glaciers between the two inventories is almost exclusively because the new World Glacier Inventory requires a listing of all permanent snow fields and glacierets in Italy having areas greater than 5 ha. Most of these small snow fields and glacierets were not included in the old "Catasto dei Ghiacciai Italiani." A revision and updating of the "Catasto dei Ghiacciai Italiani" is expected during the next few years, and the new data collected for the World Glacier Inventory project will be used.

TABLE 7.—*The largest glaciers in the Italian Alps (unpublished data from the World Glacier Inventory)*

[See figure 21 for locations of mountain groups]

Glacier	Mountain or range	Area (km^2)	Maximum length (km)	Elevation of termini (m above mean sea level)
Forni	Ortles-Cevedale	13.20	5.50	2,350
Miage	Monte Bianco	13.02	10.35	1,720
Mandrone	Adamello-Presanella	12.38	5.38	2,450
Lys	Monte Rosa	11.80	5.60	2,350
Rutor	Testa del Rutor	9.54	4.80	2,504
Malavalle	Breonie	9.42	4.40	2,460
Brenva	Monte Bianco	8.06	7.64	1,415

Italian Glaciological Research

Glaciology is a relatively recent science in Italy (Nangeroni, 1964). It was only at the beginning of this century that it found its scientific niche. Glaciology was mainly directed at an evaluation of glacial water reserves, with a view to their possible use for production of hydroelectric energy. The founding in 1914 of the Comitato Glaciologico Italiano (CGI) (still in existence with a head office in Turin) provided general coordination and great stimulus to glaciological research, which was aimed not only at descriptive geography but also at the gathering of information from geophysical, hydrological, geomorphological, and topographic viewpoints. A comprehensive bibliography of the Italian glaciers is included in the first volume of "Catasto dei Ghiacciai Italiani" (Consiglio Nazionale delle Ricerche, 1959).

Ever since its founding, one of the main activities of the CGI has been the monitoring of glacier variation by means of systematic field observations on representative glaciers. This activity began on a regular basis around 1925 and coincided with a renewed though moderate advance of the Italian glaciers after the end of the so-called "Little Ice Age" that had affected the Alpine region for more than 300 years. A very long retreat phase began a few years later and lasted uninterruptedly until the 1960's. Further advance then began for the Italian glaciers, too, and has recently become more pronounced.

Italian glacier variations were published in the "Bollettino del Comitato Glaciologico Italiano" until 1977; after 1977 publication continued in

"Geografia Fisica e Dinamica Quaternaria" (published in Turin by the CGI). On an international scale, data on Italian glaciers appeared in the various Reports of the Commission on Snow and Ice, International Association of Hydrological Sciences–International Union of Geodesy and Geophysics (IAHS–IUGG). Variations from 1959 to 1965 were edited by P. Kasser (1967) in the first of a series of volumes sponsored by the International Association of Hydrological Sciences and the United Nations Educational, Scientific, and Cultural Organization (UNESCO) entitled "Fluctuations of Glaciers," a continuation of the earlier international Reports of the Commission on Snow and Ice. Since 1967, with the creation of the Permanent Service on the Fluctuations of Glaciers (now the World Glacier Monitoring Service), Italian glacier variations have been reported in "Fluctuations of Glaciers" 1965–70 (Kasser, 1973); 1970–75 (Müller, 1977); 1975–80 (Haeberli, 1985); and 1980–85 (Haeberli and Müller, 1988). These publications also include the results of surveys on the mass balance of the Ghiacciaio di Marmolada (Alpi Dolomitiche) for 1964–65 and 1965–66, and of the Ghiacciaio di Caresèr (Ortles-Cevedale) from 1966–67 to 1984–85.

The Italian glaciers are shown on the official maps of the Istituto Geografico Militare (IGMI) at 1:25,000, 1:100,000, and, more recently, 1:50,000 scales, which are derived from the 1:25,000-scale maps. The cartography at the 1:25,000 and 1:50,000 scales, done from aerial photogrammetric surveys carried out during the early 1960's, is of good quality, but the mapping does not yet cover the entire region of the Italian Alps. During the past few years, technical regional maps also have been published at scales of 1:10,000 and 1:5,000; both map scales were produced from aerial photogrammetric surveys. However, they are still not used extensively, and glacier margins are sometimes not well defined because of less than optimum conditions at the time the flights were carried out. For some glaciers of particular research interest, special very large-scale terrestrial and aerial photogrammetric surveys were carried out over a period of many years. Examples of products from these surveys are the glacier maps of the Ghiacciai di Lys, Forni, Miage, Belvedere (Gruppo del Monte Rosa), and Pian di Neve, and the series of surveys carried out on the Ghiacciai di Caresèr and Marmolada (table 8).

TABLE 8.—*Examples of large-scale maps of Italian glaciers published by the Consiglio Nazionale delle Ricerche, Comitato Glaciologico Italiano, Turin*

Glacier name	Map scale	Year published
Lys	1:10,000	1925
Forni	1:5,000	1953
Miage	1:5,000	1957
Belvedere	1:5,000	1957
Pian di Neve	1:5,000	1959
Marmolada	1:5,000	1951
Marmolada	1:5,000	1966
Caresèr	1:8,333	1933
Caresèr	1:5,000	1967
Caresèr	1:5,000	1970
Caresèr	1:5,000	1980

534 glaciers belonged to the Po basin, 255 to the Adige basin, and 48 to other basins. It should be noted that the isolated Ghiacciaio di Calderone, not included in the above categories, the southernmost glacier in Europe, lies in the Apennines (Gran Sasso d'Italia) of central Italy(fig. 21).

Between 1980 and 1986, Italian collaboration on the World Glacier Inventory project was concluded with the identification of 1,397 glaciers distributed as follows: Piedmont (and Valle d'Aosta), 531; Lombardy, 305; and Tre Venezie, 560. The total surface area of these glaciers is 608 km^2. The large difference in the number of glaciers between the two inventories is almost exclusively because the new World Glacier Inventory requires a listing of all permanent snow fields and glacierets in Italy having areas greater than 5 ha. Most of these small snow fields and glacierets were not included in the old "Catasto dei Ghiacciai Italiani." A revision and updating of the "Catasto dei Ghiacciai Italiani" is expected during the next few years, and the new data collected for the World Glacier Inventory project will be used.

TABLE 7.—*The largest glaciers in the Italian Alps (unpublished data from the World Glacier Inventory)*

[See figure 21 for locations of mountain groups]

Glacier	Mountain or range	Area (km^2)	Maximum length (km)	Elevation of termini (m above mean sea level)
Forni	Ortles-Cevedale	13.20	5.50	2,350
Miage	Monte Bianco	13.02	10.35	1,720
Mandrone	Adamello-Presanella	12.38	5.38	2,450
Lys	Monte Rosa	11.80	5.60	2,350
Rutor	Testa del Rutor	9.54	4.80	2,504
Malavalle	Breonie	9.42	4.40	2,460
Brenva	Monte Bianco	8.06	7.64	1,415

Italian Glaciological Research

Glaciology is a relatively recent science in Italy (Nangeroni, 1964). It was only at the beginning of this century that it found its scientific niche. Glaciology was mainly directed at an evaluation of glacial water reserves, with a view to their possible use for production of hydroelectric energy. The founding in 1914 of the Comitato Glaciologico Italiano (CGI) (still in existence with a head office in Turin) provided general coordination and great stimulus to glaciological research, which was aimed not only at descriptive geography but also at the gathering of information from geophysical, hydrological, geomorphological, and topographic viewpoints. A comprehensive bibliography of the Italian glaciers is included in the first volume of "Catasto dei Ghiacciai Italiani" (Consiglio Nazionale delle Ricerche, 1959).

Ever since its founding, one of the main activities of the CGI has been the monitoring of glacier variation by means of systematic field observations on representative glaciers. This activity began on a regular basis around 1925 and coincided with a renewed though moderate advance of the Italian glaciers after the end of the so-called "Little Ice Age" that had affected the Alpine region for more than 300 years. A very long retreat phase began a few years later and lasted uninterruptedly until the 1960's. Further advance then began for the Italian glaciers, too, and has recently become more pronounced.

Italian glacier variations were published in the "Bollettino del Comitato Glaciologico Italiano" until 1977; after 1977 publication continued in

"Geografia Fisica e Dinamica Quaternaria" (published in Turin by the CGI). On an international scale, data on Italian glaciers appeared in the various Reports of the Commission on Snow and Ice, International Association of Hydrological Sciences–International Union of Geodesy and Geophysics (IAHS–IUGG). Variations from 1959 to 1965 were edited by P. Kasser (1967) in the first of a series of volumes sponsored by the International Association of Hydrological Sciences and the United Nations Educational, Scientific, and Cultural Organization (UNESCO) entitled "Fluctuations of Glaciers," a continuation of the earlier international Reports of the Commission on Snow and Ice. Since 1967, with the creation of the Permanent Service on the Fluctuations of Glaciers (now the World Glacier Monitoring Service), Italian glacier variations have been reported in "Fluctuations of Glaciers" 1965–70 (Kasser, 1973); 1970–75 (Müller, 1977); 1975–80 (Haeberli, 1985); and 1980–85 (Haeberli and Müller, 1988). These publications also include the results of surveys on the mass balance of the Ghiacciaio di Marmolada (Alpi Dolomitiche) for 1964–65 and 1965–66, and of the Ghiacciaio di Caresèr (Ortles-Cevedale) from 1966–67 to 1984–85.

The Italian glaciers are shown on the official maps of the Istituto Geografico Militare (IGMI) at 1:25,000, 1:100,000, and, more recently, 1:50,000 scales, which are derived from the 1:25,000-scale maps. The cartography at the 1:25,000 and 1:50,000 scales, done from aerial photogrammetric surveys carried out during the early 1960's, is of good quality, but the mapping does not yet cover the entire region of the Italian Alps. During the past few years, technical regional maps also have been published at scales of 1:10,000 and 1:5,000; both map scales were produced from aerial photogrammetric surveys. However, they are still not used extensively, and glacier margins are sometimes not well defined because of less than optimum conditions at the time the flights were carried out. For some glaciers of particular research interest, special very large-scale terrestrial and aerial photogrammetric surveys were carried out over a period of many years. Examples of products from these surveys are the glacier maps of the Ghiacciai di Lys, Forni, Miage, Belvedere (Gruppo del Monte Rosa), and Pian di Neve, and the series of surveys carried out on the Ghiacciai di Caresèr and Marmolada (table 8).

TABLE 8.—*Examples of large-scale maps of Italian glaciers published by the Consiglio Nazionale delle Ricerche, Comitato Glaciologico Italiano, Turin*

Glacier name	Map scale	Year published
Lys	1:10,000	1925
Forni	1:5,000	1953
Miage	1:5,000	1957
Belvedere	1:5,000	1957
Pian di Neve	1:5,000	1959
Marmolada	1:5,000	1951
Marmolada	1:5,000	1966
Caresèr	1:8,333	1933
Caresèr	1:5,000	1967
Caresèr	1:5,000	1970
Caresèr	1:5,000	1980

Glacier Surveys by Satellite Remote Sensing

Table 1 and figure 2 list the optimum Landsat 1, 2, and 3 images of the Alps and show their area of coverage. To cover the entire Italian section of the Alps, eight Landsat MSS images are required. Several images that show a part of the Alps are discussed in this section. A Landsat 2 MSS image (fig. 22) (21333–09210, band 6; 16 September 1978; Path 210, Row 28) shows part of the Western Alps, including, among the principal Italian mountain groups, Monte Bianco (A) and Monte Rosa (B). A Landsat 1 MSS false-color composite image (1021–09383; 13 August 1972; Path 208, Row 28) shows part of the Central Alps, the Alpi Retiche. The Badile-Disgrazia (A), Ortles-Cevedale (B), and Adamello-Presanella (C) areas are indicated (fig. 23). Observations by satellite remote sensing were carried out on the first group (Della Ventura and others, 1982, 1983). Mass-balance studies were completed on the second group (Zanon, 1982). A Landsat 1 MSS image (band 7; 26 October 1975; Path 207, Row 28) shows the Eastern Alps between the Alpi Venoste and the Alpi Carniche (fig. 24). In each of the illustrations, some of the glacier

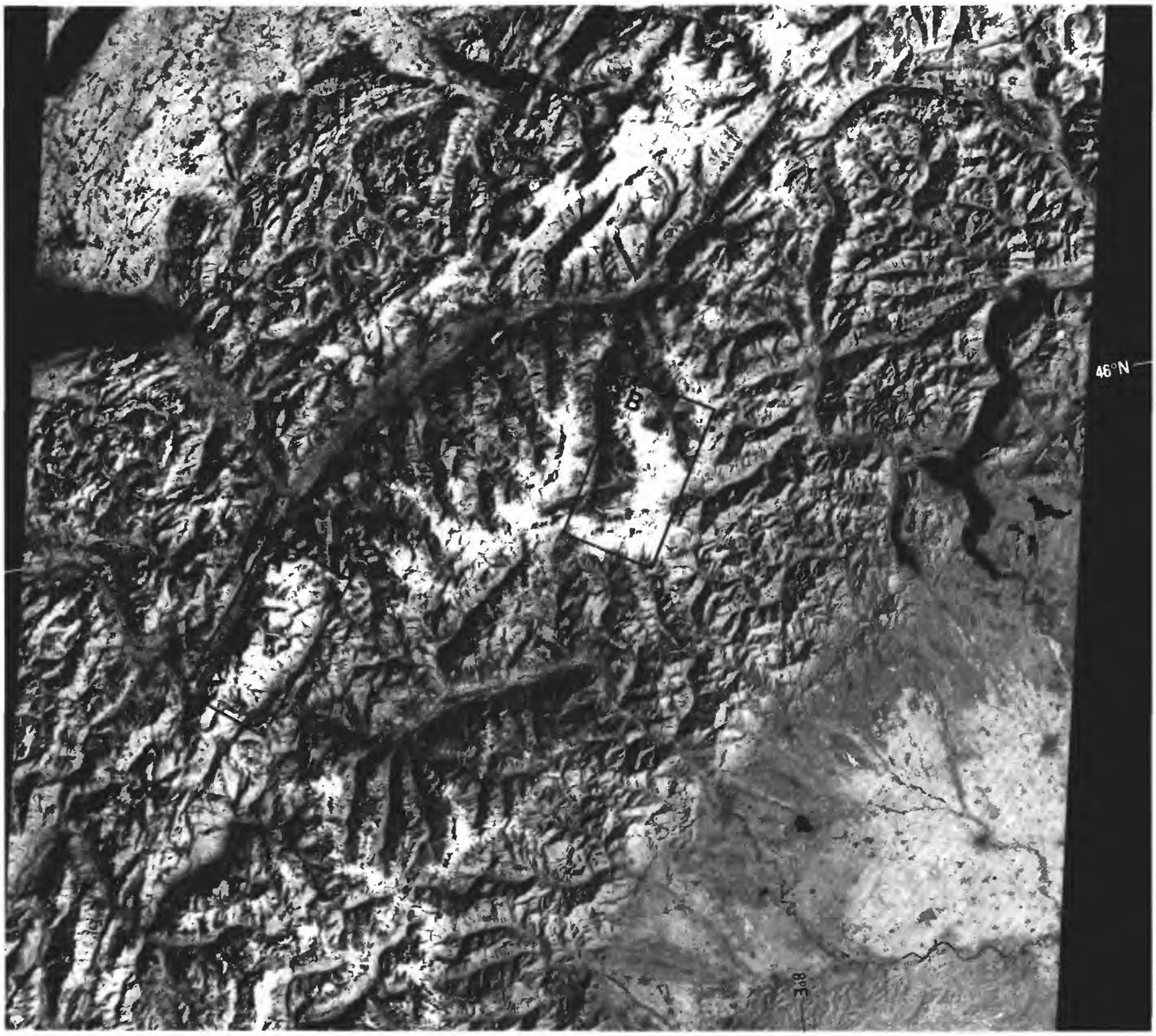

__Figure 22.__—Landsat 2 MSS image (21333–09210, band 6; 16 September 1978; Path 210, Row 28) showing part of the Monte Bianco (A) and the Monte Rosa (B) mountain groups. Landsat image courtesy of the Swiss Federal Institute of Technology, Zürich. The scale is approximately 1:1,000,000.

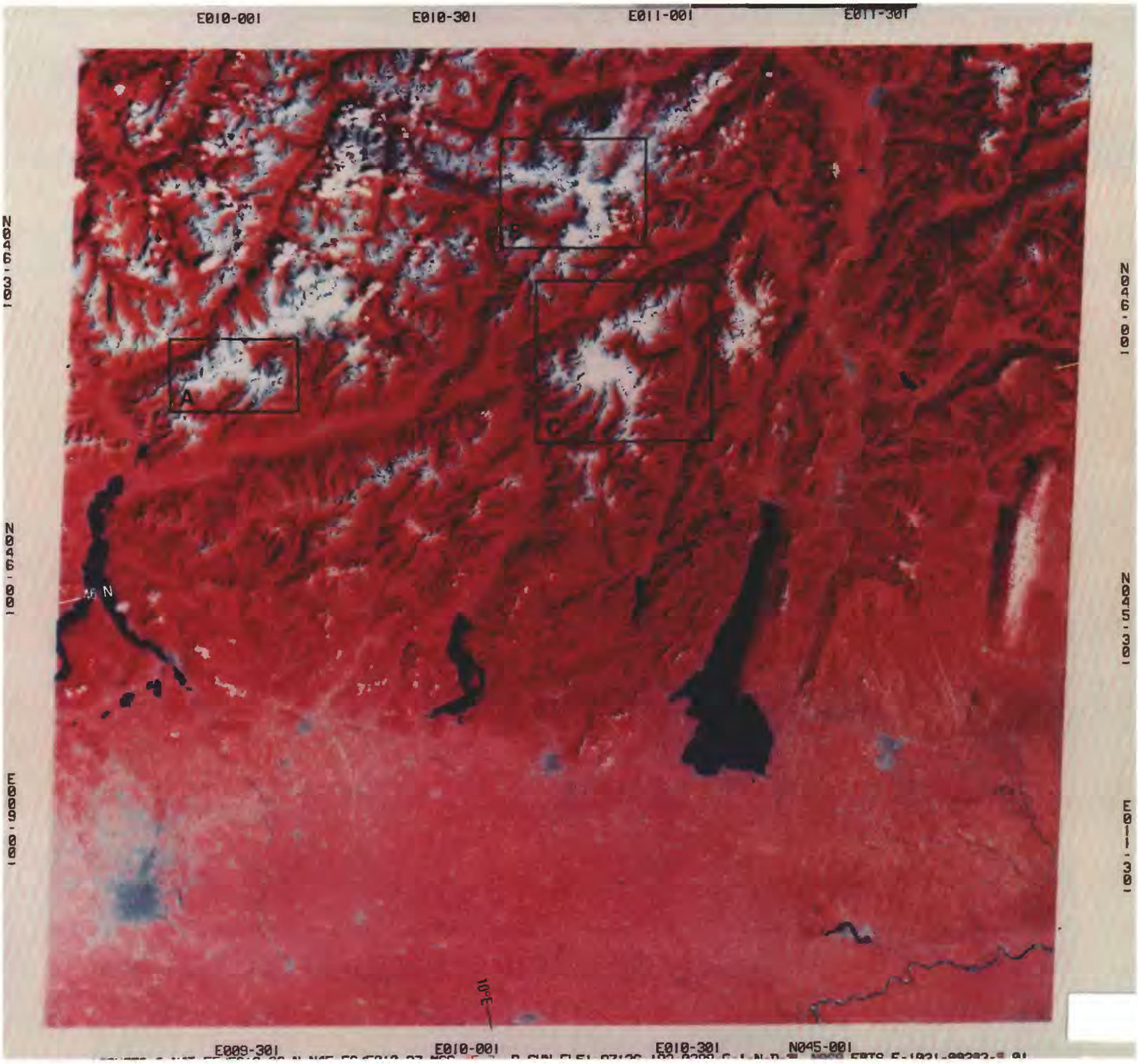

Figure 23.—Landsat 1 MSS false-color composite image (1021–09383; 13 August 1972; Path 208, Row 28) showing part of the central Italian Alps. The Badile-Disgrazia (A), Ortles-Cevedale (B), and Adamello-Presanella (C) mountain groups are shown. Landsat image from the EROS Data Center, U.S. Geological Survey, Sioux Falls, S. Dak. The scale is approximately 1:1,000,000.

features are partially obscured by clouds, snow cover, or shadows, but many of the glacier features can be seen clearly.

The high frequency and areal extent of coverage of the Alps by Landsat images, which have been acquired of the region since 1972, suggested that, despite the many factors (for example, clouds and snow cover) that decrease the number of usable images, repeated measurements of significant glaciological parameters could be made if coupled with traditional field measurements made in the Italian Alps at a few of the glaciers. At the end of the summer the total area of a glacier could be measured; the data would be useful for subsequent areal comparisons and for evaluating the extent of annual surface variations. Measurement of the area of residual snow cover on the glacier at the end of the melt season, could, with the total area of the glacier, produce an estimated Accumulation Area Ratio (AAR) computation.

Figure 24.—Landsat 1 MSS image (band 7; 26 October 1975; Path 207, Row 28) showing the eastern Italian Alps between the Alpi Venoste and the Alpi Carniche. Landsat image from the European Space Agency, Frascati, Italy. The scale is approximately 1:1,000,000.

Although visible and near-infrared satellite image data had been used frequently to carry out glaciological studies of large glaciers at high latitudes, and it was established that AAR could be computed from Landsat MSS images on a glacier with an area less than 10 km^2 (Salomonson, 1983), the question arose as to whether satellite remote sensing was applicable to glacier dimensions in the Italian Alps, where glacier areas less than 1 km^2 are common. Therefore, simple representative models were examined to see if the spatial resolution of Landsat MSS images of the Alps was sufficient to trace the dynamics of the Italian Alpine glaciers. Calculation of the variations in surface area of selected glaciers could then be correlated with fluctuations of their termini (Rabagliati and Serandrei Barbero, 1979). In spite of the small size of the glaciers, calculations of variation in surface area were, in the majority of the cases, able to be determined with the Landsat spatial resolution.

Following a systematic approach (Della Ventura and others, 1981), Della Ventura and others (1983) performed the first extensive glacier survey on Monte Disgrazia. The glaciers investigated, whose surface areas ranged between 0.2 and 2.5 km^2 (Consiglio Nazionale delle Ricerche, 1961b), lie in different orientations around Monte Disgrazia, about 100 km north-northeast of Milan, within the drainage system of the Adda, a tributary of the Po.

Landsat MSS images acquired on 13 September 1975 (20234–09320; Path 209, Row 28), 28 August 1978 (21314–09142; Path 209, Row 28), and 4 September 1980 (Path 209, Row 28) were digitally processed through four steps: preprocessing, classification of glacier surfaces, classification of morphological features, and registration. An analysis of the four Landsat MSS bands showed, in accordance with the observations made on the Ghiacciaio di Marmolada in the Alpi Dolomitiche by Pagliari and Zandonella (1982), that MSS band 5 contains the best information about the areal extent of glaciers and that MSS band 7 is optimum for delineating morphological characteristics of the glacier surface (glacier ice, snow, shadowed areas, rocky outcrops, crevasses).

The areal extent of several glaciers, which was obtained through digital image analysis of Landsat MSS images, is shown in table 9. The digital image analysis showed good agreement with traditional field measurements, but the research carried out by Della Ventura and others (1982) determined that the shadow effect caused by the time of the Landsat passage over the Alps at about 0930 hours Greenwich Mean Time caused uncertainty in the identification and analysis of Alpine glaciers that are oriented to the north and northwest. The shadow effect results from the solar azimuth and angle above the horizon in late summer, about 136° and 50°, respectively.

TABLE 9.—*Total surface area and snow-covered surface area of selected glaciers as derived from Landsat MSS images acquired on 13 September 1975 (20234–09320; Path 209, Row 28), 28 August 1978 (21314–09142; Path 209, Row 28), and 4 September 1980 (Path 209, Row 28)*

[From Della Ventura and others, 1983]

Glacier number[1]	Glacier name	Total surface area (km^2)			Variation in area	Snow-covered surface area (km^2)			Variation in area
		1975	1978	1980	1975–80	1975	1978	1980	1975–80
408	Predarossa	1.081	0.985	1.052	−0.029	0.772	0.857	0.881	+0.109
409	Corna Rossa	.046	.051	.036	−.010	.036	.046	.026	−.010
410	Cassandra Occidentale	.293	.313	.368	+.075	.233	.288	.313	+.080
411	Cassandra Orientale	.492	.616	.641	+.149	.444	.563	.588	+.144
416	Ventina	1.854	1.940	2.024	+.170	1.384	1.267	1.097	−.287
417	Canalone della Vergine	.470	.515	.566	+.096	.243	.263	.268	+.025
419	Disgrazia	2.438	2.732	2.890	+.452	1.562	1.380	1.431	−.313
				Total	+.903			Total	−.070

[1] Number assigned to each glacier in the "Catasto dei Ghiacciai Italiani" (Consiglio Nazionale delle Ricerche, 1959; 1961a,b; 1962).

The second area analyzed included the Valle Aurina glaciers (Alpi Noriche); they were specially selected to be representative of glaciers oriented to the northwest on Landsat MSS images. They have areas that range from 0.06 to 1.69 km^2 (Provincia Autonoma di Bolzano, 1983) and lie within the drainage system of the Isarco, a tributary of the Adige. The problem with their delineation on Landsat images was confronted during fieldwork in 1979, 1981, and 1983 (Della Ventura and others, 1987a). Radiance measurements made on the ground at the time of the Landsat satellite overpasses gave indications that led to using MSS band 6 combined with MSS band 5 to differentiate glaciers situated on shadowed slopes from the surrounding land.

Figure 25 is a digitally processed Landsat image that makes three classifications: other, doubtful, and ice/snow. Glaciers can be delineated in this Landsat MSS image (2 September 1980; Path 207, Row 27) as the first step in an interpretation procedure that uses the product of MSS bands 5 and 6. Figure 26 shows how the four separate MSS bands are unable, on the shaded slope, to clearly distinguish glacier ice from the surrounding area. Two other Landsat MSS images were also digitally processed (6 September 1981; Path 207, Row 27; 40389–09272; and 9 August 1983; Landsat 4 Path 192, Row 27, approximately equivalent to Landsats 1–3 Path 207, Row 27).

Figure 25.—*Digitally processed Landsat 2 MSS image (2 September 1980; Path 207, Row 27) of part of the eastern Italian Alps. The Landsat image makes three classifications: other, doubtful, and ice/snow. This classifying represents the first step in the interpretation procedure developed to calculate glacier areas. The glaciers are labeled with their catalog reference numbers. The watershed line is superimposed from cartographic data. Image processing courtesy of the Istituto di Fisica Cosmica e Tecnologie Relative-CNR, Milan.*

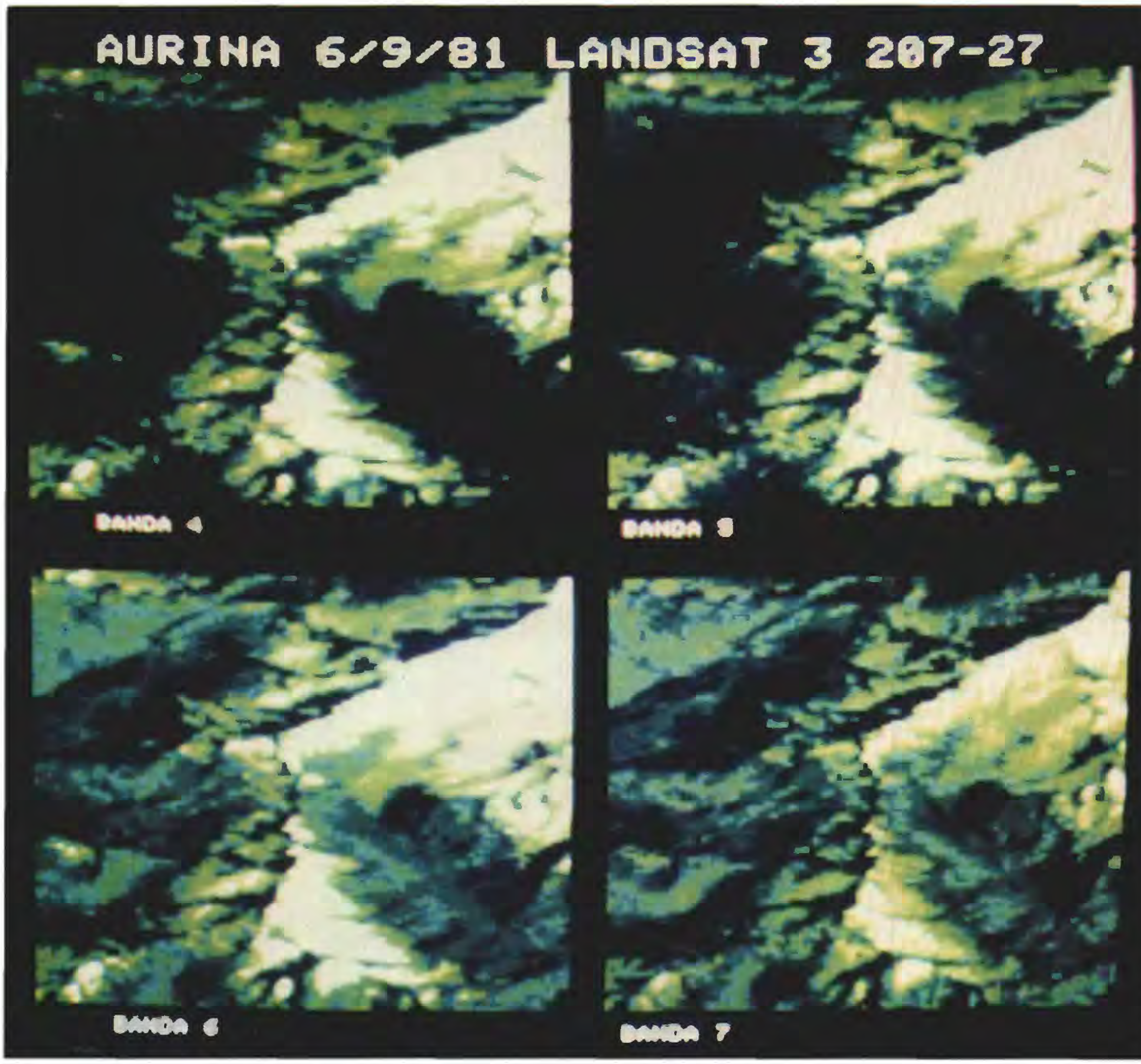

Figure 27 shows the final classification map, in which the snow-covered glacier areas are identified from the digitally processed Landsat MSS image of 9 August 1983 and additional synthesis of MSS bands 5, 6, and 7. The complete analysis gave the areas of the glaciers at the end of the summer of 1980, 1981, and 1983, the variations in area between 1980 and 1983, and the AAR (Della Ventura and others, 1987b).

In both of the regions investigated, it was possible to duplicate with the Landsat images the measurements made at glacier termini. This capability to perceive, within a given area, fluctuations in all of the existing glaciers, even those with movements opposite to those observed on the main glaciers, permits a more accurate assessment of glacier variations in a region. An analysis of problems related to the areal dimension and exposure of glaciers being studied permitted the development of a method to automatically delineate Alpine glaciers on Landsat images, in the absence of a digital model. Glacier areas are calculated by evaluating the intensity values on Landsat images combined with validity of observational conditions related to exposure, slope, and surface homoge-

Figure 26.—*Digitally processed Landsat 3 false-color MSS image (6 September 1981; Path 207, Row 27) of part of the eastern Italian Alps. False colors are used in each of the four MSS bands. The glaciers investigated are in the Valle Aurina area. The white areas on the right-hand part of the images correspond to the Austrian glaciers exposed to the south and to the southeast. Image processing courtesy of the Istituto di Fisica Cosmica e Tecnologie Relative-CNR, Milan.*

Figure 27.—Digitally processed Landsat 4 image (40389–09272; 9 August 1983; Path 192, Row 27, approximately equivalent to Landsats 1–3 Path 207, Row 27) of part of the eastern Italian Alps. This final classification map delineates snow-free and snow-covered glacier areas. Image processing courtesy of the Istituto di Fisica Cosmica e Tecnologie Relative-CNR, Milan.

neity (Della Ventura and others, 1987b). An observational accuracy value is assigned to each glacier by comparing the area recorded in existing glacier catalogs with the area calculated from the digitally processed image (MSS band 5 × MSS band 6). The low-cost methodology permits the calculation of the areas of glaciers and snow-covered regions at different years and thereby makes it possible to estimate the long-term trend of the glacierization of a region.

As an operational tool, this technique of monitoring individual glaciers and snow-covered regions in separate Alpine areas was evaluated for recognition of the extent of snow cover in the upper Piave basin (eastern Italian Alps). These data would be useful in improving models of snow-cover change (Rossi and others, 1986). Landsat images for Path 207, Row 28, which were acquired between August 1983 and July 1984, during both the snow accumulation and snow ablation seasons, were used. The results show that this technique makes possible the calibration of a snowmelt model that can be used to estimate the amount of runoff for the production of hydroelectric power in small basins.

References Cited

Consiglio Nazionale delle Ricerche, 1959, Catasto dei Ghiacciai Italiani, Anno Geofisico 1957–1958 [Inventory of Italian glaciers, geophysical year 1957–1958]: Turin, Comitato Glaciologico Italiano, v. 1, 171 p.

———1961a, Catasto dei Ghiacciai Italiani, Anno Geofisico 1957–1958 [Inventory of Italian glaciers, geophysical year 1957–1958]: Torino, Comitato Glaciologico Italiano, v. 2, 324 p.

———1961b, Catasto dei Ghiacciai Italiani, Anno Geofisico 1957–1958 [Inventory of Italian glaciers, geophysical year 1957–1958]: Torino, Comitato Glaciologico Italiano, v. 3, 389 p.

———1962, Catasto dei Ghiacciai Italiani, Anno Geofisico 1957–1958 [Inventory of Italian glaciers, geophysical year 1957–1958]: Torino, Comitato Glaciologico Italiano, v. 4, 309 p.

———Della Ventura, A., Mussio, P., Rabagliati, R., Rampini, A., and Serandrei Barbero, R., 1981, Determination of the spectral signatures of a glacier, *in* Guyot, G., and Verbrugghe, M., eds., Proceedings of the International Colloquium on Spectral Signatures of Objects in Remote Sensing: Avignon, Institut National de la Recherche Agronomique, v. 5, p. 477–485.

Della Ventura, A., Rabagliati, R., Rampini, A., and Serandrei Barbero, R., 1982, Remote sensing observation of glaciers toward their monitoring, *in* Papers Approved for Presentation at the Sixteenth Symposium on Remote Sensing of Environment: Ann Arbor, Mich., Environmental Research Institute of Michigan, v. 2, p. 723–733.

Della Ventura, A., Rampini, A., Rabagliati, R., and Serandrei Barbero, R., 1983, Glacier monitoring by satellite: Il Nuovo Cimento, Serie 1, v. 6C, p. 211–222.

Della Ventura, A., Rabagliati, R., Rampini, A., and Serandrei Barbero, R., 1987a, L'evoluzione recente del glacialismo in Valle Aurina (Alpi Pusteresi) nelle immagini Landsat MSS [Recent glacial evolution in Valle Aurina (Pusteresi Alps) by Landsat MSS images]: Geografia Fisica e Dinamica Quaternaria, v. 9, no. 1 (1986), p. 39–48.

Della Ventura, A., Rampini, A., Rabagliati, R., and Serandrei Barbero, R., 1987b, Development of a satellite remote sensing technique for the study of Alpine glaciers: International Journal of Remote Sensing, v. 8, no. 2, p. 203–215.

Haeberli, W., compiler, 1985, Fluctuations of glaciers 1975–1980: Paris, International Association of Hydrological Sciences (IAHS) and United Nations Educational, Scientific, and Cultural Organization (UNESCO), v. 4, 265 p., with 13 special topographic maps of glaciers.

Haeberli, W., and Müller, P., compilers, 1988, Fluctuations of glaciers 1980–85: Zürich, Switzerland, International Association of Hydrological Sciences (IAHS), United Nations Environment Programme (UNEP), and United Nations Educational, Scientific, and Cultural Organization (UNESCO), v. 5, 288 p., with 13 special topographic maps of glaciers.

Kasser, P., 1967, Fluctuations of glaciers 1959–1965: Paris, International Association of Scientific Hydrology (IAHS) and United Nations Educational, Scientific, and Cultural Organization (UNESCO), v. 1, 52 p., with an additional 23 tables, 7 figures, and 1:25,000-scale photogrammetric map of Aletsch-gletscher.

———1973, Fluctuations of glaciers 1965–1970: Paris, International Association of Hydrological Sciences (IAHS) and United Nations Educational, Scientific, and Cultural Organization (UNESCO), v. 2, 357 p., with 5 special topographic maps of glaciers.

Müller, F., 1977, Fluctuations of glaciers 1970–1975: Paris, International Association of Hydrological Sciences (IAHS) and United Nations Education, Scientific, and Cultural Organization (UNESCO), v. 3, 269 p., with 12 special topographic maps of glaciers.

Nangeroni, G., 1964, Ghiacciai, nevi e fenomeni periglaciali [Glaciers, snow and periglacial phenomena], *in* Un Sessantennio di Ricerca Geografica Italiana: Memorie della Società Geografica Italiana, v. 26,
p. 83–102.

Pagliari, M., and Zandonella, A., 1982, Bacino della Marmolada—Analisi multitemporale della copertura nevosa usando immagini Landsat [Marmolada basin—A multitemporal analysis of the snow cover by Landsat images]: Gargnano, Atti 4° Convegno Società Italiana Telerilevamento.

Porro, C., 1925, Elenco dei Ghiacciai Italiani [List of Italian Glaciers]: Parma, Ufficio Idrografico del Po, 61 p.

Porro, C., and Labus, P., 1927, Atlante dei Ghiacciai Italiani [Atlas of Italian Glaciers]: Firenze, Istituto Geografico Militare.

Provincia Autonoma di Bolzano, 1983, Catasto dei ghiacciai della Provincia di Bolzano [Glacier inventory of the Province of Bolzano): Ufficio Idrografico di Bolzano.

Rabagliati, R., and Serandrei Barbero, R., 1979, Possibilità di impiego del remote sensing da satellite per il controllo annuale dei ghiacciai [The possible use of satellite remote sensing in the yearly control of glaciers]: Geografia Fisica e Dinamica Quaternaria, v. 2, no. 1, p. 35–40.

Rossi, G., Tomasino, M., Della Ventura, A., Rampini, A., Serandrei Barbero, R., and Rabagliati, R., 1986, Landsat registrations for a snowmelt model of the Piave River basin, *in* Modelling snowmelt-induced processes, Proceedings of the Budapest Symposium, July 1986: International Association of Hydrological Sciences Publication No. 155, p. 215–229.

Salomonson, V.V., 1983, Water resources assessment, snow and ice mapping and monitoring, *in* Manual of remote sensing: American Society of Photogrammetry, v. 2, p. 15–22.

Zanon, G., 1980, Ghiacciai, neve e valanghe [Glaciers, snow and avalanches], *in* Associazione dei Geografi Italiani, La Ricerca Geografica in Italia 1960–1980, ASK edizioni: Varese, p. 699–702.

———1982, Recent glaciological research in the Ortles-Cevedale region (Italian Alps): Geografia Fisica e Dinamica Quaternaria, v. 5, no. 1, p. 75–81.

———1985, Glaciology, *in* Gruppo Nazionale CNR Geografia Fisica e Geomorfologia, [Italian research on physical geography and geomorphology (addendum)]: Bologna, Tecnoprint, p. 3–6.

Glaciers of Europe—

GLACIERS OF THE PYRENEES, SPAIN AND FRANCE

By DAVID SERRAT *and* JOSEP VENTURA

SATELLITE IMAGE ATLAS OF GLACIERS OF THE WORLD

Edited by RICHARD S. WILLIAMS, Jr., *and* JANE G. FERRIGNO

U.S. GEOLOGICAL SURVEY PROFESSIONAL PAPER 1386–E–2

The 41 glaciers in the Pyrenees, covering a total area of 8.10 square kilometers, have all receded since the mid-1800's although some minor advances took place in the late 1950's

CONTENTS

	Page
Abstract	E49
Introduction	49
Distribution of glaciers	50
FIGURE 1. Index map to the glaciers of the Pyrenees	50
2. Aspect diagram showing the polarized distribution of the orientation of the glaciers of the Pyrenees	52
3. A graph of the maximum altitude of the snowline at the end of the melt season on selected peaks in the Pyrenees	52
TABLE 1. Distribution and dimensions of glaciers of the Pyrenees as of 1984	51
Glacier studies	53
Glacier fluctuations	54
Available data for glacier studies	55
Maps	55
Aerial photographs	55
Satellite imagery	55
TABLE 2. Optimum Landsat 1, 2, and 3 images of glaciers of the Pyrenees	56
FIGURE 4. Index map to the optimum Landsat 1, 2, and 3 images of the glaciers of the Pyrenees	56
5. Section of annotated 1:500,000-scale enlargement of Landsat 2 false-color composite image 2185–10022, Path 214, Row 30, acquired 26 July 1975	57
6. Sketch map of Maladeta massif and its glaciers in 1979	58
7. Vertical aerial photograph of Glaciar de la Maladeta	59
8. Vertical aerial photographs of the Maladeta massif taken 5 September 1988	60
References cited	61

GLACIERS OF EUROPE—

GLACIERS OF THE PYRENEES, SPAIN AND FRANCE

By DAVID SERRAT[1] *and* JOSEP VENTURA[2]

Abstract

The glaciers of the Pyrenees, a range of Alpine mountains that extends along the border between Spain and France, are found in a 100-kilometer-long section in the central part of the range. According to the latest figures, compiled in 1984 for the Temporary Technical Secretariat for World Glacier Inventory (now the World Glacier Monitoring Service) and updated with 1988 aerial photographs, there are currently 41 glaciers in the Pyrenees with a total area of approximately 8.10 square kilometers. Thirteen peaks, all having elevations greater than 3,000 meters above mean sea level, support these 41 glaciers, generally on slopes that have a northern, northeastern, or eastern orientation. The current area of the Pyrenees calculated to be glacier covered is based on measurements made in the field or from vertical aerial photographs. Most published maps do not accurately differentiate between true glaciers and snowfields or snow patches. The glaciers are all small, with the largest, Glaciar de Aneto, only 1.32 square kilometers. Half of the glaciers are 0.1 square kilometer or less in size. The maximum altitude of the snowline at the end of the summer melt season generally rises from west to east, with a range of 2,600 to 2,850 meters in the west and 2,750 to 3,100 meters in the east. During the Pleistocene, the Pyrenees were a local center of glaciation. During the middle 1800's, glaciers in the Pyrenees were larger and more numerous than at present. Virtually all of the glaciers have been in a state of recession since the mid-1800's. Although some glaciers reached an equilibrium in the early 1950's, a few actually exhibited minor advances beginning in the late 1950's. Cloud-free Landsat multispectral scanner images of the glacier areas are available, but the imagery has limited usefulness for glacier studies because of the small size of the Pyrenean glaciers and because the snow cover makes it difficult to distinguish the margin of glaciers. Data from sensors having greater spectral or spatial resolution should contribute greatly to glacier studies and monitoring in the Pyrenees in the near future.

Introduction

The Pyrenees are an Alpine mountain range stretching across the isthmus that lies between the Iberian Peninsula and the rest of the European continent. The mountains are oriented in an east-west direction and lie between 42° and 43° N. lat. They extend almost 400 km from 2° W. long. near the Bay of Biscay on the Atlantic Ocean side to 3° E. long. near the Mediterranean Sea and are divided into two nearly equal parts by the Greenwich meridian. The glaciers are found in a 100-km-long section in the central part of the range between about 0°30′ W. and 0°50′ E. lat.

The elevations of the highest mountain peaks are about 3,000 m above mean sea level, with a maximum elevation of 3,404 m on Pico de Aneto (Maladeta massif). All glacierized peaks are higher than 3,000 m, although some peaks that reach this height do not have glaciers. The peaks that have glaciers are as follows (from west to east): Balaïtous,

[1]Department of Geomorphology and Tectonics, University of Barcelona, Barcelona, Spain.
[2]Cartographic Institute of Catalunya, Barcelona, Spain.

Picos del Infierno, Vignemale, Gavarnie, Monte Perdido, La Múnia, Pic Long, Batoua, Gourgs Blancs, Posets, Espingo, Cirque de Lys, and Maladeta. The mean elevations of the glaciers range from 2,432 to 3,169 m, with an average of 2,817 m.

Distribution of Glaciers

According to the latest figures, compiled in 1984 for the Temporary Technical Secretariat for World Glacier Inventory (now part of the World Glacier Monitoring Service in Zürich, Switzerland) and updated with 1988 aerial photographs, there are currently 41 glaciers in the Pyrenees covering a total area of approximately 8.10 km^2. The glaciers are all small, with the largest, Glaciar de Aneto, only 1.32 km^2. The smallest is Glaciar de Batoua with an area of 0.03 km^2. Half of the glaciers are 0.1 km^2 or less in size. Figure 1 shows the location of the glaciers; table 1 gives statistics for each glacier. The glaciers are primarily cirque glaciers or small strip glaciers on ledges and terraces. They are remnants of

***Figure 1.**—Glaciers of the Pyrenees. The altitude of the area is indicated by color. The areas less than 800 m are shown in yellow. Each darker shade indicates an increase in height of 400 m. The dark brown areas at the summit of the Pyrenees range from 2,400 to 3,500 m in altitude. The numbers on the map correlate to the glaciers listed in table 1.*

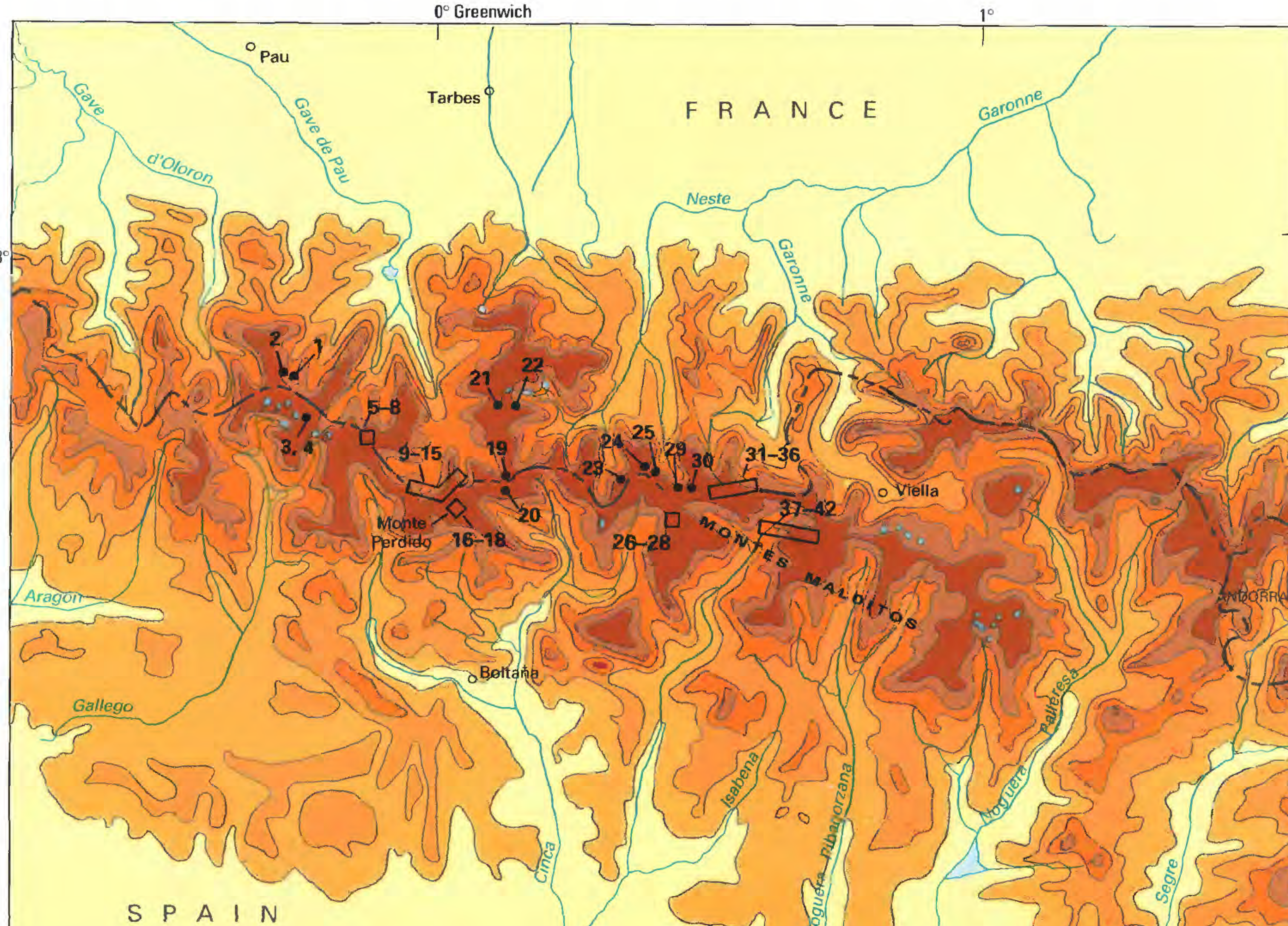

Base from International Map of the World 1:1,000,000
Madrid, Sheet NK 29 & 30, 1965;
Barcelona, Sheet NK 31. 1962

TABLE 1.—*Distribution and dimensions of glaciers of the Pyrenees as of 1984*

[In the following names of the Pyrenean glaciers, G. is an abbreviation for glacier, except where preceded by a single asterisk, in which case it stands for glaciar. Gs. indicates glaciers. (Total number is shown in parentheses.) Accum. = accumulation; Ablat. = ablation]

Number	Name	Massif	Basin	UTM coordinates	Area (km²)	Orientation (Accum. and ablat. areas)	Mean Width (m)	Mean Length (m)	Max length (m)	Elevation (meters above mean sea level) Maximum	Mean	Minimum	Massif top
1	G. de Les Néous	Balaïtous	Gave de Pau	30 TYN 222468	0.28	E	225	1,050	1,125	3,010	2,700	2,500	3,144
2	G. de Pabat			30 TYN 220474	.10	N	340	300	450	2,850	2,740	2,610	2,996
3	*G. del Infierno	Picos del Infierno	Gállego (Ebro)	30 TYN 246405	.06	N	200	400	500	2,960	2,820	2,720	3,061
4	*G. del Infierno			30 TYN 243407	.09	N	300	400	500	2,940	2,800	2,700	3,061
5	G. des Oulettes	Vignemale	Gave de Pau	30 TYN 338404	.18	N	240	500	1,010	3,152	2,490	2,340	3,298
6	G. du Petit Vignemale			30 TYN 343403	.12	N	300	400	610	2,920	2,660	2,490	3,154
7	G. d'Ossoue			30 TYN 342393	.70	E	380	1,500	1,880	3,195	3,050	2,630	3,298
8	G. du Montferrat			30 TYN 347389	.06	E	180	200	450	2,970	2,780	2,680	3,219
9	Gs. des Gabietous (3)	Gavarnie	Gave de Pau	30 TYN 414317	.26	N	640	400	800	2,935	2,650	2,380	3,144
10	G. du Taillon			30 TYN 425315	.26	NE	320	750	940	2,900	2,710	2,570	3,144
11	G. de la Brèche			30 TYN 438309	.123	N	410	300	400	2,860	2,660	2,580	3,006
12	G. de la Cascade			31 TBH 548311	.056	W	105	300	380	3,030	2,780	2,680	3,248
13	Gs. W du Marboré (2)			31 TBH 551317	.116	NW	300	270	430	2,940	2,760	2,530	3,248
14	Gs. de Paillà (2)			31 TBH 560328	.15	N	400	300	610	2,964	2,520	2,410	3,071
15	G. d'Astazou			31 TBH 570325	.085	N	280	240	450	2,670	2,500	2,400	3,071
16	*G. de Monte Perdido	Monte Perdido	Cinca (Ebro)	31 TBH 572298	.48	NE	1,200	400	700	3,180	2,980	2,690	3,355
17	*G. del Cilindro			31 TBH 565305	.05	NE	300	100	200	2,905	2,820	2,740	3,337
18	*G. de Marboré			31 TBH 561312	.07	NE	500	100	200	2,900	2,830	2,760	3,248
19	*G. de la Múnia	La Múnia	Gave de Pau	31 TBH 651336	.062	NW	250	250	290	2,850	2,775	2,710	3,133
20	*G. de Robiñera		Cinca (Ebro)	31 TBH 656321	.05	N	300	200	300	2,805	2,720	2,660	3,003
21	G. du Lac Tourrat	Pic Long	Gave de Pau	31 TBH 629433	.07	N	260	240	300	2,960	2,860	2,740	3,192
22	G. de Pays Baché		Garonne	31 TBH 634429	.154	E	380	450	590	3,080	2,980	2,860	3,192
23	*G. de Batoua	Batoua	Garonne	31 TBH 816327	.03	NW	110	180	280	2,500	2,432	2,365	3,034
24	G. de Pouchergues[3]	Gourgs Blancs	Garonne	31 TBH 921303	.062	N	290	200	250	2,750	2,700	2,650	2,967
25	G. de Gourgs Blancs			31 TBH 937311	.27	N	625	410	500	3,000	2,890	2,780	3,128
26	*G. de Llardana	Posets	Cinca (Ebro)	31 TBH 894260	.23	NW	300	700	800	3,052	2,917	2,782	3,375
27	*G. de la Paul		Esera (Ebro)	31 TBH 901265	.08	NE	400	200	300	3,076	3,016	2,850	3,375
28	*G. de Posets			31 TBH 903260	.13	E	300	400	500	3,180	3,105	2,995	3,375
29	*Gs. Sheil dera Baquo (2)[1]	Espingo	Garonne	31 TBH 948303	.39	NE	1,040	340	660	3,040	2,910	2,780	3,103
30	*Gs. du Portillon d'Oo (3)			31 TBH 959302	.164	N	316	230	725	2,950	2,766	2,583	3,222
31	G. W des Crabioules	Cirque de Lys	Garonne	31 TBH 977313	.088	N	300	200	350	2,860	2,755	2,650	3,116
32	G. E des Crabioules			31 TBH 983310	.087	NE	240	250	400	2,810	2,720	2,630	3,116
33	G. W du Maupas			31 TBH 989310	.051	N	175	170	300	3,020	2,900	2,780	3,109
34	G. E du Maupas			31 TBH 994308	.055	NE	430	120	175	2,960	2,910	2,860	3,109
35	G. du Boum			31 TCH 002307	.14	N	440	250	375	2,900	2,800	2,700	3,006
36	G. des Graoues			31 TCH 010305	.09	N	375	250	375	2,840	2,740	2,640	2,942
37	*G. de la Maladeta	Maladeta	Esera (Ebro)[2]	31 TCH 066250	.60	N	900	700	900	3,240	3,100	2,780	3,308
38	*G. de Aneto		[2]	31 TCH 075236	1.32	NE	1,600	800	1,200	3,330	3,080	2,780	3,404
39	*G. de Coronas			31 TCH 074229	.13	W	200	600	700	3,250	3,169	2,958	3,404
40	*G. de Barrancs		[2]	31 TCH 083230	.28	NW[4]	400	700	900	3,290	3,110	2,900	3,404
41	*G. de Tempestades		[2]	31 TCH 089223	.34	NE	700	400	500	3,050	2,902	2,705	3,310
42	*G. de Salenques[3]		Ribagorçana (Ebro)	31 TCH 089219	.05	E	250	250	320	3,100	2,980	2,960	3,240

[1] In French, Gs. Seil de la Baque.

[2] Draining to Garonne Basin by karstic conduction.

[3] Additional work in 1988 led to the reclassification of Glacier de Pouchergues (#24) as a snowpatch and of a snowpatch in the Maladeta Massif as a glacier (Glaciar de Salenques, #42).

[4] Ablation area is oriented northeast.

cirque and valley glaciers that were often connected on several levels by ice falls and avalanches. Recession has caused the larger glaciers to shrink and separate into smaller individual ice masses.

The glaciers are most often found on the northeastern, northern, and eastern slopes of the mountain range (fig. 2). The preferential north-northeast orientation is caused by the combined effects of precipitation pattern, prevailing winds, and solar radiation. Considerable precipitation on the northern and western slopes of the Pyrenees results from the oceanic climate. The southern slopes, influenced by a Mediterranean climate, are drier (Taillefer, 1968). The prevailing winds are westerly, and solar radiation is most intense from the south. As a result, the northern and eastern slopes receive maximum deposition of snow and maximum protection from the ablative effects of the wind and sun.

The maximum altitude of the snowline at the end of the melt season in the Pyrenees generally rises from west to east (fig. 3). Current research seems to indicate that the range of this seasonal snowline in the west is from 2,600 to 2,850 m and 2,750 to 3,100 m in the east. It is important to note that in the two instances where the seasonal snowline drops sharply, on Glacier d'Astazou and Glaciar de Batoua, the glaciers are maintained and fed by avalanche activity, an important source of nourishment for many of the glaciers in the Pyrenees. These seasonal snowline figures are not very different from those published by Höllermann (1968) of 2,900 m in the west and 3,100 m in the east, which might indicate a stablization of the glaciers since his work.

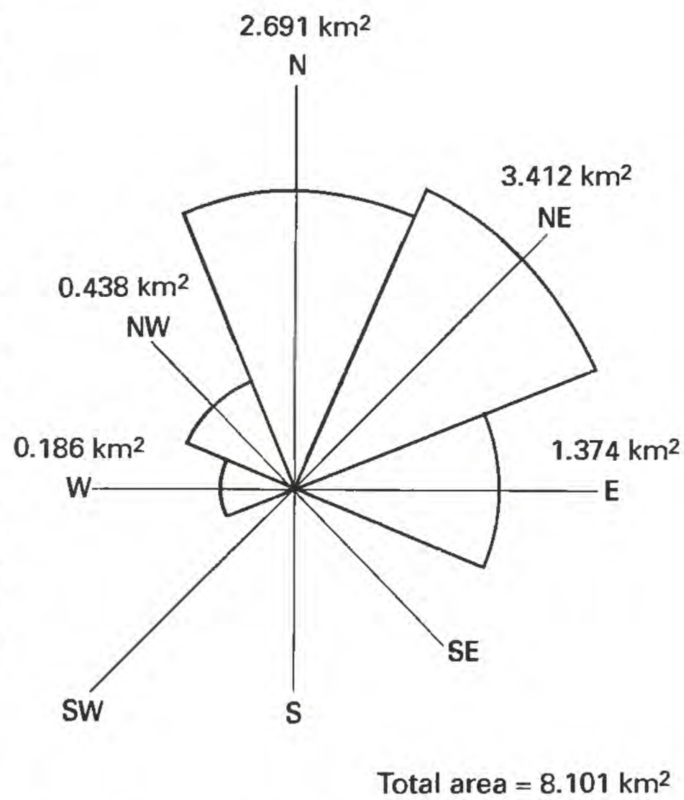

***Figure 2.**—The polarized distribution of the orientation of the glaciers of the Pyrenees. The distribution is weighted by area in square kilometers.*

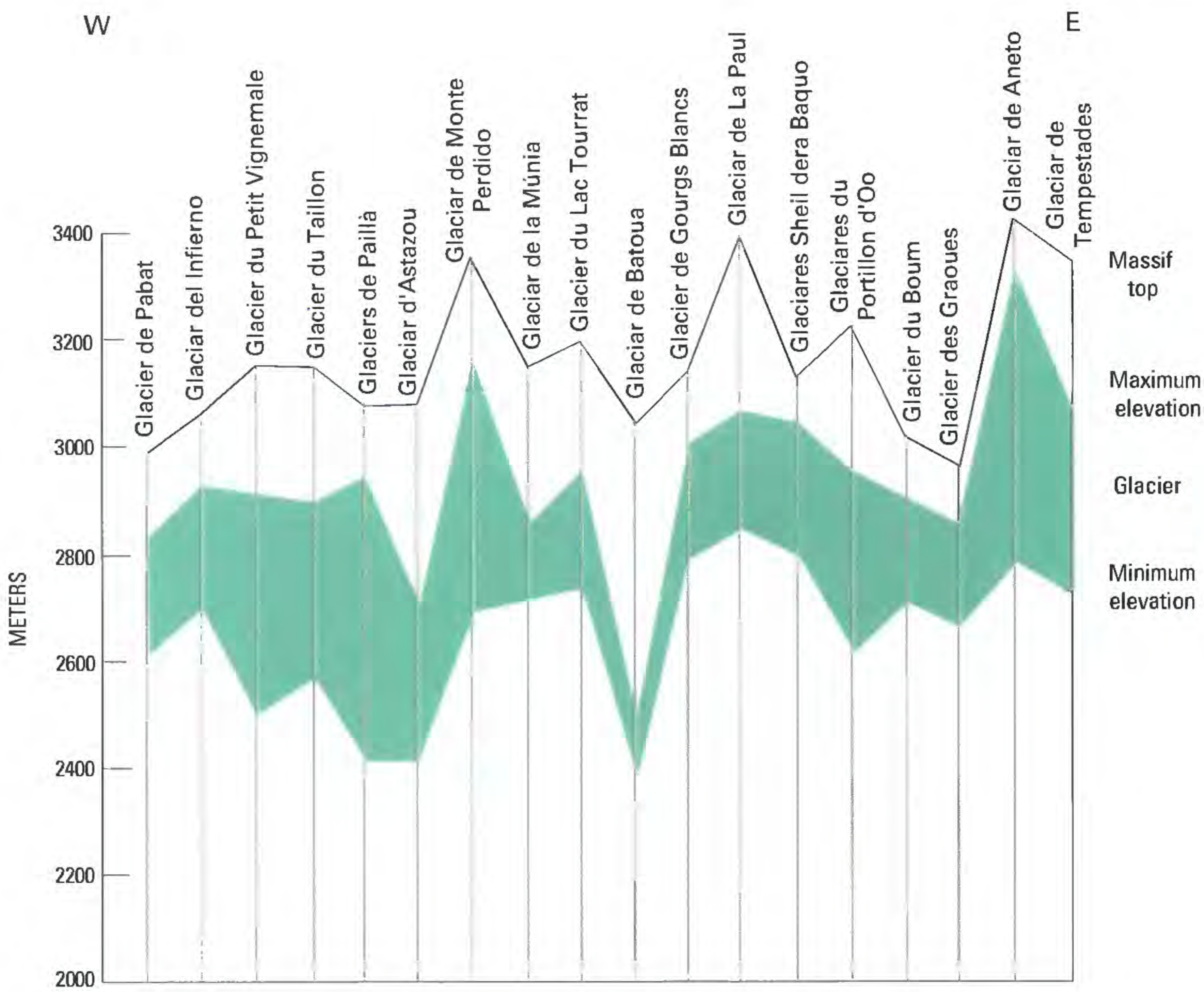

***Figure 3.**—A graph of the maximum altitude of the snowline at the end of the melt season on selected peaks in the Pyrenees. This seasonal snowline generally rises from west to east. In the two instances where this seasonal snowline drops sharply, Glacier d'Astazou and Glaciar de Batoua, the glaciers are fed by avalanche activity.*

Glacier Studies

In the past, glaciological work in the Pyrenees has been limited in scope. The relative remoteness of the region made travel and research difficult, and because of the small size of the glaciers there was little interest from an economic standpoint.

The first isolated observations on glaciers were made by Johann von Charpentier during his stay in the Pyrenees area from 1808 to 1812 (Charpentier, 1823). He described some of the more prominent glaciers on the peaks of Maladeta, Crabioules, Monte Perdido, Vignemale, and Néouvielle. The first scientific studies were carried out in the Maladeta massif by Collomb, Michelier, and Eugène Trutat (1875, 1894), Director of the Natural History Museum in Toulouse, France.

Work carried out by Franz Schrader from 1869 to 1883 in mapping the Pyrenees at a scale of 1:100,000 constituted the first attempt to evaluate the areal extent of its glaciers (Schrader, 1895). These earlier studies were continued by Prince Roland Bonaparte (1891) and Ludovic Gaurier (1921), who carried out periodic observations on Pyrenean glaciers during the period 1904 to 1931. Gaurier was President of the Commission de Glaciologie des Pyrénées and contributed to the journal "Études glaciologiques," published by the French Ministry of Agriculture until 1934. Some other interesting studies from this period were those carried out by Eydoux and Maury (1907) on the Pic Long glaciers, and by Plandé (1939).

From 1945 to 1963, French scientists directed by the engineers Chimits, Chabrol, and Sannac (Chabrol and others, 1953) studied the Ossoue, Taillon, and Sheil dera Baquo (Seil de la Baque) glaciers for hydroelectric potential. The mountaineer Raymond d'Espouy and the Geographical Institute of Toulouse have collaborated on the project since 1951. Work carried out by Barrère (1953) and Durand (1961) on glaciers of the western Pyrenean massifs (Balaïtous, Vignemale, and Picos del Infierno), including two glaciers (Néouvielle, Cambalés) which no longer exist; Brunet (1955) on Sheil dera Baquo (Seil de la Baque) glaciers; Galibert (1956), Mounier (1962), and Bellan (1963) on the glaciers of the Luchonnais area (a region that encompasses the previously cited massifs); and Taillefer (1968) on the extent of Pleistocene glaciation also fell within this period.

Up to now, Spanish studies on glaciers have been limited. During the past 60 years, however, work has been carried out by Faura (1923) on Glaciar de Aneto and Glaciar de la Maladeta (where a displacement of up to 35 m per year was calculated for the Glaciar de Aneto); by Vidal-Boix (1933) and Gómez de Llarena (1936) on Glaciar de Monte Perdido; by Vedruna (1956) and, recently, by Nicolás-Martínez (1981) on the geomorphology of Tucarroya Cirque on the Monte Perdido massif.

Surveys on the distribution and extent of glaciers have been done by van Summern and Morrison (1958) and Mercer (1975) of the American Geographical Society and by Höllermann (1968). More recently, work has been carried out by Soutadé (1982) on the Luchonnais glaciers.

The most recent data included in this paper have been collected as part of the Technical Secretariat for the World Glacier Inventory project. Information was collected during successive years of fieldwork, beginning in 1979, by geologists and geographers of the Alpine Geomorphological Group of the University of Barcelona (Josepa Brú, Joan Martí, Carme Muntaner, Joan M. Vilaplana, and the authors) with the help of others interested in Alpine research (Equip de Geomorfología Alpina, 1980).

Glacier Fluctuations

During the Pleistocene, the Pyrenees were a local center of glaciation (Penck, 1884). During historic times, the glaciers reached their recent maximum during the middle of the last century. Glacier de Pays Baché reached the crest of its end moraine in 1856 (Eydoux and Maury, 1907); Glacier des Oulettes on Vignemale massif reached its moraine in 1857 (Höllermann, 1968), but all the glaciers have receded almost continuously since that time. According to Höllermann (1968), the largest glaciers had lost 40 percent of their volume since the 19th-century maximum.

According to Barrère (1953) and Taillefer (1981), recent glacier fluctuations can be grouped in different periods:

1. In the middle of the last century ("Little Ice Age") glaciers reached their end moraines.
2. From 1850 to 1905, glaciers retreated noticeably.
3. From 1905 to 1912, glaciers advanced slightly, and new moraines were formed (Glacier des Oulettes).
4. From 1912 to about 1950, glaciers generally retreated as the climate became both warmer and drier. During this period, several glaciers vanished (Isabé and Arremoulit, for example); others were divided into small remnants (Sheil dera Baquo, or Seil de la Baque); the rest were reduced both in areal extent and volume.
5. Since 1951, an increase in precipitation has resulted in glacier stabilization. During the work carried out on Pyrenean glaciers for the World Glacier Inventory, glacier stabilization, with minor advances (Glaciar de La Paul and Glaciar de Tempestades formed push moraines), was recorded during the period from 1957 to 1979.

Up to now, data on glacier extent in the Pyrenees have been questionable and exaggerated. Confusion is mainly caused by two factors:

1. The ambiguity of early data. Many authors cite approximate data of glacier extent from the latter part of the 1800's that are very different from data for the present-day extent.
2. The small size of many glaciers makes it difficult to differentiate between glaciers and snowfields on aerial photographs unless field work has been done. The problem is complicated by the fact that many of these snowfields are remnants of old glaciers (19th century) that were in recession from 1912 to 1950. Confusion is evident when some of these snowfields exhibit end moraines that formed during the last century. French and Spanish maps, even modern ones, do not clearly differentiate between glaciers and snowfields. From the middle of the 1800's to the present time, many historic glaciers have completely vanished from several massifs (for example, Gran Bachimala, Cambalés, Punta Zarre, Bardamina, and Bessiberri). Frondellas and Brecha de Latour glaciers in the southern slopes of the Balaïtous massif turned into snowfields, and Llosas and Salenques glaciers in the Maladeta massif became snowfields between 1948 and 1957.

The first data on glacier extent in the Pyrenees were provided by Franz Schrader (1895), who calculated the area at 40 km^2. According to Taillefer (1981), Ludovic Gaurier calculated an area of 21 km^2 for the French Pyrenean glaciers in 1934, and the Direction des Eaux et Forêts (French Department of Waters and Forests) calculated an extent of 8 km^2 for the French Pyrenean glaciers in 1950. Other compilations provided rather different data. Thorarinsson (1940) gave 40 km^2 as the total area of the Pyrenean glaciers. He based his total on the work of Hess (1933) who, in turn, referred to the observations by Eydoux and Maury (1907). Van Summern and Morrison's (1958) survey of glaciers produced an estimate of 30 km^2 for the total area of glaciers. Mercer (1975) gave a total area of 15 km^2 for 70 glaciers. The figures determined for the present study are listed in table 1. Forty-one Pyrenean glaciers have a total area of about 8.10 km^2.

Available Data for Glacier Studies

Maps

Only a limited number of maps are available for glacier studies because often no differentiation between snow patches, snowfields, and true glaciers has been shown on the maps. The most useful are the 1:25,000-scale series of topographic maps published by the Institut Géographique National of Paris.

Aerial Photographs

Some vertical aerial photographs are available from a flight in 1957 along the southern slope of the mountains. The flight was unique because nearly optimal conditions allowed photographs of such quality that true glaciers can be distinguished from snow patches (see fig. 7). Aerial photographs acquired during a 1988 flight have been used to determine more accurately the glacierized area of the Pyrenees and reclassify two snow and ice areas on the Gourgs Blancs and Maladeta massifs (table 1; fig. 8).

Satellite Imagery

Satellite imagery has only limited usefulness for glacier studies in the Pyrenees at the present time. Cloud-free Landsat multispectral scanner (MSS) images of the glacier areas are available (see table 2 and fig. 4). However, the glaciers are so small that, on a standard 1:1,000,000-scale Landsat print, the largest glacier, Glaciar de Aneto, is only 1.32 mm^2, and almost half the glaciers are less than one-tenth that size. Photographic enlargements, color composites, and digital enhancement techniques make it easier to see some of the glaciological features, but these techniques also have limitations, one of the greatest being snow cover, which makes it difficult to distinguish the margins of the glaciers. Landsat MSS image 2185–10022, acquired on 26 July 1975 (Path 214, Row 30), is virtually cloud free and is the best image in the U.S. archive at the EROS Data Center that covers all the glaciers of the Pyrenees. A section of the color composite image is shown at 1:500,000 scale in figure 5. On this image it is possible to discern Glacier d'Ossoue (#7) on the Vignemale massif and to locate the rest of the glacier massifs, but, because of the snow cover, it is difficult to delineate other individual glaciers. This problem is especially noticeable on the Maladeta massif, which is the location of the highest peak in the Pyrenees, Pico de Aneto (3,404 m) and the first and third largest glaciers in the area, Glaciar de Aneto (1.32 km^2) (#38) and Glaciar de la Maladeta (0.60 km^2) (#37). A sketch map of the area (fig. 6) and aerial photographs of the Maladeta massif (figs. 7, 8) give details of the shape and location of the glaciers. Unfortunately, it is possible to determine only the general location of the glaciers on the Landsat image. The glacier boundaries are lost because of the limits of the spatial resolution and the snow cover.

TABLE 2.—*Optimum Landsat 1, 2, and 3 images of the glaciers of the Pyrenees*

[In the "Code" column, a filled-in circle indicates an excellent image]

Path-Row	Nominal scene center (lat–long)	Landsat identification number	Date	Solar elevation angle (in degrees)	Code	Cloud cover (in percent)	Remarks
214–30	043°05′N. 000°42′E.	1027–10135	19 Aug 75	52	●	0	Covers all glacier areas
214–30	043°05′N. 000°42′E.	2185–10022	26 Jul 75	55	●	0	Covers all glacier areas; snow cover slightly greater than above
215–30	043°05′N. 000°44′W.	1028–10193	20 Aug 72	51	●	0	Covers glaciers of Balaïtous, Picos del Infierno, Vignemale, Gavarnie, Monte Perdido, La Múnia, and Pic Long

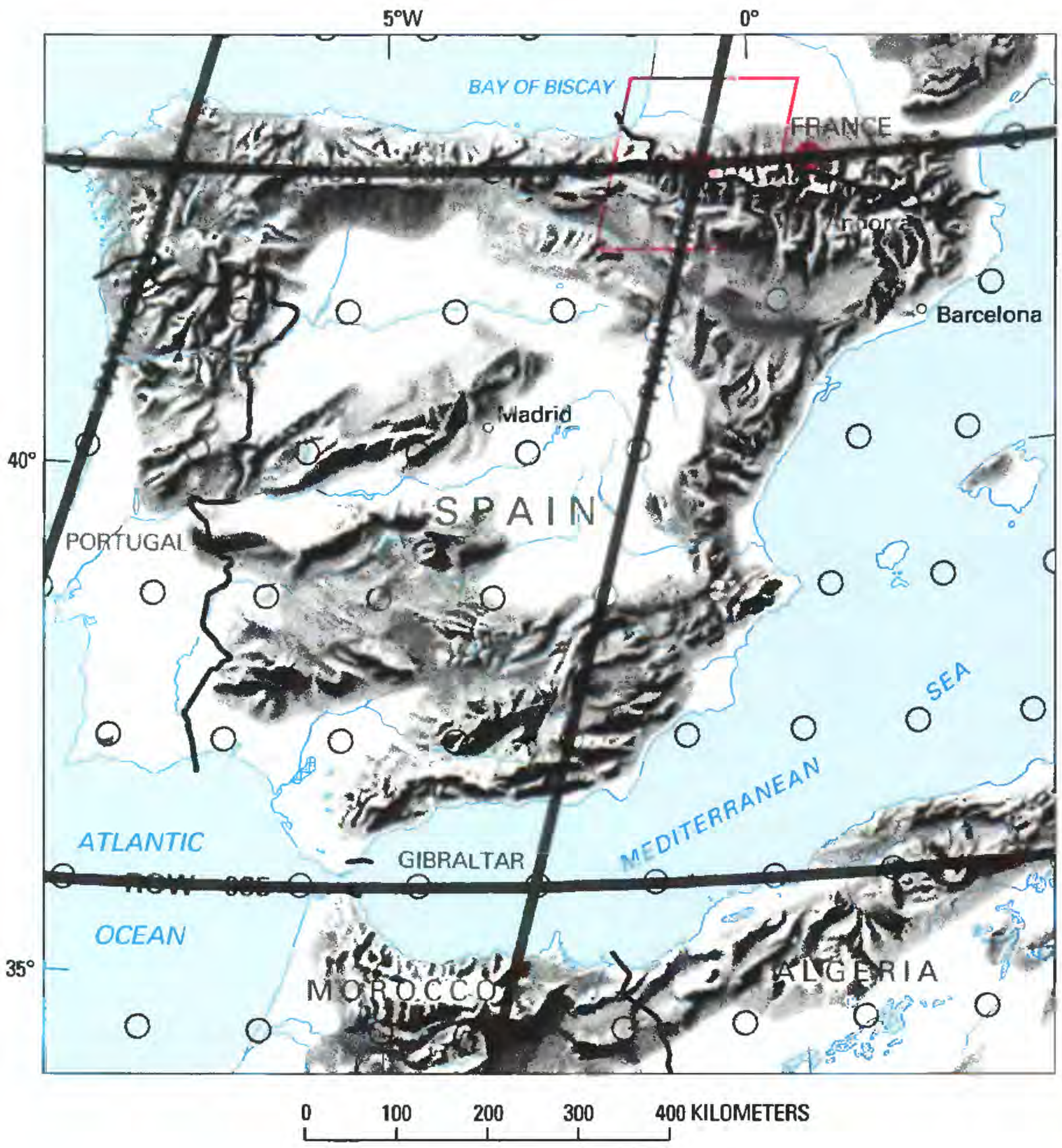

EXPLANATION OF SYMBOLS

Evaluation of image usability for glaciologic, geologic, and cartographic applications. Symbols defined as follows:

- ● Excellent image (0 to ≤5 percent cloud cover)
- ○ Nominal scene center for a Landsat image outside the area of glaciers
- ▱ Approximate size of area encompassed by nominal Landsat MSS image

***Figure 4.**—Optimum Landsat 1, 2, and 3 images of the glaciers of the Pyrenees. The vertical lines represent nominal paths. The rows (horizontal lines) have been established to indicate the latitude at which the imagery has been acquired.*

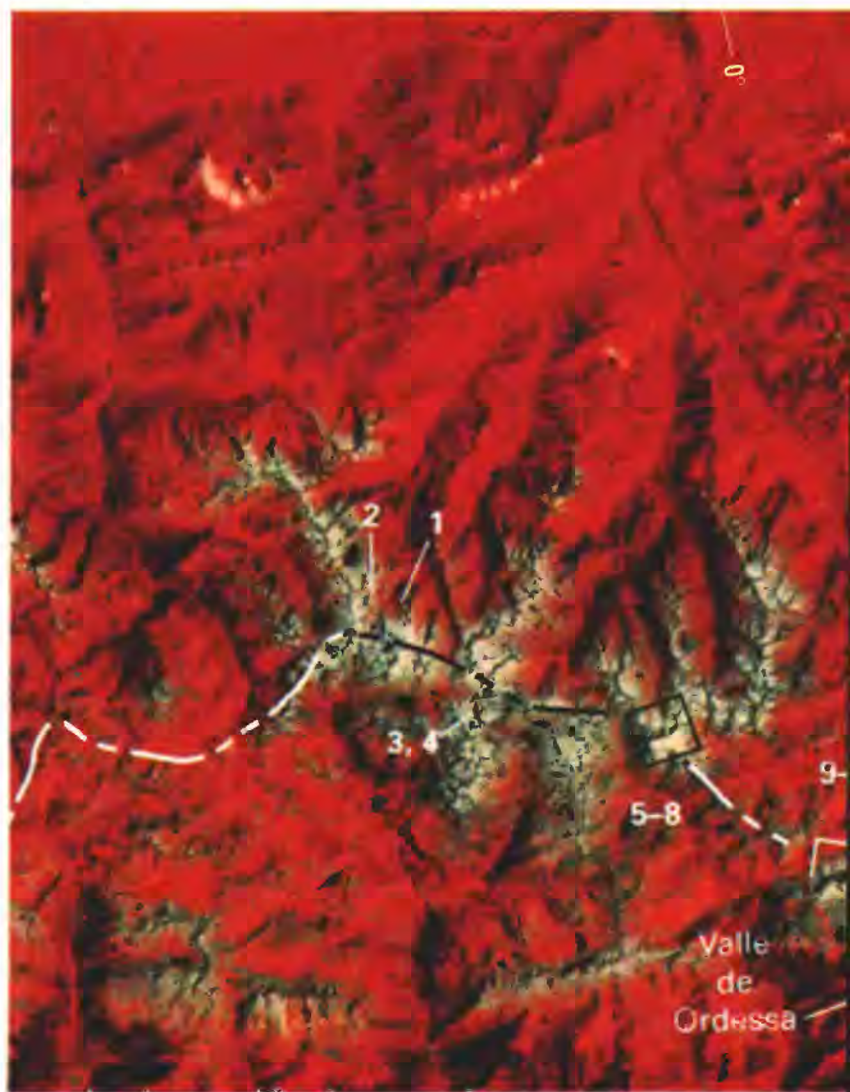

Landsat imagery can sometimes be used to indicate the former extent of glaciers by showing the location of abandoned moraines or by showing traces of glacial erosion such as cirques, arêtes, or glaciated valleys. A good example of this can be seen on figure 5. The Valle de Ordesa extends 10 km south and then west from the Gavarnie massif and has the typical appearance and shape of a valley erosionally modified by a glacier, although no glaciers can be seen today on the southern slope of the massif.

In some areas it is possible to use Landsat imagery to (1) delineate glacier distribution, (2) map glacier outlines, (3) monitor glacier fluctuations, (4) distinguish transient snowlines, and (5) even inferentially determine changes in mass balance. However, the size of the glaciers in the Pyrenees makes this difficult, given the current satellite capability. Data from sensors having greater spectral and (or) spatial resolution are now becoming available, including data from the Landsat thematic mapper, the Large Format Camera, and the French Satellite Pour l'Observation de la Terre (SPOT). Such new data will be able to contribute to glacier studies and monitoring in the Pyrenees and in other mountainous regions of the world, where the spatial resolution of the Landsat MSS sensor is not adequate.

Figure 5.—*Section of annotated 1:500,000-scale enlargement of Landsat 2 false-color composite image 2185–10022, Path 214, Row 30, acquired 26 July 1975. The image covers the entire glacier area of the Pyrenees. Numbers correlated to glaciers listed in table 1.*

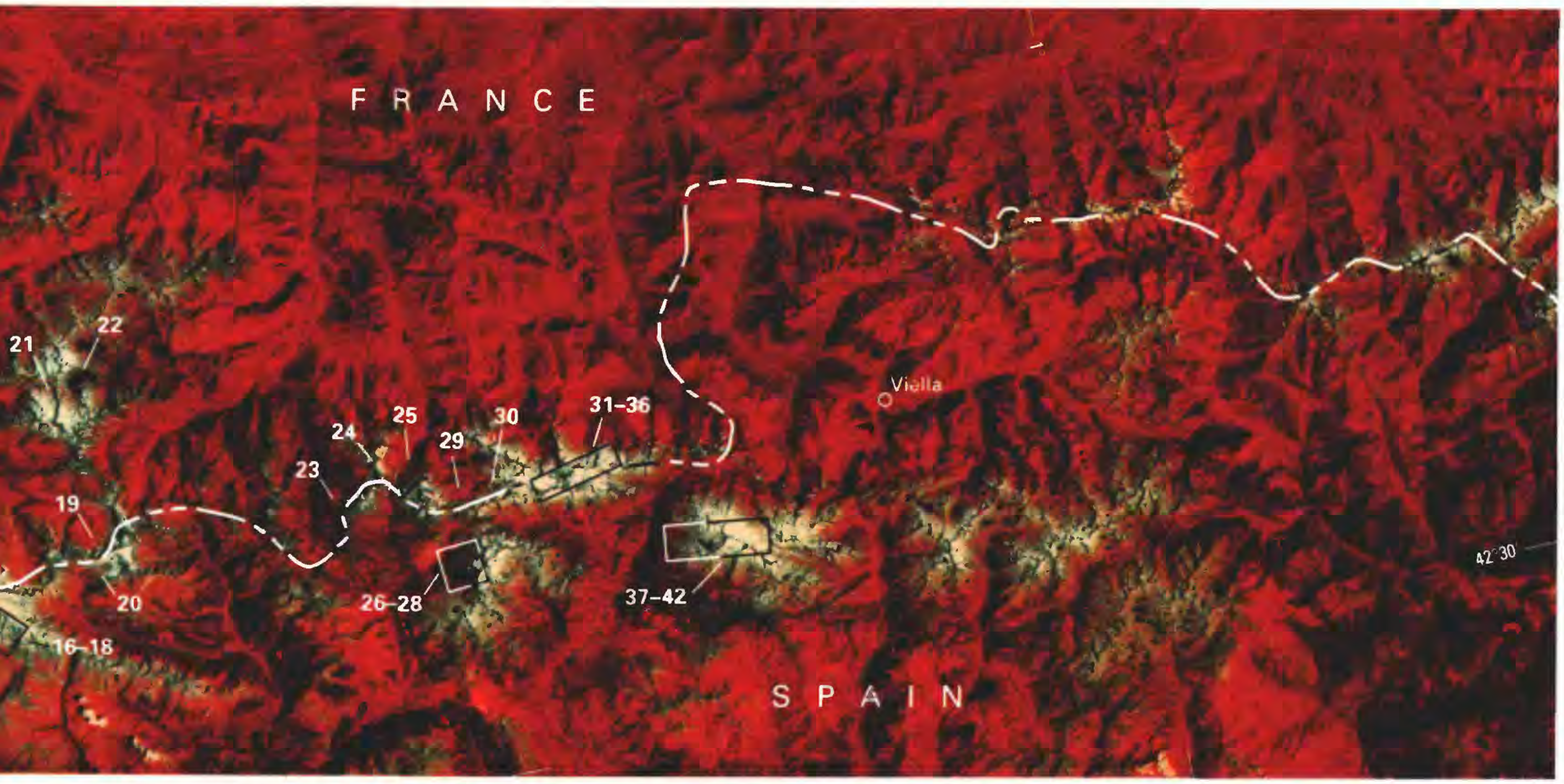

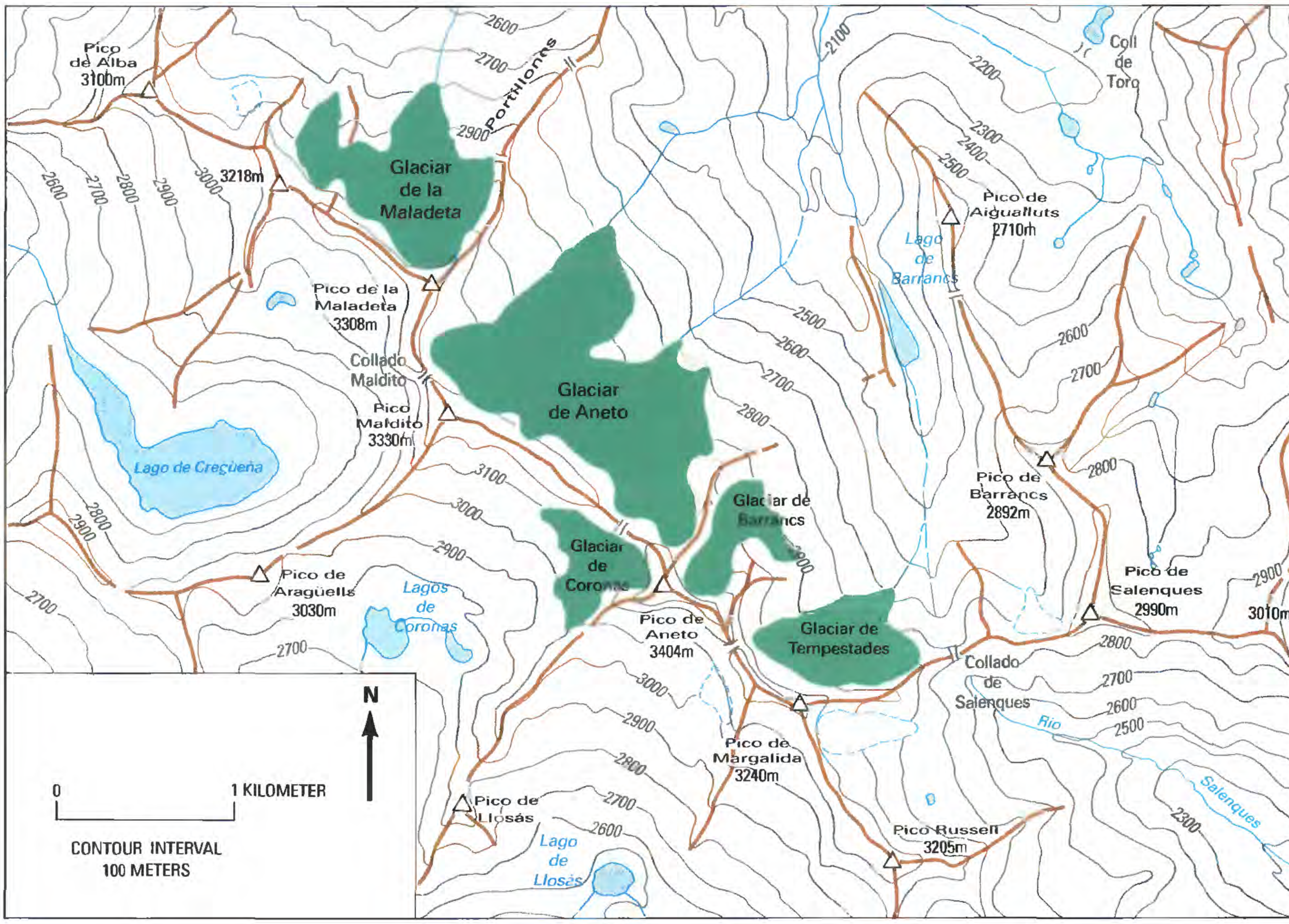

Figure 6.—*Maladeta massif and its glaciers in 1979. Former glaciers that are now reduced to snowfields are shown by dashed blue lines (northwest of Glaciar de Maladeta and south of Glaciar de Tempestades).*

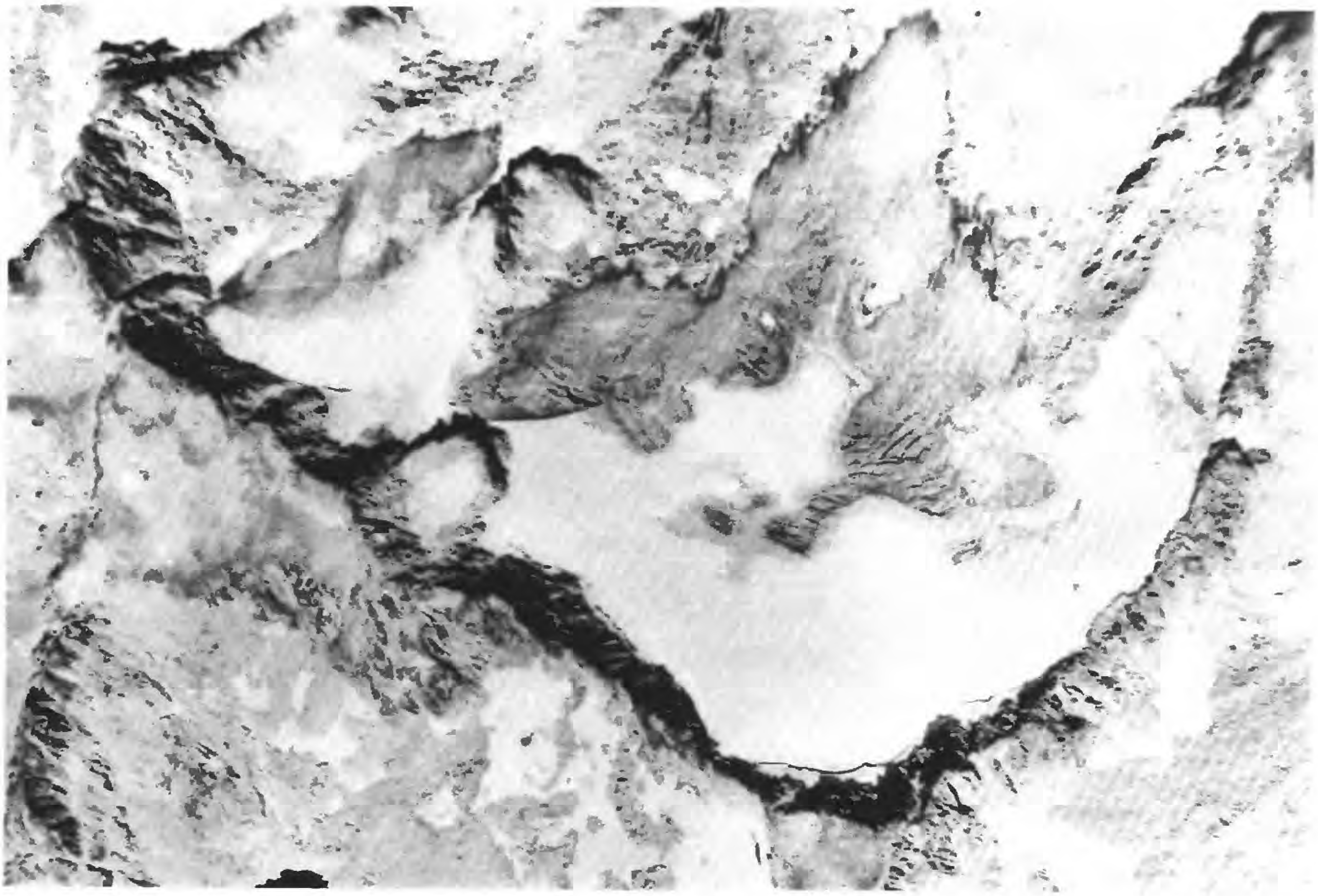

Figure 7.—*Vertical aerial photograph of Glaciar de la Maladeta. Photograph taken 26 August 1957 by the U.S. Air Force.*

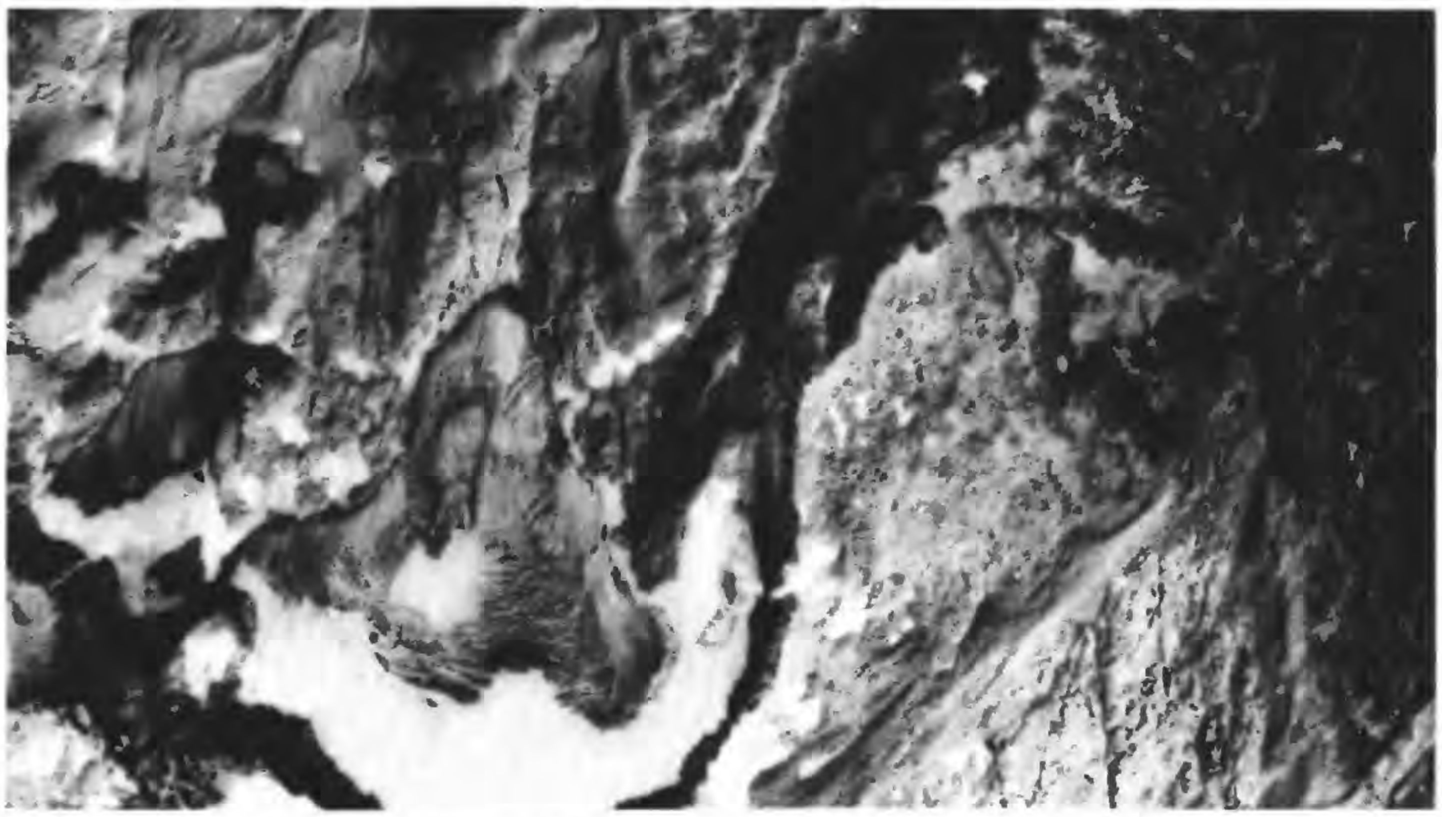

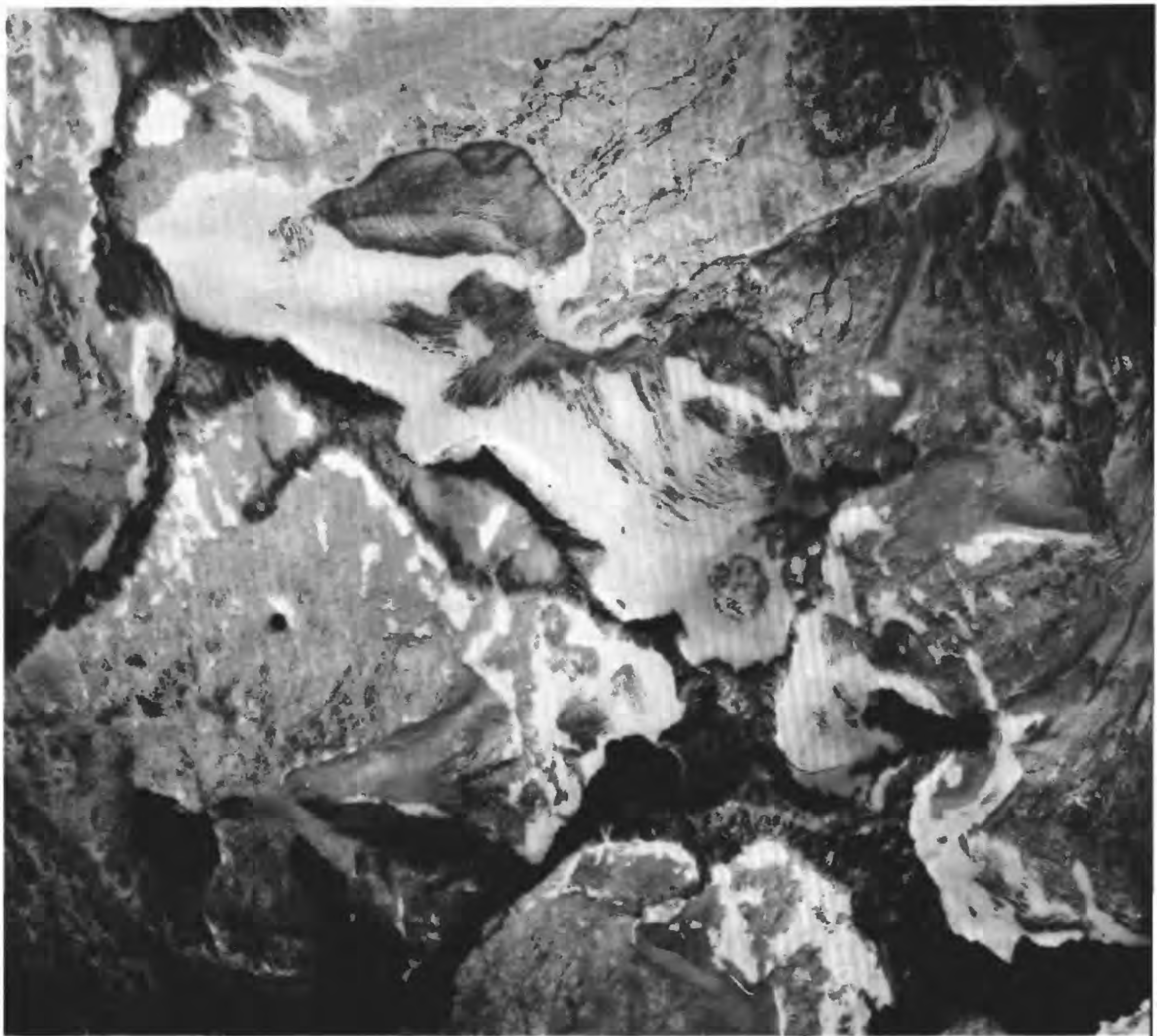

Figure 8.—*Vertical aerial photographs of the Maladeta massif taken 5 September 1988 by the Institut Cartografic de Catalunya. These photographs and others taken close to the time of maximum snowmelt have been used to determine more accurately the glacierized area of the Pyrenees. Compare with figures 6 and 7. The scale is approximately 1:22,000.*

References Cited

Barrère, P., 1953, Équilibre glaciaire actuel et Quaternaire dans l'Ouest des Pyrénées Centrales [Present and Quaternary glacier equilibrium in the west-central Pyrenees]: Revue Géographique des Pyrénées et du Sud-Ouest, v. 24, no. 2, p. 116–134.

Bellan, A., 1963, Quelques observations sur l'evolution des glaciers de la region Luchonnaise dans les Pyrénées Centrales [Some observations on the evolution of glaciers in the Luchon region of the central Pyrenees]: Grenoble, Société Hydrotechnique de France, Comptes Rendus, Section de Glaciologie, 10 p.

Bonaparte, R., 1891, Les variations périodiques des glaciers français [Periodic variations of the French glaciers]: Paris, Annuaire de Club Alpin Français, v. 17, p. 425–447.

Brúnet, R., 1955, La régression des glaciers au Celh de la Baque (Pyrénées Garonnaises) [Glacier recession in the Celh de la Baque (Garonnais Pyrenees)]: Revue Géographique des Pyrénées et du Sud-Ouest, v. 26, no. 1, p. 70–71.

Chabrol and others, 1953, Travaux de glaciologie effectués en 1952 sur les glaciers des Pyrénées Centrales [Glaciological studies in 1952 of the glaciers of the central Pyrenees]: Grenoble, Société Hydrotechnique de France, Comptes Rendus, Section de Glaciologie, 113 p.

Charpentier, J. von, 1823, Essai sur la constitution géognostique des Pyrénées [Essay on the geologic framework of the Pyrenees]: Paris, F.G. Levrault, 633 p.

Durand, M.-C., 1961, L'influence des glaciers sur les cours d'eau Pyrénéens (Bassins du Gave de Pau et de la Neste d'Aure) [The influence of glaciers on Pyrenees stream basins (Basins of Gave de Pau and Neste d'Aure)]: Revue Géographique des Pyrénées et du Sud-Ouest, v. 32, no. 4, p. 289–318.

Equip de Geomorfología Alpina, 1980, Catálogo de los glaciares de la Península Ibérica [Catalog of the glaciers of the Iberian Peninsula]: Notes de Geografia Física, no. 3, p. 35–55.

Eydoux, D., and Maury, L., 1907, Les glaciers orientaux du Pic Long (Pyrénées centrales) [Eastern glaciers of Pic Long (central Pyrenees)]: La Géographie (Bulletin de la Société de Géographie, Paris), v. 16, no. 1, p. 1–18.

Faura, M., 1923, Avenç de les geleres d'Aneto i Maladeta [Advance of Aneto and Maladeta glaciers]: Butlletí del Ciència e Culture, no. 347, p. 343–346.

Galibert, G., 1956, Le relief de haute montagne dans les massifs de Luchon et des Monts Maudits [The topography of the high mountains in the Luchonnais massif and Monts Maudits]: Revue Géographique des Pyrénées et du Sud-Ouest, v. 27, p. 41–73.

Gaurier, L., 1921, Études glaciaires dans les Pyrénées françaises et espagnolles de 1900 à 1909 [Glaciological studies in the French and Spanish Pyrenees from 1900 to 1909]: Pau, Garet-Haristoy, 363 p.

Gómez de Llarena, J., 1936, Algunos datos sobre el glaciar actual del Monte Perdido (Pirineos) [Some facts about the present glacier of Monte Perdido (Pyrenees)]: Boletín de la Real Sociedad Española de Historia Natural, v. 36, p. 327–343.

Hess, H., 1933, Das Eis der Erde [The glaciers of the world]: Handbuch der Geophysik, v. 7, no. 1, p. 1–121.

Höllermann, P., 1968, Die rezenten Gletscher der Pyrenäen [The recent glaciers of the Pyrenees]: Geographica Helvetica, v. 23, no. 4, p. 157–168.

Mercer, J.H., 1975, Glaciers of the Pyrenees, *in* Field, W.O., ed., Mountain glaciers of the northern hemisphere: Hanover, N.H., U.S. Army Cold Regions Research and Engineering Laboratory, p. 141–155.

Mounier, J., 1962, La tournée glaciologique 1961 dans les Pyrénées françaises et españoles [Glaciological tour in 1961 in the French and Spanish Pyrenees]: Revue Géographique des Pyrénées et du Sud-Ouest, v. 33, no. 1, p. 113–120.

Nicolás-Martínez, P.M., 1981, Morfología del Circo de Tucarroya (Macizo del Monte Perdido, Pirineo Aragonés) [Morphology of the Circo de Tucarroya (Massif of Monte Perdido, Aragon Pyrenees)]: Cuadernos de Investigación Geográfica, v. 7, no. 1-2, p. 51–80.

Penck, A., 1884, Die Eiszeit in den Pyrenäen [The ice age in the Pyrenees]: Mitteilungen des Vereins für Erdkunde zu Leipzig, v. 23, p. 163–231.

Plandé, R., 1939, Neiges et glaces d'aujourd'hui dans les Pyrénées [Snow and ice in the Pyrenees today]: Revue Géographique des Pyrénées et du Sud-Ouest, v. 10, p. 85–106.

Schrader, F., 1895, Sur l'étendue des glaciers des Pyrénées (On the extent of the glaciers of the Pyrenees): Paris, Annuaire de Club Alpin Français, v. 21, p. 403–423. (Reprinted as The Pyrenees, Edition Privat-Didier, Toulouse, 1936, v. 2, p. 201–221).

Soutadé, G., 1982, La haute montagne pyrénéenne dans le massif du Luchonnais [The high mountain Pyrenees in the Luchonnais massif]: Recherches Géographiques à Strasbourg, v. 16–17, (Hommages à R. Raynal), p. 143–145.

Taillefer, F., 1968, Extent of Pleistocene glaciation in the Pyrenees, *in* Wright, H.E., Jr., and Osburn, W.H., eds., Arctic and Alpine environments: International Association for Quaternary Research, v. 10, Indiana University Press, p. 255–266.

———1981, Glaciers des Pyrénées, reponse à quelques questions [Glaciers of the Pyrenees, response to some questions]: Revue Pyrénéenne, 6 Serie, v. 15, p. 11–14.

Thorarinsson, S., 1940, Present glacier shrinkage, and eustatic changes of sea-level: Geografiska Annaler, v. 22, no. 3–4, p. 131–159.

Trutat, E., 1875, Les glaciers de la Maladeta et le Pic de Posets [The glaciers of Maladeta and Pic de Posets]: Paris, Annuaire de Club Alpin Français, 440 p.

———1894, Les Pyrénées; les montagnes, les glaciers, les eaux minerales, les phénomènes de l'atmosphère, la flore, la faune et l'homme [The Pyrenees, the mountains, the glaciers, the mineral waters, the phenomena of the atmosphere, the flora, the fauna, and the inhabitants]: Paris, J.-B. Baillière et fils, 371 p.

van Summern, J., and Morrison, C.C., 1958, Glaciers of the Pyrenees, *in* Geographical study of mountain glaciation in the northern hemisphere: New York, American Geographical Society, p. 5.3.1–5.3.10.

Vedruna, J.M., 1956, Características de los glaciares del Macizo de la Maladeta [Characteristics of the glaciers of the Maladeta massif]: Ibérica, v. 24, no. 334, p. 109–117.

Vidal-Boix, C., 1933, Notas sobre la glaciología pirenaica [Facts about the Pyrenean glaciology]: Boletín de la Real Sociedad Española de Historia Natural, v. 33, p. 273–285.

Glaciers of Europe—

GLACIERS OF NORWAY

By GUNNAR ØSTREM *and* NILS HAAKENSEN

SATELLITE IMAGE ATLAS OF GLACIERS OF THE WORLD

Edited by RICHARD S. WILLIAMS, Jr., *and* JANE G. FERRIGNO

U.S. GEOLOGICAL SURVEY PROFESSIONAL PAPER 1386–E–3

Norway has 1,627 glaciers that total 2,595 square kilometers in area; these glaciers, most commonly ice caps, outlet, cirque, and valley glaciers, have been receding since about 1750

CONTENTS

Page

Abstract ---------- E63

Introduction ---------- 63

FIGURE 1. Index map showing areas covered by the three regional maps of Norwegian glaciers ---------- 65

2. *A*, Index map of glaciers in southern Norway; *B*, Index map of glaciers in the southern section of northern Scandinavia (Norway and Sweden); *C*, Index map of glaciers in the northern section of northern Scandinavia (Norway and Sweden) ---------- 66

TABLE 1. The size and location of the 34 largest glaciers in Norway ---------- 64

Occurrence of glaciers ---------- 67

Historical review ---------- 70

FIGURE 3. Oblique aerial photograph of Nigardsbreen and its valley, named Mjølverdalen, taken in 1951 by Olav Liestøl ---------- 71

TABLE 2. Variation of the terminus of Nigardsbreen outlet glacier during the period 1710–1991 ---------- 72

Modern glaciological investigations ---------- 73

FIGURE 4. Graph of glacier terminus observations at Bondhusbreen ---------- 73

5. Map showing the retreat of Nigardsbreen ---------- 74

6. Mass-balance diagram for the glacier Storbreen in Jotunheimen during the period 1949–89, combined with a line for the 5-year running mean ---------- 74

Mapping of glaciers ---------- 75

FIGURE 7. The oldest existing glacier map in Norway, published by J.D. Forbes in 1853, showing the glaciers in central Jotunheimen, southern Norway ---------- 75

8. The first glacier map of the Folgefonni ice cap and its surroundings, drawn by S.A. Sexe in 1864 ---------- 76

9. Nigardsbreen, mapped in 1937 by terrestrial photogrammetry by the German professor W. Pillewizer (1950) ---------- 77

10. *A*, Sketch of the Memuru glaciers in Jotunheimen, showing differences in glacier area and outline as depicted on an old map surveyed in 1849 and on a modern topographic map surveyed in 1938; *B*, Part of the Norwegian Series M 711, 1:50,000-scale topographic map (Sheet 1418 III–Jostedalen) of Nigardsbreen outlet glacier from Jostedalsbreen prepared from 1966 aerial photographs ---------- 77

11. A modern glacier map of Trollbergdalsbreen, northern Norway, compiled from aerial photographs ---------- 80

12. Index map to location of modern large-scale glacier maps of Norway published during the period 1952–88 ---------- 81

TABLE 3. Glacier maps published in Norway during the period 1952–88 - 80

Historic and modern photographs and satellite images ---------- 82

FIGURE 13. Two of the earliest pictures of Norwegian glaciers: *A*, An artistic portrayal of Bondhusbreen, an outlet glacier from the Folgefonni ice cap, which was painted by Niels Hertzberg in 1801; *B*, Nigardsbreen shown in great detail in an 1822 painting by the well-known Norwegian artist Johannes Flintoe ---------- 82

14. *A*, Nigardsbreen in 1851 from an illustration by J.D. Forbes (1853); *B*, Nigardsbreen in 1864 from a photograph by the pharmacist/photographer Selmer ---------- 83

15. One of the oldest known photographs of Nigardsbreen, taken by J.B. Rekstad in 1899 ---------- 84

16. Engabreen, an outlet glacier from the northwestern part of the Svartisen ice cap, photographed in 1883 by Charles Rabot ---------- 85

Page

FIGURE 17. Photograph of Engabreen in 1974 ---------- E85
18. One of the first known vertical aerial photographs of a Norwegian glacier, showing the snout of Nigardsbreen and its associated terminal moraine system ---------- 86
19. Vertical aerial photograph of the terminus of Nigardsbreen taken in August 1974 ---------- 87
20. Nigardsbreen, in July 1959, photographed from nearly the same position as that illustrated by Forbes (fig. 14*A*) and photographed by Rekstad (fig. 15) ---------- 88
21. Nigardsbreen, photographed in 1980 from nearly the same position as shown in figures 13*B*, 14, 15, and 20 ---------- 88
22. Two photographs showing the retreat of Mjølkevoldsbreen (western side of the Jostedalsbreen ice cap) between 1933 and 1939 ---------- 89
23. Landsat MSS false-color composite image of Seilandsjøkulen, the northernmost glacier in Norway, taken on 29 July 1972 (1006–09481, MSS band 5 with a red filter, MSS band 6 with a blue filter, and MSS band 7 with a green filter; Path 211, Row 10) ---------- 90
24. Vertical aerial photograph of the small Seilandsjøkulen ice cap, the northernmost glacier in Norway ---------- 91
25. A "map" of Seilandsjøkulen ice cap produced as a computer-generated dotprint from Landsat MSS band 7 digital data (1006–09481; 29 July 1972; Path 211, Row 10) ---------- 91
26. NOAA image of southern Norway taken on 1 June 1982 ---------- 92
27. NOAA image of southern Norway taken on 30 July 1982 ---------- 92
28. A section of a Landsat MSS false-color composite image (2565–10004; MSS band 4 with a blue filter, MSS band 5 with a green filter, and MSS band 7 with a red filter; 9 August 1976; Path 216, Row 17) showing the Jostedalsbreen ice cap, the largest continuous ice mass in continental Europe ---------- 93
29. A section of Landsat MSS image 22059–10083 (11 September 1980; Path 216, Row 18) showing the Hardangervidda mountain plateau in central southern Norway ---------- 94

Glaciological phenomena ---------- 95

FIGURE 30. Diagram showing the clear linear relation between the elevation of the equilibrium line at the end of the ablation season and the specific net balance of a glacier ---------- 95
31. Landsat special MSS false-color composite image of the Jostedalsbreen ice cap (2583–10001; MSS band 4 in blue, MSS band 7 in yellow; 27 August 1976; Path 216, Row 17) ---------- 96
32. Map of areas of exposed ice as of 27 August 1976 that were determined on 24 outlet glaciers in the Jostedalsbreen area from the Landsat MSS image (2583–10001; 27 August 1976; Path 216, Row 17) ---------- 97
33. Part of a special false-color composite Landsat MSS image of the Jotunheimen area (2583–10001; MSS band 4 in blue, MSS band 7 in yellow; 27 August 1976; Path 216, Row 17), covering approximately 45 × 55 km ---------- 98
34. Map of the Jotunheimen high-mountain area in the central part of southern Norway ---------- 99
35. A Landsat MSS special false-color composite image (2187–10082; 28 July 1975; Path 216, Row 17) of the high-altitude areas of the central part of southern Norway ---------- 100
36. A digital printout (dotprint) from Landsat MSS image 1336–10260; band 4; 24 June 1973; Path 217, Row 17 ---------- 101
37. Map showing the specific discharge in the area around the Hardangerjøkulen ice cap ---------- 101

TABLE 4. Results of height determinations of the transient snowline level on 27 August 1976 from a Landsat image of the area of the Jostedalsbreen ice cap ---------- 97
5. Results of height determinations of the transient snowline level on 27 August 1976 from a Landsat image of the Jotunheimen area, central southern Norway ---------- 100

Page

Glaciers on Landsat images ---------- E102

FIGURE 38. Landsat MSS image (2186–10005; band 7; 27 July 1975; Path 215, Row 13) showing glaciers in the southern part of northern Norway ---------- 102

39. Map of the Svartisen-Blåmannsisen area in northern Norway showing the second, fourth, and fifth largest glaciers in Norway ---------- 103

40. Index map to the optimum Landsat 1, 2, and 3 images of the glaciers of Norway ---------- 104

TABLE 6. A list of the most useful Landsat images of the glaciers of Norway as of the end of 1980 ---------- 105

7. Optimum Landsat 1, 2, and 3 images of the glaciers of Norway ---------- 106

Acknowledgments ---------- 108

References cited ---------- 109

GLACIERS OF EUROPE—

GLACIERS OF NORWAY

By GUNNAR ØSTREM[1] *and* NILS HAAKENSEN[1]

Abstract

Detailed glacier inventories made in 1969, 1973, and, finally, in 1988 for a modern glacier atlas of Scandinavia list 1,627 glaciers in Norway that have a total area of 2,595 square kilometers. Glaciers occur principally as ice caps, outlet glaciers, cirque glaciers, and small valley glaciers. The largest ice cap, Jostedalsbreen, covers 487 square kilometers and is the largest continuous ice mass in continental Europe. Since the "Little Ice Age" (culminating in about 1750 in Norway), when glaciers reached their greatest extent in historic time, the glaciers have retreated almost continuously, and advances have been relatively small. Minor glacier advances occurred during the first part of this century, but a major glacier recession started about 1930. Systematic measurements of glaciers in Norway began in the late 19th century, although the earliest recorded observation of termini fluctuation was made in 1742. The longest series of mass-balance observations are those of Storbreen, begun in 1949. Mass-balance measurements are carried out for other selected glaciers for hydropower purposes. High quality aerial photographs are available for almost all glacierized areas in Norway, and 31 modern glacier maps have been published at 1:10,000 to 1:50,000 scales. Landsat images have limited value in Norway for most glaciological studies, but the satellite data have been used to qualitatively evaluate suspended sediment in lakes and fjords and to monitor the transient snowline as an indication of the approximate net mass balance.

Introduction

Norway is a relatively small country, 323,000 km^2, but the total area covered by glaciers is proportionally higher than for most other countries in Europe. According to glacier inventories made during 1969 and 1988 in southern Norway and during 1973 in northern Norway, about 2,595 km^2 of the land is covered by glaciers (Østrem and Ziegler, 1969; Østrem and others, 1973, 1988). In the compilation of these inventories, which were made in accordance with criteria recommended by UNESCO (1970), all glacier masses were divided according to a system based on hydrological factors. This system was chosen because the information obtained would be used mainly for hydrological purposes. It was also decided that glaciers that drain into different rivers should be subdivided into separate "glacier units," each unit draining into one river. The total number of such glacier units amounts to 2,113, whereas the number of "glaciers," continuous masses of ice regarded as one glacier body, amounts to 1,627.

The largest ice cap in Norway, the Jostedalsbreen, covers 487 km^2 and is the largest continuous ice mass in continental Europe. Only Iceland and Spitzbergen (Svalbard) have larger glaciers. For the hydrological reasons discussed above, Jostedalsbreen was divided into 61 individual glacier units. On the other hand, the smaller Norwegian glaciers are, in general, not subdivided, because most valley glaciers and cirque glaciers drain into only one river. Table 1 lists the size and location of the 34 largest glaciers of Norway.

---

[1]Norwegian Water Resources and Energy Administration, P.O. Box 5091, Majorstuen, N-0301, Oslo 3, Norway.

TABLE 1.—*The size and location of the 34 largest glaciers in Norway (from Østrem and others, 1988)*

Glacier name	Area (km^2)	Height in meters		Location	
		maximum	minimum	East long	North lat
1. Jostedalsbreen	487	2,000	350	7°00′	61°40′
2. Vestre Svartisen	221	1,580	20	14°00′	66°40′
3. Søndre Folgefonni	168	1,660	490	6°20′	60°00′
4. Østre Svartisen	148	1,550	208	14°10′	66°40′
5. Blåmannsisen	87	1,560	810	16°00′	67°20′
6. Hardangerjøkulen	73	1,850	1,050	7°20′	60°30′
7. Myklebustbreen (Snønipbreen)	50	1,830	890	6°40′	61°40′
8. Okstindbreen	46	1,740	750	14°10′	66°00′
9. Øksfjordjøkulen	41	1,170	330	22°00′	70°10′
10. Harbardsbreen	36	1,950	1,250	7°40′	61°40′
11. Salajekna	33	1,680	830	16°20′	67°10′
12. Spørteggbreen	28	1,750	1,270	7°30′	61°40′
13. Nordre Folgefonni	26	1,640	990	6°30′	60°10′
14. Giččečåkka	25	1,500	870	16°50′	68°00′
15. Frostisen	25	1,710	840	17°10′	68°10′
16. Sekke/Sikilbreen	24	1,930	1,330	7°40′	61°50′
17. Tindefjellbreen	22	1,850	940	7°10′	61°50′
18. Simlebreen	21	1,320	780	14°30′	66°50′
19. Tystigbreen	21	1,900	1,220	7°20′	62°00′
20. Holåbreen	20	2,020	1,320	7°50′	61°50′
21. Grovabreen	20	1,640	1,090	6°30′	61°30′
22. Ålfotbreen	17	1,380	890	5°40′	61°40′
23. Fresvikbreen	15	1,660	1,270	6°50′	61°00′
24. Seilandsjøkulen	14	940	480	23°20′	70°20′
25. Strupbreen/Koppangsbreen	14	1,400	320	20°10′	69°40′
26. Smørstabbreen	14	2,070	1,390	8°05′	61°35′
27. Gjegnalundsbreen	13	1,590	900	5°50′	61°50′
28. Hellstugu/Vestre Memurubre	12	2,200	1,470	8°30′	61°30′
29. Unnamed glacier in Beiardalen	12	1,560	760	14°20′	66°40′
30. Storsteinsfjellbreen	12	1,850	930	18°00′	68°40′
31. Søndre Jostefonn	11	1,620	960	6°35′	61°25′
32. Midtre Folgefonni	11	1,570	1,100	6°30′	60°10′
33. Langfjordjøkulen	10	1,020	360	21°40′	70°10′
34. Veobreen	9	2,300	1,530	8°30′	61°35′

More detailed information about the length of glaciers, their orientation, the date of aerial photography, and similar information can be found in the two glacier atlases of Norway ((Østrem and Ziegler, 1969, revised edition by Østrem and others, 1988; Østrem and others, 1973). The glacier atlases also contain considerable geomorphological information, such as surface characteristics, morainal features, proglacial lakes, and other data related to each glacier unit listed.

The distribution of glaciers in Norway is shown on figures 1 and 2. These glacier index maps show that a concentration of glaciers exists in southwestern Norway and also in certain parts of northern Norway. Because glaciers seem to "attract more precipitation" than glacier-free areas in the mountainous parts of Norway, the glacierized areas have gained increased interest from waterpower engineers. During the last several decades, several hydroelectric powerplants have been considered for construction near the glacier-capped mountains because of the quantity of water available at high altitudes and the relatively short distances to sea level. In connection with this, mass-balance investigations have been undertaken at a number of selected glaciers, and special, highly detailed maps have been prepared for several glaciers in Norway during the last two decades (see table 3). Because glaciers have, in the past, been regarded as a remote and relatively uninteresting aspect of the landscape, very little information has been recorded on their behavior.

Figure 1.—The areas covered by the three regional maps of Norwegian glaciers. Numbers correlate with the three maps in figure 2.

Only in a few cases, for example, Nigardsbreen and Engabreen, have accurate measurements been made of their variations prior to the end of the last century (Øyen, 1898).

Aerial photographs have been available during the last few decades, and detailed measurements of glacier mass balance were begun in 1948 when Dr. Olav Liestøl initiated systematic glaciologic investigations at Storbreen in Jotunheimen, southern Norway. His series of observations on Storbreen is the second longest of its kind in the world. Observations of variations in the position of termini of glaciers in Norway have been made on various occasions dating from about 1740 (see the section entitled "Historical Review").

Satellite images represent a new tool for glaciologists. In Norway, however, where good maps and aerial photographs exist and where glaciers are relatively small and accessible for detailed observations, Landsat images are of limited value for most types of glaciological studies. Due to the fact, however, that the elevation of the transient snowline (TSL) can be determined easily from Landsat images when compared with topographic maps of an area, and because there is a relation between this elevation at the end of the summer and the mass balance of the glacier, it seems possible that satellite images in the future may become a valuable tool for glacier-hydrologic studies. A high TSL indicates a negative mass balance, whereas the TSL will be situated at a lower altitude in years of positive mass balance. Thus, it is hoped that the high costs associated with fieldwork for the determination of selected glaciers' mass balance can be reduced, provided that optimum satellite

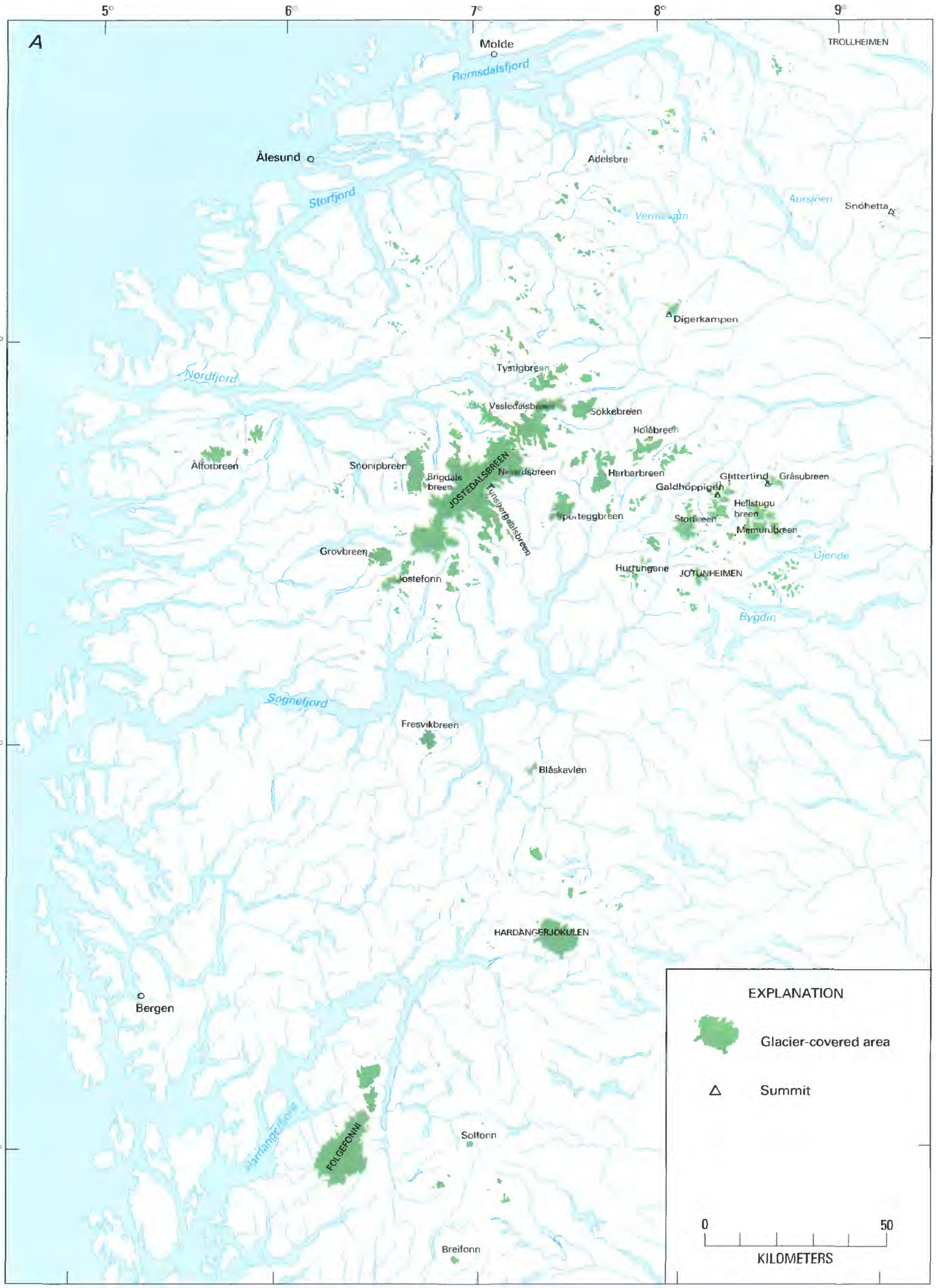
A
5°
6°
7°
8°
9°
62°
61°
60°
Molde
Romsdalsfjord
TROLLHEIMEN
Ålesund
Storfjord
Adelsbre
Aursjøen
Snøhetta
Digerkampen
Nordfjord
Tystigbreen
Vesledalsbreen
Sokkebreen
Holåbreen
Ålfotbreen
Snønipbreen
Brigdalsbreen
JOSTEDALSBREEN
Harbarbreen
Glittertind
Gråsubreen
Galdhøppigen
Hellstugubreen
Storbreen
Memurubreen
Gjende
Grovbreen
Jostefonn
Hurrungane
JOTUNHEIMEN
Bygdin
Sognefjord
Fresvikbreen
Blåskavlen
HARDANGERJØKULEN
Bergen
FOLGEFONNI
Hardangerfjord
Solfonn
Breifonn
EXPLANATION
Glacier-covered area
Summit
0
50
KILOMETERS

◀ *Figure 2A.—The glaciers in southern Norway (from Østrem and Ziegler, 1969). Map location shown by number 1 on figure 1. Base from Norges Vassdrags- og Elektrisitetsvesen, 1:500,000, Glacier Map of Southern Norway, 1969.*

images can be acquired at the end of the summer ablation season. However, cloud cover presents a serious problem that may be solved in the future, if cloud-penetrating sensors (such as radar images) can produce images that have sufficient detail.

In the text that follows, the occurrence, observational history, modern investigations, mapping, photographing and imaging, glaciological phenomena, and Landsat images of Norway's glaciers will be discussed. In Norway, glaciers occur principally as ice caps, outlet glaciers from these ice caps, cirque glaciers, and small valley glaciers. In the Norwegian language, several words are used to describe the term "glacier." Perhaps the oldest word still in use is "jøkul" (ice cap). The most common word used for glacier in modern Norwegian is "bre." "Fonn" and "is" are also used, although more commonly on the island of Svalbard (see "Modern Glaciological Investigations") than in Norway. "Botn" is used in reference to a cirque glacier, and "skåkje" is used locally in the Hardanger area in reference to three outlet glaciers of Hardangerjøkulen. In a few places "skavl" (snow drift) is used for small glaciers. Most geographic names of Norway's glaciers are compounds, as in Jostedalsbreen. Jostedals-bre-en is composed of a descriptive location name, followed by the word for glacier and the definite article in Norwegian, or literally, Joste Valley–glacier–the. Another example is Storbreen or, literally, large–glacier–the. In northern Norway, several ice caps carry Lappish names, such as Salajekna and Giččečåkka (see table 1). The Lappish word for glacier is variously spelled as jekna, jiek'ki, jietna, and so on.

Occurrence of Glaciers

The glaciers in Norway are concentrated in two areas: (1) the high-mountain area in the central and western part of southern Norway that has the dominating ice caps Jostedalsbreen, Hardangerjøkulen, and Folgefonni, and the numerous valley and cirque glaciers in the Jotunheimen mountain area and (2) northern Norway, where most of the glaciers are concentrated in Nordland County—the narrowest part of Norway— approximately between 66° N. and 68° N. latitude. However, a number of valley glaciers and small ice caps are also distributed farther north, particularly on the Lyngen peninsula, east of Tromsø. The northernmost glacier in continental Europe is found on the island Seiland, 70°25′ N. latitude (see the Landsat image and the aerial photograph of Seilandsjøkulen in figures 23 and 24, respectively).

The largest glaciers in Norway are ice caps. Valley glaciers are of reasonable length—normally not longer than a few times their width. The smallest are cirque glaciers, with an almost circular outline.

Very early descriptions of permanent ice and snow do exist (for example, the work by P.C. Friis in 1632), but no area measurements were made. The oldest known Norwegian glacier map, published in 1853 of the Jotunheimen area, is discussed in the section "Mapping of Glaciers."

Inventories of the glaciers in Norway have been made at various intervals. The first really complete inventory was made by Olav Liestøl in 1958, however. His inventory was first printed as a small booklet but was later included in the comprehensive publication "Glaciers and Snowfields in Norway" (Liestøl, 1962a). According to Liestøl's inventory, the total number of glaciers and snow fields in Norway amounted to approximately 1,750 and covered a total area of about 3,900 km^2. This figure is considerably higher than the figure given in the modern glacier atlases (1,627 glaciers covering 2,595 km^2), but this discrepancy is mainly due to the fact that Liestøl's inventory included both glaciers and snow-

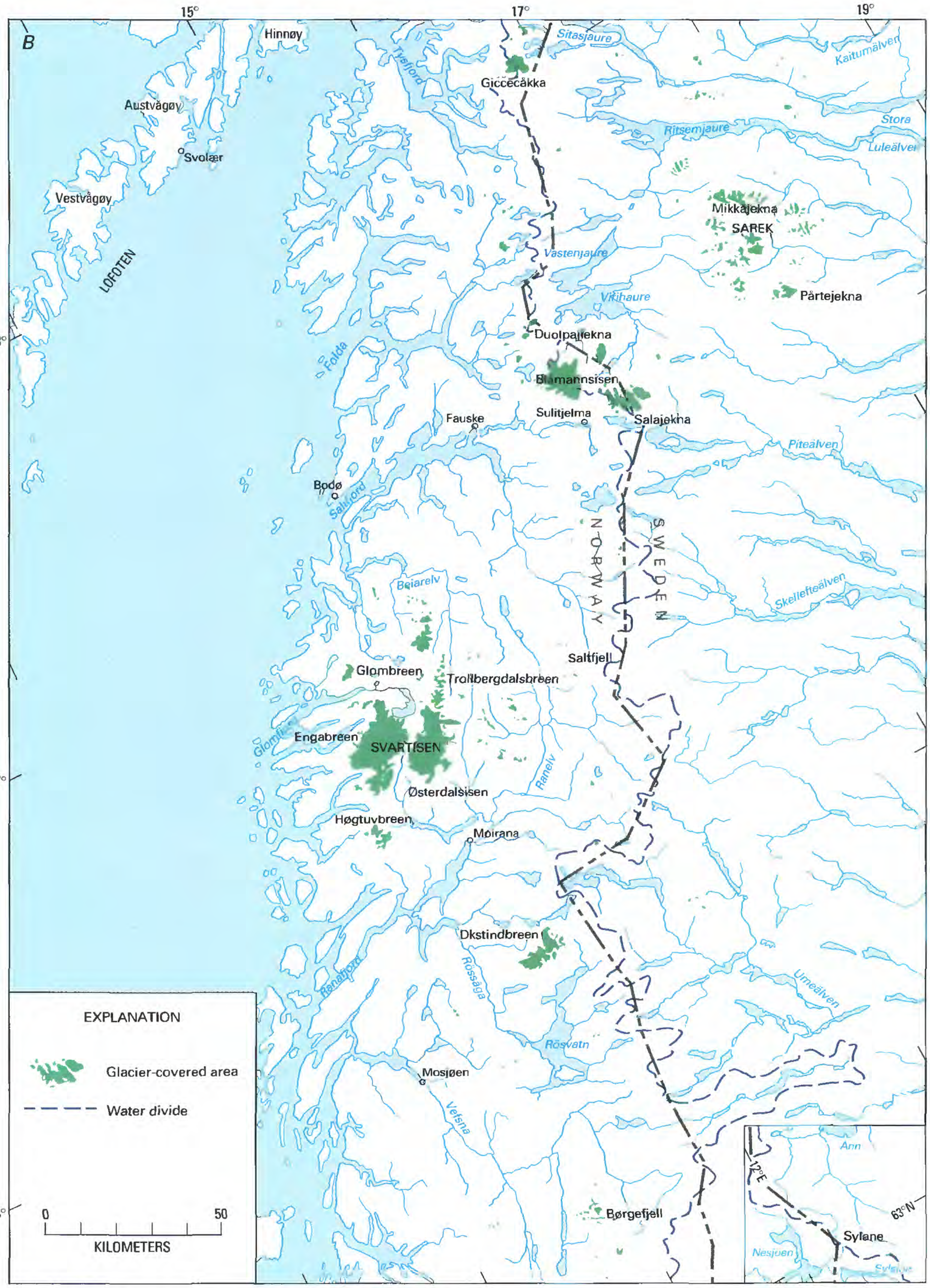

Figure 2B.—The glaciers in the southern section of northern Scandinavia (Norway and Sweden) (from Østrem and others, 1973). Map location shown by number 2 on figure 1. Base from Norges Vassdrags- og Elektrisitetsvesen og Stockholms Universitet, 1:500,000, Glacier Map of Northern Scandinavia, Southern Sheet, 1972.

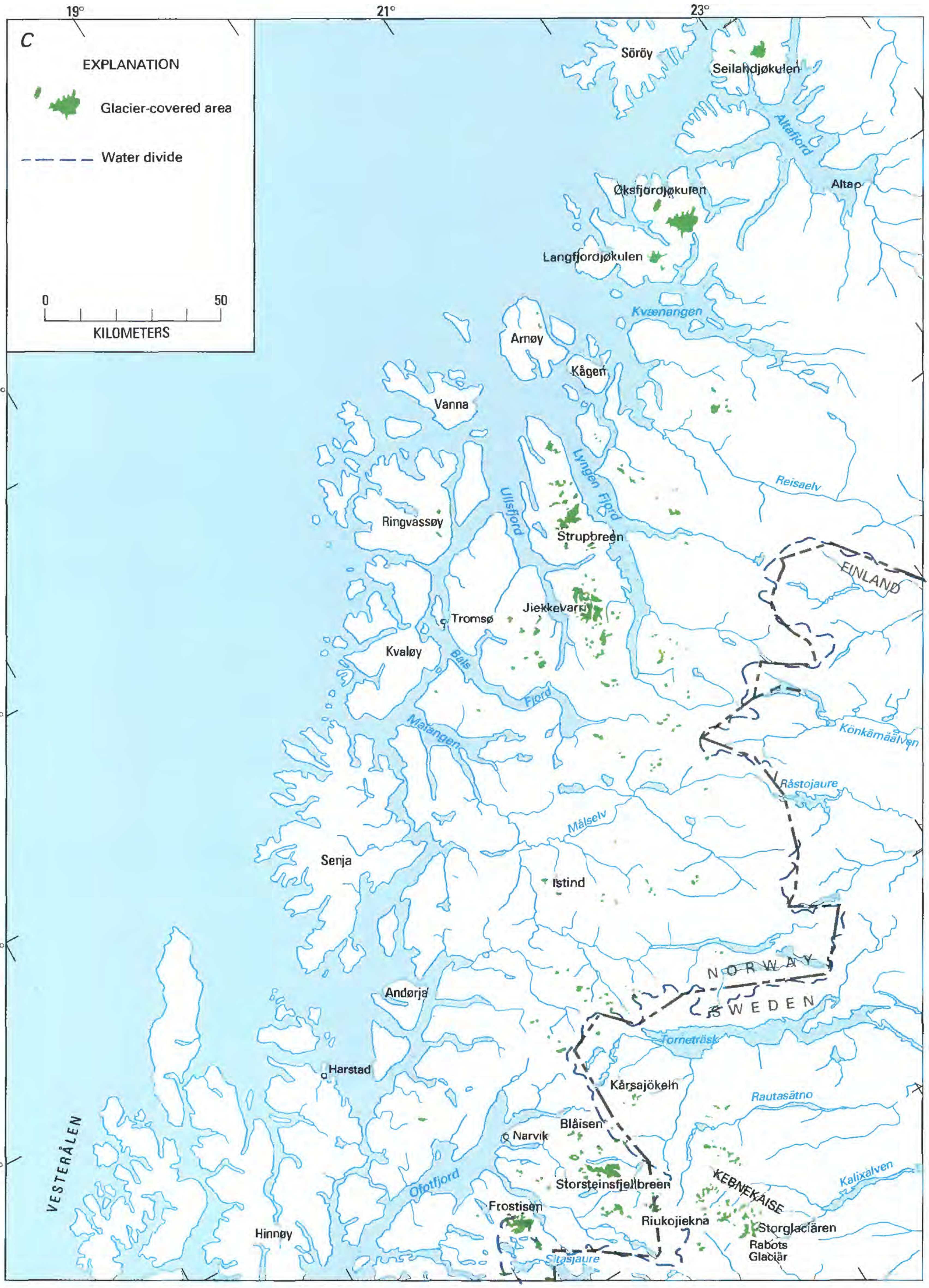

***Figure 2C.**—The glaciers in the northern section of northern Scandinavia (Norway and Sweden) (from Østrem and others, 1973). Map location shown by number 3 on figure 1. Base from Norges Vassdrags- og Elektrisitetsvesen og Stockholms Universitet, 1:500,000, Glacier Map of Northern Scandinavia, Northern Sheet, 1972.*

fields. The topographic maps that Liestøl used as source materials did not distinguish cartographically between true glaciers and snow fields.

Another inventory, which was less detailed, was made by Østrem (1963). He prepared an index map at a scale of 1:1,800,000 showing all glaciers in Scandinavia. An improved version of the southern part of this map was made in 1963, when a glacier map of southern Norway was issued at a scale of 1:500,000 and printed in three colors (Liestøl and Østrem, 1963). Detailed glacier inventories were prepared of southern Norway in the late 1960's (Østrem and Ziegler, 1969) and of northern Norway and Sweden in the early 1970's (Østrem and others, 1973). A second glacier inventory for southern Norway was completed in the late 1980's (Østrem and others, 1988).

A concept related to the existence of glaciers is the so-called *glaciation level*. This term is defined as the critical mountain height above which glaciers can form. A mountain that is higher than the glaciation level will normally carry one or more glaciers, provided the topography is suitable for glacier formation. Mountains lower than the critical level will not collect sufficient snow to form a glacier, or complete disappearance of the snow during the summer makes glacier formation impossible.

On the western coast of southern Norway, this critical level is about 1,200 m, so that mountains higher than this level normally carry glaciers. In the eastern part of Jotunheimen, the glaciation level is about 2,200 m; consequently, all glaciers there are situated at much higher elevations than those near the coast. Similar conditions prevail in northern Norway, where glaciers form at considerably lower elevations in the coastal districts than in the more continental inland part of the Scandinavian peninsula. For further details please refer to Østrem (1964, p. 333–335; 1966, p. 128).

Another concept, the *equilibrium line*, is directly related to the mass balance of glaciers. It divides the glaciers in two parts: the accumulation area and the ablation area. Strictly speaking this is a theoretical and invisible line across the glacier, the exact determination of which is a complicated procedure. It is situated higher up on the glaciers during years of negative mass balance and lower during years of positive mass balance. For most temperate glaciers, however, the equilibrium line coincides quite well with the TSL at the end of the melt season, and this line is fully visible on the glacier because it forms the transition between remaining snow and uncovered (bare) glacier ice. Its position can be determined on satellite images, and certain conclusions can be drawn about the "health" of the glacier (see the section entitled "Glaciological Phenomena").

Historical Review

During historic time there have been several periods of glacier advance and retreat. However, very little has been written about these events in Norway, mainly because glaciers were relatively far from populated areas and generally of little interest to people. However, some documentation exists concerning the last large glacier advance, called "The Little Ice Age," which culminated about 1750 in Norway. As a result of several years of climatic deterioration, most glaciers advanced considerably, and, in many cases, the outermost moraine at any glacier today was deposited during this large advance. The first known direct measurement of a glacier terminus in relation to a fixed point was made in 1742 at Tverråbreen in the Jostedalen area (Hoel and Norvik, 1962, p. 9).

The first written documentation of glacier measurements made in Norway was of the outlet glacier Nigardsbreen, which drains southeastward from the Jostedalsbreen ice cap. This glacier advanced so far that it reached cultivated land and even destroyed houses. Farmers who lost their fertile land wrote to the king, Fredrik V, and asked for tax exemption because they had lost their grazing fields. The local judge and the minister were sent to the area to inspect the damage. The minister, Matthias Foss, wrote a "Short description from Justedalen 1750," which was published somewhat later (Foss, 1803). He wrote:

> In the year 1742, in the middle of August, his Majesty's representative and the judge went to observe the areas which had been destroyed by the glacier. A measurement was made from the glacier to the nearest house, and this distance was then 200 feet. On the same day next year, 1743, the glacier had not only moved forward these 200 feet, but it also increased in width and had pushed away the houses and tumbled them around. The ice had also plowed up large amounts of soil and gravel and large rocks and crushed these rocks into small pieces which are still visible. The owner of the farm had to leave his house in a great hurry to try to find another place to stay. His farm, named Nigard, was destroyed together with all its fertile land, and the glacier had also approached other areas during the following years. The farm Bjerkehougen lost cultivated land so that only the houses were left, and it is not possible to live there any more. However, we have noted that the ice has retreated since 1748 but only very slowly. In addition to the destroyed arable land the glacier is also harmful because it produces cold winds so that rime on the ground is not unusual during the summer.

Since this disastrous advance, the glacier has retreated almost continuously, interrupted only by relatively small advances. From 1748 until the present time, the retreat amounts to about 5 km (table 2). The effect from the small advances can be seen easily on the photograph (fig. 3). The series of small morainal ridges has been dated and described in detail by Faegri (1933) and by Andersen and Sollid (1971). A map showing the various moraines and the time of their formation has been constructed on the basis of all available information.

As a curiosity, it should be mentioned that glacier ice has been a commercial product in Norway for some time. From the beginning of the

Figure 3.—*Oblique aerial photograph of Nigardsbreen and its valley, named Mjølverdalen, taken in 1951 by Olav Liestøl. The terminal moraines from the 1750 advance are in the lower left of the picture. The distance between the 1750 moraine and the present position of the glacier terminus is about 5 km.*

TABLE 2.—*Variation of the terminus of Nigardsbreen outlet glacier during the period 1710–1991 (based upon data in Østrem and others, 1976, and additional information)*

Year	Variation (in meters)	Year	Variation (in meters)
1710–35	+2,800[1]	1940–41	−41
1735–42	0	1941–42	−19
1742–43	+100[1]	1942–43	−38
1743–48	+50[1]	1943–44	−10
1748–1818	−540	1944–45	−43
1818–23	−70[1]	1945–46	−35
1823–45	−80[1]	1946–47	−113
1845–73	−710	1947–48	−145
1873–99	−595	1948–49	−92
1899–1903	−73	1949–50	−47
1903–07	+8	1950–51	−56
1907–08	−10	1951–52	−87
1908–09	+18	1952–53	−60
1909–10	−31	1953–54	−41
1910–11	+5	1954–55	−72
1911–12	−40	1955–56	−53
1912–13	−11	1956–57	−34
1913–14	−13	1957–58	−49
1914–15	−25	1958–59	−66
1915–16	−20	1959–60	−87
1916–17	−19	1960–61	−55
1917–18	−16	1961–62	−30
1918–19	−21	1962–63	−65
1919–20	−14	1963–64	−65
1920–21	−16	1964–72	−515
1921–22	+7	1972–73	−65
1922–23	−23	1973–74	−46
1923–24	−13	1974–75	−16
1924–25	+10	1975–76	−1
1925–26	+16	1976–78	−14
1926–27	−16	1978–79	+3
1927–28	+12	1979–80	+1
1928–29	+20	1980–81	−11
1929–30	+6	1981–82	+4
1930–31	−9	1982–83	−6
1931–32	−15	1983–84	−2
1932–33	−15	1984–85	−4
1933–34	−45	1985–86	−7
1934–35	−25	1986–87	+11
1935–36	+5	1987–88	−18
1936–37	−17	1988–89	+1
1937–38	−21	1989–90	+7
1938–39	−50	1990–91	+10
1939–40	−28		

[1] Approximative values only.

last century it is reported that quantities of ice were carried from the Bondhusbreen outlet glacier (from the Folgefonni ice cap) down to the small community of Sunndal for sale to fishermen who used it for preservation of their fish. The first known ice export dates from 1822, when a ship carried glacier ice to Scotland. Later, in 1863, a small road was built up the valley to facilitate ice transport. Similarly, ice was taken for the same reason from a small regenerated glacier in Jøkulfjord, near the Øksfjordjøkulen ice cap in northern Norway. Here, during recent years, ice was blasted off the cone-shaped glacier that reaches sea level. However, this activity ceased in 1949 when a refrigeration plant was built in the area.

Modern Glaciological Investigations

More systematic measurements of glaciers in Norway started about 100 years ago, when some scientists began to establish survey points in front of selected glaciers for annual position measurements of each terminus. This kind of systematic measurement was first made by the geologist P.A. Øyen, who published his figures in annual reports (Øyen, 1898, 1907, 1915), and by J.B. Rekstad (1905), who also photographed many glaciers. His historic glass negatives contain a wealth of information from 1890 to about 1910. C. de Seue, a Norwegian Army officer and meteorologist, took several photographs of the Jostedalsbreen and Svartisen ice caps in 1868 (de Seue, 1870). The famous French geographer Charles Rabot took many photographs in Scandinavia during the 1880's. Several of his photographs provide considerable information about the position of selected glacier termini at that time. Later, Professor Werner Werenskiold began a long series of glacier-termini measurements in the Jotunheimen mountains. Many of his research students did their fieldwork in glaciology under his guidance. His interest in glaciology is recorded in several scientific papers, and he also reviewed the history of glaciological research in Norway (Hoel and Werenskiold, 1962, p. 14–18) in a work that contains a listing of many old sources. An extensive bibliography is also given in Hoel and Norvik (1962).

We know that minor glacier advances have occurred during the first part of this century (Liestøl, 1962b), but a period of major glacier retreat started about 1930 (fig. 4). One of the best studied glaciers in modern time is the Nigardsbreen outlet glacier, where several scientists, both

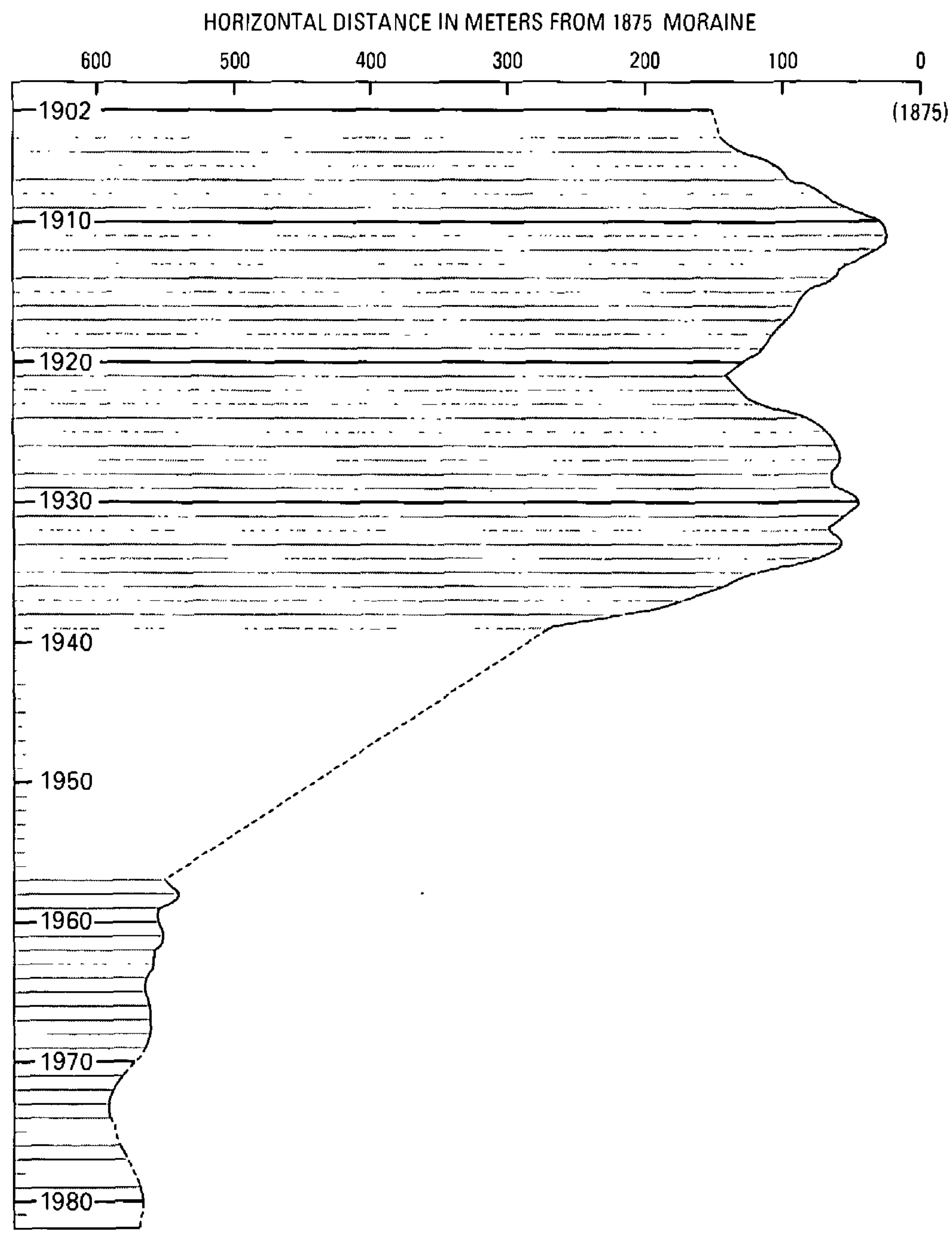

***Figure 4.**—Glacier terminus observations at Bondhusbreen. Distances given are in meters, measured horizontally from the 1875 terminal moraine (modified from the text accompanying the 1979 map of Bondhusbreen noted on table 3).*

Norwegian and foreign, have carried out various types of glaciological studies. Detailed mass-balance investigations were started there in 1962. A map showing the retreat of Nigardsbreen since the 1750's is shown on figure 5, and the results of termini measurements are plotted in table 2. The longest mass-balance-observation series made in Norway concerns Storbreen, a valley glacier in the Jotunheimen mountain massif where measurements have been made since 1949 (fig. 6). For five other glaciers in Norway there are observations covering a time span of almost 30 years or longer (Haakensen, 1982, p. 49). At least some of these observations will continue in the future because of the need to gather hydrological data for various waterpower developments in Norway.

Continuous mass-balance investigations have also been carried out at intervals of 5 to 6 years for other selected glaciers in Norway (Roland and Haakensen, 1985; Østrem and others, 1991; Haakensen and Elvehøy, 1992). These studies have also been done mainly for hydrologic purposes.

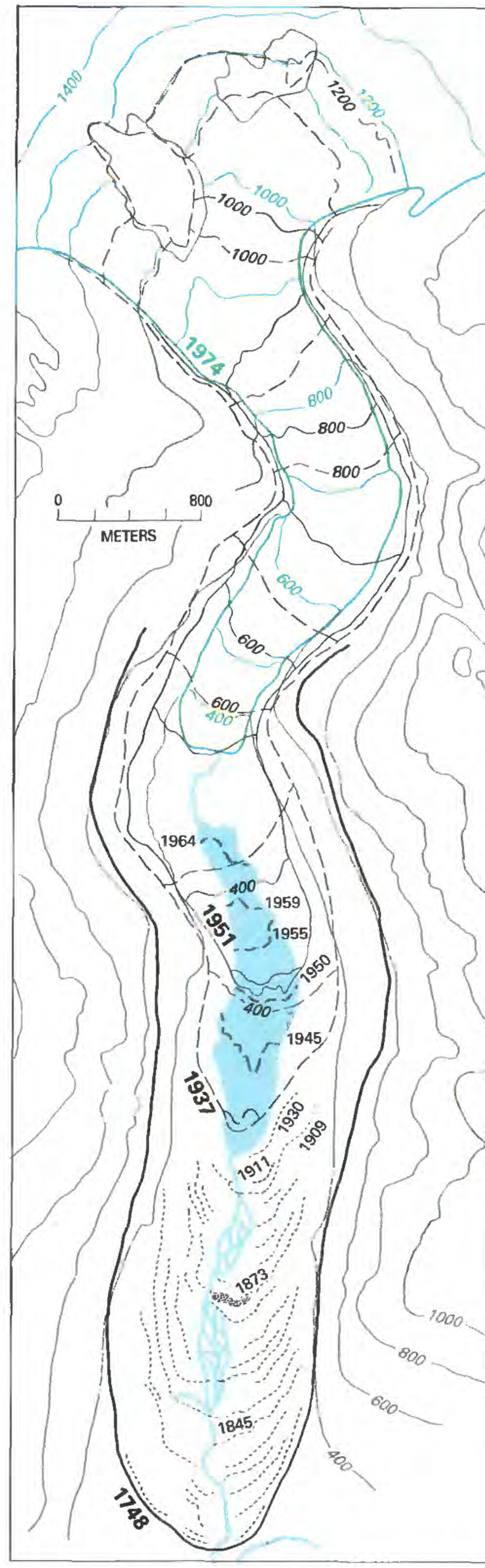

Figure 5.*—Map of the retreat of Nigardsbreen. The information is based upon various datings of existing moraine ridges (oldest stages) and direct observations made in recent years. The dotted lines represent location of moraine ridges. The dashed lines represent 1937 glacier terminus and contours. The solid black lines represent 1951 glacier terminus and contours. The green lines represent 1974 glacier terminus and contours. The contours on the surrounding landscape are shown in gray (from Østrem and others, 1976). Since 1974, the retreat of the terminus of Nigardsbreen has been only 42 m. For more details, see Andersen and Sollid (1971). (See also table 2.)*

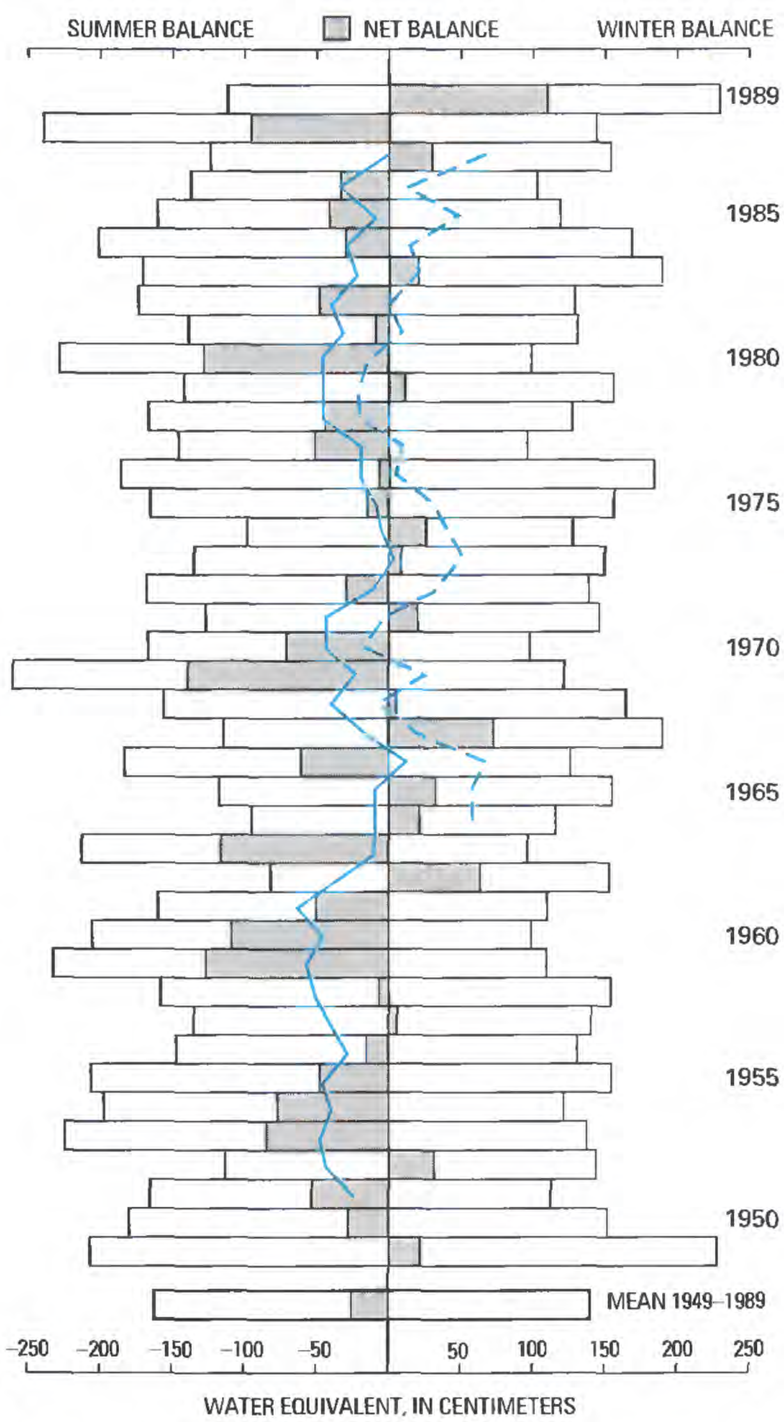

◀ ***Figure 6.****—Mass-balance diagram for the glacier Storbreen in Jotunheimen during the period 1949–89, combined with a line for the 5-year running mean. The total mass loss in 41 years amounts to 10.5 m of water equivalent. For comparison, the 5-year running mean for Nigardsbreen is also indicated (dashed line). The average net balance for Nigardsbreen is about 0.6 m higher than that for Storbreen.*

Mapping of Glaciers

__Figure 7.__—The oldest existing glacier map in Norway, published by J.D. Forbes in 1853, showing the glaciers in central Jotunheimen, southern Norway.

No real glacier maps were made in Norway until the British Professor J.D. Forbes produced a map (fig. 7) of some of the most important glaciers in Jotunheimen during his visit to Norway in 1851 (Forbes, 1853). Another early glacier map was produced by Professor S.A. Sexe at

the University of Oslo. He studied the ice cap Folgefonni and produced a color map (fig. 8) (Sexe, 1864). In the 1920's, the famous Swedish Professor H.W:son Ahlmann started a glaciological research program on Styggedalsbreen in western Jotunheimen. Professor Ahlmann produced two glacier maps (Ahlmann, 1922) that were printed in color at a scale of 1:20,000. The Norwegian professors Adolf Hoel and Werner Werenskiold produced a glacier map (1:10,000) of Tverråbreen in Jotunheimen by terrestrial photogrammetry in 1927 (Hoel and Werenskiold, 1962). Some German scientific expeditions were also active in the production of glacier maps during the 1930's. An example is Wolfgang Pillewizer's map (Pillewizer, 1950) of the lower part of Nigardsbreen from 1937 (fig. 9).

Topographic maps also contain some glacier information, but the oldest maps (called Amtskart and at a scale of 1:250,000) produced in the last

Figure 8.—The first glacier map of the Folgefonni ice cap and its surroundings, drawn by S.A. Sexe in 1864.

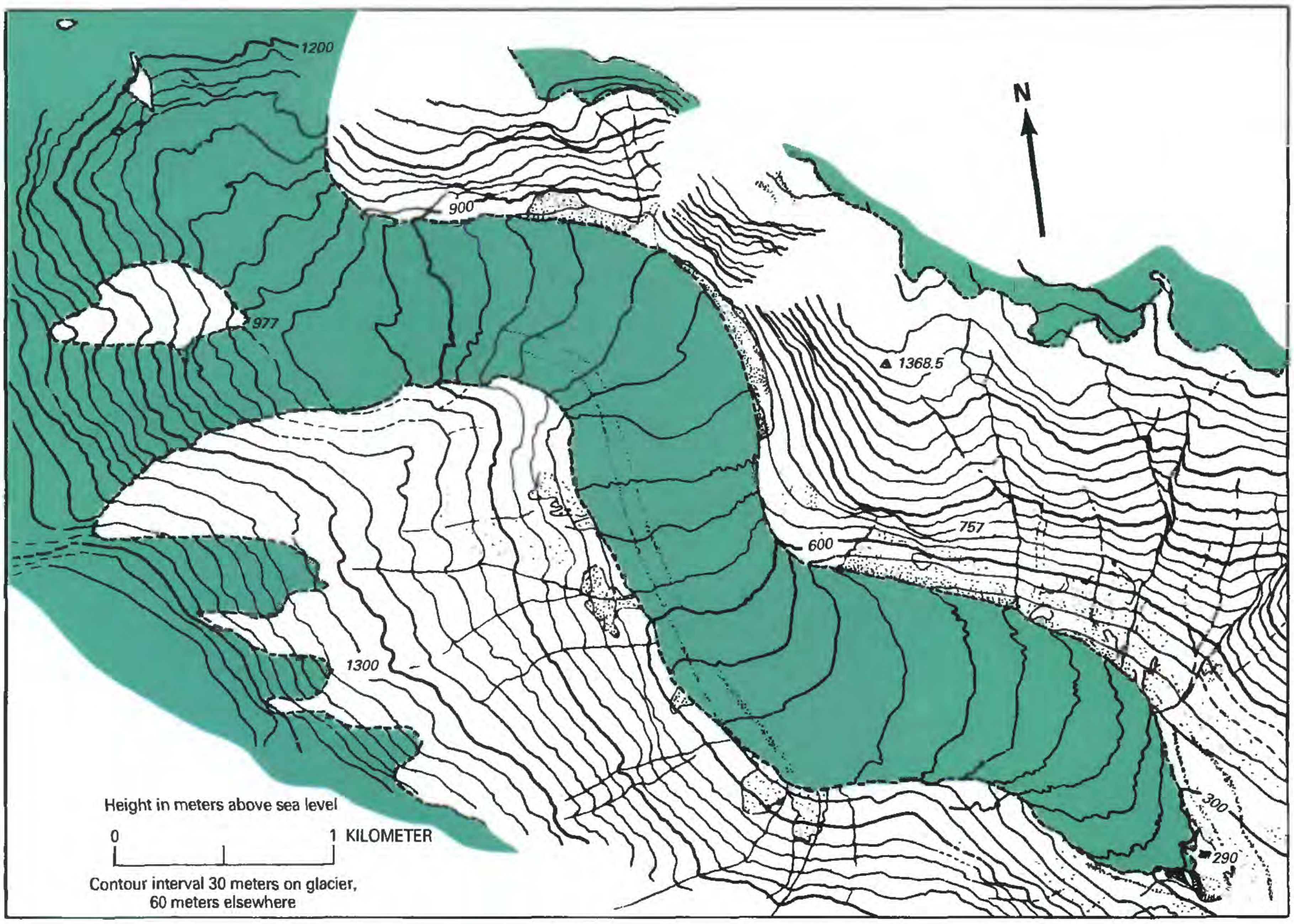

Figure 9.—Nigardsbreen, mapped in 1937 by terrestrial photogrammetry by the German professor W. Pillewizer (1950).

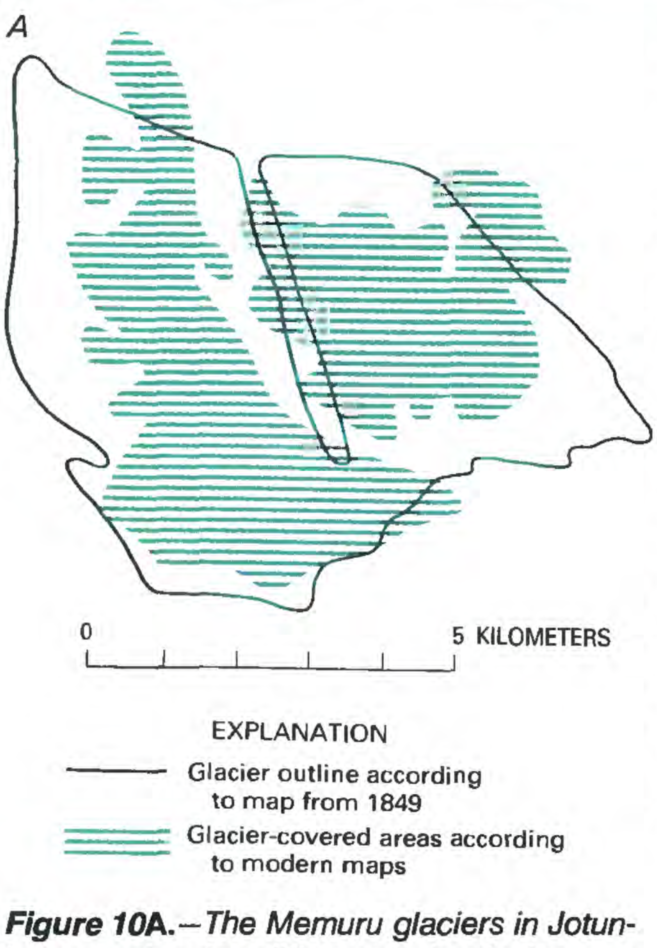

Figure 10A.—*The Memuru glaciers in Jotunheimen, showing differences in glacier area and outline as depicted on an old map surveyed in 1849 (Amtskart, scale 1:250,000) and on a modern topographic map surveyed in 1938 (scale 1:100,000; from Østrem, 1960). Compare with figure 7.*

century were not very reliable concerning the existence or size of glaciers (fig. 10*A*). Modern topographic maps are much better (fig. 10*B*), but the relatively small scale often limits the value of the information for glaciological studies. Furthermore, in some cases, permanent snow fields are interpreted as glaciers and marked as such on the maps.

Modern glacier maps are defined as maps produced according to standards established during the First International Symposium on Glacier Mapping held in Ottawa, Canada, in 1965. Such maps have been prepared for selected glaciers in connection with studies by the Norwegian Water Resources and Energy Administration (NVE) for planning of future hydroelectric power developments (fig. 11) and by the Norwegian Polar Research Institute for scientific purposes. Some glacier maps have also been produced for other reasons, such as special research projects. A list of all published glacier maps is given in table 3, and an index map showing the location of each map is shown in figure 12.

Figure 10B.—*Part of the Norwegian Series M 711, 1:50,000-scale topographic map (Sheet 1418 III—Jostedalen) of Nigardsbreen outlet glacier from Jostedalsbreen prepared from 1966 aerial photographs. Map published in 1973 by the Norwegian Geographical Survey (NGO).* ▶


Kjenndalskruna
Kjenndalsbreen
JOSTEDALSBREEN
Högste Breakulen
Steinmannen
Tuftebreen
Kvitekulen
Kråfjellet
Bergset-
breen
Vetlenibba
Vetledalsbreen
Höganibba

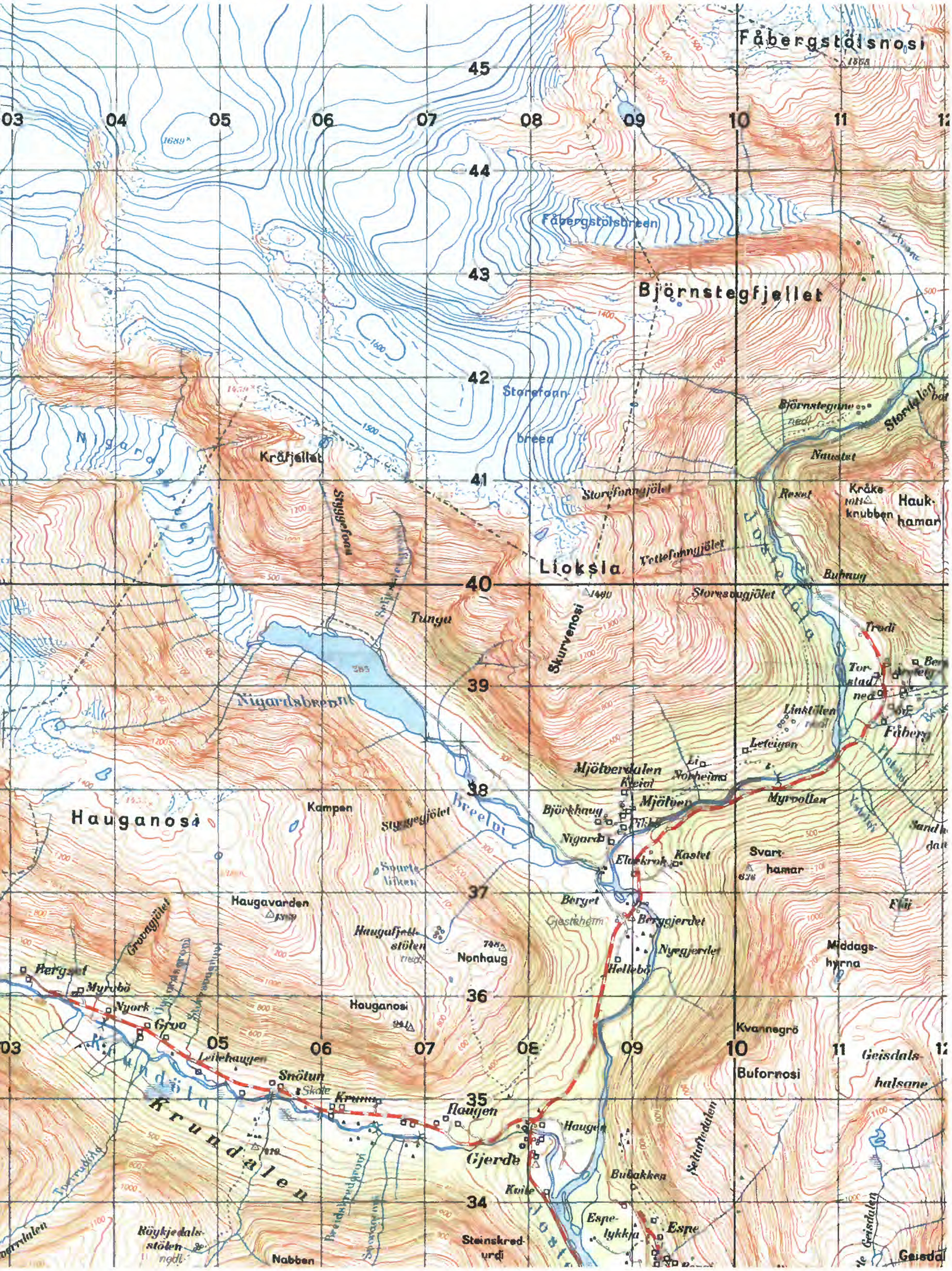

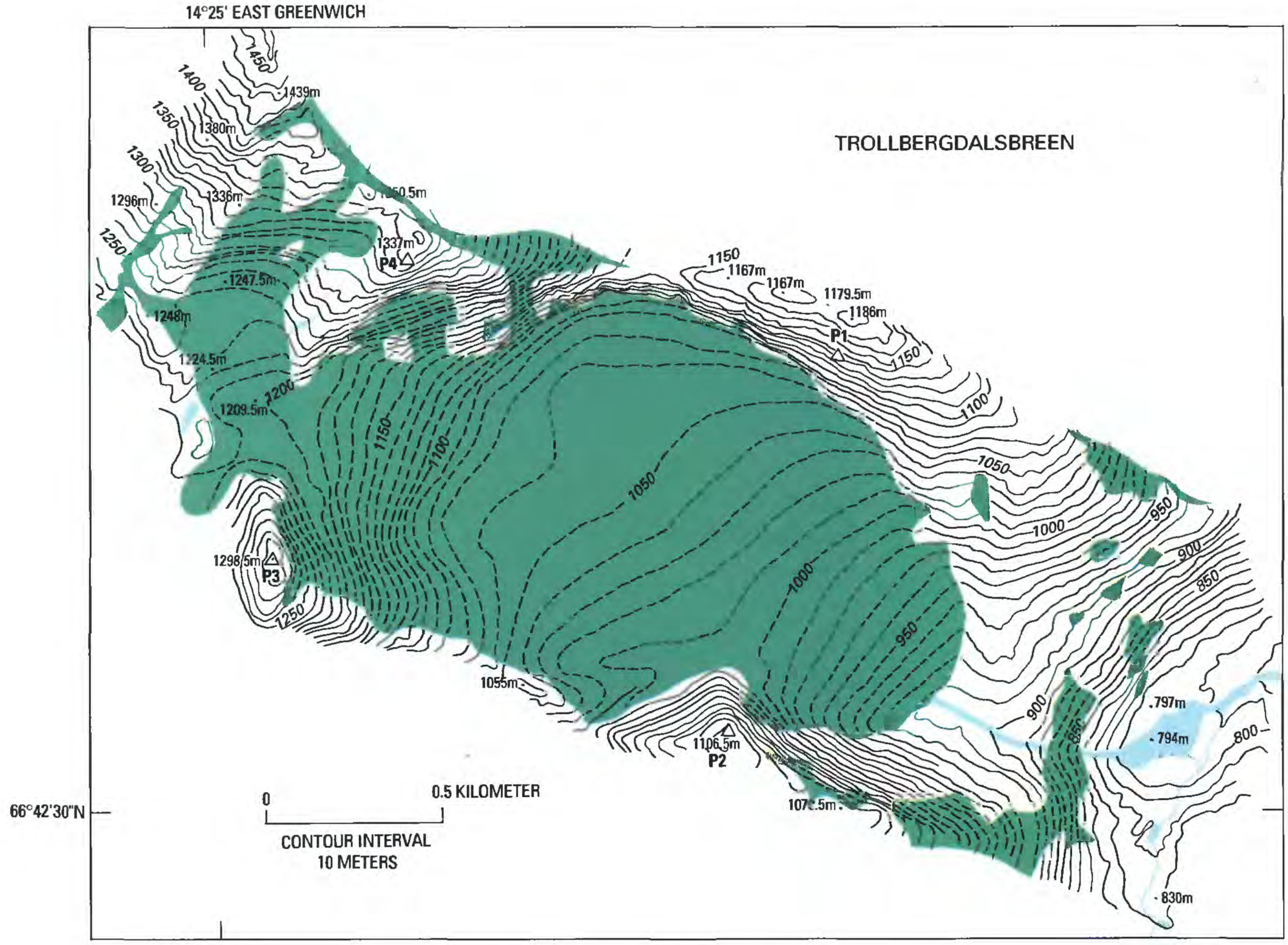

***Figure 11.**—A modern glacier map of Trollbergdalsbreen, northern Norway, compiled from aerial photographs taken on 25 August 1968. The original map was printed in 1970 in four colors at a scale of 1:10,000 with 10-m contour intervals, in accordance with guidelines proposed by the First International Symposium on Glacier Mapping, which was held in Ottawa, 1965.*

TABLE 3.—*Glacier maps published in Norway during the period 1952–88 (see also fig. 12)*

[NPI, Norwegian Polar Research Institute; NVE, Norwegian Water Resources and Energy Administration; SU, University of Stockholm]

Map name	Scale	Year of aerial photography	Year of issue	Issued by	Colors	Remarks
Storbreen	1:10,000	1951	1952	NPI	Three	
Østerdalsisen	1:20,000	1954	1956	NPI	One	Manuscript; only lower part.
Tverråbreen	1:10,000	1927	1962	NPI	Three	
Hellstugubreen	1:10,000	1941	1962	NPI	Three	
Blåisen ved Sildvikvann	1:10,000	1960	1963	NVE	One	Manuscript.
Part of Folgefonni	1:10,000	1959	1964	NVE	Three	
Storsteinsfjell	1:10,000	1960	1964	NVE	Four	
Nigardsbreen	1:20,000	1955,1964	1965	NVE	Three	
Hellstugubreen	1:10,000	1962	1965	NVE	Three	
Tunsbergdalsbreen	1:20,000	1955,1964	1966	NVE	Four	
Cainhavarrebreen	1:10,000	1960	1967	NVE	Two	
Erdalsbreen–Vesledalsbreen	1,20,000	1966	1967	NVE	Four	
Gråsubreen	1:10,000	1968	1968	NVE	Four	
Austre Memurubre	1:10,000	1966	1968	NVE	Four	
Vestre Memurubre	1:10,000	1966	1968	NVE	Four	
Ålfotbreen	1:10,000	1968	1969	NVE	Four	

TABLE 3.—*Glacier maps published in Norway during the period 1952–88 (see also fig. 12)*—Continued

[NPI, Norwegian Polar Research Institute; NVE, Norwegian Water Resources and Energy Administration; SU, University of Stockholm]

Map name	Scale	Year of aerial photography	Year of issue	Issued by	Colors	Remarks
Hellstugubreen	1:10,000	1968	1969	NPI	One	Manuscript.
Engabreen	1:20,000	1968	1970	NVE	Four	
Trollbergdalsbreen	1:10,000	1968	1970	NVE	Four	
Storbreen	1:10,000	1968	1971	NPI	Four	
Høgtuvbreen	1:10,000	1972	1973	NVE	Four	
Nigardsbreen	1:20,000	1966, 1974	1975	NVE	Four	
Bondhusbreen	1:10,000	1959, 1979	1979	NVE	Five	
Hellstugubreen	1:10,000	1980	1980	NVE and NPI	Four	
Riukojietna[1]	1:10,000	1960, 1978	1983	NVE and SU	Three	Two maps.
Salajekna (Sulitjelma)[1]	1:50,000 1:20,000	1950, 1957–58 1971, 1980–82	1983	NVE and SU	Four	Four maps.
Midtre Folgefonni	1:20,000 1:10,000	1959 1981	1984	NVE and SU	Four	Two maps.
Gråsubreen	1:10,000	1984	1985	NVE and SU	Four	
Strupbreen	1:20,000 1:10,000	1952, 1978 1985	1985	NVE and SU	Four	Three maps.
Sylglaciären[2]	1:10,000	1958, 1966, 1971, 1975, 1982	1985	NVE and SU	Four	Five maps.
Nigardsbreen	1:20,000	1984	1988	NVE	Four	

[1] The glacier is partly located in Sweden.
[2] The glacier is located in Sweden.

Figure 12.—Location of modern large-scale glacier maps of Norway published during the period 1952–88. Because some glaciers have been mapped more than once (red squares), one number may represent more than one glacier map.

Historic and Modern Photographs and Satellite Images

Because of the distance from most glaciers to inhabited areas in Norway, there is a lack of historic pictures depicting glacier termini. However, some Norwegian paintings from the last century do exist, but they were not intended to show ice and snow; glaciers were included by chance only if the artist happened to have them within the field of view. In most cases the glaciers portrayed are so distant that the painting has very little value from a glaciological point of view.

The first "artistic" representation of glaciers in Norway was probably made by the Norwegian minister Niels Hertzberg, who portrayed the outlet glacier Bondhusbreen in August 1801 (fig. 13*A*). Another early glacier picture was made by the painter Johannes Flintoe; his product shows Nigardsbreen in 1822 in great detail—almost as good as that of a photograph (fig. 13*B*). Later, Professor J.D. Forbes from Edinburgh, who visited Norway in 1851, made a good drawing of Nigardsbreen that was printed in color (Forbes, 1853; fig. 14*A*). A photograph of

Figure 13A.*—An artistic portrayal of Bondhusbreen, an outlet glacier from the Folgefonni ice cap, painted by Niels Hertzberg in 1801. This is the earliest known picture of a Norwegian glacier.*

__Figure 13B.__—Nigardsbreen shown in great detail in an 1822 painting by the well-known Norwegian artist Johannes Flintoe.

__Figure 14A.__—Nigardsbreen in 1851 from an illustration by J.D. Forbes (1853).

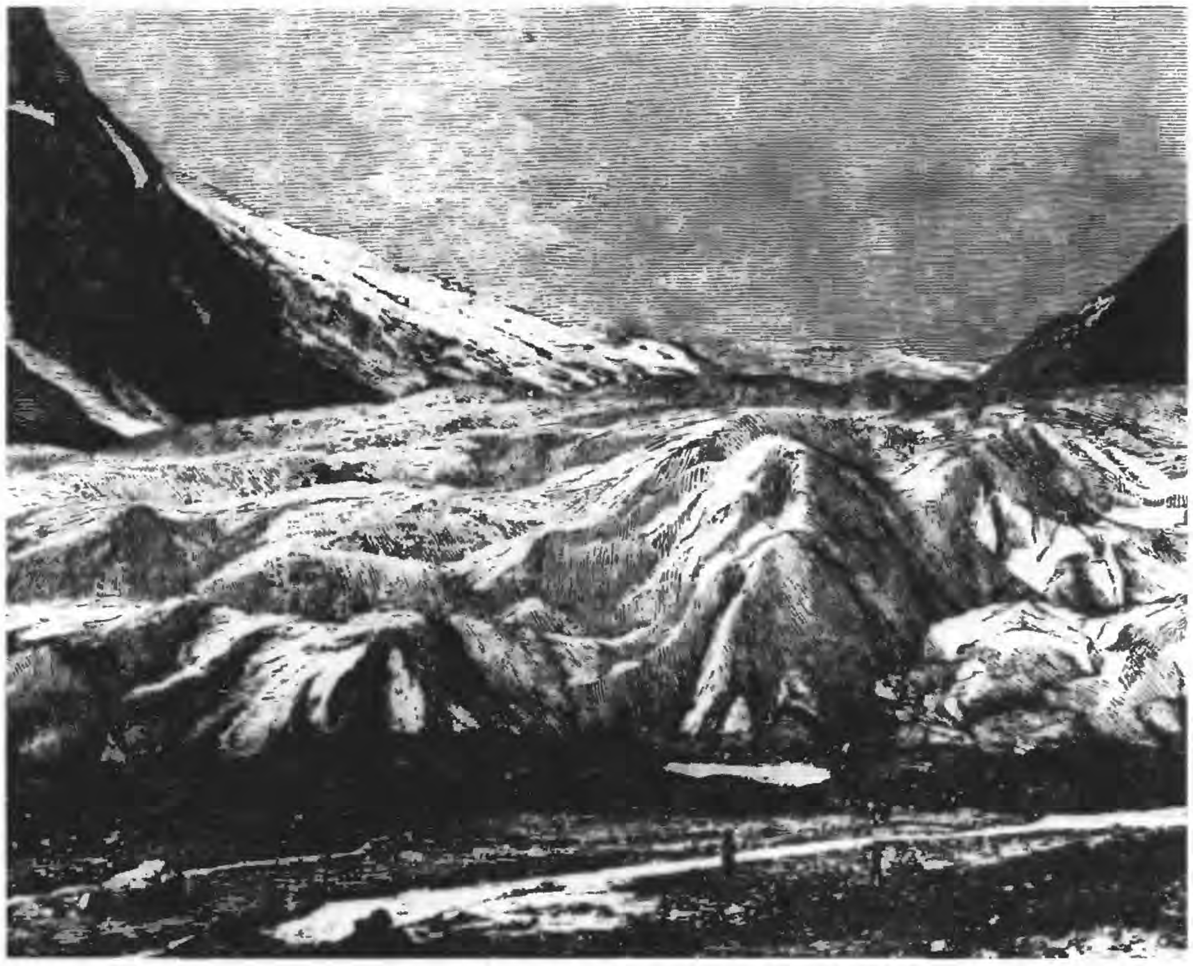

Figure 14B.—Nigardsbreen in 1864 from a photograph by the pharmacist/photographer Selmer that was published in Illustreret Nyhedsblad. The original photograph was copied in a woodcut by H.P. Hansen in Leipzig so that it could be printed in the newspaper.

Figure 15.—One of the oldest known photographs of Nigardsbreen, taken by J.B. Rekstad in 1899. The glacier front had then retreated more than 1 km since J.D. Forbes made his drawing in 1851. (See fig. 14A.)

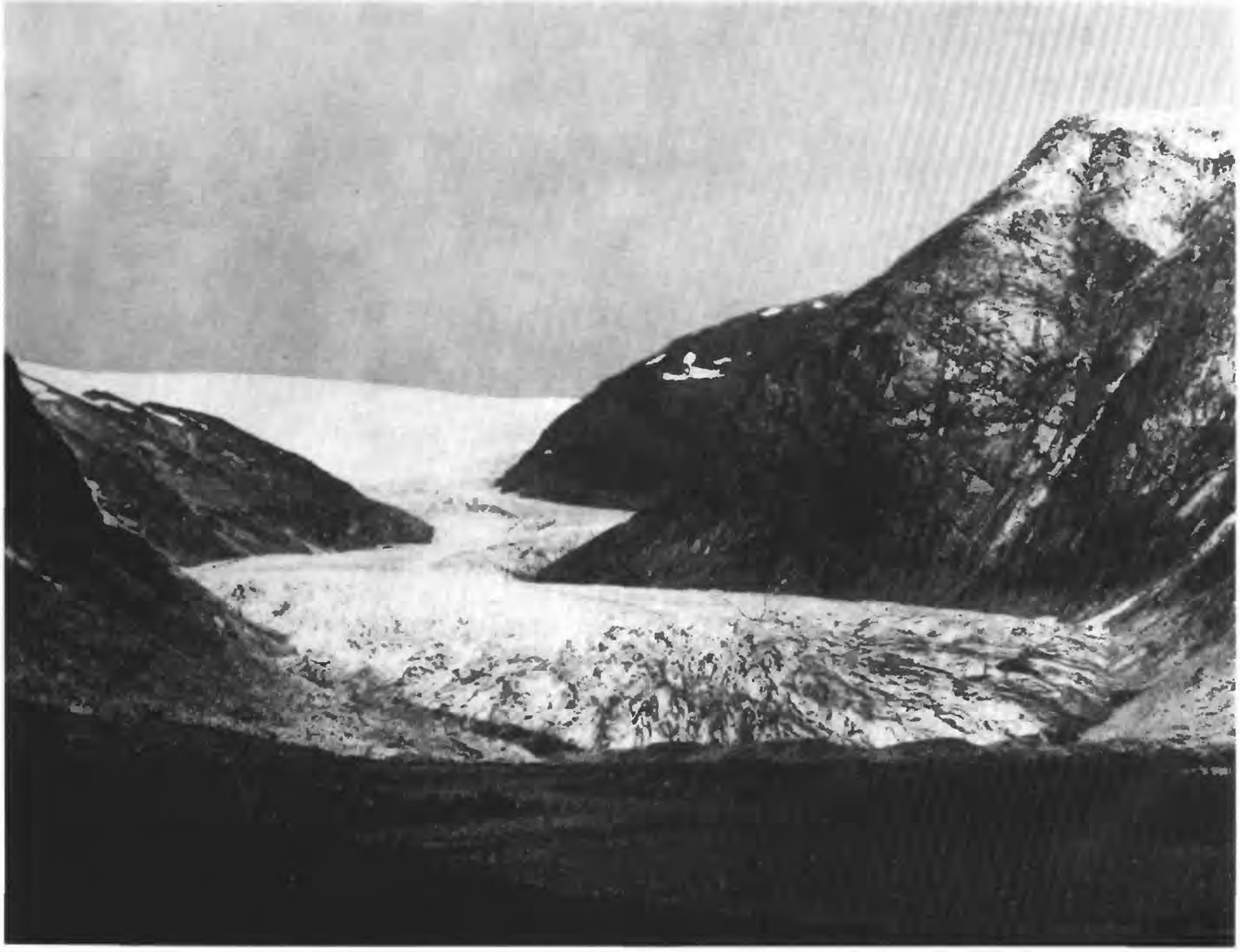

Figure 16.—Engabreen, an outlet glacier from the northwestern part of the Svartisen ice cap, photographed in 1883 by Charles Rabot. Compare with figure 17 (below), a photograph of the same area 91 years later that demonstrates about 2 km retreat.

Figure 17.—Engabreen in 1974. The glacier has retreated about 2 km since 1883 (compare with fig. 16), and most of the recession has occurred since 1930. Photograph by Nils Haakensen.

Nigardsbreen by Selmer was made into a woodcut and published in *Illustreret Nyhedsblad* in 1864 (fig. 14*B*). Some of these artworks are so detailed that they can be used for calculations of the glacier volume at that time, but some are too "artistic" to be used in this context. The Norwegian scientist J.B. Rekstad, geologist and photographer, took numerous pictures of various glacier termini from the same viewpoint in different years (fig. 15). Also, the French geographer Charles Rabot took several photographs during the period 1880–90 of various geographical subjects, particularly in northern Norway, including some glaciers, and his pictures are of high quality (fig. 16). Engabreen has retreated 2 km between Rabot's photographs in 1883 and recent studies in 1974 (fig. 17).

A professional photographer, Mr. Knud Knudsen from Bergen, traveled extensively in Norway, particularly in western Norway during the years 1860–1900. He took numerous beautiful photographs, mainly to prepare postcards, but among them are a lot of good glacier photographs. Some of these can be dated. Most of his 20,000–25,000 glass negatives and some of his postcards were taken over by the University Library in Bergen and are now accessible to researchers.

The first commercial aerial photographs showing a Norwegian glacier were taken in 1937 and show part of the Folgefonni ice cap (Widerøe's Contract No. 14), but the negatives have been lost. A German scientific expedition arranged for vertical aerial photographs of selected glaciers in southern Norway in the 1930's, and an example is shown in figure 18. Unfortunately, in this case also, the negatives have been lost. Since

Figure 18.*—One of the first known vertical aerial photographs of a Norwegian glacier, showing the snout of Nigardsbreen and its associated terminal moraine system. The photograph was taken in 1938 by the Norwegian Surveying Company Widerøe under contract from a German scientific expedition. The scale is approximately 1:37,000.*

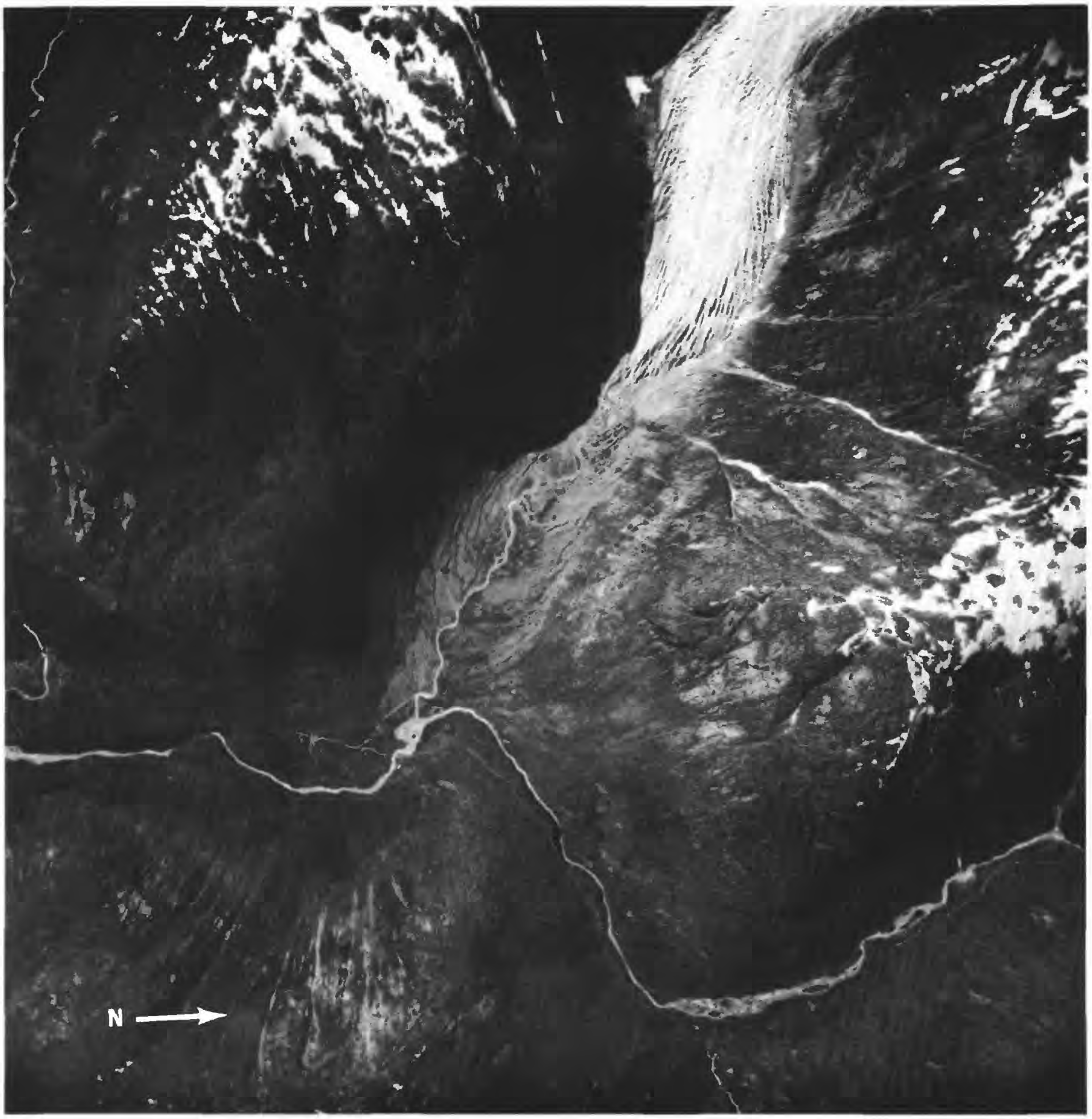

World War II a great number of vertical aerial photographs have been taken, particularly for production of the new 1:50,000-scale topographic map series of Norway.

Aerial photographs, taken from various altitudes, are now available of almost every glacier in Norway. Repeated aerial photographic surveys make possible comparisons of volume changes of glaciers during intervals of several years. A modern vertical aerial photograph is shown in figure 19 and can be compared with the old German aerial photograph (fig. 18). Another interesting comparison can be made between terrestrial photographs of Nigaardsbreen that were taken in 1959 and 1981. They show

Figure 19.*—Vertical aerial photograph of the terminus of Nigardsbreen taken in August 1974 (Fjellanger-Widerøe No. 4409–A3). The length of the lake is about 1.9 km, and the scale is approximately 1:18,000. In 1938 (see fig. 18), the snout was located just at the lower end of the lake.*

continuous retreat (figs. 20 and 21). Similarly, the outlet glacier Mjølkevoldsbreen, on the western side of the Jostedalsbreen ice cap, has receded most dramatically (fig. 22), in one of the most rapid retreats seen in Norway over such a short period of time.

It is quite obvious that similar comparisons will be possible through the use of satellite images taken at intervals of several years. Thus, an archive of images showing glaciers on a global scale will be most valuable in the future.

As a historical note, it should be mentioned that one of the very first images produced by Landsat 1 in 1972 (on the sixth day of its operation

Figure 20.—*Nigardsbreen, in July 1959, photographed from nearly the same position as that illustrated by Forbes (see fig. 14A) and photographed by Rekstad (see fig. 15). Photograph by Olav Liestøl, Norsk Polarinstitutt.*

Figure 21.—*Nigardsbreen, photographed in 1980 from nearly the same position as in figures 13B, 14, 15, and 20. Photograph by Nils Haakensen.*

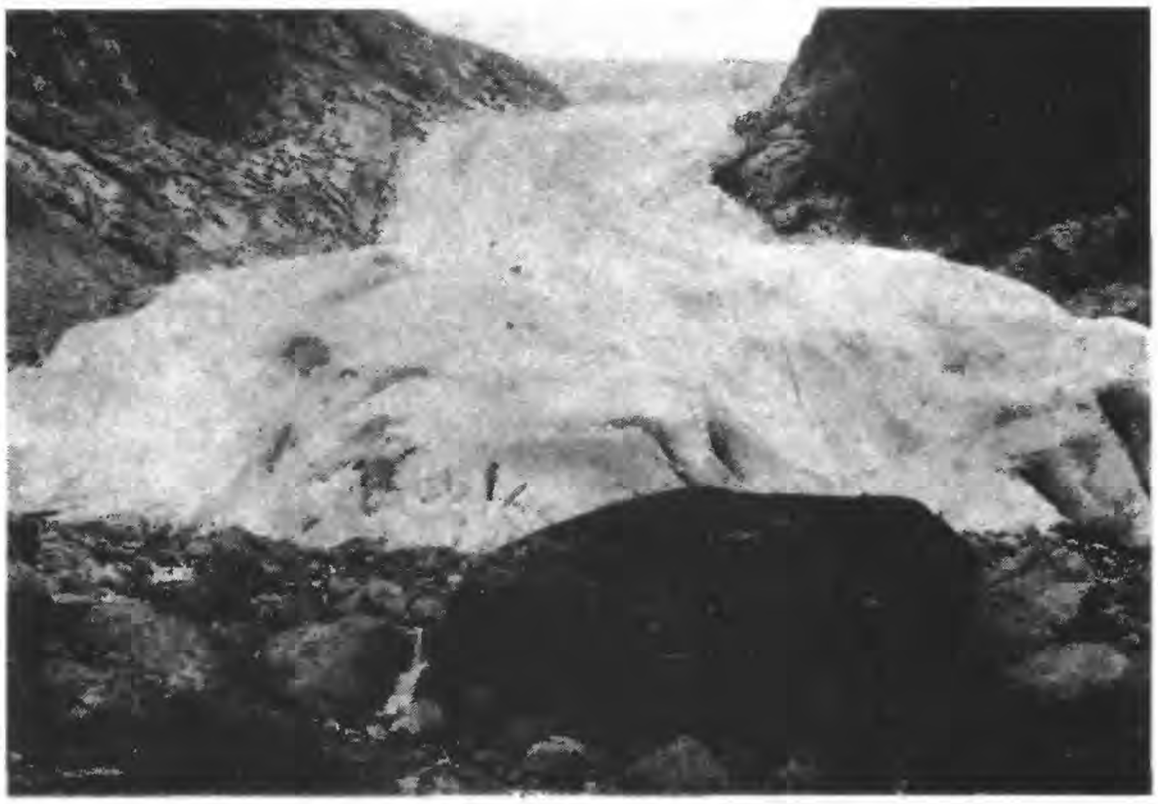

Figure 22.—Two photographs showing the retreat of Mjølkevoldsbreen (western side of the Jostedalsbreen ice cap) between 1933 (top) and 1939 (bottom) (from Fægri, 1940).

since its launch on 22 July 1972) was of the northernmost glacier in continental Europe, Seilandsjøkulen. The transient snowline could be seen easily on the image. This almost "historical image" (fig. 23) is compared with a vertical aerial photograph taken 2 years earlier (fig. 24), where a similar, but not identical, snowline can be seen. From the Landsat digital (computer-compatible tape, or CCT) data a dotprint "map" of this glacier was also made (fig. 25).

Investigations have been made to evaluate usefulness for hydrological purposes of image data from meteorological satellites (Østrem and others, 1979). It is obvious that the resolution in images from the television and infrared observation satellite (TIROS) or the National Oceanic and Atmospheric Administration (NOAA) satellites, about 1.1 km, cannot give the same glaciological information as Landsat data, but the location of glaciers, their approximate size, and so on can be obtained from analysis of such images (figs. 26 and 27).

A much better tool in glaciological research is, of course, the Landsat image taken under cloud-free conditions. For many purposes the MSS

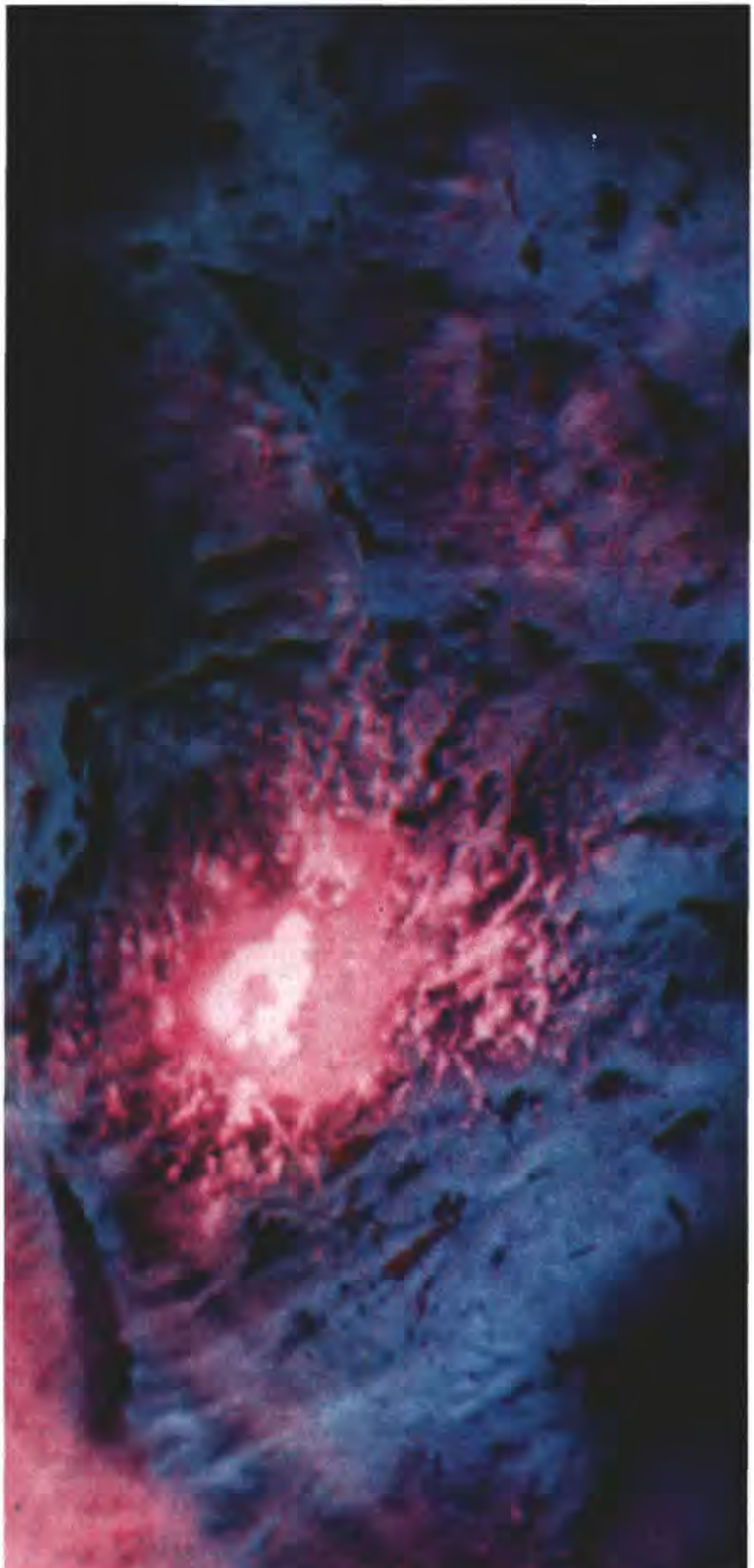

Figure 23.—*Landsat MSS false-color composite image of Seilandsjøkulen, the northernmost glacier in Norway, taken on 29 July 1972 (1006–09481, MSS band 5 with a red filter, MSS band 6 with a blue filter, and MSS band 7 with a green filter; Path 211, Row 10). Snow is white and bare ice is red. Sediment-laden water appears red, whereas clear water is black. The bedrock is blue. This is the first Landsat 1 image acquired over Norwegian territory. The image covers an area of approximately 25 km × 50 km.*

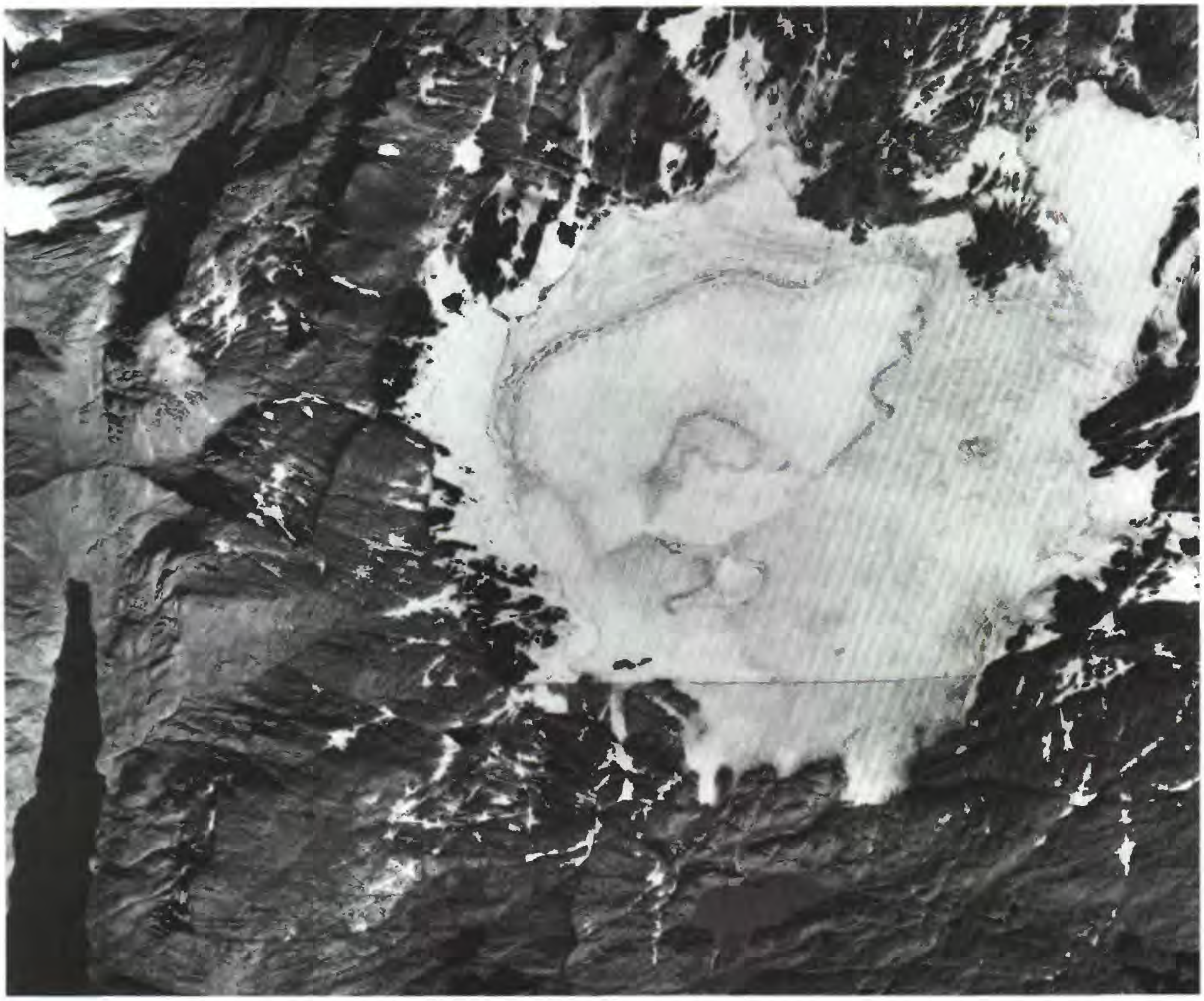

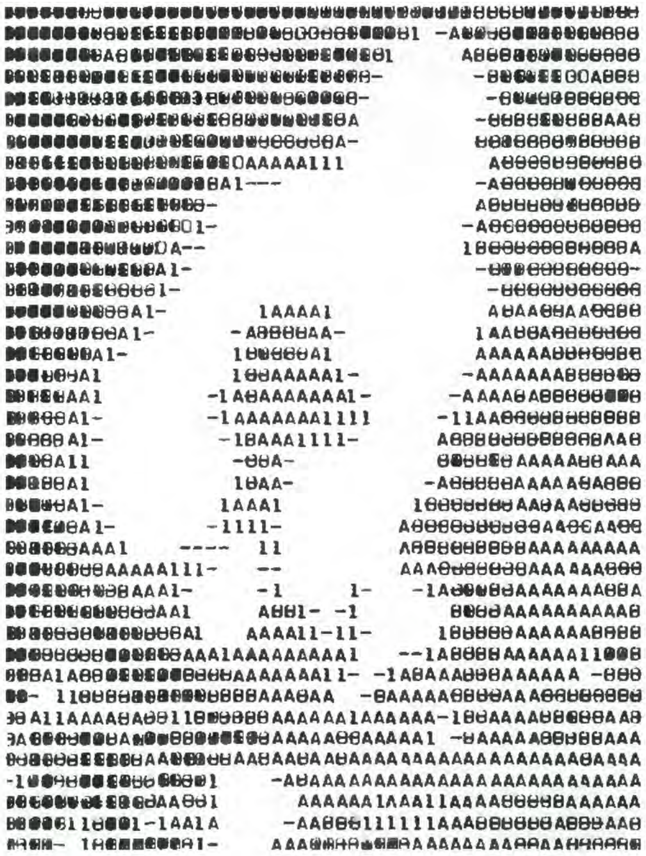

▲

Figure 24.—*Vertical aerial photograph of the small Seilandsjøkulen ice cap, the northernmost glacier in Norway (Fjellanger-Widerøe No. 3615, August 1970). The scale is approximately 1:45,000.*

Figure 25.—*A "map" of Seilandsjøkulen ice cap produced as a computer-generated dotprint from Landsat MSS band 7 digital data (1006–09481; 29 July 1972; Path 211, Row 10). The white areas represent residual snow from the past winter; the gray areas (in general marked by –, 1, A, or Θ) represent bare glacier ice, whereas darker areas and overprinted characters indicate bedrock or water. Each character represents one pixel (about 60 × 80 m). The scale is approximately 1:50,000. From Østrem (1975); reproduced from the Journal of Glaciology, v. 15, no. 73, p. 403–415, by courtesy of the International Glaciological Society.*

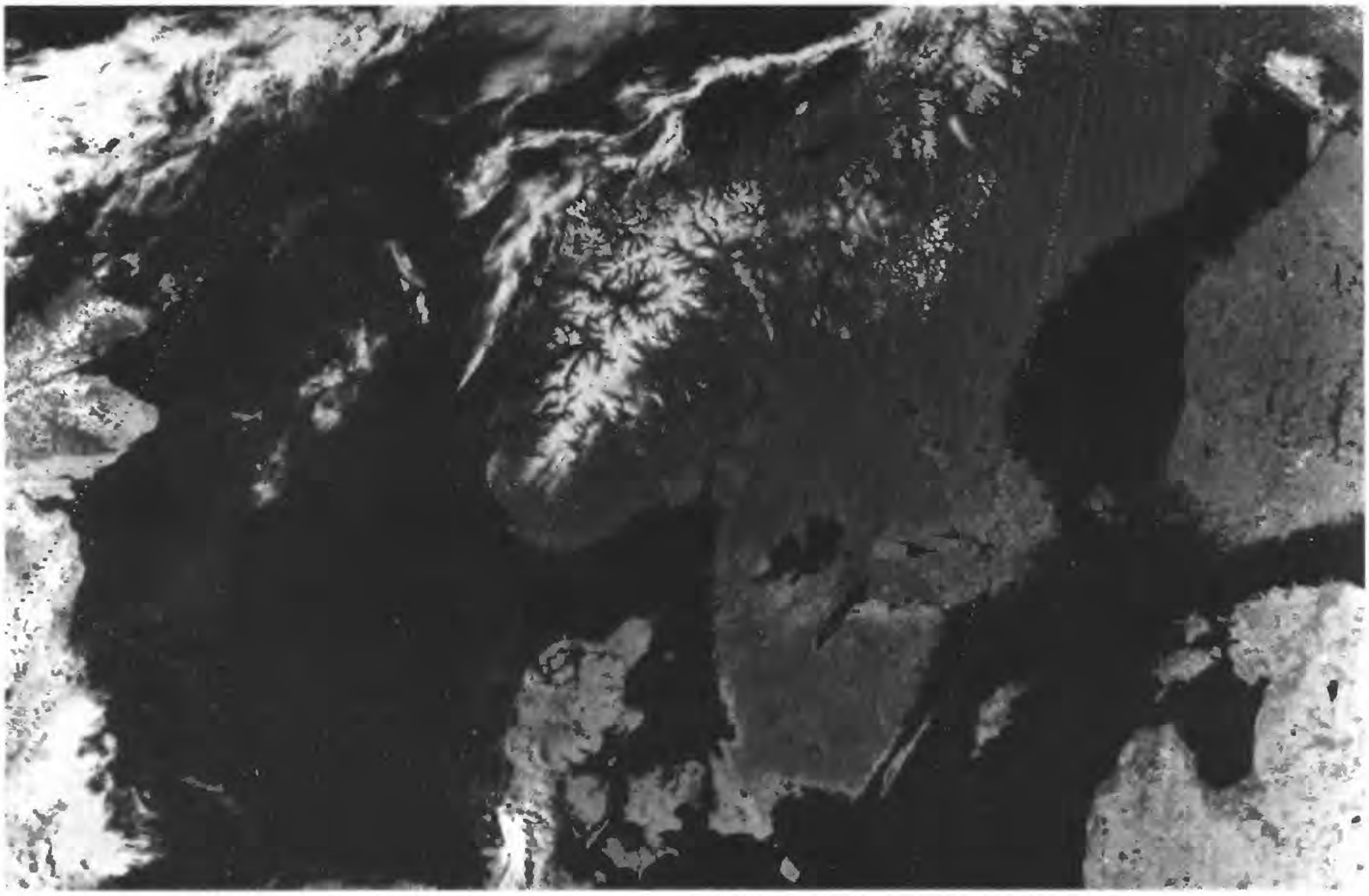

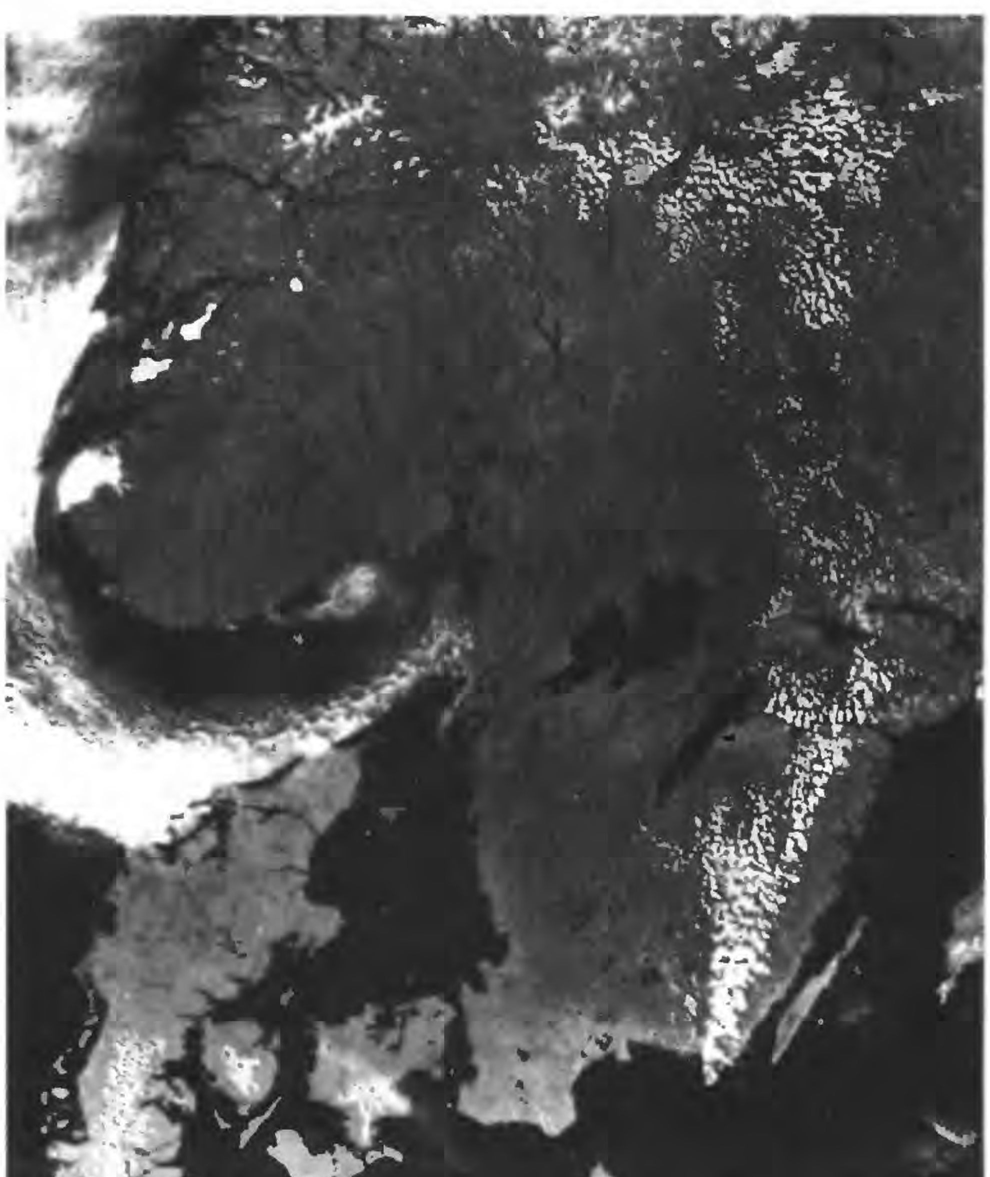

Figure 26.—*NOAA image of southern Norway taken on 1 June 1982. The high-altitude areas (about 1,000 m above mean sea level) are still snow covered. Scale approximately 1:10,000,000. NOAA image received and processed by the Norwegian Telemetry Station in Tromsø.*

Figure 27.—*NOAA image of southern Norway taken on 30 July 1982. The snow has disappeared, and the glaciers appear as white areas. The large white dot in the southwest is a cloud. In the northeast some cumulus clouds are visible. Scale approximately 1:8,000,000. NOAA image received and processed by the Norwegian Telemetry Station in Tromsø.*

false-color composite images may be even more useful. The EROS Data Center (EDC) standard MSS false-color composite (MSS band 4 through a blue filter, MSS band 5 through a green filter, and MSS band 7 through a red filter) distributed by EDC will normally show bare glacier ice in blue and the rest of the glacier in white (fig. 28). It is, however, possible to change the color filters or vary the intensity of the colors in order to emphasize glaciological features, such as sediment in glacier streams and lakes. A good example is the image of Hardangervidda shown in figure 29, where sediment in lakes can be seen easily. A decreasing amount of suspended sediment is apparent at increasing distance from the terminus of the glacier. It may be possible, in the future, to calibrate satellite images so that the sediment concentration in lakes could be calculated from satellite data. So far, this task has proven difficult; a qualitative determination is possible, but reliable *quantitative* calculations are still impossible.

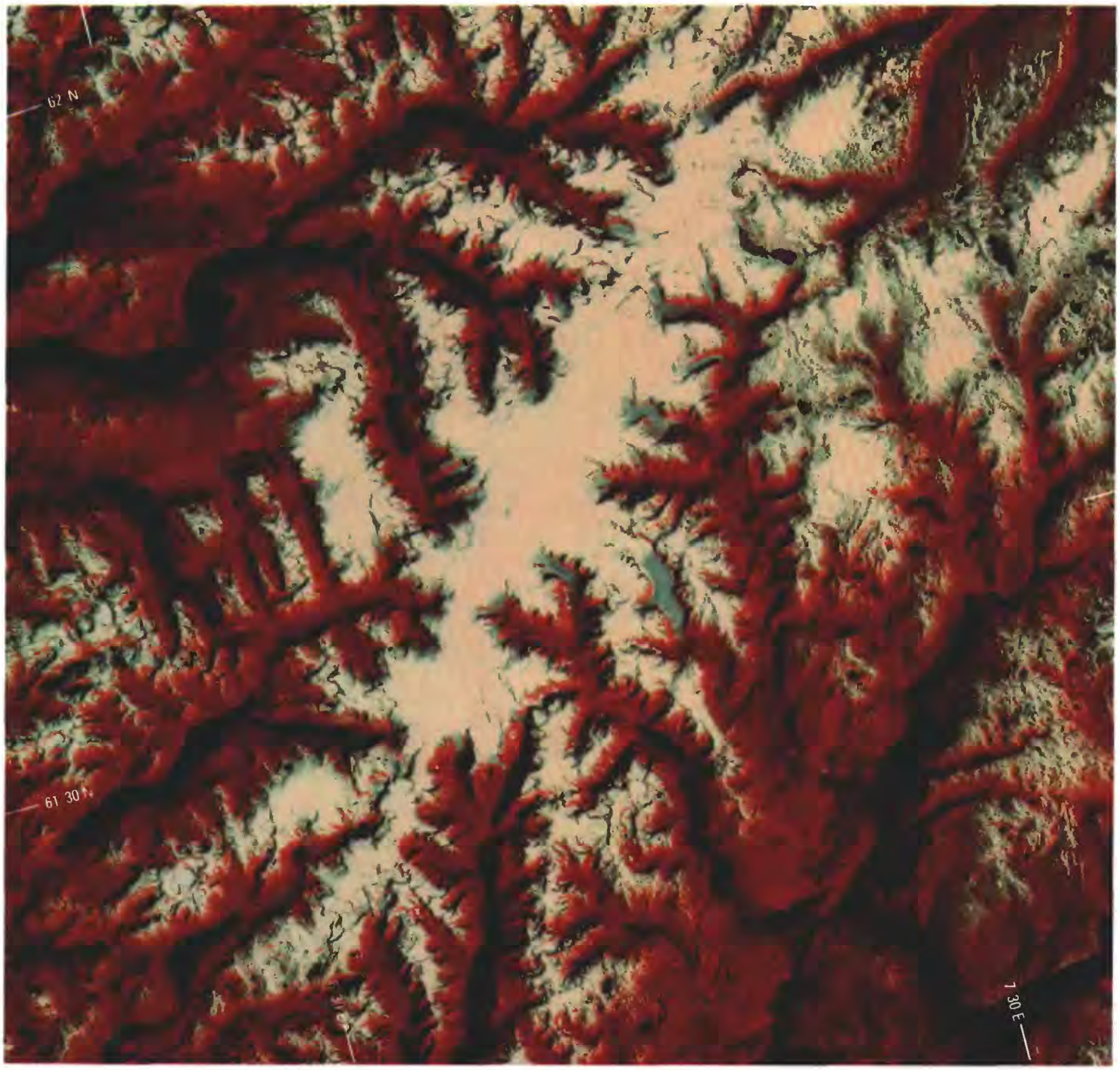

Figure 28.*—A section of a Landsat MSS false-color composite image (2565–10004; MSS band 4 with a blue filter, MSS band 5 with a green filter, and MSS band 7 with a red filter; 9 August 1976; Path 216, Row 17) showing the Jostedalsbreen ice cap, the largest continuous ice mass in continental Europe. The section covers approximately 90 × 85 km.*

Glaciological Phenomena

The transient snowline (TSL) on a glacier is defined as the transition line between exposed (bare) glacier ice and snow or firn. This line is situated somewhere on the lower part of the glacier at the beginning of the melt season when last winter's snow disappears and the bare glacier ice is gradually exposed. It moves to higher altitudes throughout the melt season and reaches its highest position at the end of the summer. If this highest position, given in meters above sea level, is plotted against the net mass balance, given in meters of water equivalent, this relation is expressed by a straight line (see Liestøl, 1967, p. 46; Østrem, 1975; and figure 30). Each single dot in this diagram is a result of 1 year's field and office work. For Nigardsbreen this means an annual cost in the order of several thousand dollars.

After this diagram has been established for a particular glacier, however, it becomes possible to determine the approximate net mass balance directly from the height of the TSL at the end of the summer, provided its position (and elevation) can be identified. By an appropriate, very simple color coding of Landsat images it may be easy to distinguish exposed glacier ice from the snow-covered areas on glaciers (fig. 31). If the Landsat image is compared with a topographic map, the height of the TSL can be determined, as has been done in figure 32 for Jostedalsbreen and environs. At Jostedalsbreen the height of the TSL was between 1,160 m and 1,360 m above sea level on 27 August 1976 (table 4). It increases eastward as can be seen on Spørteggbreen and Holåbreen. Within a limited area the height of the TSL does not vary very much. The steepest glaciers, however, show a tendency for a higher TSL level.

Similarly, for the cirque and valley glaciers in Jotunheimen (figs. 33 and 34) the TSL on 27 August 1976 could be determined for 15 glaciers (table 5). Also, the TSL in the Jotunheimen area shows a consistent increase in altitude toward the east, the more continental part of Norway.

◀ *Figure 29.—A section of Landsat MSS image 22059–10083 (11 September 1980; Path 216, Row 18) showing the Hardangervidda mountain plateau in the central part of southern Norway. Note the ice caps of Folgefonni in the west and Hardangerjøkulen in the north. The northern part of the latter ice cap drains eastward, and the sediment is clearly visible (light bluish color) in the lakes in the upper right part of the image. The sediment content decreases with increasing distance from the glacier. Approximate scale 1:42,000. Special MSS false-color composite processing by Fjellanger-Widerøe, Oslo, with MSS band 4 in blue, MSS band 5 in green, and MSS band 7 in red.*

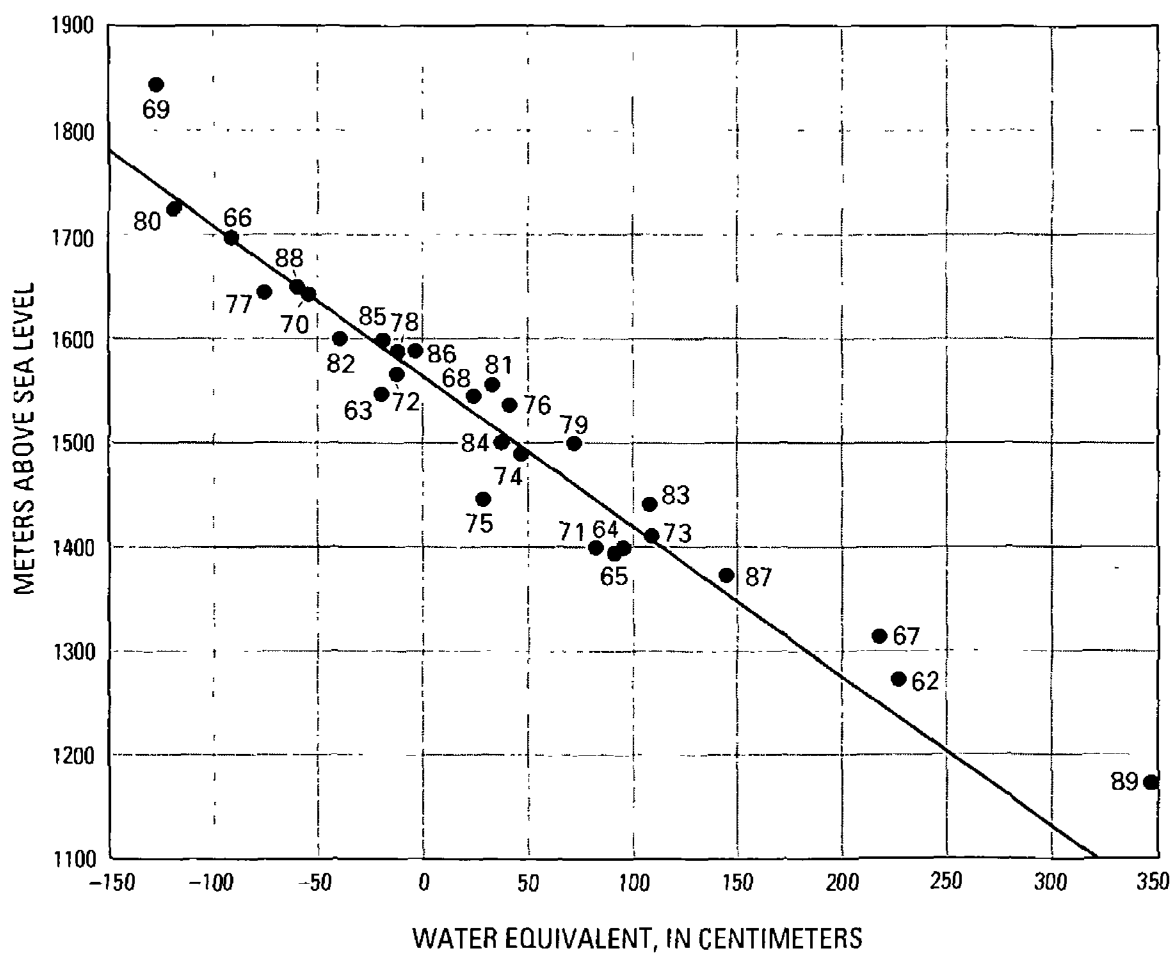

***Figure 30.**—The clear linear relation between the elevation of the equilibrium line at the end of the ablation season and the specific net balance of a glacier. This example is from Nigardsbreen, where mass-balance studies have been performed continuously since 1962. The plotted points show the relations for each year from 1962 to 1989. Similar diagrams have been made for several other glaciers. From Østrem, 1975; reproduced from the Journal of Glaciology, v. 15, no. 73, p. 403–415, by courtesy of the International Glaciological Society.*

Figure 31.—*Landsat special MSS false-color composite image of the Jostedalsbreen ice cap (2583–10001; MSS band 4 in blue, MSS band 7 in yellow; 27 August 1976; Path 216, Row 17). The transient snowline is clearly visible on many outlet glaciers as the border between white snow-covered areas and bluish areas representing exposed or bare glacier ice. Black areas are lakes, fjords, or shadows in narrow valleys. (The image covers the same area as shown on the map in fig. 32, or approximately 60 × 75 km.)*

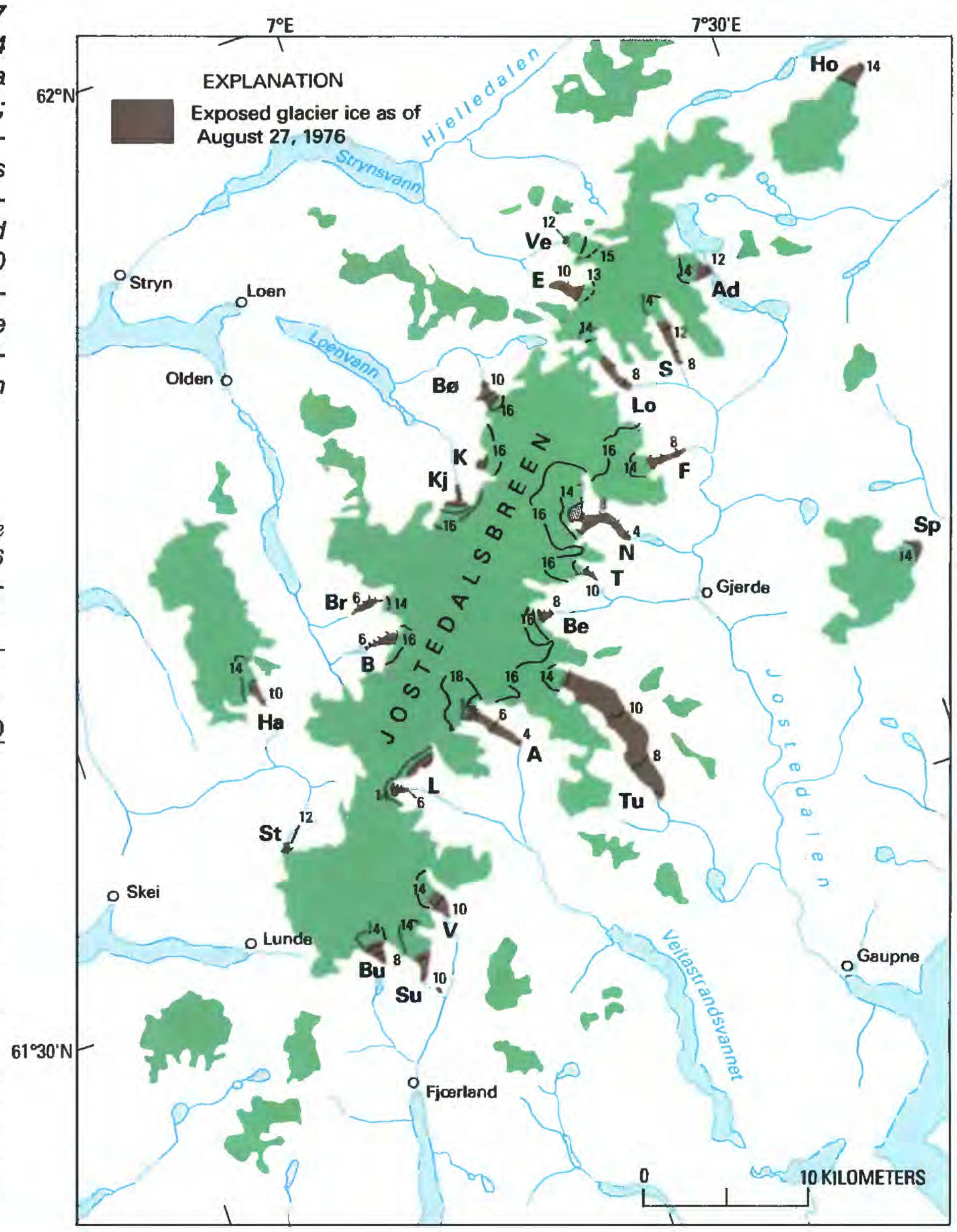

***Figure 32.**—Areas of exposed ice as of 27 August 1976 that were determined on 24 outlet glaciers in the Jostedalsbreen area from the Landsat MSS image (2583–10001; 27 August 1976; Path 216, Row 17). (Compare also with fig. 31.) The contour interval is 200 m, heights in 100's of meters. The altitude of the transient snowline, as determined from topographic maps, was between 1,160 and 1,360 m above sea level at Jostedalsbreen (average 1,242 m) but a little higher farther east. Abbreviations and individual transient snowline altitudes are shown in table 4.*

TABLE 4.—*Results of height determinations of the transient snowline (TSL) level on 27 August 1976 from a Landsat image of the area of the Jostedalsbreen ice cap (compare with figs. 31 and 32)*

Abbreviation	Glacier name	Height of TSL (meters)
A	Austerdalsbreen	1,200
Ad	Austdalsbreen	1,280
B	Briksdalsbreen	1,300
Be	Bergsetbreen	1,200
Br	Brenndalsbreen	1,250
Bu	Bøyumsbreen	1,300
Bø	Bødalsbreen	1,360
E	Erdalsbreen	1,220
F	Fåbergstølsbreen	1,200
Ha	Haugabreen	1,200
Ho	Holåbreen	1,580
K	Krunebreen	1,300
Kj	Kjenndalsbreen	1,240
L	Langedalsbreen	1,200
Lo	Lodalsbreen	1,160
N	Nigardsbreen	1,220
S	Stegholtbreen	1,240
Sp	Spørteggbreen	1,400
St	Strupebreen	1,240
Su	Supphellebreen	1,220
T	Tuftebreen	1,300
Tu	Tunsbergdalsbreen	1,240
V	Veslebreen	1,250
Ve	Vesledalsbreen	1,200

Consequently, if good satellite images are available at the end of the melt season and the above-mentioned relation has already been established, it is obvious that great savings could be made in the cost of glacier mass-balance work. However, several constraints remain. Many glaciers are located in areas of frequent bad weather or heavy cloud cover, and it might be difficult to accurately define the end of the melt season. Furthermore, this method gives the *net* balance only; data on the two most important factors that determine it, the winter accumulation and the summer ablation, cannot be obtained so easily. For an operational use of this method it is necessary to obtain images that are not obscured by clouds and that give good temporal coverage during a period near the end of the melt season.

Glaciers, in the course of their movement, produce copious amounts of sediment (fine-grained, about 50 percent; coarse material, about 50 percent), that is carried away by melt water. Large rocks, gravel, and some finer material carried within the ice will be deposited in the front as terminal moraines. Suspended sediment, sometimes called glacier rock flour, gives the characteristic milky color to glacier rivers and lakes downstream. One example of this was shown in figure 29 in the previous section. Another example is shown in figure 35, where the suspended

***Figure 33.**—Part of a special false-color composite Landsat MSS image of the Jotunheimen area (2583–10001; MSS band 4 in blue, MSS band 7 in yellow; 27 August 1976; Path 216, Row 17), covering approximately 45 × 55 km, the same area as the map shown in fig. 34. White regions represent snow-covered areas (mainly on glaciers), and light-blue areas represent exposed ice. The height of the transient snowline can be defined at 15 glaciers by comparison with a topographic map, and it has been determined to lie between 1,690 and 2,130 m above sea level, with a mean value of 1,853 m above sea level. The height of the transient snowline increases eastward (that is, with increasing continentality) (compare with table 5).*

sediment has been discharged into an arm of the Sognefjord. Even a very weak concentration of suspended sediment in various lakes is here visible on the special color-coded Landsat image. A digital printout from MSS band 4 shows the plume of sediment in the Gaupnefjord (fig. 36).

During recent years, waterpower engineers have requested that special investigations be directed at suspended sediment transport in glacier streams. Small rock particles cause increased wear in turbines, so data on the amount and characteristics of suspended sediment are of great interest. These investigations require, however, continuous fieldwork, because water samples must be taken several times daily to give data for a reliable calculation. We have seen that Landsat images clearly indicate those lakes and fjords where suspended sediment is present, and the data can also indicate variations in sediment concentration, although the calibration problem is still unsolved. At present the repetition time and weather constraints limit the usefulness of satellite data in this application.

Figure 34.—*Map of the Jotunheimen high-mountain area in the central part of southern Norway. The highest summits reach about 2,400 m above sea level, and the area includes many cirque glaciers and small valley glaciers (from Østrem and Ziegler, 1969). Compare with figure 33, a Landsat image of the same area. The transient snowlines were determined for 15 of the glaciers in this area. They are listed in table 5.*

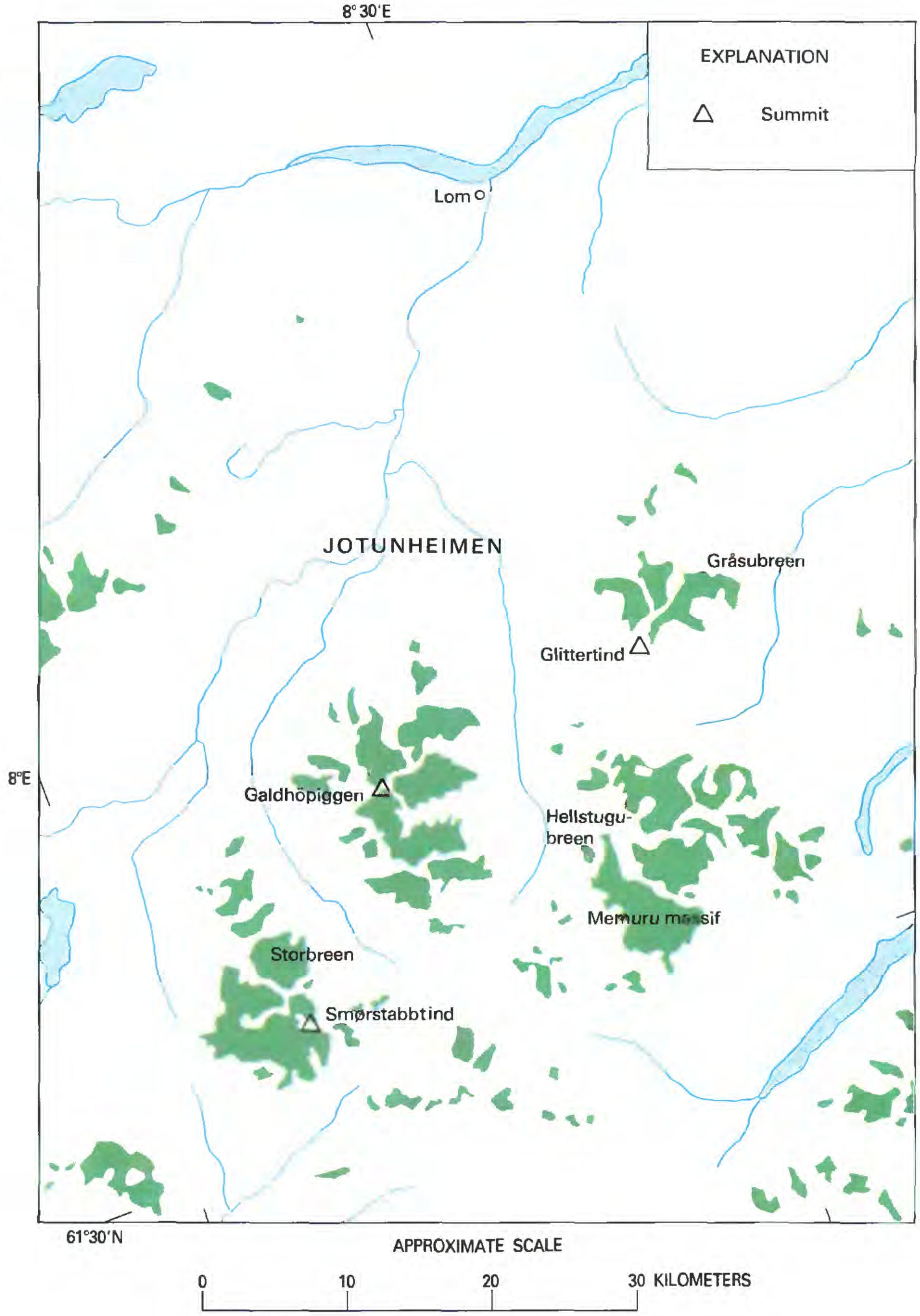

The special map shown in figure 37 demonstrates the economic importance of glaciers in waterpower-producing catchments. The map shows the specific water yield near a small ice cap (Hardangerjøkulen) in southwestern Norway; it also indicates an increasing quantity of water yield near the glacier. The water yield from a glacierized basin determines, of course, the production at a power station. Such basins are therefore very attractive for hydroelectric power developments. The map shows a very water-rich area, an area also shown on figure 29 in the previous section. The data on water discharge were taken from hydrological sources; satellite images cannot give such information as yet, but data collection platforms (DCP's) equipped with stream-gaging sensors have been used to transmit stream discharge measurements from field sites to a hydrological service. Polar-orbiting or geostationary weather satellites are used to relay the information.

TABLE 5.—*Results of height determinations of the transient snowline (TSL) level on 27 August 1976 from a Landsat image of the Jotunheimen area, central southern Norway (compare with figs. 33 and 34)*

[Height of transient snowline on 27 August 1976 increased more than 300 m toward continental areas (D) in the Jotunheimen area (fig. 34). Heights were taken from topographic maps]

Glacier group (fig. 34)	Glacier name	Number of height determinations	Height of TSL (meters)
A. Smørstabbtind massif		3	1,720±22
	Bøverbreen		1,740
	Storbreen		1,730
	Veslebreen		1,690
B. Galdhøpiggen massif		6	1,835±47
	South Illåbre		1,800
	Tverråbreen		1,770
	North Illåbre		1,870
	Svellnosbreen		1,800
	Styggebreen		1,870
	Storgjuvbreen		1,900
C. Memuru massif		4	1,855±23
	Hellstugubreen		1,860
	West Memurubre		1,830
	Veobreen		1,890
	Blåbreen		1,840
D. Glittertind		2	2,100±30
	West Grotbre		2,070
	Gråsubreen		2,130

***Figure 35.**—A Landsat MSS special false-color composite image (2187–10082; 28 July 1975; Path 216, Row 17) of the high-altitude areas of the central part of southern Norway (MSS band 4 in red, MSS band 5 in green, and MSS band 7 in blue). The Jostedalsbreen ice cap is situated in the left-central part of the image. Glacier sediment in lakes and fjords appears a very distinct red. Exposed ice appears yellow.*

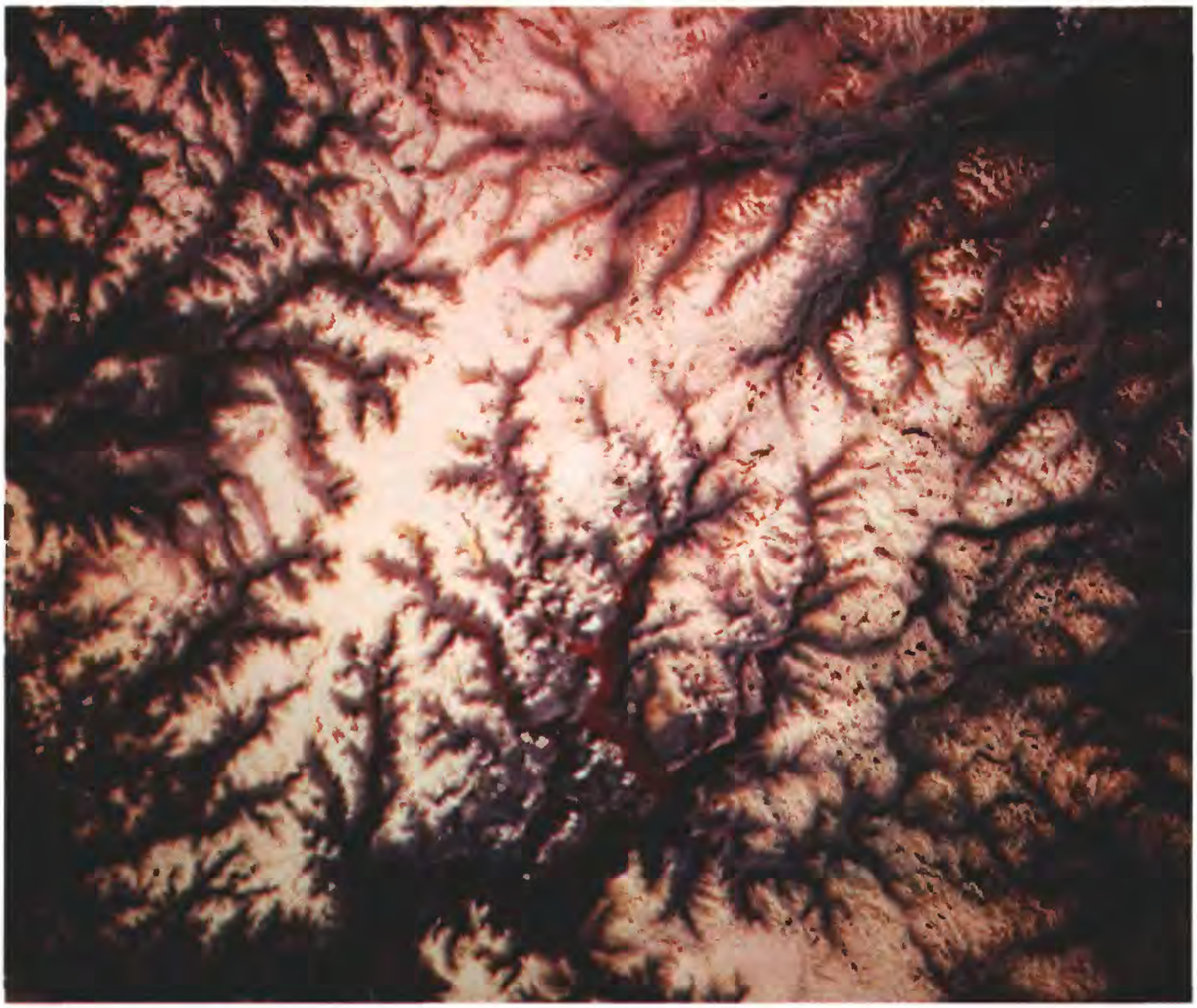

Figure 36.—A digital printout (dotprint) from Landsat MSS image 1336–10260; band 4; 24 June 1973; Path 217, Row 17. The coast is indicated by a heavy line. The Jostedal River, which drains the eastern part of the Jostedalsbreen ice cap, carries a large sediment load into the Gaupnefjord (center). Sediment-laden water is indicated by light areas, whereas dark areas represent clear water. The white areas are clouds. Each character represents one pixel (about 60 × 80 m). The scale is approximately 1:66,000 (from Østrem, 1976).

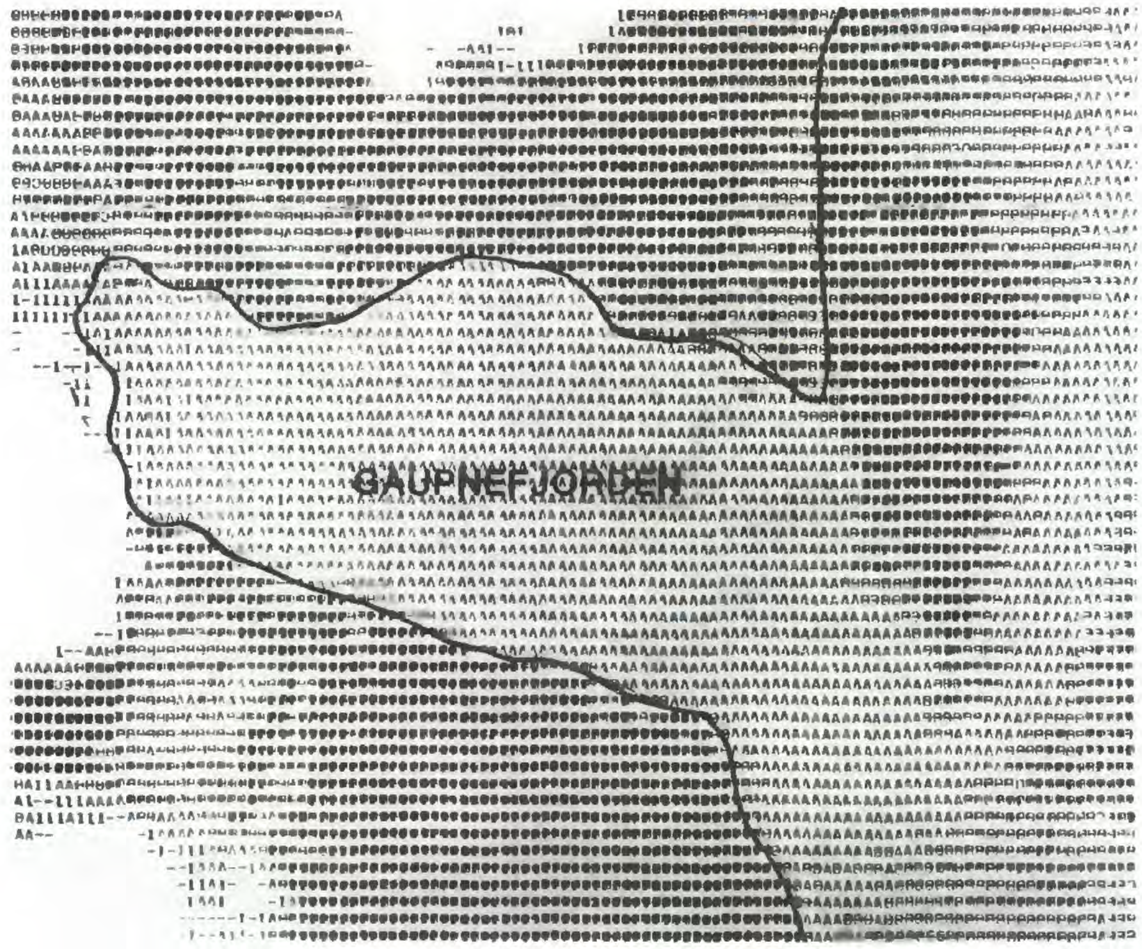

Figure 37.—Specific discharge in the area around the Hardangerjøkulen ice cap. This map clearly shows that the water yield from the glacierized areas is large and is increasing toward the glacier. Contours are in liters per second per square kilometer. One liter per second per square kilometer corresponds to 66 acre-feet per square mile.

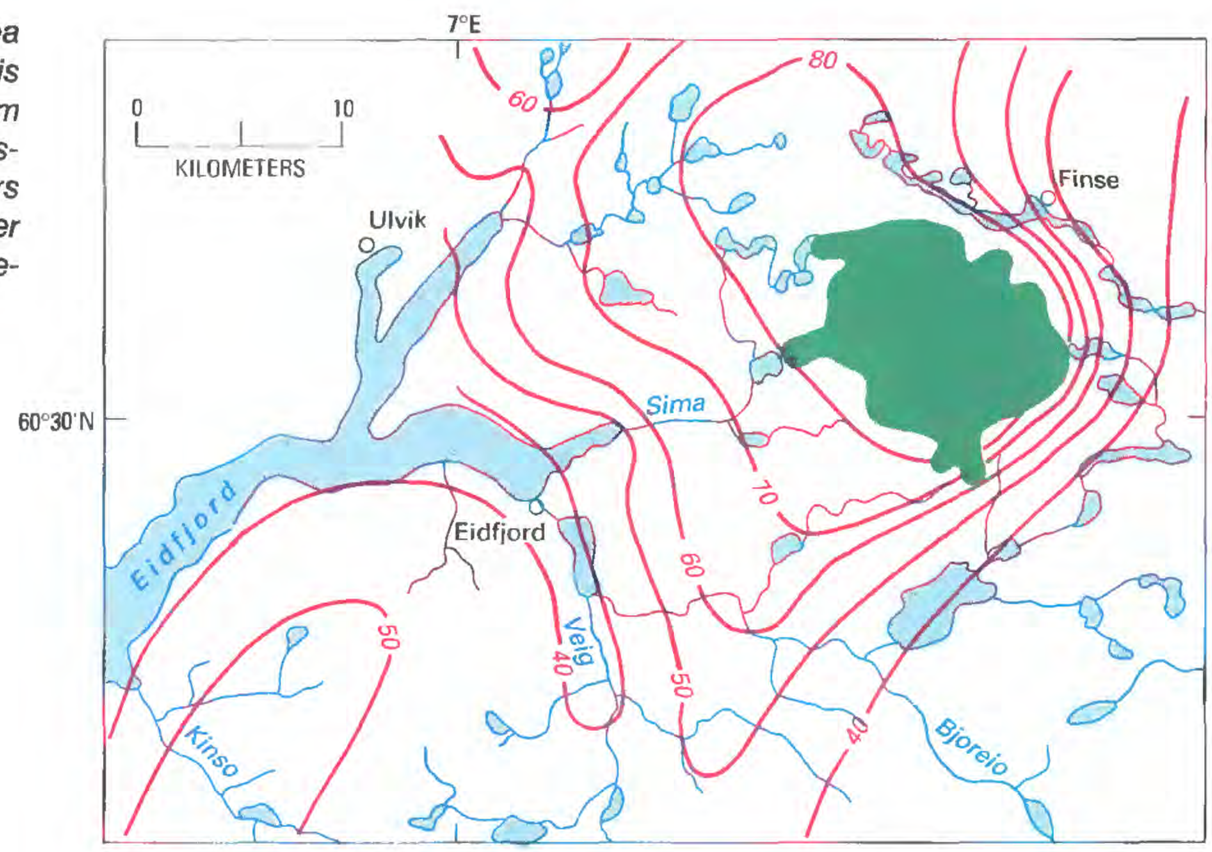

Glaciers on Landsat Images

Good coverage with high-quality aerial photographs is available for nearly all glacierized areas in Norway. A detailed inventory of all ice masses in Norway has been made, and the results have been published in two glacier atlases (Østrem and Haakensen, 1980). These atlases, containing data for all glaciers on the Scandinavian peninsula, were produced before detailed satellite images were commonly available. Both aerial photographs and topographic maps formed the source of information for this inventory. For inventory purposes, no presently available satellite data can replace the excellent vertical aerial photography available in Norway. Some types of glaciological phenomena, however, can be better obtained from satellite imagery. These phenomena have been discussed earlier in this section.

Figure 38.—*Landsat MSS image (2186–10005; band 7; 27 July 1975; Path 215, Row 13) showing glaciers in the southern part of northern Norway. Svartisen is situated in the lower part and Blåmannsisen and the Sulitjelma glaciers (near the Swedish border) in the upper part. The image covers approximately 120 × 150 km. (See map of area in figure 39.)*

To demonstrate the potential of using Landsat imagery for glacier inventories, an enlarged part of a Landsat image showing valley glaciers and cirque glaciers in the Jotunheimen area (fig. 33) can be compared with the field observations and a map taken from the glacier atlas that is based upon aerial photographs (fig. 34). Another example is demonstrated in figure 38 for glaciers in northern Norway. The true glacier distribution is shown on the map, figure 39. It is clear that even relatively small glaciers are easily determined on images of good quality; their outline can be drawn and transferred to a map. This method is certainly valuable in areas where other sources of information are lacking.

For all Norwegian glacier areas, a survey was made to find the most useful Landsat images for glaciological work. The result is shown on the map of the Path/Row positions (fig. 40) and in table 6. Table 7 provides information on the availability of optimum Landsat 1, 2, and 3 images for all nominal scene centers of glacierized areas of Norway. Percent cloud cover refers only to glacierized part of image.

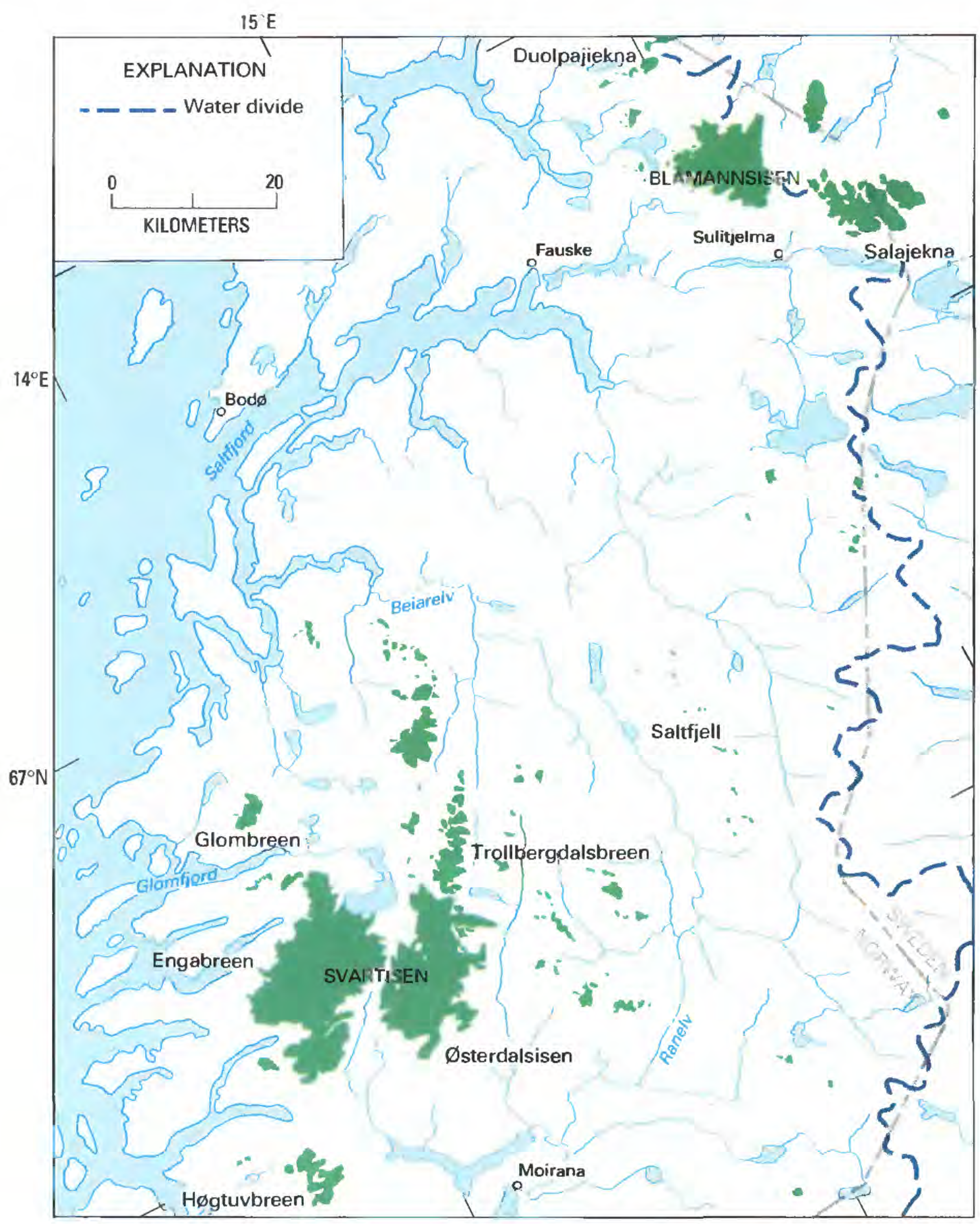

Figure 39.—Map of the Svartisen-Blåmannsisen area in northern Norway showing the second, fourth, and fifth largest glaciers in Norway (from Østrem and others, 1973). (See Landsat image of area in figure 38.)

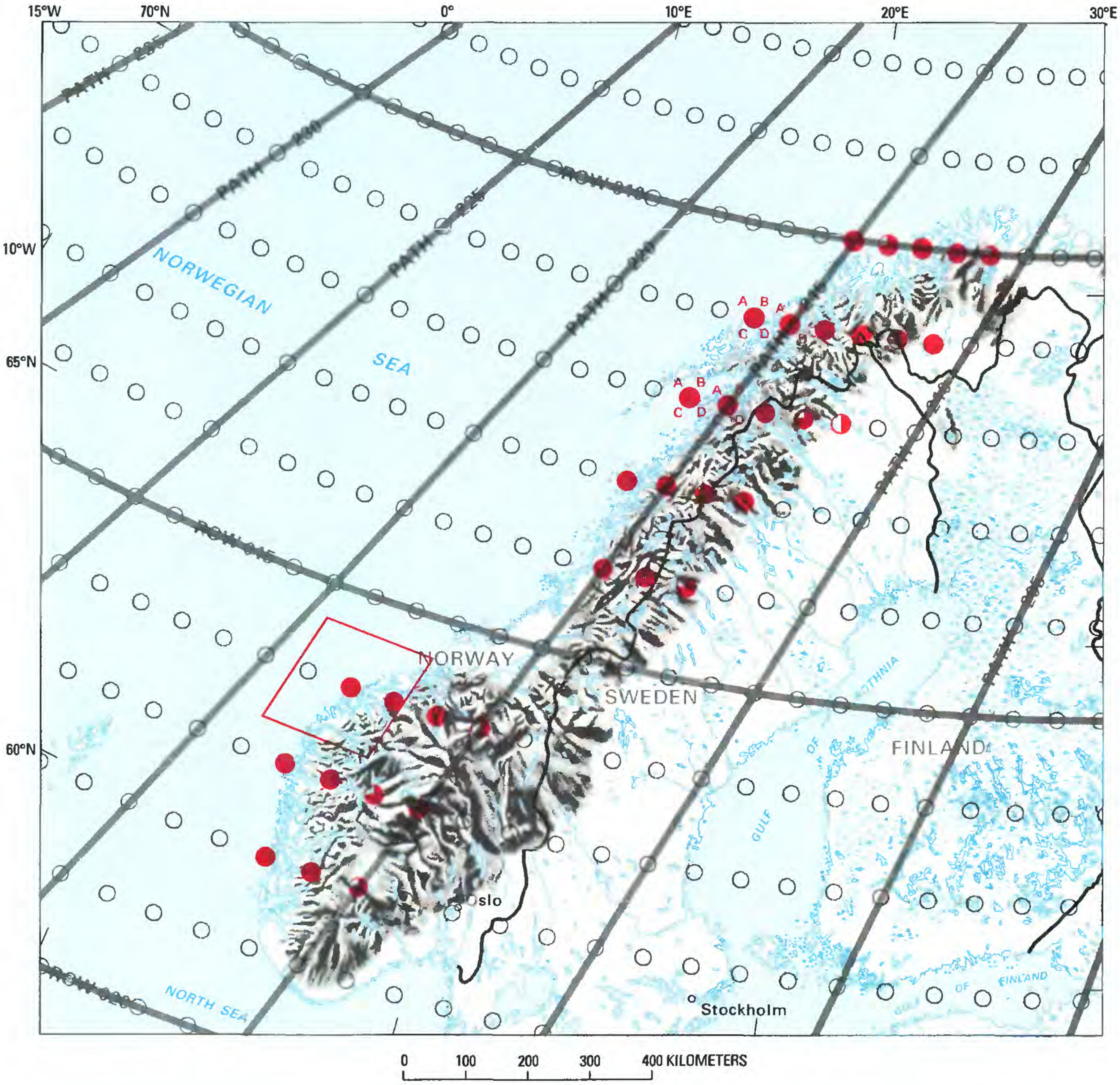

EXPLANATION OF SYMBOLS

Evaluation of image usability for glaciologic, geologic, and cartographic applications. Symbols defined as follows:

- Excellent image (0 to ≤5 percent cloud cover)
- Good image (>5 to ≤10 percent cloud cover)
- Fair to poor image (>10 to ≤100 percent cloud cover)
- A B C D Usable Landsat 3 return beam vidicon (RBV) scenes A, B, C, D refer to usable RBV subscenes
- Nominal scene center for a Landsat image outside the area of glaciers
- Approximate size of area encompassed by nominal Landsat MSS image

Figure 40.*—Optimum Landsat 1, 2, and 3 images of the glaciers of Norway. The vertical lines represent nominal paths. The rows (horizontal lines) have been established to indicate the latitude at which the imagery has been acquired.*

TABLE 6.—*A list of the most useful Landsat images of the glaciers of Norway as of the end of 1980*

Path-Row	Date	Landsat identification number	Cloud cover[1] (in percent)	Remarks
211–10	29 Jul 72	1006–09481	10	
211–11	29 Jul 72	1006–09484	0	
213–12	8 Jul 73	1350–10005	10	
214–12	25 Jul 73	1367–09545	50	
215–13	9 Jul 75	2168–10012	20	
	27 Jul 75	2186–10005	5	
	28 May 75	2492–09552	10	
215–14	9 Jul 75	2168–10014	10	
215–17	6 Mar 73	1226–10151	20	
	17 Jun 74	1694–10071	25	
	15 Feb 75	2024–10031	0	Completely snow covered
	9 Jul 75	2168–10030	10	
215–18	15 Feb 75	2024–10034	0	Excellent; completely snow covered
	9 Jul 75	2168–10032	0	
216–16	23 Jun 73	1335–10195	10	
	18 Jun 74	1695–10123	10	
	9 Aug 76	2565–10002	10	
	27 Aug 76	2583–09595	0	
216–17	18 May 73	1299–10204	0	
	18 Jun 74	1695–10125	30	
	22 Jun 75	2151–10085	20	
	10 Jul 75	2169–10084	20	
	28 Jul 75	2187–10082	0	Excellent; good snowline; sediment in lakes and fjords
	9 Aug 76	2565–10004	10	
	27 Aug 76	2583–10001	0	Excellent
216–18	22 Jun 75	2151–10091	20	
	28 Jul 75	2187–10084	20	
	9 Aug 76	2565–10011	10	
	27 Aug 76	2583–10004	10	
	11 Aug 80	22059–10083	0	Excellent
217–16	5 Jul 76	2530–10070	0	
217–17	24 Jun 73	1336–10260	0	Excellent; sediment in lakes and fjords visible
	5 Jul 76	2530–10073	0	
217–18	27 Sep 72	1066–10255	10	
	24 Jun 73	1336–10263	0	Excellent
	5 Jul 76	2530–10075	5	
218–16	25 Jun 73	1337–10312	0	

[1] Cloud cover given only for glacierized parts of image.

TABLE 7.—*Optimum Landsat 1, 2, and 3 images of the glaciers of Norway*

Path-Row	Nominal scene center (lat-long)	Landsat identification number	Date	Solar elevation angle (in degrees)	Code	Cloud cover (in percent)	Remarks
211–10	070°35′N. 025°20′E.	1006–09481	29 Jul 72	38	◕	10	Seilandsjøkulen, Øksfjordjøkulen, east part of Langfjordjøkulen; image used for figure 23
211–11	069°17′N. 023°18′E.	1006–09484	29 Jul 72	39	●	0	
212–10	070°35′N. 023°54′E.	22019–09420	02 Aug 80	36	●	0	Archived by ESA[1]
212–11	069°17′N. 021°52′E.	22019–09422	02 Aug 80	37	◑	30	Strupbreen, Jiekkevarri; archived by ESA
212–12	067°59′N. 020°03′E.	1367–09545	25 Jul 73	40	◑	50	
213–10	070°35′N. 022°28′E.	22020–09474	03 Aug 80	36	●	0	Archived by ESA
213–11	069°17′N. 020°26′E.	22434–09442	21 Sep 81	20	●	0	Archived by ESA
213–12	067°59′N. 018°37′E.	1350–10005	08 Jul 73	43	◕	10	Blåisen, Storsteinsfjellbreen, Frostisen
213–13	066°40′N. 016°59′E.	20940–09255	19 Aug 77		●	0	Archived by ESA; not physically examined
213–14	065°20′N. 015°30′E.	1422–10003	18 Sep 73	25	◕	10	Børgefjell
214–10	070°35′N. 021°02′E.	31612–09573	03 Aug 82	36	◕	10	Partial scene includes all glacier areas; archived by ESA
214–11	069°17′N. 019°00′E.	22075–09541	27 Sep 80	18	●	0	Archived by ESA
214–12	067°59′N. 017°11′E.	22075–09543	27 Sep 70	19	◑	20	Archived by ESA
214–12	067°59′N. 017°11′E.	31612–09582	03 Aug 82	38	●	0	Partial scene; archived by ESA
214–13	066°40′N. 015°33′E.	22075–09550	27 Sep 80	20	◑	30	Archived by ESA
214–13	066°40′N. 015°33′E.	31612–09585	03 Aug 82	39	●	0	Partial scene, does not include western glacier area; archived by ESA
214–14	065°20′N. 014°04′E.	20941–09320	20 Aug 77		●	0	Archived by ESA; not physically examined
215–10	070°35′N. 019°36′E.	21302–09404	16 Aug 78	32	●	0	Archived by ESA
215–11	069°17′N. 017°34′E.	21302–09410	16 Aug 78	32	●	0	Archived by ESA
215–11	069°17′N. 017°34′E.	30893–09500 A,B,C,D	14 Aug 80	34	A ○ B C D	10– 50	Landsat 3 RBV images
215–12	067°59′N. 015°45′E.	30893–09503 A,B,C,D	14 Aug 80	35	A ○ B C D	10– 70	Landsat 3 RBV images
215–12	067°59′N. 015°45′E.	31613–10041	04 Aug 82	38	●	5	Partial scene, includes all glacier areas; archived by ESA

Table 7.—*Optimum Landsat 1, 2, and 3 images of the glaciers of Norway*—Continued

[See fig. 40 for explanation of symbols used in "Code" column]

Path-Row	Nominal scene center (lat-long)	Landsat identification number	Date	Solar elevation angle (in degrees)	Code	Cloud cover (in percent)	Remarks
215–13	066°40′N. 014°06′E.	2186–10005	27 Jul 75	41	●	5	Blåmannsisen, Svartisen; image used for figure 38
215–14	065°20′N. 012°38′E.	2186–10012	27 Jul 75	42	●	0	Okstindbreen
215–16	062°38′N. 010°03′E.	21626–09554	06 Jul 79	47	◑	30	Archived by ESA
215–17	061°16′N. 008°56′E.	2168–10030	09 Jul 75	48	◕	10	Jotunheimen
215–18	059°54′N. 007°52′E.	2168–10032	09 Jul 75	49	◕	10	Folgefonni, Hardangerjøkulen
216–11	069°17′N. 016°08′E.	21321–09474	04 Sep 78	26	●	0	Archived by ESA
216–11	069°17′N. 016°08′E.	30894–09554 A,B,C,D	15 Aug 80	33	A ○ B C D	0– 50	Landsat 3 RBV images
216–12	067°59′N. 014°19′E.	21321–09481	04 Sep 78	27	●	0	Archived by ESA
216–12	067°59′N. 014°19′E.	30894–09561 A,B,C,D	15 Aug 80	34	A ○ B C D	10– 50	Landsat 3 RBV images
216–13	066°40′N. 012°40′E.	31614–10102	05 Aug 82	38	●	0	Partial scene, includes all glacier areas; archived by ESA
216–16	062°38′N. 008°37′E.	2583–09595	27 Aug 76	34	●	0	Adelsbre
216–17	061°16′N. 007°30′E.	2565–10004	09 Aug 76	41	◕	10	Jostedalsbreen, Jotunheimen; image used for figure 28
216–18	059°54′N. 006°27′E.	22059–10083	11 Sep 80	31	●	0	Folgefonni, Hardangerjøkulen; image used for figure 29; archived by ESA
217–16	062°38′N. 007°11′E.	2530–10070	05 Jul 76	47	●	0	Adelsbre
217–17	061°16′N. 006°04′E.	2530–10073	05 Jul 76	48	●	0	Jostedalsbreen
217–18	059°54′N. 005°01′E.	21682–10091	31 Aug 79	35	●	0	Folgefonni; archived by ESA
218–16	062°38′N. 005°45′E.	21305–10003	19 Aug 78		●	0	Archived by ESA; not physically examined
218–17	061°16′N. 004°38′E.	21305–10010	19 Aug 78		●	0	Ålfotbreen; archived by ESA; not physically examined

[1] ESA is the European Space Agency, which archives Landsat imagery in Fucino, Italy, and Kiruna, Sweden.

Acknowledgments

The authors are indebted to the U.S. Geological Survey, particularly Dr. Richard S. Williams, Jr., and Jane G. Ferrigno, who sent us a great number of Landsat images. Furthermore, the Norwegian Water Resources and Energy Administration provided resources for the work in several ways. Its chief hydrologist, Dr. Jakob Otnes, supplied ample historic material; Mr. Bård Braskerud drafted many of the illustrations; Mrs. Evy Vollmo, Mrs. Rigmor Haugunn, and Miss Eva Klausen typed the manuscript. The photographer, Mr. Henrik Svedahl, carried out the tedious task of recording parts of Landsat images from the screen of a color-additive viewer and also assisted in making enlargements. Dr. Olav Liestøl, a glaciologist at the Norwegian Polar Research Institute, read the manuscript and made valuable comments.

The authors express their sincere thanks to all those who have contributed in one way or another to assist us in preparing "Glaciers of Norway."

References Cited

Ahlmann, H.W:son, 1922, Glaciers in Jotunheimen and their physiography: Geografiska Annaler, v. 4, no. 1, p. 1–57.

Andersen, J.L., and Sollid, J.L., 1971, Glacial chronology and glacier geomorphology in the marginal zones of the glaciers Midtdalsbreen and Nigardsbreen, south Norway: Norsk Geografisk Tidsskrift, v. 25, no. 1, p. 1–38.

de Seue, C., 1870, Le nevé de Justedal et ses glaciers (Publié par S.A. Sexe) [The firn of Justedal and its glaciers (Published by S.A. Sexe)]: University Programme, Christiania, 55 p.

Faegri, K., 1933, Über die Längenvariation einiger Gletscher des Jostedalsbre und die dadurch bedingten Pflanzensukzessionen [The fluctuation of some outlet glaciers of Jostedalsbre and the resulting plant succession]: Bergens Museums Årbok 1933, no. 2, p. 1–255.

———1940, Forandringer ved norske breer 1937–39 [Changes of Norwegian glaciers]: Bergens Museums Årbok 1939–40, Naturvitenskapelig rekke, no. 3, 9 p.

Forbes, J.D., 1853, Justedalen-Fillefield, *in* Norway and its glaciers visited in 1851; followed by journals of excursions in the high Alps of Dauphiné, Berne, and Savoy: Edinburgh, A. & C. Black (Publishers) Ltd., Chap. 7, 349 p.

Foss, M., 1803, Justedalens kortelige Beskrivelse [Short description of the Jostedalen valley]: Magazin for Danmarks og Norges topografiske, oeconomiske og statistiske Beskrivelse, v. 2, p. 1–42.

Friis, P.C., 1632, Om Quindhaerrit oc Fuglesand [On the parish Kvinnherad and Folgefonni], *in* Storm, Gustav, ed., Norriges Bescrifuelse: Samlede Skrifter, v. 83, 493 p.

Haakensen, N., 1982, Glasiologiske undersøkelser i Norge 1980 [Glaciological investigations in Norway]: Hydrologisk avdeling, Norges vassdrags- og elektrisitetsvesen, Oslo, Report No. 1–82, 87 p. [In Norwegian with a summary in English.]

Haakensen, N., and Elvehøy H., 1992, Massebalansemålinger på norske breer 1990 [Mass-balance measurements on Norwegian glaciers, 1990]: NVE-Publikasjon no. XX fra Hydrologisk avdeling, Norges vassdrags- og energiverk (In Norwegian with a summary in English).

Hoel, A., and Norvik, J., 1962, Glaciological bibliography of Norway: Norsk Polarinstitutt, Skrifter No. 126, 242 p.

Hoel, A., and Werenskiold, W., 1962, Glaciers and snowfields in Norway: Norsk Polarinstitutt, Skrifter No. 114, 291 p.

Illustreret Nyhedsblad, 1864, Nigaardsbraeen i Justedalen [Woodcut]: 13th year, no. 10 (6 March 1864), p. 51.

Liestøl, O., 1962a, List of the area and numbers of glaciers, *in* Hoel, A., and Werenskiold, W., eds., Glaciers and snowfields in Norway: Norsk Polarinstitutt, Skrifter No. 114, p. 35–54.

———1962b, Glacier fluctuations, *in* Hoel, A., and Werenskiold, W., eds., Glaciers and snowfields in Norway: Norsk Polarinstitutt, Skrifter No. 114, p. 57–79.

———1967, Storbreen Glacier in Jotunheimen, Norway: Norsk Polarinstitutt, Skrifter No. 141, 63 p.

Liestøl, O., and Østrem, G., 1963, Brekart over Sør-Norge [Glacier map of southern Norway]: 1:500,000-scale map mostly compiled from aerial photographs from the year 1955, Norges vassdrags- og elektrisitetsvesen, Oslo [In Norwegian and English].

Østrem, G., 1960, Breer og morener i Jotunheimen: Norsk Geografisk Tidsskrift, no. 17, p. 210–243.

———1963, Oversikt over breer i Skandinavia. [Glaciers in Scandinavia]: 1:1,800,000-scale map, Hydrologisk avdeling, Norges vassdrags- og elektrisitetsvesen, Oslo [In Norwegian and English].

———1964, Ice-cored moraines in Scandinavia: Geografiska Annaler, v. 46, no. 3, p. 282–337.

———1966, The height of the glaciation limit in southern British Columbia and Alberta: Geografiska Annaler, Series A, v. 48, no. 3, p. 126–138.

———1975, ERTS data in glaciology-An effort to monitor glacier mass balance from satellite imagery: Journal of Glaciology, v. 15, no. 73, p. 403–415.

———1976, Fjernanalyse [Remote sensing]: Naturen, v. 100, no. 5–6, p. 329–338.

Østrem, G., Andersen, T., Ødegaard, H., and del Llano, R., 1979, Snow and ice mapping: Norwegian examples for run-off prediction, *in* Use of data from meteorological satellites, Proceedings of a Technical Conference, Lannion, September 1979, European Space Agency Special Publication 143, p. 177–181.

Østrem, G., Dale Selvig, K., and Tandberg, K., 1988, Atlas over breer i Sør-Norge [Atlas of glaciers in south Norway] (revised ed.): Meddelelse No. 61 fra Hydrologisk avdeling, Norges Vassdrags- og Energiverk, Oslo, 248 p. [in Norwegian and English].

Østrem, G., and Haakensen, N., 1980, The Scandinavian glacier inventory-Two glacier atlases, *in* Proceedings of the Workshop on the World Glacier Inventory (Riederalp, Switzerland; September 1978): International Association of Hydrological Sciences-Association Internationale des Sciences Hydrologiques Publication No. 126, p. 161–171.

Østrem, G., Haakensen, N., Kjøllmoen, B., Laumann, T., and Wold, B., 1991, Massebalansemålinger på norske breer 1988 og 1989 [Mass-balance measurements on Norwegian glaciers, 1988 and 1989]: NVE-Publikasjon no. 11 fra Hydrologisk avdeling, Norges vassdrags- og energiverk, 78 p. (In Norwegian with a summary in English).

Østrem, G., Haakensen, N., and Melander, O., 1973, Atlas over breer i Nord-Skandinavia [Atlas of glaciers in northern Scandinavia]: Meddelelse No. 22 fra Hydrologisk avdeling, Norges vassdrags- og elektrisitetsvesen, 315 p. [In Norwegian and English].

Østrem, G., Liestøl, O., and Wold, B., 1976, Glaciological Investigations at Nigardsbreen, Norway: Norsk Geografisk Tidsskrift, v. 30, p. 187–209.

Østrem, G., and Ziegler, T., 1969, Atlas over breer i Sør-Norge [Atlas of glaciers in southern Norway]: Meddelelse No. 20 fra Hydrologisk avdeling, Norges vassdrags- og Elektrisitetsvesen, Oslo, 207 p. [In Norwegian and English].

Øyen, P.A., 1898, Norvège—Les variations periodique des glaciers. 3[e] rapport. [Norway—The periodic variations of its glaciers, Report 3]: Archives Sciences et Physique Naturelle, Tome 6, Genève, p. 40–41.

———1907, Klima und Gletscherschwankungen in Norwegen [Climate and glacier variations in Norway]: Zeitschrift für Gletscherkunde, v. 1, no. 1, p. 46–61.

———1915, Norvège—Les variations periodique des glaciers. 19[e] rapport. [Norway—The periodic variations of its glaciers, Report 19]: Zeitschrift für Gletscherkunde, v. 9, p. 53–55.

Pillewizer, W., 1950, Bewegungsstudien an Gletschern des Jostedalsbre in Sud-Norwegian [Studies of the movement on glaciers of Jostedalsbreen in southern Norway]: Erdkunde, v. 4, no. 3/4, p. 201–206.

Rekstad, J.B., 1905, Fra Jostedalsbreen [From Jostedalsbreen]: Bergens Museums Aarbog 1904, Naturvidenskabelig rekke No. 1, 95 p.

Roland, E., and Haakensen, N., 1985, Glasiologiske undersøkelser i Norge 1982 [Glaciological investigations in Norway 1982]: Hydrologisk avdeling, Norges vassdrags- og elektrisitetsvesen: Oslo, Report No. 1–85, 102 p. [In Norwegian with a summary in English].

Sexe, S.A., 1864, Om Sneebraeen Folgefond [About the Folgefonni ice cap]: University Programme, Christiania, 36 p.

UNESCO, 1970, Combined heat, ice and water balance at selected glacier basins: Technical Papers in Hydrology, no. 5, 20 p.

Glaciers of Europe—

GLACIERS OF SWEDEN

By VALTER SCHYTT

SATELLITE IMAGE ATLAS OF GLACIERS OF THE WORLD

Edited by RICHARD S. WILLIAMS, Jr., *and* JANE G. FERRIGNO

U.S. GEOLOGICAL SURVEY PROFESSIONAL PAPER 1386–E–4

Sweden has a total area of 314 square kilometers covered by glaciers, one of which (Storglaciären, in Swedish Lapland) is subject of the longest continuous series of mass-balance measurements in the world, initiated in 1945–46

CONTENTS

Page

Abstract ---------- E111
Introduction ---------- 111
Occurrence of glaciers ---------- 111
Observation of glaciers ---------- 112

FIGURE 1. Index map of Sweden showing the location of the 20 largest glaciers listed in table 2 ---------- 113
2. Graph of winter, summer, and net mass-balance measurements of Storglaciären, Kebnekaise, Lapland, Sweden, for the period 1945–46 through 1983–84 ---------- 114
3. Terrestrial photographs of the terminus of Storglaciären taken 52 years apart ---------- 115

TABLE 1. Glacier inventories of Sweden ---------- 112
2. Areas of the largest glaciers in Sweden ---------- 113

Mapping of glaciers ---------- 114
Aerial photography ---------- 117
Satellite imagery ---------- 117

FIGURE 4. *A*, Map of the lower part of Storglaciären showing the results of radio-echosounding; *B*, Isometric diagram of the subglacial bedrock topography of Storglaciären and Isfallsglaciären derived from radio-echosounding data ---------- 116
5. A portion of the map of the Tarfala Valley area and part of the Kebnekaise massif area, Sweden, compiled by stereophotogrammetric methods from the 14 September 1969 vertical aerial photographs ---------- 118
6. Index map to the optimum Landsat 1, 2, and 3 images of the glaciers of Sweden ---------- 120
7. Annotated 1:500,000-scale enlargement of a Landsat image (1350–10005; band 7; 8 July 1973; Path 213, Row 12) of the Storglaciären and other glaciers in the Kebnekaise massif area ---------- 122
8. Vertical aerial photograph of the Kebnekaise massif and its glaciers on 29 August 1972 ---------- 123
9. Part of a vertical aerial photograph of the central part of the Kebnekaise massif on 29 July 1980, with Storglaciären in the lower part of the photograph ---------- 123
10. Vertical aerial photograph of the terminus of Storglaciären on 22 August 1968 ---------- 123

TABLE 3. Optimum Landsat 1, 2, and 3 images of the glaciers of Sweden ---------- 121

Conclusions ---------- 124
Acknowledgments ---------- 124
References cited ---------- 125

GLACIERS OF EUROPE—

GLACIERS OF SWEDEN

By VALTER SCHYTT[1] [2]

Abstract

The most recent glacier inventory lists a total glacier area for Sweden of 314 square kilometers. The first glaciological observations were made in 1807, but no further studies were carried out until the end of the century. The modern center for the study of Swedish glaciers is the Tarfala Glaciological Station in Kebnekaise, Lapland. At Storglaciären, in Kebnekaise, winter, summer, and net mass-balance measurements were begun in 1945–46, the longest continuous mass-balance series in the world. The first map of the Swedish glaciers was published in 1910, but it was not until good-quality topographic maps and aerial photographs were available in the 1960's that it was possible to produce an accurate map of the shape and extent of Swedish glaciers. This map was published in 1973 as part of the "Atlas of Glaciers in Northern Scandinavia." It includes maps at scales of 1:1,500,000, 1:600,000, 1:500,000, and 1:250,000. However, a few of the Swedish glaciers, for example Kårsajökeln and Storglaciären, had been mapped previously at larger scales. Satellite imagery has a very limited application for glaciological studies in Sweden because most of Sweden's glaciers are too small for the spatial resolution of the Landsat MSS sensors. Repetitive aerial photographic coverage is available.

Introduction

Occurrence of Glaciers

The total number of glaciers in Sweden has varied from one climatic epoch to another and from one glacier inventory to the next. Many glaciers are so small that a climatic warming, like the one experienced in the period between 1910 and 1940, could markedly reduce the area and volume of active glaciers to tiny patches of ice. All modern glacier inventories of Sweden have been based on aerial photographs, and it is often very difficult to distinguish between a small glacier and a large snow field, especially if the photographs happen to have been taken during a cold summer, when there is much residual snowpack.

However, the more recent inventories should be better than previous ones, because more photographic material has become available and all deviations from previous glacier maps have been assessed carefully. The results of three complete glacier inventories (Schytt, 1959; Vilborg, 1962; and Østrem and others, 1973) are summarized in table 1.

It was found during these inventories that the quality of the topographic maps, the scale of the aerial photographs, and the availability of several years of photographic coverage were the most important factors in achieving an acceptable final result. Table 2 provides information on the areas of the 20 largest glaciers in Sweden. Their locations are shown on figure 1.

---

[1] Stockholm University, Department of Physical Geography, S–10691 Stockholm, Sweden.
[2] Deceased on 30 March 1985.

TABLE 1.—*Glacier inventories of Sweden*

Glaciologist	Source of data	Number of glaciers	Area of glaciers (km^2)
Schytt (1959)	One set of 1:65,000-scale aerial photographs acquired in 1958 and 1:200,000-scale topographic maps compiled from plane-table surveys in the late 1800's (ca. 1890).	237	310
Vilborg (1962)	Modification of Schytt's 1959 map, aerial photographs acquired during the years 1959–61, and extensive field observations.	287	329
Østrem and others (1973)	1959 and 1963 aerial photographs and the new 1:100,000-scale topographic map series compiled from aerial stereophotogrammetric methods.	294	314

Observation of Glaciers

The Swedish high mountains are situated in a much more continental type of climate than most of the Norwegian mountains. Therefore, only a few massifs reach above the present-day glaciation level, and, when they do, the areas are too small to support any really large glaciers. There are nearly 30 glaciers in Norway, for example, that are larger than Sweden's largest glacier, Stourrajekna. Norway's largest glacier, Jostedalsbreen (487 km^2), covers 50 percent more area than all the Swedish glaciers combined. Furthermore, the Swedish glaciers are all situated far from populated areas and did not attract people's attention until the 1800's.

Although the first scientific glaciological observations were made by Göran Wahlenberg in 1807 (Wahlenberg, 1808), no further studies were carried out until the end of the century, when Fredrik Svenonius, Jonas Westman, Axel Hamberg, Axel Gavelin, and Fredrik Enquist became interested in them. Together they published "Die Gletscher Schwedens im Jahre 1908" ["The Swedish Glaciers in the Year 1908"] for the International Geological Congress, which was held in Stockholm in 1910 (Svenonius and others, 1910). Their publication is of great value, because it describes several glaciers before the great glacier retreat that started in about 1915.

Another important contribution to historical study of Swedish glaciers was Fredrik Enquist's terrestrial photogrammetric mapping of the Kebnekaise glaciers in 1910. For this purpose he took a set of excellent-quality terrestrial photographs on 18- by 24-cm glass plates; these photographs show all glaciers and glacier termini in August 1910. Axel Hamberg began a comprehensive study of glaciers in the Sarek Mountains, especially of the glacier Mikkajekna (Mikkajökeln), in 1895 (Hamberg, 1896), but the longest and most continuous study of the variation in termini of a glacier is that of the glacier Kårsajökeln (fig. 1), which lies farther north (Ahlmann, 1929; Schytt, 1963).

The modern center for the study of Swedish glaciers is the Tarfala Glaciological Station in Kebnekaise, Lapland (see fig. 5). The station is situated 70 km west of Kiruna, 30 km from the end of the road, at 1,130 m elevation, about 400 m above the tree line. Two glaciers in the Tarfala Valley were surveyed in 1897 and several times between 1908 and 1920. In the spring of 1946, this author began a series of mass-balance studies of Storglaciären that are still going on (Schytt, 1981; Grudd and Jannson,

TABLE 2.—*Areas of the largest glaciers in Sweden (Information from Østrem and others, 1973)*

Number (see fig. 1)	Glacier name	Area (km^2)
1..........	Stourrajekna	12.75
2..........	Ålmaijekna	12.15
3..........	Salajekna	11.10
4..........	Pårtejekna	11.10
5..........	Jåkåtjkaskajekna	9.96
6..........	Suottasjekna	8.11
7..........	Mikkajekna	7.62
8..........	Å. Ålkatj-jekna	6.56
9..........	Å. Ruotesjekna	5.41
10..........	Riukojietna	4.99
11..........	Buchtglaciären	4.65
12..........	Rabots Glaciär	4.22
13..........	W. Sarekglaciären	4.00
14..........	S. Akkajekna	3.94
15..........	Mårmaglaciären	3.93
16..........	Vartasjekna	3.64
17..........	Ruopsokjekna	3.63
18..........	Svenonius Glaciär	3.50
19..........	Vuoinesjekna	3.35
20..........	Storglaciären	3.06

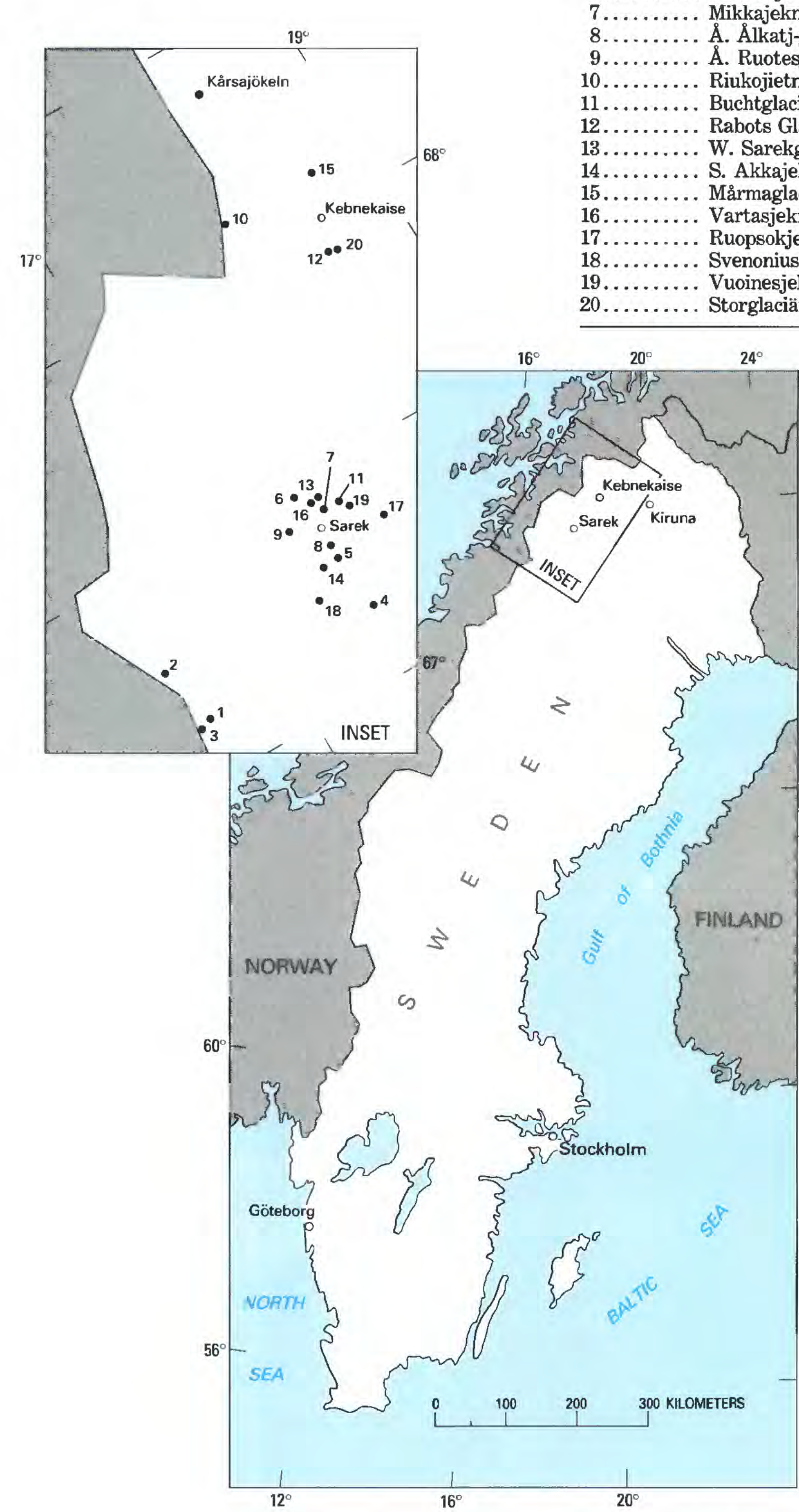

***Figure 1.**—Index map of Sweden showing the location of the 20 largest glaciers listed in table 2.*

1986; Naturgeografiska Institutionen, 1987–90). Storglaciären is one of only a very few glaciers in the world in which all three balance terms are known—winter balance, summer balance, and net balance, for each year, starting in 1945–46 (fig. 2). Several other studies have been or are being carried out on Storglaciären: movement, debris content and transport, glacier drainage, crystallography, ice temperatures, and thickness, for example (figs. 3 and 4).

To ensure that Storglaciären is reasonably representative of the glaciers in Lapland, 20 other glacier termini are also surveyed quite regularly, from Kårsajökeln in the north (at 68°22′N. lat) to Salajekna in the south (at 67°08′N. lat). Glacier recession was still taking place in 1981 at all Swedish glaciers, although at a slower rate than was the case during the 1940's and 1950's.

Mapping of Glaciers

In "Die Gletscher Schwedens im Jahre 1908," Axel Hamberg published a map of the Swedish glaciers (Svenonius and others, 1910), but it was the areal distribution rather than the characteristics of the individual glaciers that was of prime importance to him. At that time it was next to impossible to make a good glacier map, because the National Land Survey maps of the Lappish mountains were all compiled around 1890 and were published at a scale of 1:200,000. There were no railroads at the time, and hardly any roads led to the mountains, so it is remarkable that the cartographers managed to make a map that had all major features in the right place. It is not surprising that many glaciers were not shown and that many snow fields were mapped as glaciers. Anyone who knows what the field conditions were like in the 1880's and 1890's can appreciate the difficulties in preparing an accurate topographic map.

The next attempt to map the glaciers was made by Fredrik Enquist in 1918 when he made a study of the height of the glaciation level (Enquist,

Figure 2.—Winter, summer, and net mass-balance measurements of Storglaciären, Kebnekaise, Lapland, Sweden, for the period 1945–46 through 1983–84. Summer balance and net balance both show a periodic variation of 12 years. Solid lines indicate a moving 3-year average for winter balance (top), net balance (middle), and summer balance (bottom). The net balance figures indicate glacier recession has been taking place since 1945, but the rate in recent years is slower than in the 1940's and 1950's (modified from fig. 2 in Schytt, 1981, p. 220).

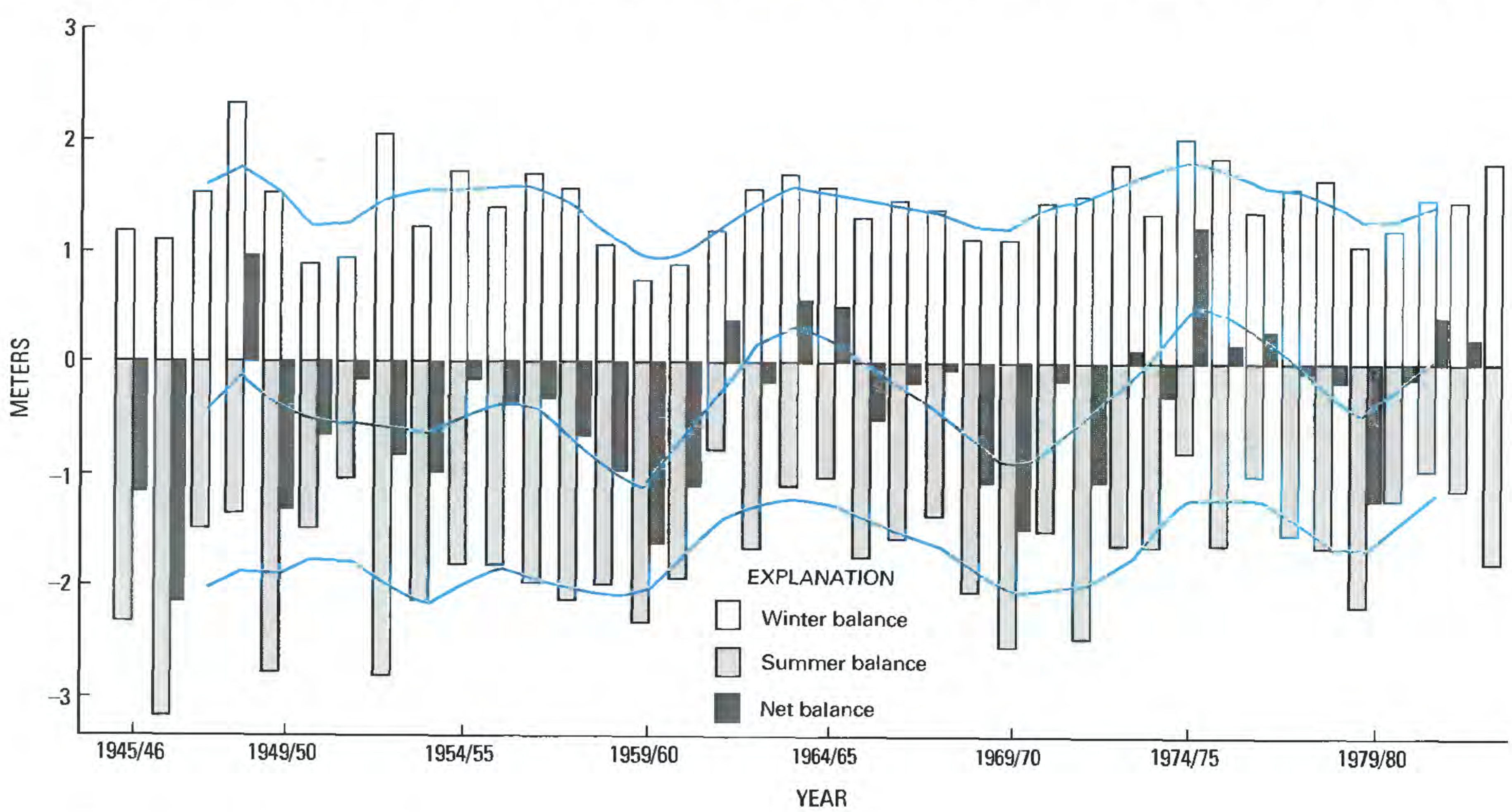

*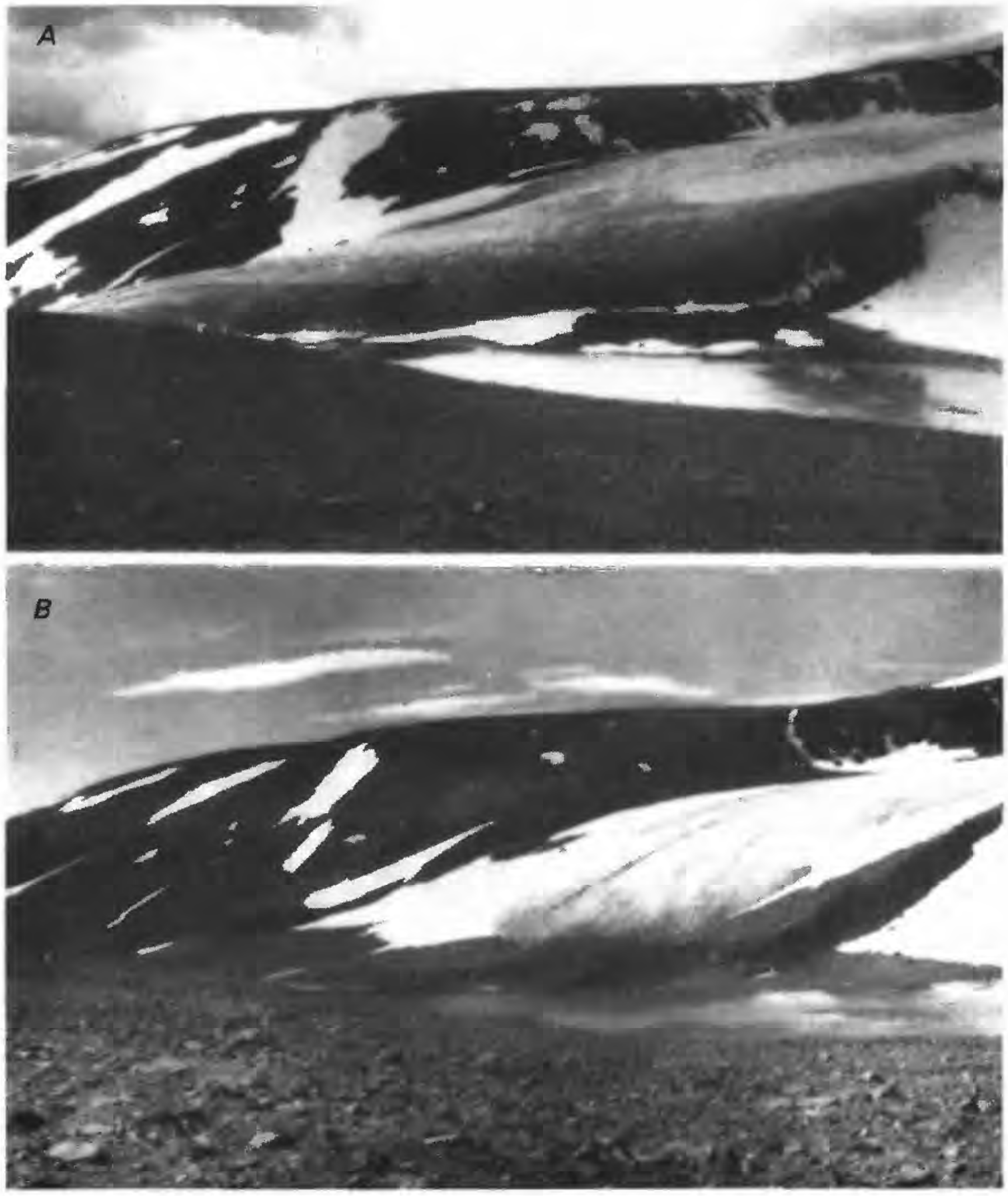

Figure 3.—Terrestrial photographs of the terminus of Storglaciären taken 52 years apart. These two photographs of Storglaciären were taken from the same vantage point, but 52 years separate them in time. When the upper photograph (A) was taken in August 1910 by Fredrik Enquist, the glacier reached all the way down into the valley, and one part extended all the way up the other side. The summer 1962 photograph (B) by Valter Schytt shows a markedly thinned glacier that ends high up on the mountainside a long way from its "days of glory," as shown by the huge terminal and lateral moraines (from Schytt, 1963).*

1918). However, his map shows all glacierized mountainous areas in Sweden but not the individual glaciers themselves.

The poor-quality topographic maps available made good glacier inventories more or less impossible. A few glaciers were mapped quite well during the early half of the century (Kårsajökeln in 1925 and 1943; Storglaciären in 1910, 1922, and 1949), but the topographic maps could not be adjusted to accept this detailed information.

In 1958, however, the entire mountainous part of western Sweden was photographed at a scale of 1:65,000 by the Swedish Air Force at the request of the National Land Survey. These aerial photographs were used for the preparation of the first modern glacier inventory of Sweden by this author. Schytt's map in Geografiska Annaler (Schytt, 1959) was the first detailed compilation. However, his map, as well as Vilborg's improved version in 1962, was based on the older topographic map sheets and could not possibly attain a very high degree of accuracy.

A great step forward was taken in 1973, when the "Atlas over breer i Nord-Skandinavia" ["Atlas of Glaciers in Northern Scandinavia"] was published by Østrem and others (1973). Melander, who was responsible for the Swedish part of this comprehensive inventory, used a completely new set of 1:100,000-scale photogrammetric maps of very good quality, with most of the glaciers already well portrayed. The photographic coverage was also far better, both in terms of higher quality and larger scale, than that which was available to the author in the late 1950's. Schytt's map (1959) was published at a scale of 1:600,000, and the glacier atlas contains maps with scales of 1:1,500,000, 1:600,000, 1:500,000, and 1:250,000. The glacier atlas and the ordinary topographic maps together give a very good record of the shape and extent of Swedish glaciers during the 1960's.

Besides the small-scale maps of the regional glacier inventory, a few of the Swedish glaciers have also been mapped at larger scales for scientific purposes. Kårsajökeln, for example, was mapped by Hans Ahlmann in 1926 (Ahlmann, 1929); by this author, based on 1943 aerial photographs (Wallén, 1948); and by the Durham University Exploration Society in 1961 (Schytt, 1963). Storglaciären was mapped by terrestrial photogrammetry from photographs acquired in 1910 (fig. 3*A*) and 1949, by aerial photogrammetry from photographs acquired in 1959, 1969 (fig. 5), and 1980, and by radio-echosounding methods in 1979 (Björnsson, 1981) (fig. 4).

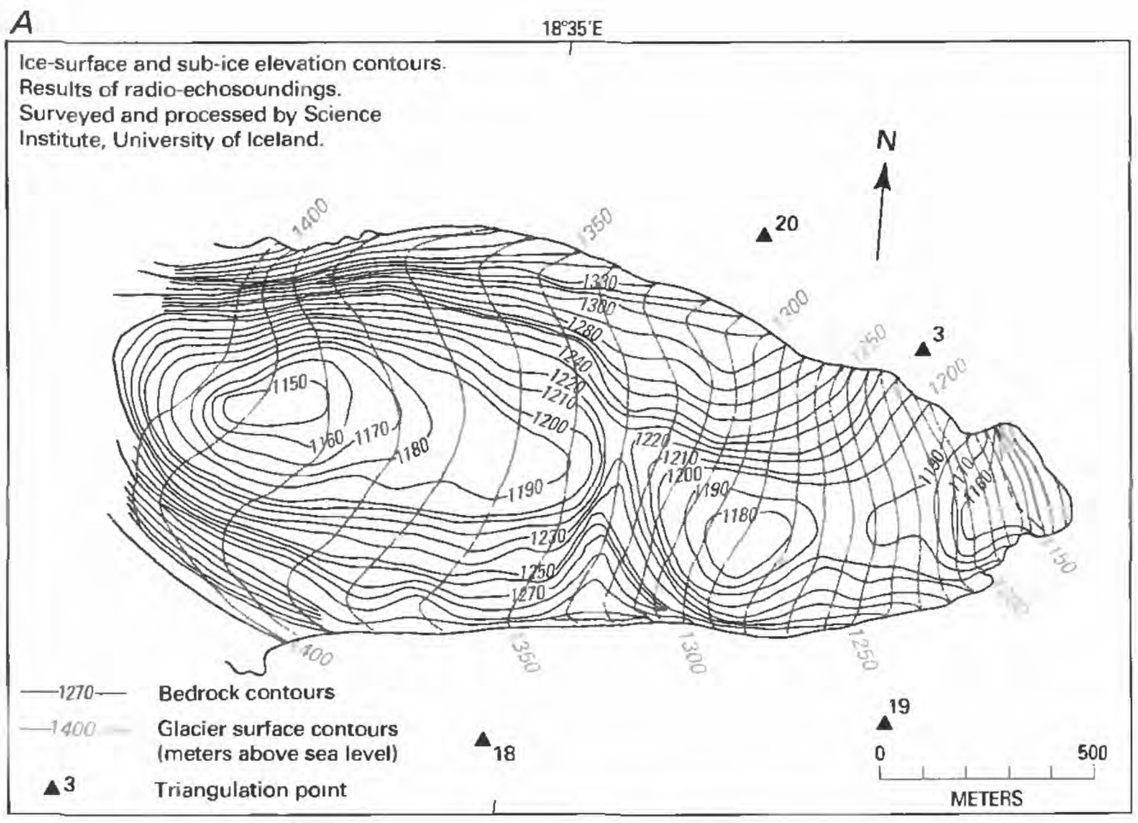

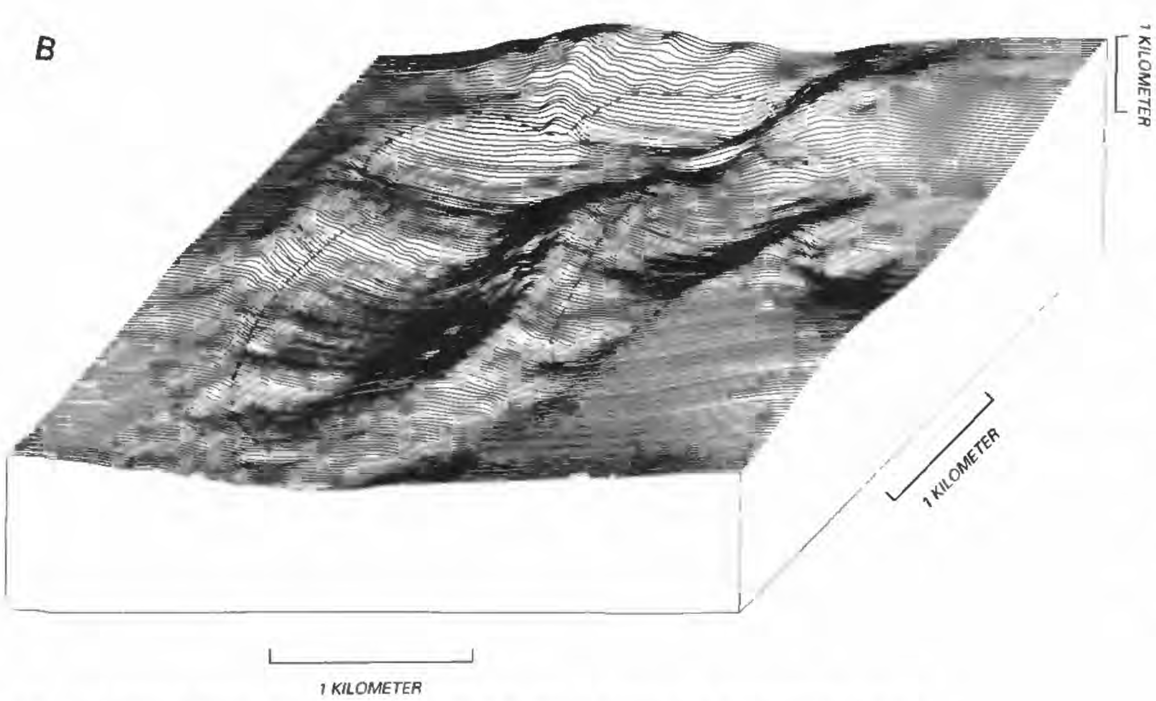

Figure 4.—*A, Map of the lower part of Storglaciären showing the results of radio-echosounding. Ice-surface and subglacial-bedrock elevation contours plotted at 10-m intervals. B, Isometric diagram of the subglacial bedrock topography of Storglaciären (left) and Isfallsglaciären (right) derived from radio-echosounding data. The dashed line shows the present margin of the two glaciers (from figs. 3 and 4 in Björnsson, 1981, p. 227).*

TARFALA RESEARCH STATION, SWEDEN

The Tarfala Research Station in the Kebnekaise area of Sweden is the principal field research facility for long-term observations of Swedish glaciers. The station is situated about 150 km north of the Arctic Circle at lat 67° 54′ N., long 18° 34′ E. (60 km west of Kiruna, or 30 km by foot-trail from the village of Nikkalaukta) and provides ready access to the surrounding glacierized region. The mass balance of Storglaciären, for example, has been measured every year since 1946, the longest continuous series for any of the Earth's glaciers. At any one time, a number of large and small field-based research projects in various scientific specialties are underway at the station; these are carried out by established scientists and students from many different countries. The Tarfala Research Station can accommodate about 35 people at one time and is operated by the Department of Physical Geography at the University of Stockholm. (Information derived from a brochure on the "Tarfala Research Station" provided to the editors by Per Holmlund.)

Aerial Photography

Much has already been mentioned above about the aerial photographic coverage of Swedish glaciers. The earliest aerial photographs used in glaciological research were made to satisfy military mapping requirements during World War II. They were exposed on 18-cm roll film (with a frame of 18 cm by 18 cm) with a 10-cm lens from 3,000 m elevation. Because they were acquired in 1943, they have great historical value, particularly for the studies of Kårsajökeln. In 1958, the Swedish Air Force photographed all Swedish mountains by vertical aerial photography at a scale of 1:65,000.

Since 1960, the aerial photographic archives of Sweden's glaciers have expanded rapidly. Aerial photographs at a scale of 1:30,000 are now available for nearly all the glaciers, and many special aerial surveys of selected glaciers have also been made. Most aerial photographs are black-and-white, but several glaciers have now been photographed with false color-infrared film. Special photographic missions can be flown by National Land Survey aircraft at reasonable cost, so the availability of aerial photographs for special studies is no longer much of a problem.

Satellite Imagery

The Landsat multispectral scanner (MSS) images of Sweden's glaciers (figs. 6 and 7 and table 3) cannot compete with the aerial photographs, because most of Sweden's glaciers are too small for the pixel resolution (79 m) of the MSS. To prepare new glacier inventories by using Landsat MSS images is not practical because of the low spatial resolution and lack of information content when compared with large-scale vertical aerial photographs (compare fig. 7 with figs. 8, 9, and 10). The same is true for studies of accumulation, ablation, drainage, morainic features, and so on. No glaciologic or glacial geologic features cover an area large enough to be properly imaged in the Landsat images.

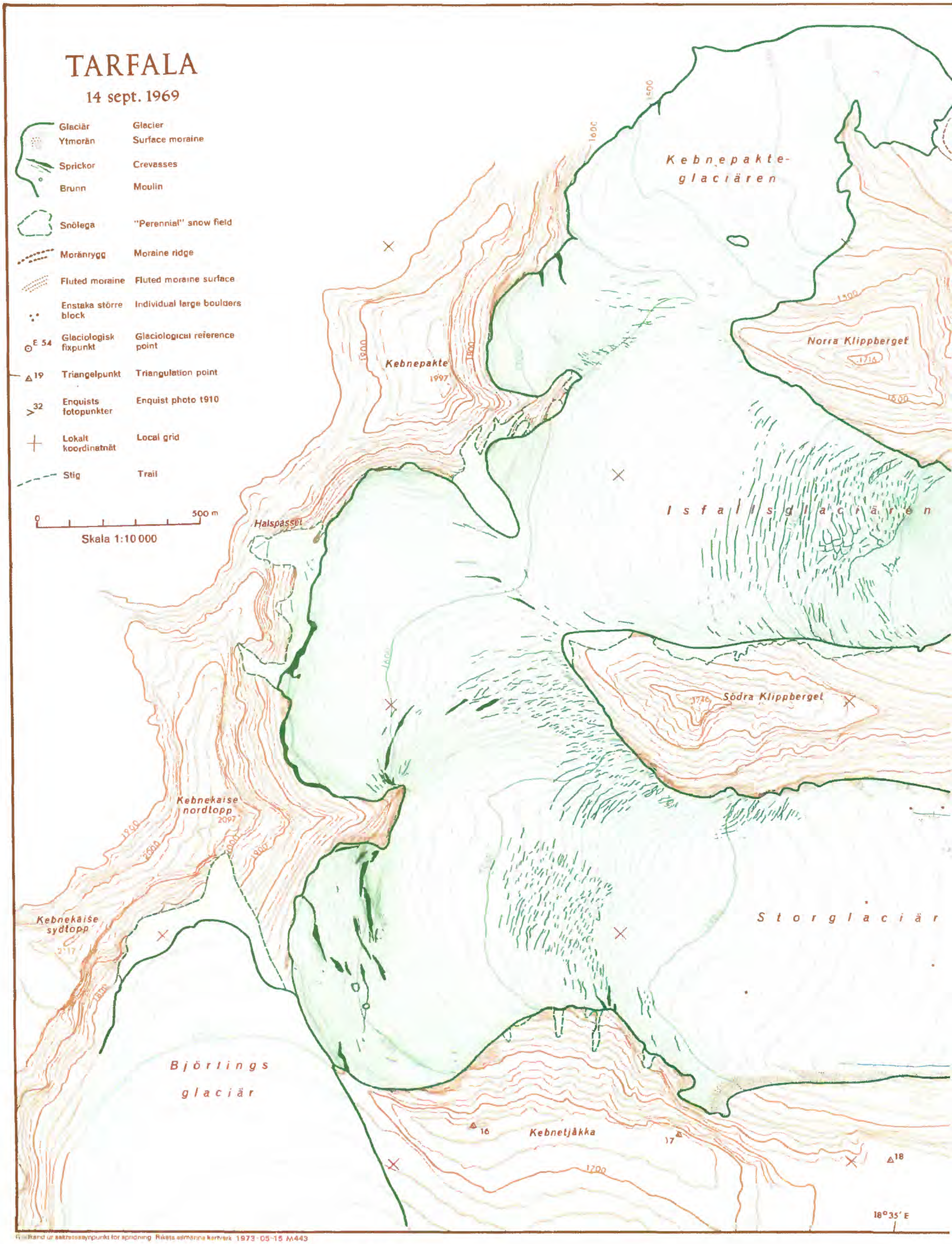

TARFALA
14 sept. 1969
Glaciär
Glacier
Ytmorän
Surface moraine
Sprickor
Crevasses
Brunn
Moulin
Snölega
"Perennial" snow field
Moränrygg
Moraine ridge
Fluted moraine
Fluted moraine surface
Enstaka större block
Individual large boulders
E 54
Glaciologisk fixpunkt
Glaciological reference point
19
Triangelpunkt
Triangulation point
32
Enquists fotopunkter
Enquist photo 1910
Lokalt koordinatnät
Local grid
Stig
Trail
0
500 m
Skala 1:10 000
Kebnepakte-glaciären
Kebnepakte
1997
Norra Klippberget
Halspasset
Isfallsglaciären
Södra Klippberget
1746
Kebnekaise nordtopp
2097
Kebnekaise sydtopp
Storglaciär
Björlings glaciär
Kebnetjåkka
16
17
18
1700
18°35′ E
1973-05-15 M443

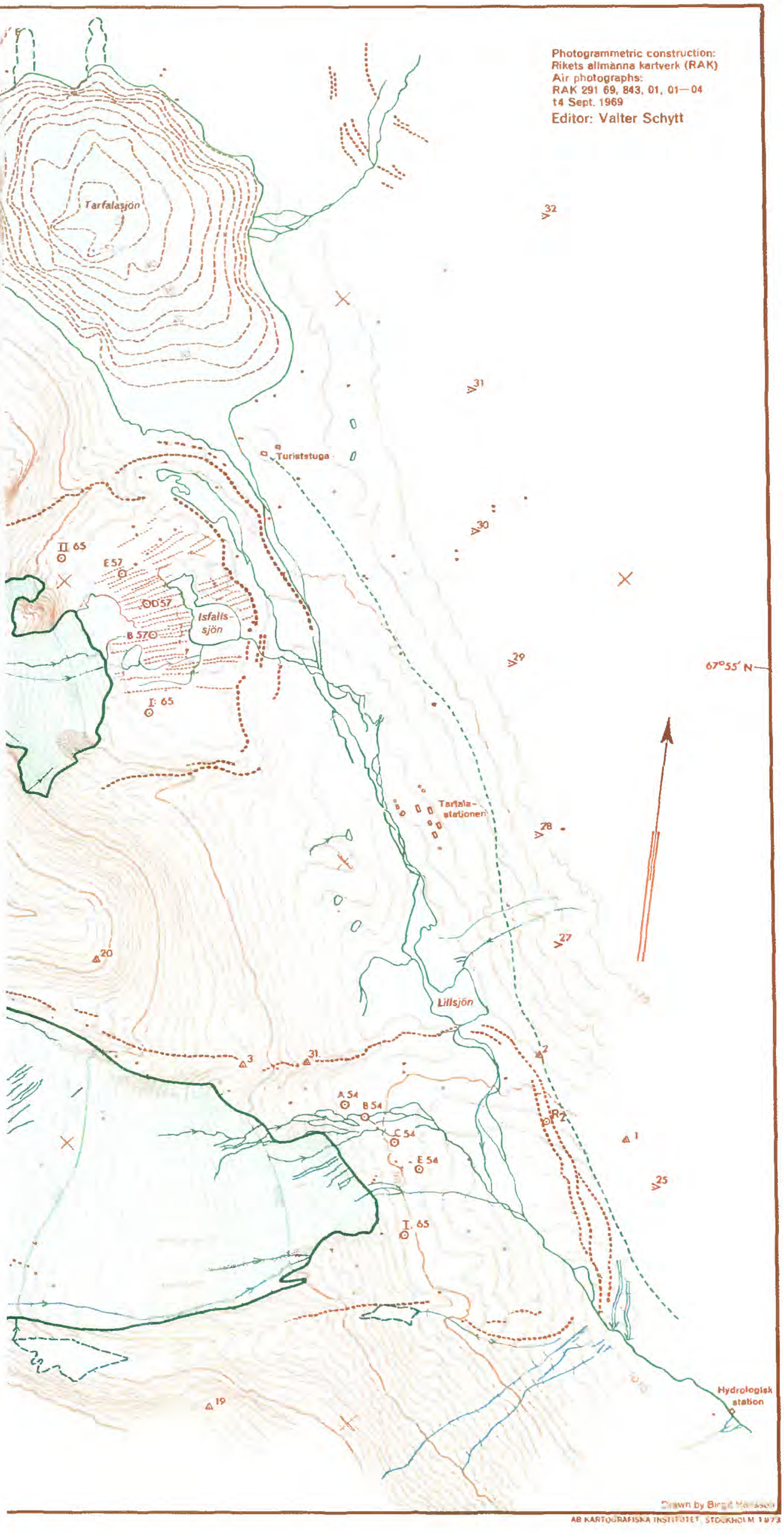

***Figure 5.**—A portion of the map of the Tarfala Valley area and part of the Kebnekaise massif area, Sweden, compiled by stereophotogrammetric methods from the 14 September 1969 vertical aerial photographs (Schytt, 1973). Storglaciären is the largest (3.06 km²) of the glaciers originally mapped at a scale of 1:10,000.*

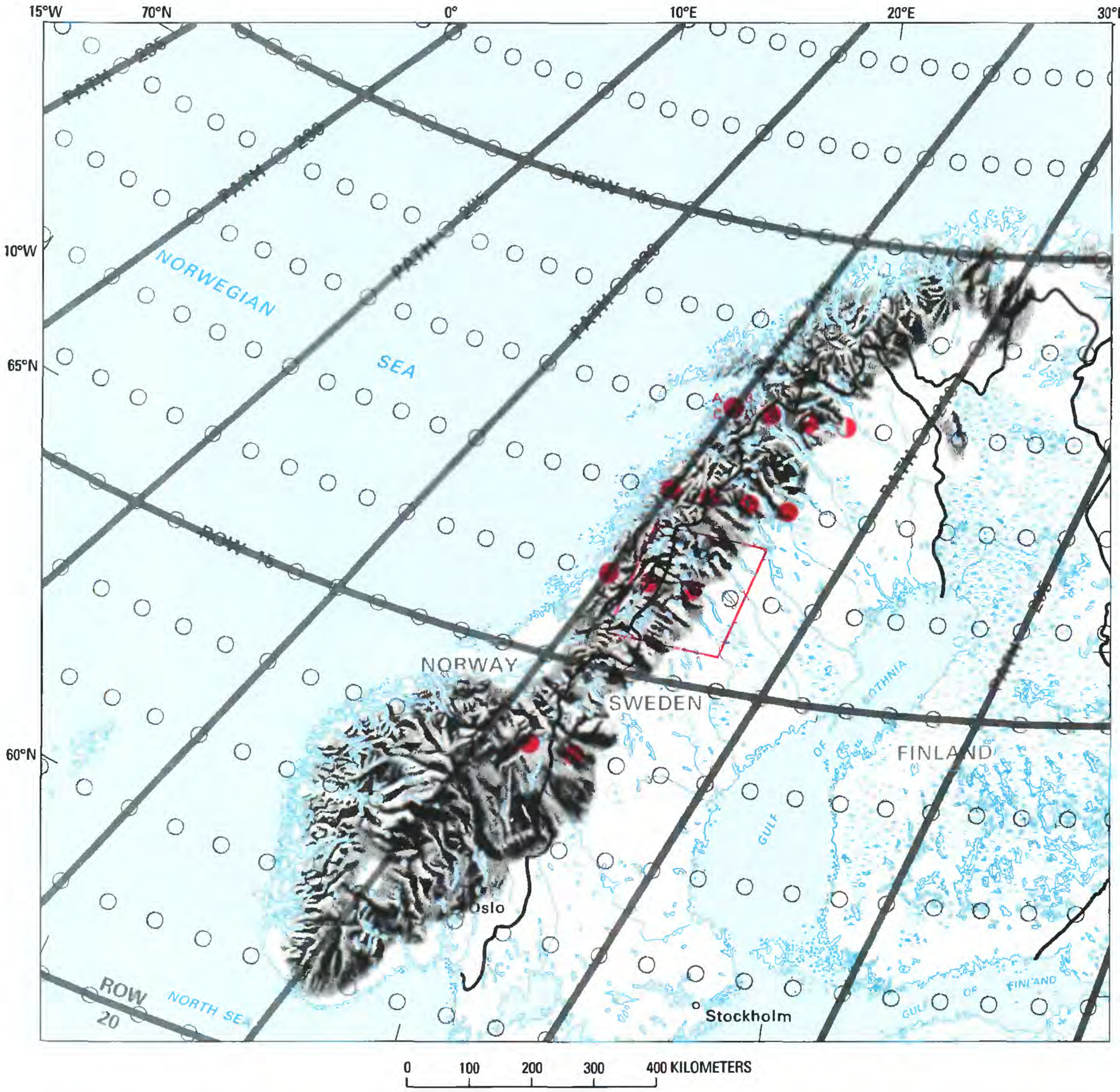

EXPLANATION OF SYMBOLS

Evaluation of image usability for glaciologic, geologic, and cartographic applications. Symbols defined as follows:

- Excellent image (0 to ≤5 percent cloud cover)
- Good image (>5 to ≤10 percent cloud cover)
- Fair to poor image (>10 to ≤100 percent cloud cover)
- A B C D — Usable Landsat 3 return beam vidicon (RBV) scenes A, B, C, D refer to usable RBV subscenes
- Nominal scene center for a Landsat image outside the area of glaciers
- Approximate size of aree encompassed by nominal Landsat MSS image

Figure 6.—*Optimum Landsat 1, 2, and 3 images of the glaciers of Sweden. The vertical lines represent nominal paths. The rows (horizontal lines) have been established to indicate the latitude at which the imagery has been acquired.*

TABLE 3.—*Optimum Landsat 1, 2, and 3 images of the glaciers of Sweden*

[See fig. 6 for explanation of symbols used in the "Code" column]

Path-Row	Nominal scene center (lat-long)	Landsat identification number	Date	Solar elevation angle (in degrees)	Code	Cloud cover (in percent)	Remarks
212–12	067°59′N. 020°03′E.	1367–09545	25 Jul 73	40	◑	50	
212–13	066°40′N. 018°25′E.	12081–09023	19 Sep 76		●	0	Sarek; archived by ESA[1]; not physically examined
213–12	067°59′N. 018°37′E.	1350–10005	08 Jul 73	43	◕	10	Kebnekaise, Storglaciären, Kårsajökeln; image used for figure 6
213–13	066°40′N. 016°59′E.	20940–09255	19 Aug 77		●	0	Archived by ESA; not physically examined
213–14	065°20′N. 015°30′E.	1422–10003	18 Sep 73	25	◕	10	
213–16	062°38′N. 012°56′E.	1422–10012	18 Sep 73	28	●	0	Sylarne
214–12	067°59′N. 017°11′E.	22075–09543	27 Sep 80	19	◑	20	Archived by ESA
214–12	067°59′N. 017°11′E.	31612–09582	03 Aug 82	38	●	0	Partial scene (75%) includes eastern glacier areas; archived by ESA
214–13	066°40′N. 015°33′E.	21301–09361	15 Aug 78	35	◑	20	Archived by ESA
214–13	066°40′N. 015°33′E.	31612–09585	03 Aug 82	39	●	0	Partial scene (75%) includes eastern glacier areas; archived by ESA
214–14	065°20′N. 014°04′E.	20941–09320	20 Aug 77		●	0	Archived by ESA; not physically examined
214–16	062°38′N. 011°30′E.	12047–09181	16 Aug 76		●	0	Archived by ESA; not physically examined
215–12	067°59′N. 015°45′E.	30893–09503–ABCD	14 Aug 80	35	A B ○ C D	10–70	Landsat 3 RBV
215–12	067°59′N. 015°45′E.	31613–10041	04 Aug 82	38	●	0	Partial scene, includes all glacier areas; archived by ESA
215–13	066°40′N. 014°06′E.	2186–10005	27 Jul 75	41	●	0	Salajekna
215–14	065°20′N. 012°38′E.	2186–10012	27 Jul 75	42	●	0	

[1] ESA is the abbreviation for the European Space Agency.

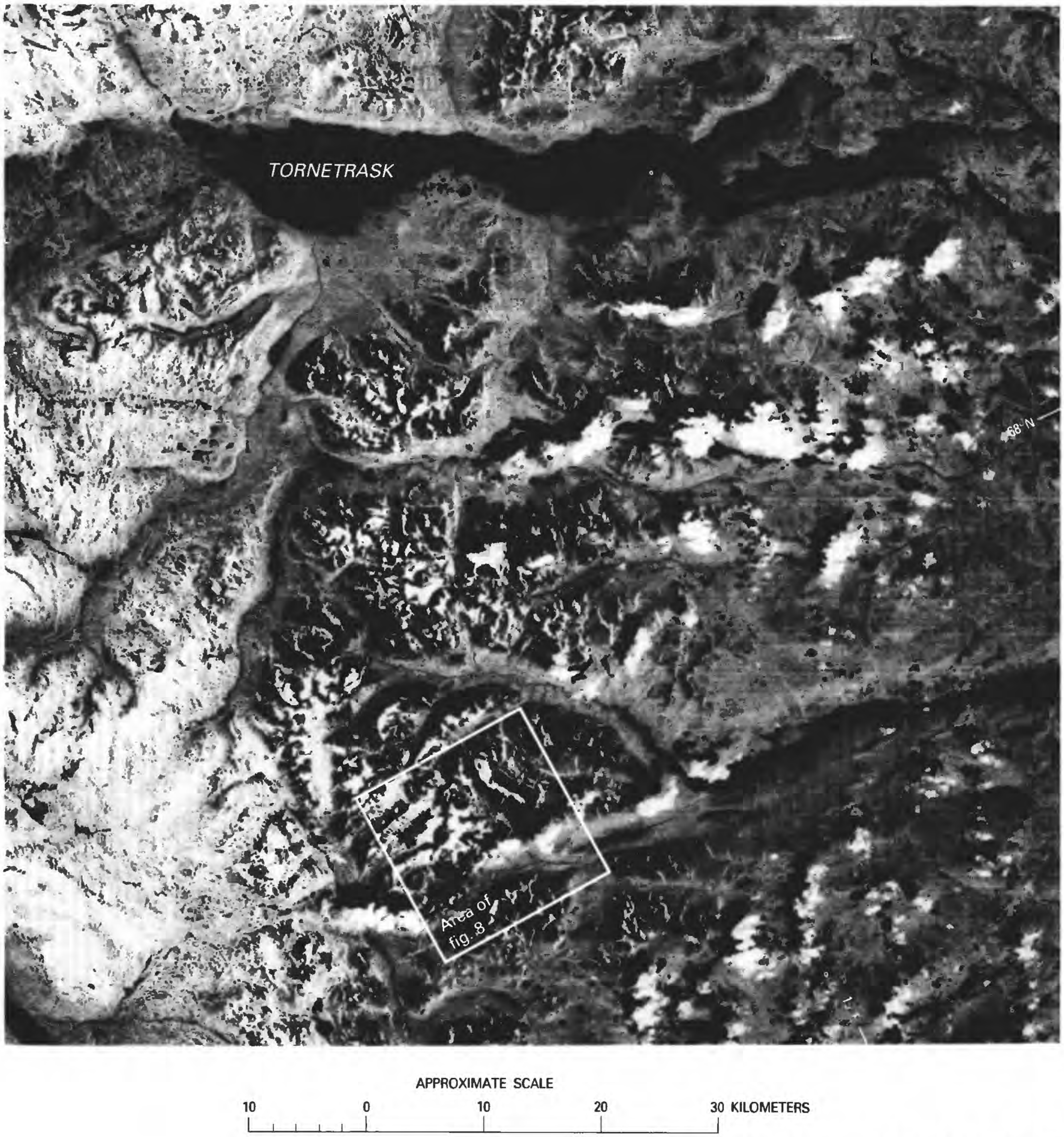

Figure 7.—*Annotated 1:500,000-scale enlargement of a Landsat image (1350–10005; band 7; 8 July 1973; Path 213, Row 12) of the Storglaciären and other glaciers in the Kebnekaise massif area. The area of figure 8 is outlined. Four of the 20 largest glaciers of Sweden listed in table 2 and located in figure 1 are in the Kebnekaise area.*

Figure 8.—*Vertical aerial photograph of the Kebnekaise massif and its glaciers on 29 August 1972. The survey aircraft flew at an altitude of 6,000 m above sea level. The camera focal length was 4.4 cm. The approximate scale of the photograph at Storglaciären is 1:150,000. The area of figure 9 is outlined; see also figure 7. Photograph no. 92–256-11–15, courtesy of the Swedish Air Force.*

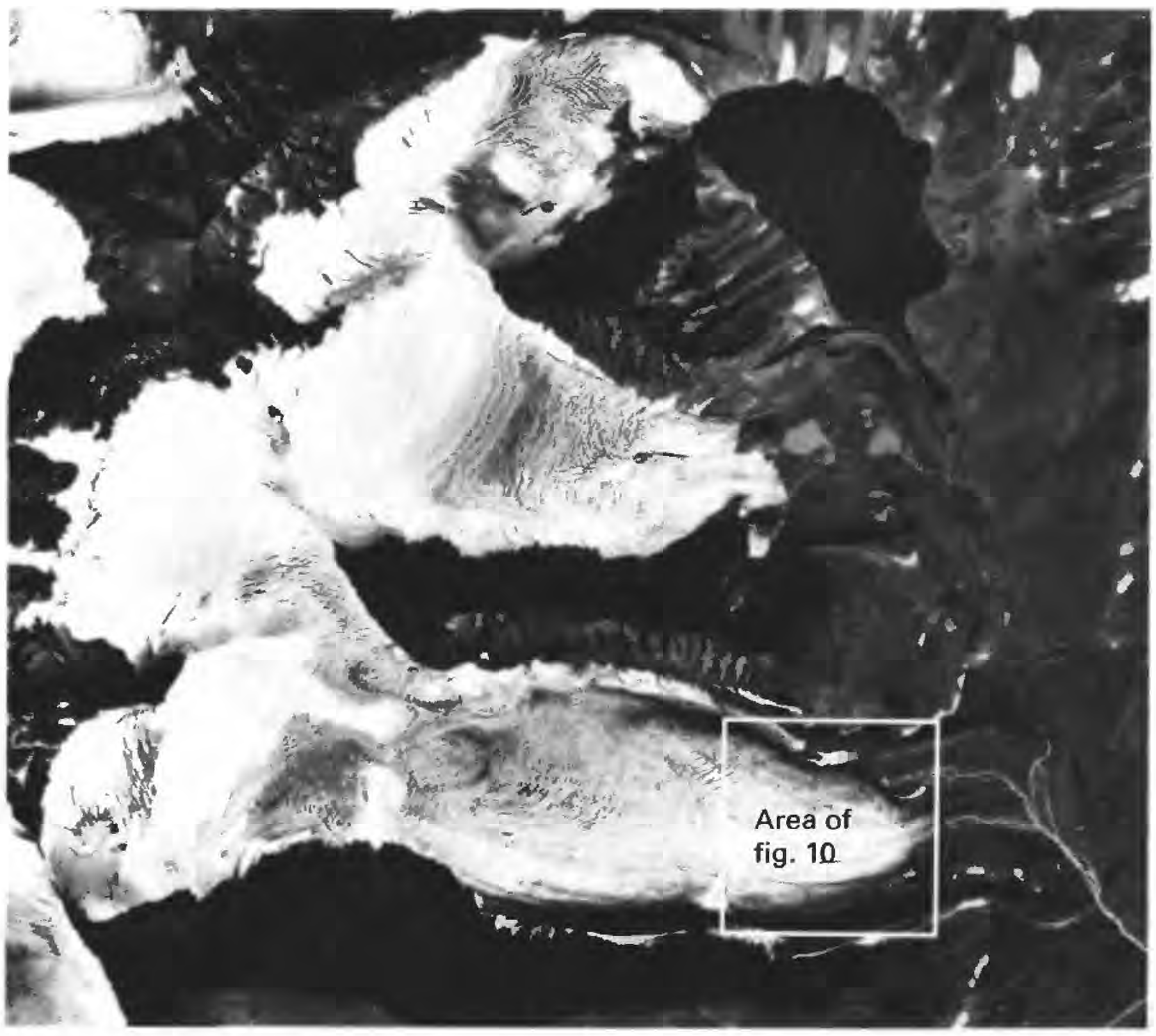

Figure 9.—*Part of a vertical aerial photograph of the central part of the Kebnekaise massif on 29 July 1980, with Storglaciären in the lower part of the photograph. The area of figure 10 is outlined. Approximate scale is 1:40,000. See also figures 7, 8, and 10 for the comparison in glaciological information available with the larger scale aerial photographs and the satellite image. Photograph No. 80–537–11–04 (SV 298) courtesy of the Swedish National Land Survey (Lantmäteriverket).*

Figure 10.—*Vertical aerial photograph of the terminus of Storglaciären on 22 August 1968. Approximate scale is 1:8,000. Photograph No. 0Y8–764–6–2, courtesy of the Swedish Air Force.*

Conclusions

The need for a good glacier map of Sweden was satisfied when the "Atlas of Glaciers in Northern Scandinavia" was published (Østrem and others, 1973). Besides containing a suite of glacier maps at scales of 1:1,500,000, 1:600,000, 1:500,000, and 1:250,000, this atlas also contains a wealth of information on each glacier, such as length, area, elevation, morainal features, glacier lakes, and glacier orientation. Over the Earth's large ice sheets, satellite images can do what no aerial photographic survey can do. In Arctic regions or remote mountains, satellite images can also be extremely valuable in the study of ice fields and ice caps. For small glaciers, especially those readily accessible to glaciologists in highly developed countries, Landsat MSS images have only limited value mainly due to spatial resolution limitations. Also, small glaciers in developed countries are often photographed at regular intervals during the course of regional aerial photogrammetric or thematic mapping surveys. Stereopairs of large-scale vertical aerial photographs are the best source material for the study of these smaller glaciers. Even in the future, when higher resolution (1:50,000-scale, 8-m spatial resolution) stereopairs of satellite photographs become available (for example, Large Format Camera photographs), it seems likely that larger scale vertical aerial photographs of the smaller glaciers will still be more useful than satellite photographs.

Acknowledgments

The editors thank Dr. Gunnar Østrem, Norges Vassdrags- og Energiverk, and Dr. Wibjörn Karlén, Stockholms Universitet, who reviewed the manuscript after the author's death and updated information in the text.

References Cited

Ahlmann, H.W:son, 1929, Kårsajökeln. Karta i skalan 1:20,000 jämte vägledning för besökande [Kårsajökeln. A map at 1:20,000-scale including a guide for visiting the area]: Svenska Turistföreningen Publication No. 451, p. 1–4.

Björnsson, H., 1981, Radio-echosounding maps of Storglaciären, Isfallsglaciären and Rabots Glaciär, northern Sweden: Geografiska Annaler, v. 63A, no. 3–4, p. 225–231.

Enquist, F., 1918, Die glaziale Entwicklungsgeschichte Nordwestskandinaviens [The glacial history of northwestern Scandinavia]: Sveriges geologiska undersökning, Series C, no. 285, Årsbok 12, no. 2, p. 1–143.

Grudd, H., and Jansson, P., 1986, The 1984/85 mass balance of Storglaciären, Kebnekaise, Swedish Lapland: University of Stockholm, Department of Physical Geography, 13 p.

Hamberg, A., 1896, Berättelse om en resa i Sarekfjällen [Report of a trip to the Sarek Highlands]: Svenska Turistföreningens årsbok 1896, p. 152–192.

Naturgeografiska Institutionen, 1987, Årsrapport från Tarfala forskningsstation 1986, Jansson, P., ed.: Stockholm, University of Stockholm, 95 p.

———1988, Årsrapport 1987: Tarfala research station, Rosqvist, G., ed.: Stockholm, University of Stockholm, 103 p.

———1989, Årsrapport 1988: Tarfala research station, Stroeven, A., ed.: Stockholm, University of Stockholm, 85 p.

———1990, Årsrapport 1989: Tarfala research station, Stroeven, A., and Eriksson, M., eds.: Stockholm, University of Stockholm, 76 p.

Østrem, G., Haakensen, N., and Melander, O., 1973, Atlas over breer i Nord-Skandinavia [Atlas of glaciers in northern Scandinavia]: Meddelelse nr. 22 fra Hydrologisk avdeling, Norges vassdrags-og elektrisitetsvesen; also published as Meddelande nr. 46 från Naturgeografiska Institutionen, Stockholms Universitet, 315 p. [In Norwegian, Swedish, and English].

Schytt, V., 1959, The glaciers of the Kebnekajse-massif: Geografiska Annaler, v. 41, no. 4, p. 213–227.

———1963, Glaciärernas liv [The life of glaciers]: Svenska Turistföreningens Årsskrift 1963, p. 144–158.

———ed., 1973, Tarfala. 14 Sept. 1969: (Special 1:10,000-scale map of glaciers in the central part of the Kebnekaise massif, Lapland, Sweden): Stockholm, AB Kartografiska Institutet.

———1981, The net mass balance of Storglaciären, Kebnekaise, Sweden, related to the height of the equilibrium line and to the height of the 500 mb surface: Geografiska Annaler, v. 63A, no. 3–4, p. 219–223.

Svenonius, F., Westman, J., Hamberg, A., Gavelin, A., and Enquist, F., 1910, Die Gletscher Schwedens im Jahre 1908 [The Swedish glaciers in the year 1908]: Stockholm, Kungl. boktryckeriet, P.A. Norstedt och söner. Sveriges geologiska undersökning, Series Ca (Avhandlingar och uppsatser i kvarto och folio), no. 5, in 6 parts, 212 p. (I. Studien über den Kårso und die Kebnegletscher nebst Notizen über andere Gletscher im Jukksajärvigebirge [Studies of the Kårsa and Kebne glaciers with notes about other glaciers in the Jukkasjärvi Mountains], by Fredrik Svenonius; II. Beobachtungen über die Sulitälmagletscher im Sommer 1908 [Observations of the Sulitälma glaciers in the summer of 1908], by Jonas Westman; III. Die Gletscher des Sarekgebirges und ihre Untersuchung. Eine kurze Übersicht [Investigation of the glaciers of the Sarek Mountains. A short review], by Axel Hamberg; IV. Über die Gletscher des Norra Storfjället und des Ammarfjället [The glaciers of northern Storfjället and Ammarfjället], by Axel Gavelin; V. Über die jetzigen und ehemaligen lokalen Gletscher in den Gebirgen von Jämtland und Härjedalen [The present and former glacier locations in the mountains of Jämtland and Härjedalen], by Fredrik Enquist; VI. Kurze Übersicht der Gletscher Schwedens [A short review of the Swedish glaciers], by Axel Hamberg.)

Vilborg, L., 1962, The recent glaciation in Sweden: Geografiska Annaler, v. 44, no. 3–4, p. 405–406.

Wahlenberg, G., 1808, Berättelse om mätningar och observationer för att bestämma lappska fjällens höjd och temperatur vid 67 graders polhöjd, förrättade år 1807 [Report on the measurements and observations to determine the height of the Lappish Mountains and the temperature near 67° latitude, carried out in 1807]: Stockholm, 58 p.

Wallén, C.C., 1948, Glacial-meteorological investigations on the Kårsa Glacier in Swedish Lappland 1942–1948: Geografiska Annaler, v. 30, no. 3–4, p. 453–672.

Glaciers of Europe—

GLACIERS OF SVALBARD, NORWAY

By OLAV LIESTØL

SATELLITE IMAGE ATLAS OF GLACIERS OF THE WORLD

Edited by RICHARD S. WILLIAMS, Jr., *and* JANE G. FERRIGNO

U.S. GEOLOGICAL SURVEY PROFESSIONAL PAPER 1386–E–5

Svalbard, Norway, an archipelago in the North Atlantic Ocean, has more than 2,100 glaciers that cover 36,591 square kilometers, or 59 percent of the total area of the islands; Landsat images have been used to monitor fluctuations in the equilibrium line and glacier termini and to revise maps

CONTENTS

		Page
Abstract		E127
Introduction		127
FIGURE 1.	Index map showing the location of Svalbard, the islands that make up the archipelago, the areas covered by glaciers, and the glaciers mentioned in the text	128
TABLE 1.	Area encompassed by glaciers on each of the islands in the Svalbard archipelago	129
Previous glacier investigations		127
FIGURE 2.	Index to photogrammetric satellite image and map coverage of glaciers of Svalbard and location of mass-balance measurements made by Norwegian and Soviet glaciologists	130
3.	Color terrestrial photograph of the grounded front of the Kongsvegen glacier at the head of Kongsfjorden, Spitsbergen, in August 1974	131
4.	Radio-echosounding cross section (*A–A'*) through the southeastern part of the Austfonna ice cap, Nordaustlandet	131
TABLE 2.	Specific mass balance, annual equilibrium line altitude, and accumulation area ratio for Austre Brøggerbreen and Midtre Lovénbreen, 1967–90	129
3.	Mass-balance measurements of five glaciers in Svalbard made by the Institute of Geography of the USSR Academy of Sciences during the period 1966–67 to 1979–80	131
Climate		132
The equilibrium line		132
FIGURE 5.	Map of Svalbard showing isolines of the height of the equilibrium line	133
Glacier fluctuations		133
FIGURE 6.	Landsat image (24 August 1979; band 7; Path 235, Row 3) of the central part of Spitsbergen showing the grounded front of the surging glacier Negribreen in the right center	134
7.	Oblique aerial photograph of the grounded front of Freemanbreen on the southern coast of Barentsøya in August 1956 showing the heavily crevassed section of the lower part of the glacier during a surge	135
8.	Oblique aerial photograph of Penckbreen on the south side of Van Keulenfjorden, Spitsbergen, in August 1936	136
TABLE 4.	Glaciers of Svalbard that have been observed to surge in the last century	137
Glacier types		138
FIGURE 9.	Oblique aerial photograph of glaciers on the east coast of Spitsbergen in August 1936	138
10.	Oblique aerial photograph of the typical glacierized landscape of northwestern Spitsbergen in August 1936	139
11.	Vertical profile along the center line of Hessbreen, southern Spitsbergen, surveyed during 4 different years: 1898, 1952, 1970, and 1974	140
12.	Cross-sectional view of the Foxfonna glacier, central Spitsbergen	140

Page

Areas of principal glaciers of Svalbard ---------- E141

TABLE 5. Areas of the largest ice caps and ice fields in Svalbard ---------- 141
6. Areas of the largest outlet glaciers and ice streams in Svalbard ---------- 141

Use of Landsat images ---------- 141

FIGURE 13. Sketch map showing the islands in the eastern part of Svalbard for which new maps have been published that used Landsat images to correct older, inaccurate maps ---------- 141
14. Landsat MSS false-color composite digital image mosaic of Svalbard giving cloud-free coverage of the glaciers ---------- 142
15. Landsat MSS false-color composite image (2543–11162; 18 July 1976; Path 230, Row 4) of the southern and central part of Spitsbergen and the western part of Edgeøya showing the transient snowline on the glaciers ---------- 143
16. Landsat MSS image (30161–12143; 13 August 1978; Path 238, Row 1) of Nordaustlandet showing supraglacial lakes on Austfonna and outlet glaciers and ice divides on Austfonna and Vestfonna ---------- 144
17. Landsat MSS image (2534–12074; 9 July 1976; Path 239, Row 3) of Prins Karls Forland, Svalbard, showing sediment-laden meltwater discharging into coastal waters ---------- 145
18. Index map to the optimum Landsat 1, 2, and 3 images of the glaciers of Svalbard, Norway ---------- 150

TABLE 7. Optimum Landsat 1, 2, and 3 images of glaciers of Svalbard, Norway ---------- 146

Acknowledgments ---------- 144
References cited ---------- 151

GLACIERS OF EUROPE—

GLACIERS OF SVALBARD, NORWAY

By OLAV LIESTØL[1]

Abstract

Svalbard, Norway, an archipelago in the North Atlantic Ocean (74° to 81° N. lat), has a total area of 62,248 square kilometers, mostly contained in the four main islands, Spitsbergen, Nordaustlandet, Edgeøya, and Barentsøya. More than 2,100 glaciers cover 36,591 square kilometers, or about 59 percent of the total area. All types of glaciers are represented in Svalbard, but the most numerous are the valley and cirque glaciers, especially on Spitsbergen; large ice caps are common on Nordaustlandet, Edgeøya, and Barentsøya. Glaciological investigations began in the late 19th century and became numerous in the 20th century. They include ice-core studies and research in meteorology, mass balance, glacier flow, glacial erosion, and radio echosounding. Mass-balance measurements in Svalbard show a continuous negative mass balance since 1966–67; the net balance has probably been negative since the end of the last century. The height of the equilibrium line, a good indicator of climatic conditions in Svalbard, is about 150 meters above mean sea level in the southeastern part of the archipelago and greater than 800 meters above mean sea level in the central parts. Many of the glaciers in Svalbard are known to surge (86 since the end of the 19th century), and the frequent surging makes it difficult to use fluctuations of glaciers as climatic indicators. Landsat images have been used successfully to trace equilibrium-line variations, monitor glacier variation and surging events, delineate glacier basins on the basis of ice divides on ice caps, and revise maps for areas in which aerial photographs are not available.

Introduction

Svalbard is a part of Norway that includes the islands between lat 74° N. to 81° N. and long 10° E. to 35° E. (fig. 1). The main area consists of Spitsbergen, by far the largest island at 39,000 km^2, followed by Nordaustlandet with 14,600 km^2, Edgeøya at 5,000 km^2, Barentsøya with 1,300 km^2, and a number of smaller islands. The total area of the islands is 62,248 km^2, and, of this total, about 59 percent is covered by more than 2,100 glaciers (table 1). Most of the information provided in this subchapter is also included in the "Glacier Atlas of Svalbard and Jan Mayen" that was compiled by the Norwegian Polar Research Institute (Hagen and others, in press).

Previous Glacier Investigations

Nowhere in the Arctic can ships sail so far north as along the west coast of Spitsbergen. Therefore, numerous expeditions reached and visited the land during the past 300 years. As early as the 17th century, Dutch and English whalers made maps of the islands that contained information of glaciological interest. Swedish scientists were active in the study of Svalbard glaciers during the 19th century with glacial geology investigations and preparation of maps (Nathorst and others, 1909). A few glacier surges also were observed, and Hamberg (1932) described the phenomenon long before the concept was generally known among glaciologists.

[1] Norwegian Polar Research Institute, P.O. Box 158, 1330 Oslo Lufthavn, Norway.

***Figure 1.**—The location of Svalbard, the islands that make up the archipelago, the areas covered by glaciers, and the glaciers mentioned in the text. Base map courtesy of Norsk Polarinstitutt, Oslo. The glaciers are indicated in white. (See fig. 4 for cross section.)*

TABLE 1.—*Area encompassed by glaciers on each of the islands in the Svalbard archipelago*

Island	Area (km^2)	Glacier area (km^2)	Glacier cover (percent)	Number of glaciers
Spitsbergen..............	38,612	21,767	56.4	1,598
Nordaustlandet...........	15,193	11,309	74.7	210
Edgeøya..................	5,230	2,130	40.7	110
Barentsøya...............	1,321	575	43.5	126
Kvitøya..................	710	705	99.3	1
Prins Karls Forland......	622	83.4	13.4	33
Kongsøya.................	195	13.7	7.0	30
Svenskøya................	140	8.0	5.7	20
Bjørnøya.................	178	0	0	0
Hopen....................	47	0	0	0
Total....................	62,248	36,591	58.8	2,128

In the 20th century, numerous expeditions from different countries have done glaciological research as the main objective or as part of a broader scientific program (Ahlmann, 1933). One of the best known is the Norwegian-Swedish expedition to Isachsenfonna in 1934 led by Ahlmann and Sverdrup. The research papers published by this expedition remain as classic works in glacial meteorology (Sverdrup, 1935). German scientists carried out a program of mapping and glaciological studies in Spitsbergen in 1938 (Pillewizer, 1939).

In 1950, the Norwegian Polar Research Institute (Norsk Polarinstitutt) started systematic mass-balance studies on Svalbard glaciers, first on Finsterwalderbreen, a glacier on the south side of Van Keulenfjorden, and later on two glaciers in the Kongsfjorden area. The results have been published annually in the Norsk Polarinstitutt Årbok. Elverhøi and others (1980) also carried out glacial erosion and related studies in the

TABLE 2.—*Specific mass balance (b_w, winter; b_s, summer; b_n, net) in meters per year water equivalent, annual equilibrium line altitude (ELA) given in meters, and accumulation area ratio (AAR) in percent for Austre Brøggerbreen (6.1 km^2) and Midtre Lovénbreen (5.5 km^2), 1967–90 (Hagen and Liestøl, 1990)*

[Both glaciers are at lat 79° N. and long 12° E. in Svalbard; — indicates measurements are not available]

Balance year	Austre Brøggerbreen					Midre Lovénbreen				
	b_w	b_s	b_n	ELA	AAR	b_w	b_s	b_n	ELA	AAR
1966–67....	77	142	−65	—	—	—	—	—	—	—
1967–68....	57	67	−10	295	54	48	51	−3	295	54
1968–69....	40	133	−93	650	0	41	125	−84	650	0
1969–70....	37	91	−54	490	7	36	89	−53	500	6
1970–71....	65	123	−58	400	23	70	116	−46	385	37
1971–72....	95	126	−31	360	32	98	120	−22	350	46
1972–73....	74	82	−8	270	60	82	84	−2	310	58
1973–74....	75	167	−92	550	2	70	159	−89	550	2
1974–75....	78	109	−31	340	35	83	104	−21	340	48
1975–76....	72	117	−45	410	20	75	110	−35	420	29
1976–77....	76	87	−11	320	45	80	84	−4	300	60
1977–78....	75	131	−56	410	20	81	129	−48	420	29
1978–79....	77	148	−71	550	2	80	146	−66	480	9
1979–80....	75	127	−52	430	17	83	126	−43	415	30
1980–81....	46	101	−55	450	14	51	97	−46	435	23
1981–82....	64	68	−4	280	56	66	64	2	290	62
1982–83....	70	97	−27	345	34	75	92	−17	330	52
1983–84....	69	142	−73	500	6	74	142	−68	440	21
1984–85....	93	148	−55	450	14	98	146	−48	445	20
1985–86....	98	130	−32	380	25	6	127	−21	370	42
1986–87....	82	60	22	200	83	82	58	24	225	77
1987–88....	61	113	−52	440	15	56	105	−49	425	27
1988–89....	56	101	−45	440	15	63	87	−24	375	41
1989–90....	75	141	−66	500	8	87	138	−51	450	19
1967–90....	71	115	−44	417	19	74	110	−36	400	33

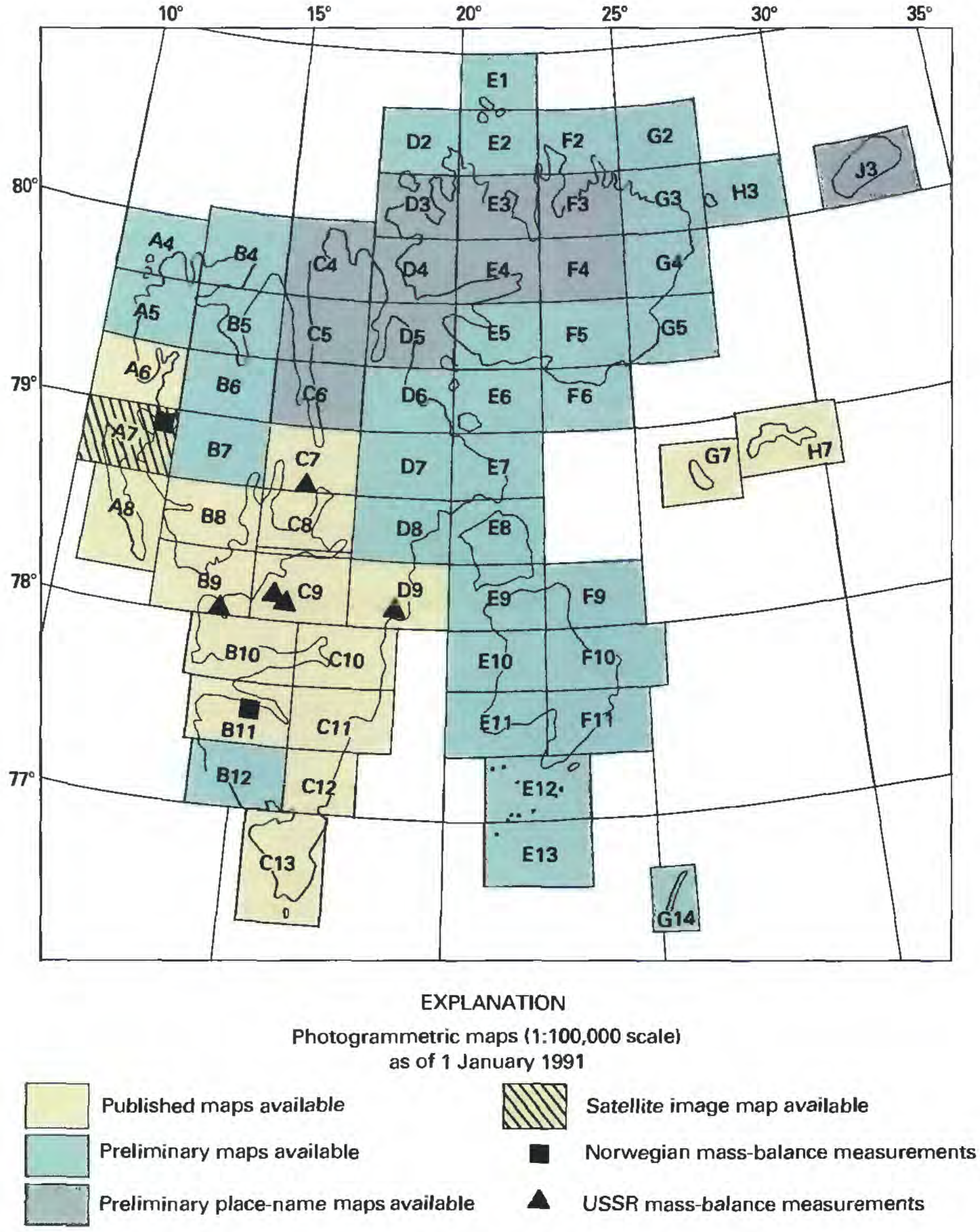

***Figure 2.**—Photogrammetric and satellite image map coverage of glaciers of Svalbard and location of mass-balance measurements made by Norwegian (table 2) and Soviet (table 3) glaciologists.*

inner part of the Kongsfjorden area. In 1957 and 1958, a team of Swedish scientists conducted glaciological studies on Nordaustlandet (Schytt, 1964). In 1966, Soviet glaciologists also worked in Spitsbergen (Markin, 1969). They started systematic yearly mass-balance measurements on five glaciers in central Spitsbergen. Their results are published in Gus'kov (1983). Figure 2 shows the location of mass-balance measurements and the map or photo coverage of the areas. The results of the Norwegian measurements are shown in table 2, and Soviet results in table 3. The detailed Polish work on mass balance and flow measurements should be mentioned also (Baranowski, 1977). One of the most extensive and detailed works on glacier flow ever made was carried out by German Democratic Republic (DDR) scientists in 1962–65 in the Kongsfjorden area. The fast-flowing Kongsvegen glacier stream (fig. 3) was the main objective of the research, and photogrammetric methods were used. The flow was of a block-movement type with maximum velocity up to 4 m/h^{-1} (meters per hour) (Voight, 1967; Pillewizer and others, 1967, and Voigt, 1979). Core drilling has been carried out on different glaciers by Soviet glaciologists in recent years. The deepest hole (586 m) was drilled through Amundsenisen. A review of the Soviet research on the glaciation of Spitsbergen was published by Troitskiy and others (1975).

Radio-echosounding surveys were also started by Soviet scientists, but later, in 1980 and 1983, scientists from the Norwegian Polar Research

***Figure 4.**—Radio-echosounding cross section (A–A′) through the southeastern part of the Austfonna ice cap, Nordaustlandet (see fig. 1 for location of survey traverse line).*

TABLE 3.—*Mass-balance measurements of five glaciers in Svalbard made by the Institute of Geography of the USSR Academy of Sciences during the period 1966–67 to 1979–80*

[Measurements are given in centimeters of water equivalent; — indicates measurements are not available]

Year	Vøringbreen			Bogerbreen			Longyearbreen			Bertilbreen			Daudbreen		
	Average total accumulation	Average total ablation	Average mass balance	Average total accumulation	Average total ablation	Average mass balance	Average total accumulation	Average total ablation	Average mass balance	Average total accumulation	Average total ablation	Average mass balance	Average total accumulation	Average total ablation	Average mass balance
1966–67...	87	107	−20	—	—	—	—	—	—	—	—	—	—	—	—
1973–74...	64	180	−116	—	—	—	—	—	—	—	—	—	—	—	—
1974–75...	73	99	−26	57	57	0	—	—	—	—	—	−29	—	—	—
1975–76...	44	161	−117	—	—	−20	—	—	—	34	106	−72	72	—	—
1976–77...	62	75	−13	62	88	−26	57	99	−42	48	107	−59	—	—	—
1977–78...	50	166	−116	34	115	−81	45	118	−73	44	144	−100	69	135	−66
1978–79...	54	143	−89	61	168	−107	48	171	−123	50	135	−85	54	112	−58
1979–80...	55	105	−50	48	113	−65	50	119	−69	31	123	−73	67	124	−57

***Figure 3.**—Color terrestrial photograph of the grounded front of the Kongsvegen glacier at the head of Kongsfjorden, Spitsbergen, in August 1974. Photograph by Olav Liestøl, Norsk Polarinstitutt, Oslo.*

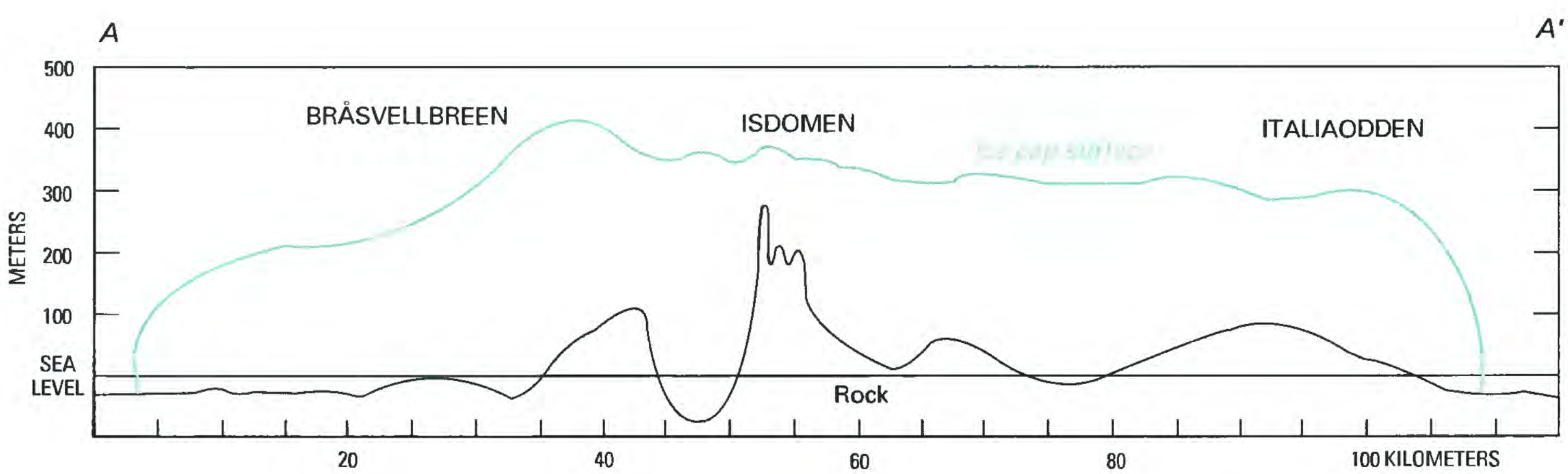

Institute (NP) and Scott Polar Research Institute (SPRI) sounded more than 100 glaciers, including a detailed survey of Austfonna, the largest ice cap in Svalbard (fig. 4) (Dowdeswell and others, 1984; Drewry and Liestøl, 1985).

Climate

The mean temperature during the winter is remarkably high, considering Svalbard's northern position. The immediate reason for the favorable temperature is the frequent transport of milder air from lower latitudes, usually in connection with the passage of low-pressure frontal systems over or near the Svalbard area. The North Atlantic Current transports warmer Atlantic water to the west coast of Spitsbergen. This current also influences the climate and keeps the sea free from ice even during the winter. Great temperature fluctuations are characteristic of Svalbard and are primarily caused by the alternate passage of warm and cold fronts: first a milder air mass from the south, followed by an Arctic air mass invading the islands from northerly or easterly directions. Temperatures above the freezing point occur even in midwinter. When accumulation is measured on the glaciers in the spring, traces of these mild periods are found as ice layers in snow pits. On the other hand, snow may fall at any time during the summer months.

On the west coast of Spitsbergen, the mean temperature in July is about 5 °C, but temperatures outside the range of 1 to 10 °C are not very common. In the same area, the mean temperature for February–March, normally the coldest part of the year, is usually between −8 and −16 °C, although the temperature is somewhat lower toward the east and north. In the inner fjord areas, the climate is slightly more continental, with temperatures 2 to 4 °C lower during wintertime and a couple of degrees higher in the summer.

The amount of precipitation is small, normally not more than 400 mm per year on the west coast of Spitsbergen and even less in the inner parts of the fjords. The greatest amount of precipitation, more than 1,000 mm, is found over glacier and mountain slopes freely exposed to winds in the southeastern part of Spitsbergen (Hisdal, 1985).

The Equilibrium Line

The height of the equilibrium line, the boundary between areas of acumulation and areas of ablation, is a good indicator of climatic conditions throughout Svalbard. Figure 5, which shows the height of the equilibrium line in Svalbard, is based on a combination of data derived from satellite images, aerial photographs, maps, and mass-balance observations. As a very rough assumption, we can say that glacier mass balance is determined by winter precipitation and summer temperature. The temperature, and thereby the ablation, varies less than the precipitation (accumulation) from one region to another. The equilibrium line altitude shown on figure 5 more or less reflects, therefore, the precipitation pattern. By looking at this map, one can see that precipitation is primarily caused by moisture-laden southeasterly winds. On Nordaustlandet, Edgeøya, and Spitsbergen, the equilibrium line is much lower on the southeastern side than on the northwestern side. On Spitsbergen, the equilibrium line is less than 200 m above sea level on the east side of Sørkapplandet, whereas its height in the inner part of Wijdefjorden is more than 800 m above sea level.

Figure 5.—Isolines of the height of the equilibrium line (the boundary between areas of accumulation and areas of ablation) in Svalbard. Compiled by Olav Liestøl and Erik Roland, Norwegian Polar Research Institute.

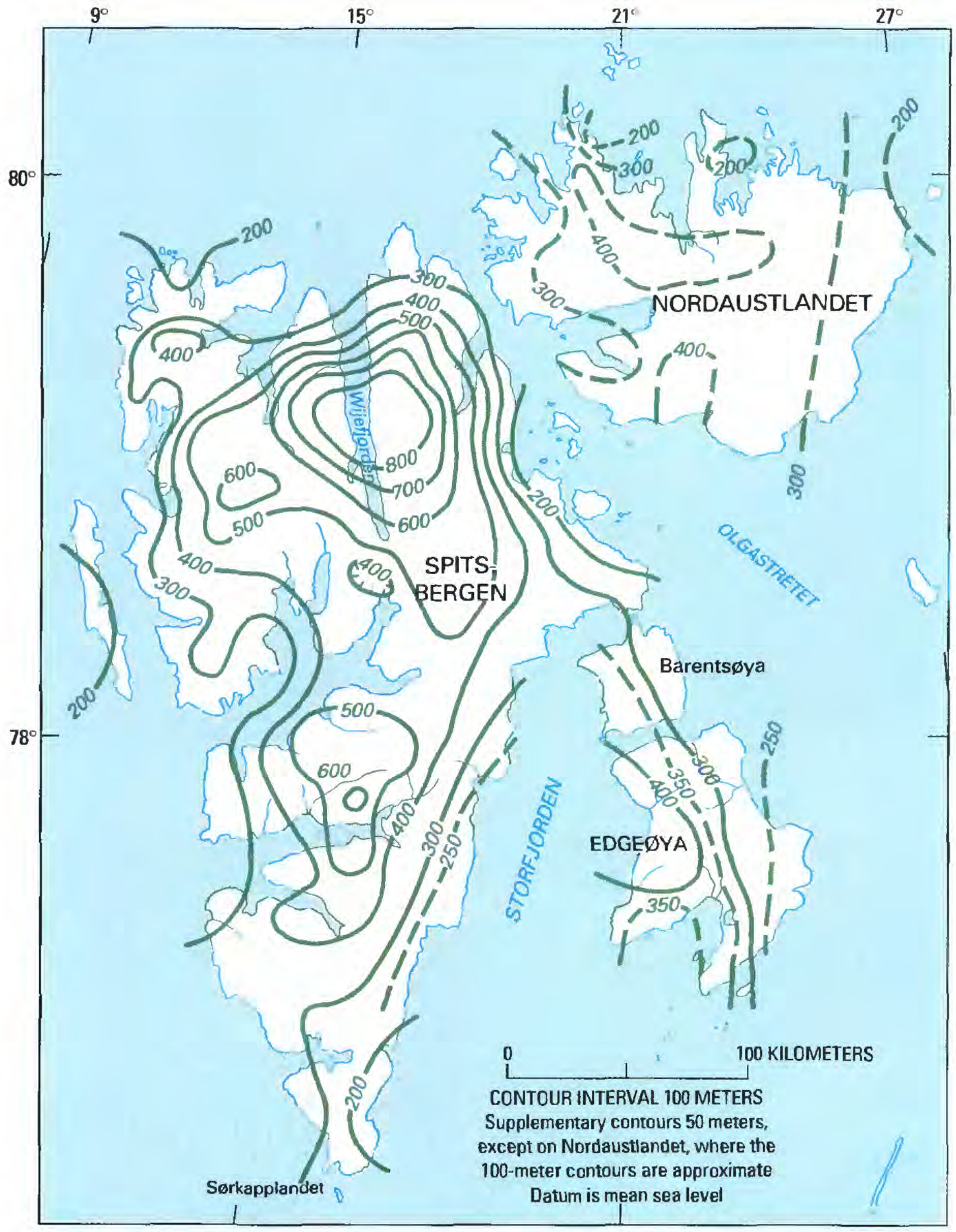

Glacier Fluctuations

As previously discussed, some information on glacier extent is available from rather early observations by sailors. In the 17th and 18th centuries, Dutch and English whalers plotted glacier fronts, or "ysbergs," on their maps. Though the maps are often quite poor, they do provide some evidence that the glacier fronts were then situated in about the same position as they are today. There are, however, some interesting exceptions. For example, on Dutch maps dating from about 1620, a valley and a river are indicated at the head of Recherchefjord on the west coast of Spitsbergen. The river even had a name: "Sardammer rivier." Today the large Recherchebreen fills the entire valley and the inner part of the fjord. Scientists on the Recherche Expedition in 1838 also commented on this fact. According to their quite accurate map, the glacier then covered the entire fjord, and their drawings showed an extremely crevassed glacier. This was, in fact, the first account of a surging glacier, a relatively common phenomenon in Svalbard and a characteristic of many of its glaciers (figs. 6–9). Table 4 lists 86 of Svalbard's glaciers that have been observed to surge in the last century. It is obvious that many more have surged but have not been observed.

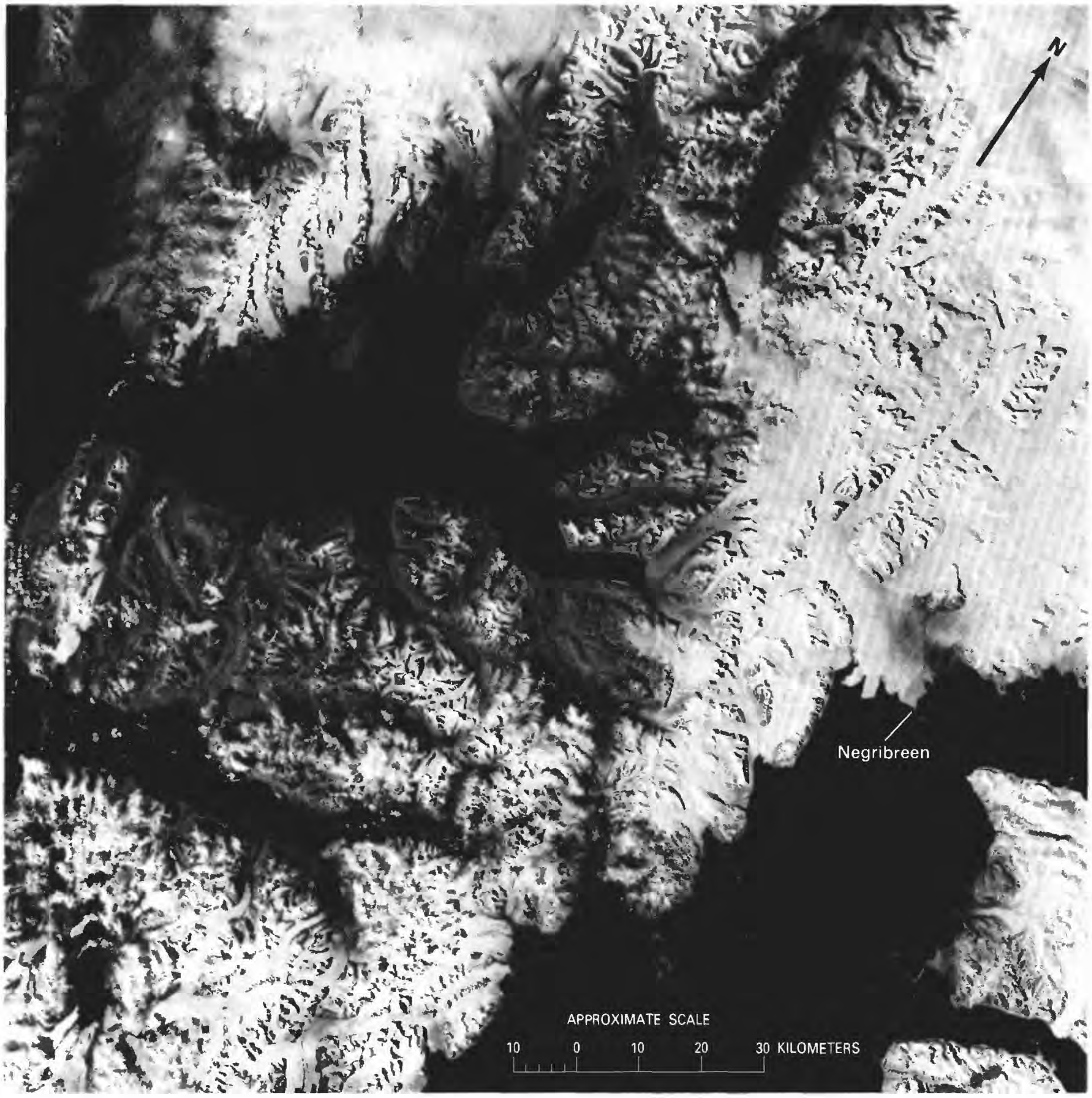

Figure 6.—Landsat image (24 August 1979; band 7; Path 235, Row 3) of the central part of Spitsbergen showing the grounded front of the surging glacier Negribreen in the right center. The image was acquired on 24 August 1979 by the Swedish Landsat receiving station at Kiruna. Negribreen advanced about 12 km between 1935 and 1936 and has now retreated about the same distance. Note the difference in area covered by glacier ice between the eastern coastal and central parts of this part of Spitsbergen.

The frequent surging makes it difficult to use glaciers as climatic indicators. The surging glaciers have their own fluctuation pattern, which depends primarily on their size, variations in mass balance, and dynamics of flow. Quick, violent advance followed by long periods of retreat, at intervals of perhaps 20 to 100 years, is a normal pattern of behavior. The only way to register shorter term variations in glacier volume, therefore, is to do mass-balance measurements.

The largest glacier surge observed was that of Bråsvellbreen, an outlet glacier from Austfonna on Nordaustlandet. The glacier advanced about 10 km along about a 30-km-wide front within less than a year (Schytt, 1969).

Negribreen, at the head of Storfjorden (fig. 6), advanced about 12 km within a year's time (1935–36), which gives a minimum velocity of approximately 30 m per day. Taking into account that the surge most probably was of a much shorter duration, the velocity may have reached as much as 100 m per day at its maximum (Liestøl, 1969).

Until the first Landsat images became available, the monitoring of surge events within the entire archipelago was impossible. The slow advance of glaciers known from studies of areas with temperate glaciers is almost unknown in Svalbard.

If terrestrial photographs used in the topographic survey at the beginning of this century are compared with more recent terrestrial and aerial photographs, it becomes obvious that most of the glaciers in Spitsbergen have decreased considerably during this period. Some of the smaller cirque glaciers have lost more than half their volume.

The mass-balance measurements on Brøggerbreen and Lovénbreen in the Kongsfjorden area show a continuous negative mass balance since investigations were begun in 1966 (Hagen and Liestøl, 1990) (table 2). The net mass balance has probably been negative in the majority of the years since the end of the last century (Lefauconnier and Hagen, 1990). Because the summer temperature during the same period has remained relatively constant, the cause of the decrease in glacier volume is most likely a result of lower annual precipitation; that is to say, below what is needed to keep the present volume constant (Steffensen, 1969).

Figure 7.*—Oblique aerial photograph of the grounded front of Freemanbreen on the southern coast of Barentsøya in August 1956 showing the heavily crevassed section of the lower part of the glacier during a surge. Approximate width of the glacier at its narrowest (before it fans out) is 2.5 km. Photograph No. S56 1393 from Norsk Polarinstitutt, Oslo.*

Figure 8.—*Oblique aerial photograph of Penckbreen on the south side of Van Keulenfjorden, Spitsbergen, in August 1936. The glacier has advanced into and folded marine sediments during a surge. A small cirque glacier and one of many glacier-dammed lakes common in Spitsbergen, Ny- Märjelen, is visible just to the right of the center of the photograph. Approximate width of the glacier is 3 km. Photograph No. S36 3207 from Norsk Polarinstitutt, Oslo.*

TABLE 4—*Glaciers of Svalbard that have been observed to surge in the last century*

[Identification number according to UNESCO's World Glacier Monitoring Service; c, circa; b, between]

Glacier	Year(s) of surge
East-central Spitsbergen	
1 11 01 Pedasjenkobreen	b 1925–35
1 11 02 Ganskijbreen	b 1925–35
1 11 03 Sonklarbreen	c 1910
1 11 05 Negribreen	1935–36
1 12 01 Hayesbreen	1901
1 12 04 Usherbreen	1978–85
1 12 04 Ulvebreen	b 1896–1900
1 13 07 Elfenbeinbreen	1903
1 13 08 Skruisbreen	1920
1 13 09 Sveigbreen	1960
1 14 06 Inglefieldbreen	1952
1 14 07 Arnesenbreen	b 1925–35
1 14 12 Thomsonbreen	b 1950–60
1 15 02 Strongbreen	b 1870–76
1 15 05 Jemelianovbreen	1971
1 15 06 Anna Margrethebreen	1970
1 15 09 Davisbreen	c 1960
Southern Spitsbergen	
1 21 02 Markhambreen	b 1930–36
1 21 03 Staupbreen	c 1960
1 21 04 Hambergbreen	c 1890 and c 1960
1 22 02 Vasilievbreen (tributary)	c 1961
1 24 04 Körberbreen	1938
Bellsund	
1 31 11 Scottbreen	c 1880
1 31 16 Recherchebreen	1838 and 1945
1 32 01 Hessbreen	1974
1 32 02 Finsterwalderbreen	c 1900
1 32 07 Siegerbreen	1940
1 32 26 Martinbreen	b 1898–1936
1 32 27 Charpentierbreen	c 1890
1 34 10 Bakaninbreen	1985–90
1 35 05 Hyllingebreen	1970–80
1 35 12 Skutbreen	1930
1 35 13 Upper Storknausen E.	1960
1 35 14 Upper Slottsmøya SW.	1960
1 36 13 Marthabreen	c 1925
1 36 15 Lunckebreen	c 1930
1 36 18 Arebreen	1985
1 37 08 Fridtjovbreen	1861
Isfjorden	
1 42 11 Scott Turnerbreen	c 1930
1 42 17 Drønbreen	1900
1 42 16 Moysalbreen (part of Gløttfjellbreen)	c 1925
1 43 12 Vendombreen	c 1934
1 43 18 Marmorbreen	1965–70
1 44 02 Von Postbreen	1870
1 44 02 Bogebreen (part of Von Postbreen)	1980
Isfjorden—Continued	
1 44 03 Tunabreen	1930 and 1970
1 45 22 Skansdalsbreen (part of Frostisen)	c 1930
1 46 17 Fyrisbreen	1960
1 46 22 Upper Brenna NW.	c 1937
1 47 16 Sefströmbreen	1896
1 48 05 Wahlenbergbreen	1908
1 49 02 Nansenbreen	1947
Northwestern Spitsbergen	
1 53 13 Osbornebreen	1987
1 55 04 E. Brøggerbreen	c 1890
1 55 06 Midre Lovénbreen	c 1890
1 55 10 Kongsvegen	1948
1 55 11 Kronebreen	1869
1 55 15 Blomstrandbreen	1960
Woodfjorden/Wijdefjorden	
1 64 11 Elnabreen	c 1930
1 64 17 Abrahamsenbreen	1978
1 64 26 Upper Svelgfjellet S.	1969
1 69 10 Longstaffbreen (part of Åsgårdsfonna)	1960
Northeastern Spitsbergen	
1 72 14 Unnamed part of Odinjøkulen	b 1965–70
1 73 05 Kosterbreen	c 1930
1 73 10 Hinlopenbreen	1969–72
1 74 02 N. Karpinskifjellet	b 1970–80
1 74 06 Hochstetterbreen	b 1895–1900
Nordaustlandet	
2 11 08 Part of Austfonna	b 1850–73
2 11 10 Bråsvellbreen	1937–38
2 21 01 Clasebreen (part of Glitnbreen)	1938
2 21 02 Palanderbreen	1969–70
2 22 03 Etonbreen	1938
2 22 06 Bodleybreen	1973–80
2 32 03 Søre Franklinbreen	1956
2 42 01 Rijpbreen	1938
Eastern islands	
3 11 01 Kvitkåpa SW.	c 1965
3 12 27 Kvitisen E.	1936
3 13 06 Bergfonna SE.	1930
3 13 12 Marsjørreen	b 1936–71
3 13 18 Stonebreen	b 1936–71
3 13 19 Kong Johans Bre	b 1925–30
3 13 22 Pettersenbreen	c 1925
3 21 01 Freemanbreen	1956–56
3 21 02 Duckwitzbreen	1918
3 22 07 Reymondbreen	1956
3 22 08 Hübnerbreen	b 1930–36

***Figure 9.**—Oblique aerial photograph of glaciers on the east coast of Spitsbergen in August 1936. The long, crevassed glacier in the center of the photograph, Arnesenbreen, is surging. Photograph No. S36 1766 from Norsk Polarinstitutt, Oslo.*

Glacier Types

If classified morphologically, all types of glaciers are represented in Svalbard, although the most common are valley and cirque glaciers. It has been difficult to classify the complex glacier system because of the intricate network of ice that covers the large inland areas of Spitsbergen, however (figs. 6, 9, and 10). Tyrrell (1922) used the term "reticular glaciers" and Ahlmann (1948) proposed "transection glaciers" for parts of the glaciated areas. Some typical piedmont glaciers are also found along the west coast, with especially fine examples resting on the strandflat of Prince Karls Forland. Ice caps are common on the relatively flat islands on the eastern half of the archipelago: Edgeøya, Barentsøya and Nordaustlandet (see fig. 16). Ice shelves, such as are common in Antarctica, do not exist, because all glacier fronts terminating in the sea are grounded (figs. 3 and 7). Cirque glaciers are most common in the high

Figure 10.—Oblique aerial photograph of the typical glacierized landscape of northwestern Spitsbergen in August 1936. To the left of center is the stagnant valley glacier, Sefstrømbreen, which last surged in 1896. Since that time, however, it has been undergoing steady retreat. Supraglacial lakes are evident on the surfce of the glacier. Photograph No. S36 628 from Norsk Polarinstitutt, Oslo.

mountain (alpine) ranges along the west coast, but even the flat mountains of sedimentary-rock origin in the central part of Spitsbergen have, to a large extent, been eroded by cirque glaciers.

If classified geophysically, the majority of Svalbard's glaciers belong to the subpolar type; that is, the accumulation area is at the pressure-melting point, and the ablation zone is below the freezing point and partly frozen to the ground. When this type of glacier surges, the lateral parts of the glacier remain frozen to the valley walls (fig. 11). Many of the small cirque and valley glaciers could be classified as polar glaciers, because the entire ice mass is below 0 °C in winter (fig. 12). In summer, however, melting takes place on the surface of all the glaciers even at the highest elevations. Subpolar glaciers can be distinguished from polar ones by large accumulations of ice (icings) in front of their termini, which are produced by the drainage of subglacial water throughout the entire winter season.

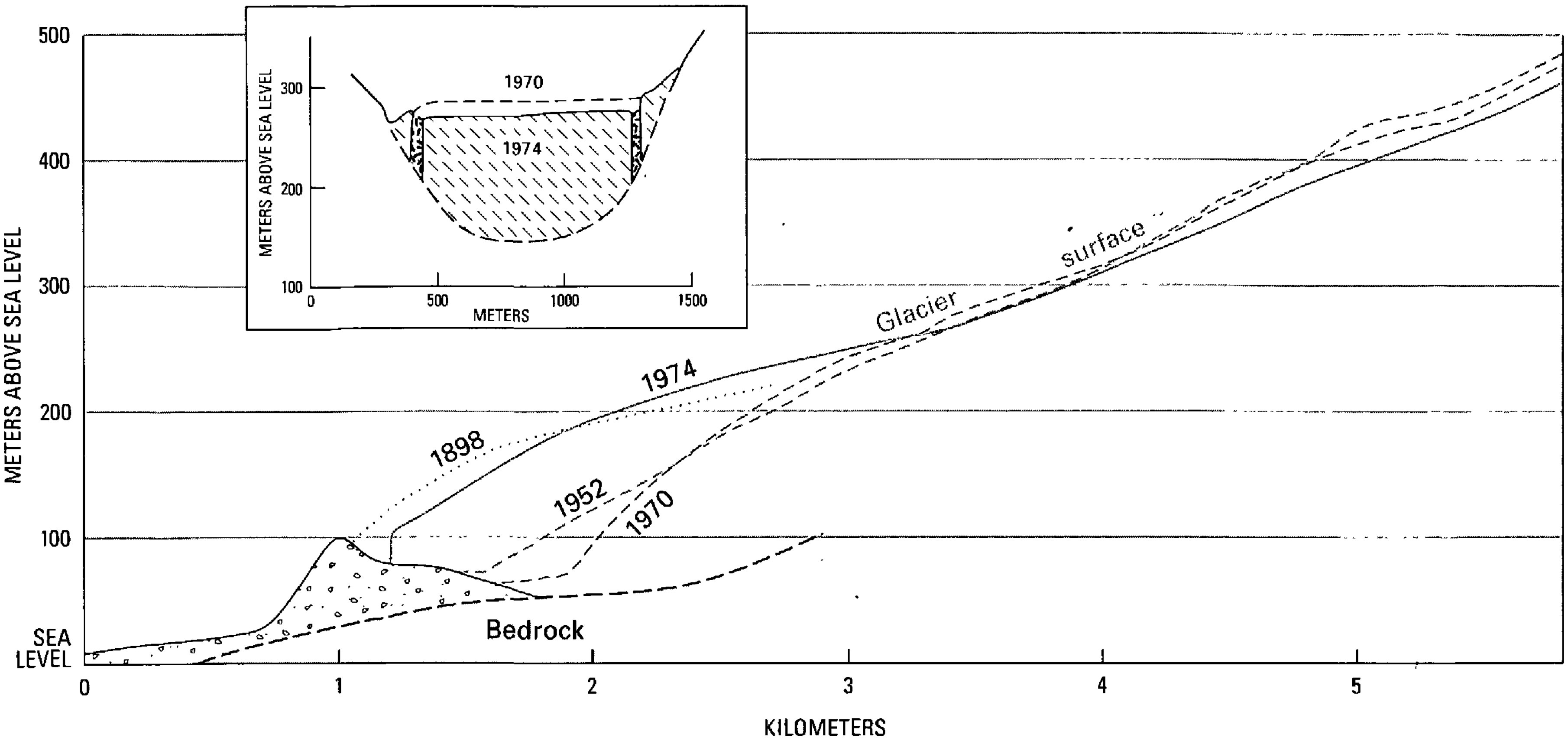

Figure 11.—*Vertical profile along the center line of Hessbreen, southern Spitsbergen, surveyed during 4 different years: 1898, 1952, 1970, and 1974. The glacier had been decreasing in the lower part and increasing in the upper part until 1974, when a surge occurred. In the transverse profile in the inset diagram, the lateral parts of the glacier are shown to have frozen to the valley walls, while the main body of the glacier surged (Liestøl, 1976).*

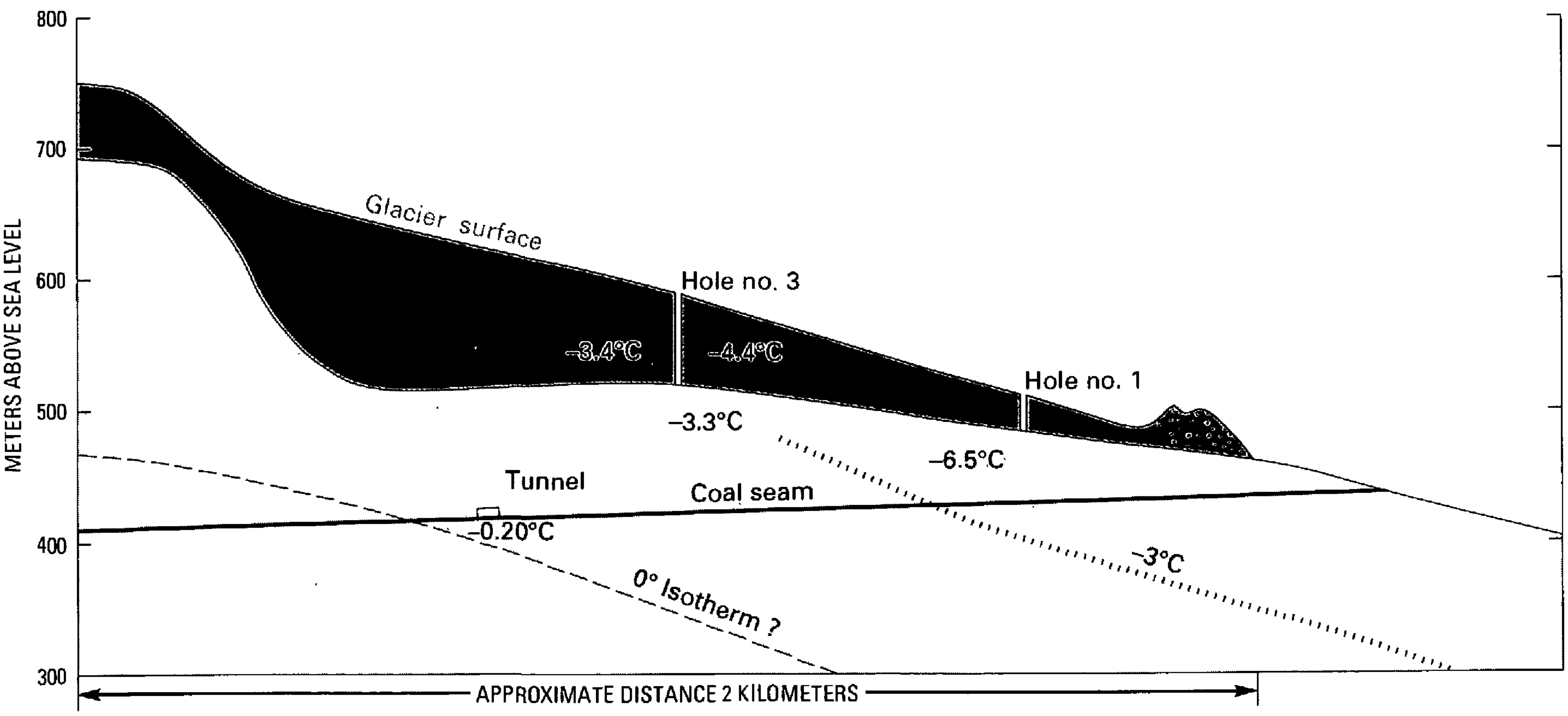

Figure 12.—*Cross-sectional view of the Foxfonna glacier, central Spitsbergen. Temperature measurements in boreholes are negative from the surface to the bed of the glacier. During the summer, melting occurs over all the surface of the glacier. The bottom profile is drawn from a radio-echosounding survey of ice thickness (Liestøl, 1974).*

Areas of Principal Glaciers of Svalbard

Table 1 provides information on the area of glaciers on each of the islands in the Svalbard archipelago. Kvitøya has a single glacier, the Kvitøyjøkulen ice cap, which covers 99.3 percent of the island (Bamber and Dowdeswell, 1990). Svenskøya has 20 glaciers, which cover only 5.7 percent of the area. Spitsbergen has 1,598 glaciers, which cover 56.4 percent of its area. The two small, low-lying islands of Bjørnøya and Hopen have no glaciers.

Table 5 provides information on the area of the 9 largest ice caps and ice fields in Svalbard; table 6 gives the same information about Svalbard's 10 largest outlet glaciers and ice streams.

Use of Landsat Images

Vertical aerial photographs are available for the entire archipelago except the eastern part of Nordaustlandet and Kvitøya. The older maps were very inaccurate in this part of Svalbard, and Landsat images were used to improve the maps. Figure 13 shows coastline changes in these areas. New maps prepared from Landsat images, such as the 1:1,000,000-scale Norsk Polarinstitutt map of Svalbard (1983), added 500 km^2 to the

TABLE 5.—*Areas of the largest ice caps and ice fields in Svalbard*

Name	Area (km^2)
Austfonna	8,413
Ice field in Olav V Land	~3,000
Vestfonna	2,505
Åsgårdfonna	1,645
Edgeøyjøkulen	1,300
Holtedahlfonna and Isachsenfonna	~900
Kvitøyjøkulen	705
Barentsjøkulen	571
Balderfonna	543

TABLE 6.—*Areas of the largest outlet glaciers and ice streams in Svalbard*

Name	Area (km^2)
Hinlopenbreen	1,248
Negribreen	1,182
Bråsvellbreen	1,160
Etonbreen	1,070
Leighbreen	925
Stonebreen	700
Kronebreen	693
Hochstetterbreen	581
Nathorstbreen	489
Monacobreen	408

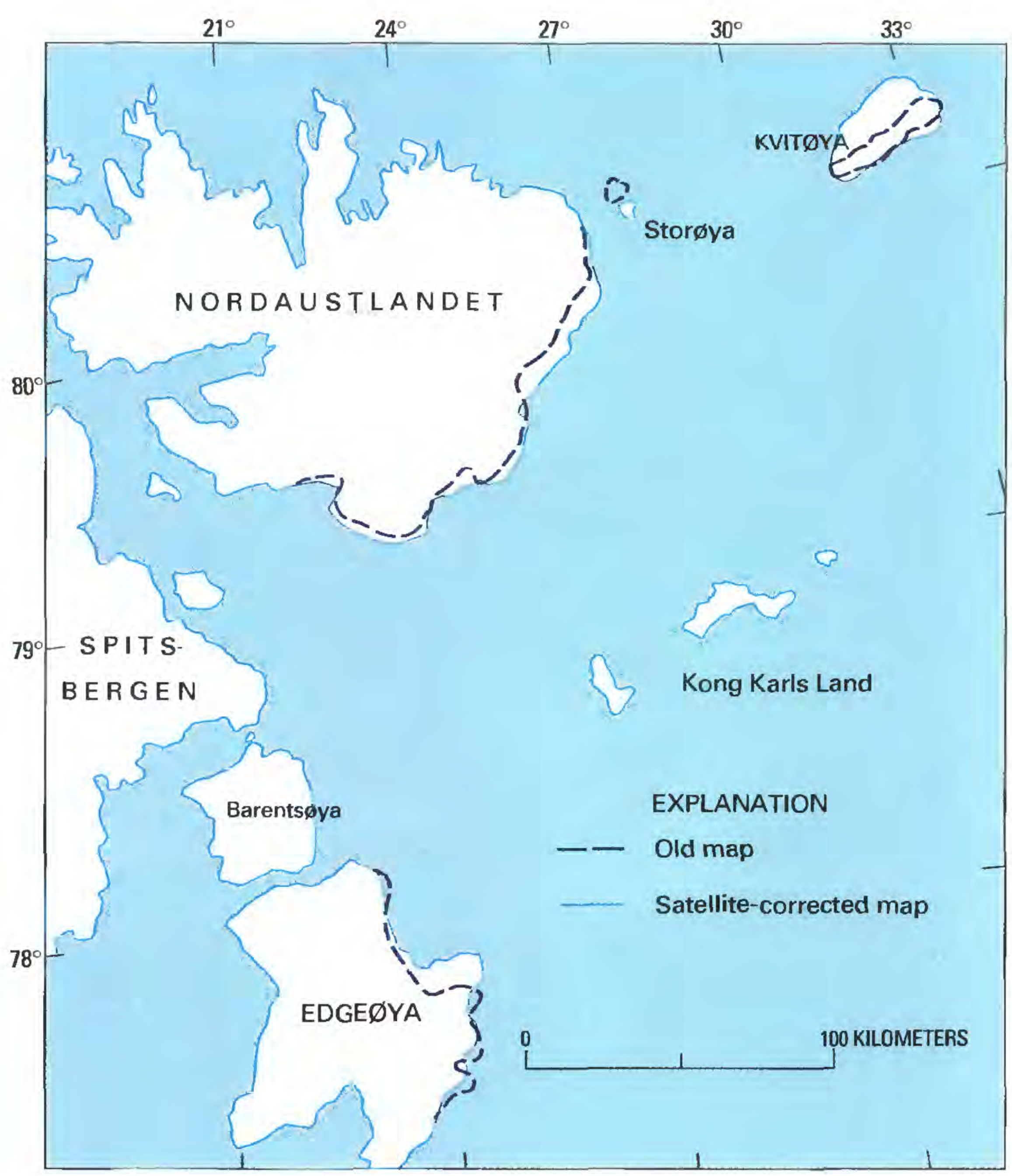

Figure 13.*—Islands in the eastern part of Svalbard for which new maps have been published that used Landsat images to correct older, inaccurate maps. Most of the corrected coastlines are represented by grounded glacier fronts. The changes are not, however, the result of glacier fluctuations but rather the result of the poor quality of the older maps.*

area of Nordaustlandet (Dowdeswell and Cooper, 1986). The area of Kvitøya, an island that is almost totally ice covered, was more than doubled, and its geometric configuration totally altered from a cigar-shaped to a more egg-shaped island. In the early 1980's, Fjellanger Widerøe A-S of Oslo produced a digital mosaic of Svalbard by using Landsat imagery. The mosaic is shown in figure 14, and the imagery used is listed in table 7.

Satellite imagery makes it possible to carry out simultaneous observations over large areas. It is, therefore, a useful tool in tracing the variation of the transient snowline in different localities (Dowdeswell and Drewry, 1989) (fig. 15). With the large amount of superimposed ice, the equilibrium line is not identical with the snowline but lies farther down the glacier. With some experience it is, however, possible even on the

***Figure 14.**—Landsat MSS false-color composite digital image mosaic of Svalbard giving cloud-free coverage of the glaciers. Mosaic was produced by Fjellanger Widerøe A-S, Norway, and is reproduced here with permission. Images used to produce the mosaic are included in table 7.*

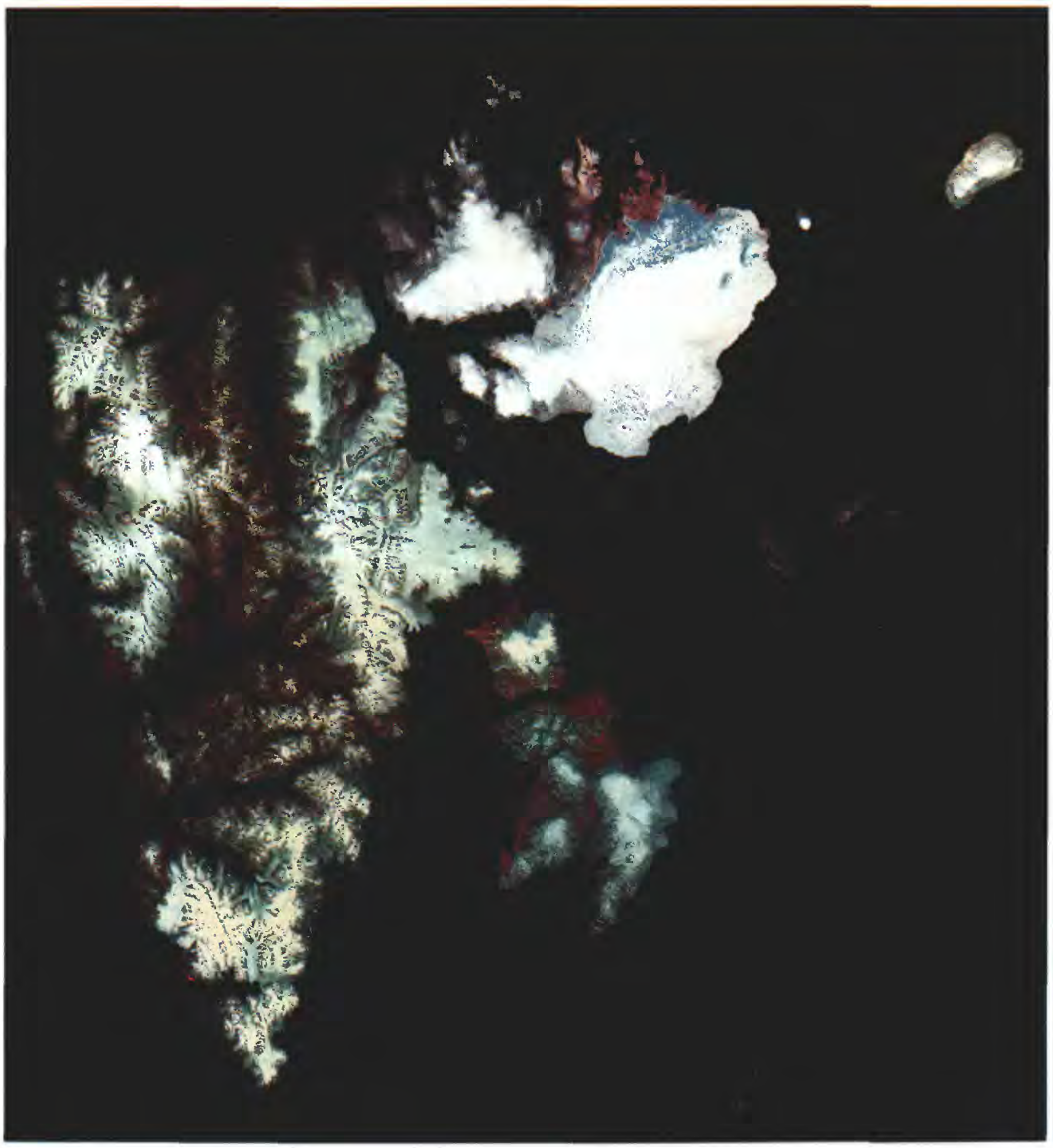

satellite imagery to locate the border between the old glacier ice and the superimposed ice. As noted earlier, Landsat images are used to monitor glacier variations and especially to detect and to monitor any surging events (Dowdeswell, 1986; Dowdeswell and others, 1991). Landsat images can also be used to delineate glacier basins and ice divides on ice caps (fig. 16) (Dowdeswell, 1984; Dowdeswell and Drewry, 1985). The imagery is useful for qualitatively evaluating or monitoring sediment-laden meltwater discharged into coastal waters (Dowdeswell and Drewry, 1989; Pfirman and Solheim, 1989) (fig. 17). An important aspect of several of these studies of Svalbard ice masses is the integration of evidence from the analysis of Landsat digital and photographic imagery

***Figure 15.**—Landsat MSS false-color composite image (2543–11162; 18 July 1976; Path 230, Row 4) of the southern and central part of Spitsbergen and the western part of Edgeøya showing the transient snowline on the glaciers.*

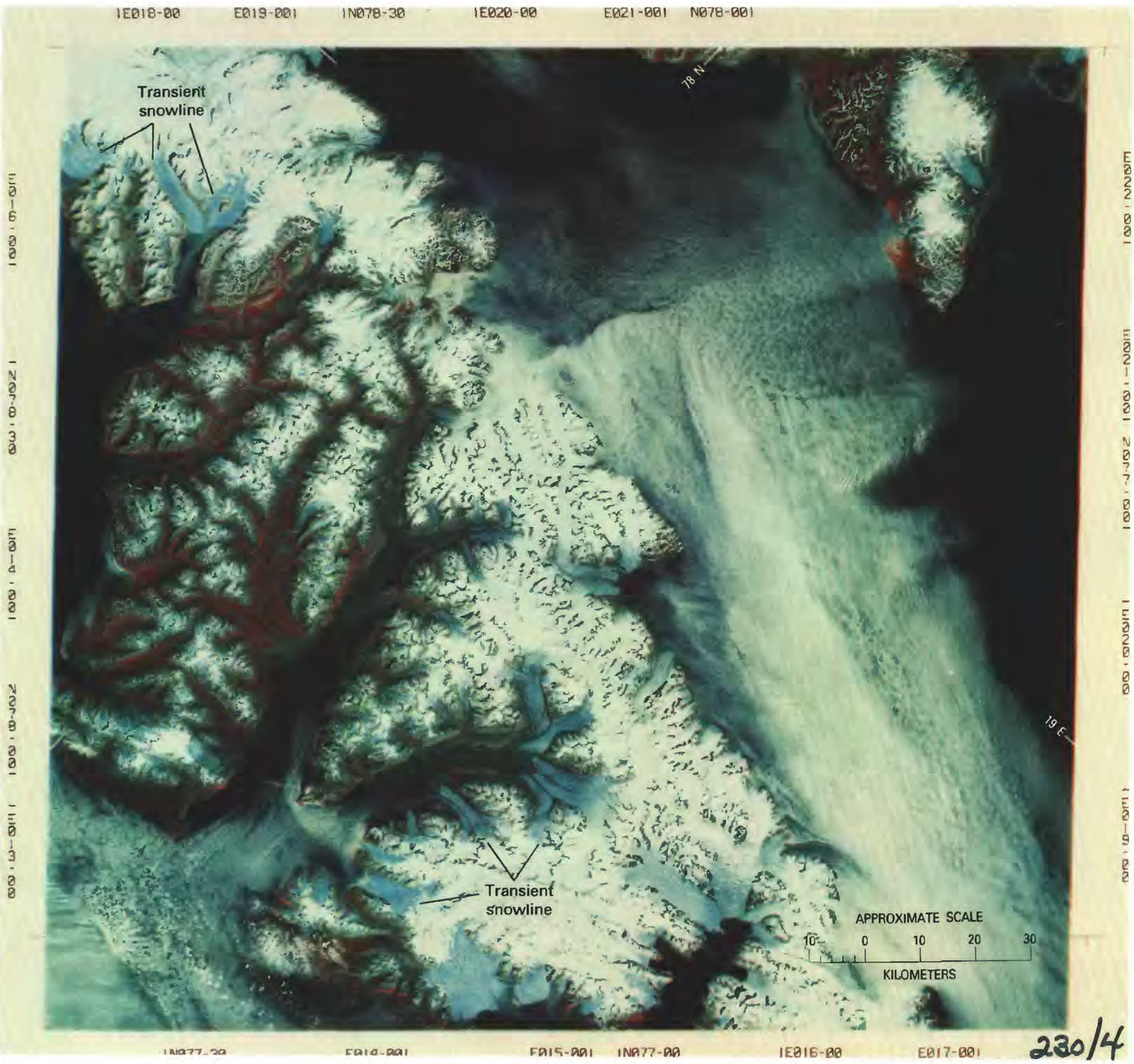

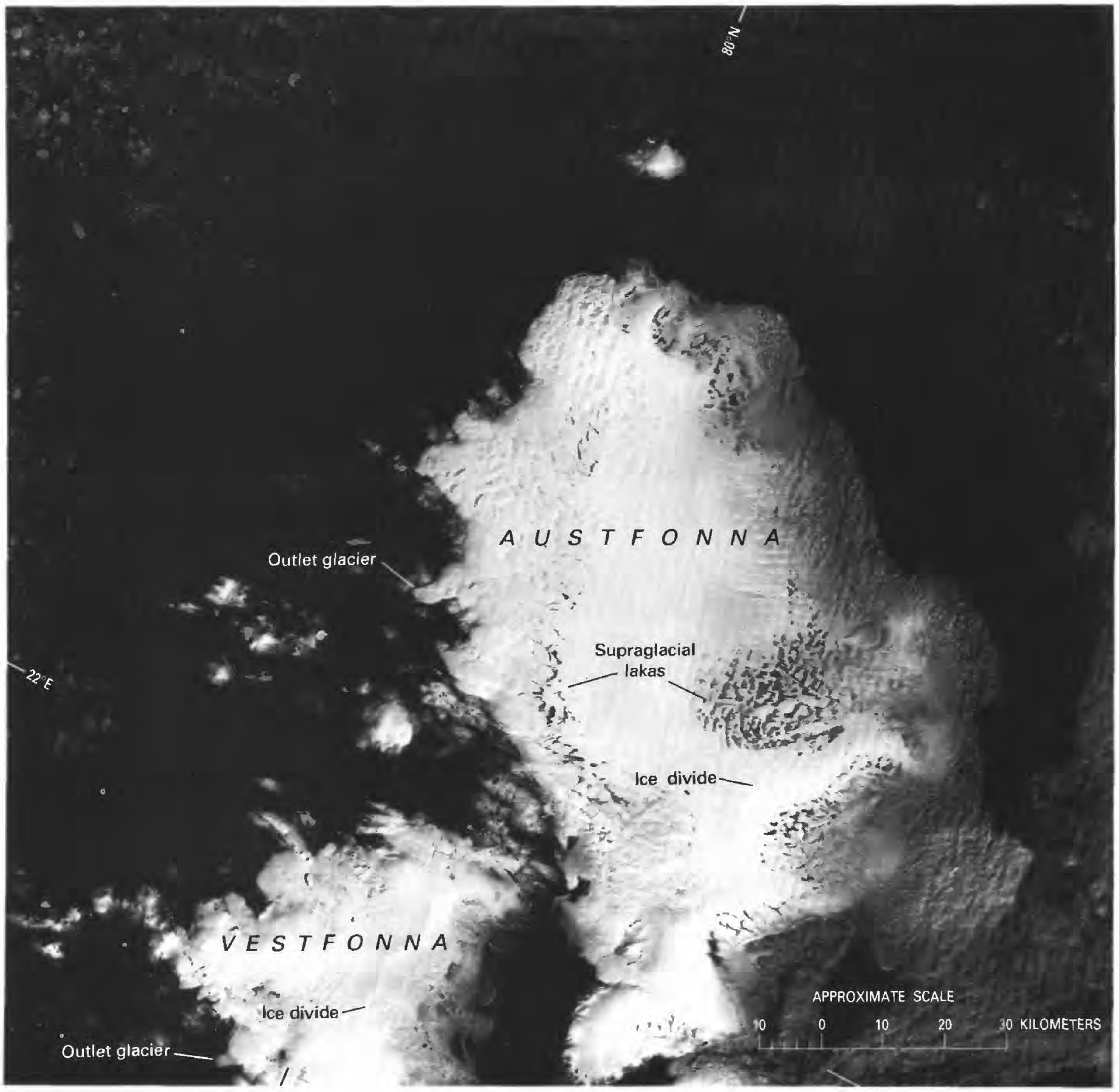

with other glaciological datasets in order to investigate the dynamics of these ice masses (Dowdeswell and Drewry, 1989; Dowdeswell and Collin, 1990).

Figure 18 is an index map showing the nominal scene centers and evaluation of the optimum Landsat images of Svalbard. Table 7 provides more-detailed information on each of the optimum Landsat images.

***Figure 16.**—Landsat MSS image (30161–12143; 13 August 1978; Path 238, Row 1) of Nordaustlandet showing supraglacial lakes on Austfonna and outlet glaciers and ice divides on Austfonna and Vestfonna. This image was used to delineate outlet-glacier basins and ice divides on these two ice caps.*

Acknowledgments

The editors thank Dr. Gunnar Østrem, Norges Vassdrags-og Energiverk, Dr. Jon Ove Hagen, Norsk Polarinstitutt, and Dr. Julian A. Dowdeswell, Scott Polar Research Institute, who reviewed the manuscript and made valuable contributions.

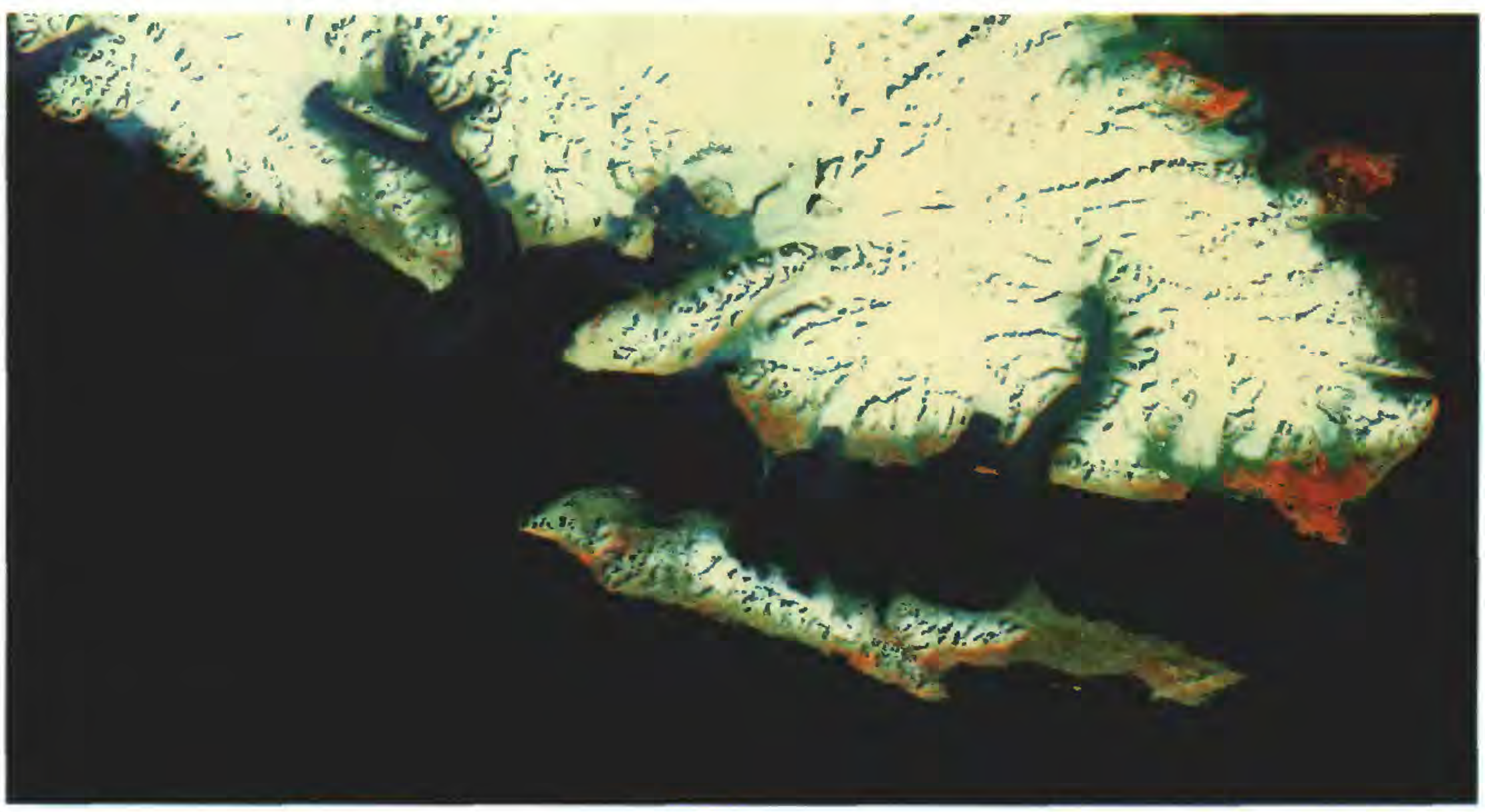

***Figure 17.**—Landsat MSS image (2534–12074; 9 July 1976; Path 239, Row 3) of Prins Karls Forland, Svalbard, showing sediment-laden meltwater discharging into coastal waters. The sediment can be seen as lighter blue patterns in the water on the false-color composite. It can be seen more clearly on the black-and-white print of MSS band 4 data.*

TABLE 7.—*Optimum Landsat 1, 2, and 3 images of the glaciers of Svalbard, Norway*

[See fig. 18 for explanation of symbols used in the "Code" column]

Path-Row	Nominal scene center (lat-long)	Landsat identification number	Date	Solar elevation angle (in degrees)	Code	Cloud cover (in percent)	Remarks
223–4	77°33′N. 28°01′E.	22066–10425	18 Sep 80	13	◑	70	Archived by ESA[1]
224–3	78°29′N. 31°58′E.	22013–10474	27 Jul 80	30	◑	20	Good image of Kongsøya; archived by ESA
224–4	77°33′N. 26°35′E.	21257–10274	02 Jul 78	35	●	0	Edgeøya-Kong Johans Breen; archived by ESA
224–5	76°31′N. 21°58′E.	2501–10432	06 Jun 76	36	◕	10	
225–3	78°29′N. 30°32′E.	30849–10461	01 Jul 80	34	●	0	Cloud free, but several line drops over islands; archived by ESA
225–4	77°33′N. 25°09′E.	2502-10484	07 Jun 76	35	◑	30	
225–4	77°33′N. 25°09′E.	30849-10464	01 Jul 80	35	◑	40	Several line drops; used to produce digital mosaic shown in figure 14; archived by ESA
225–5	76°31′N. 20°32′E.	22068-10545	20 Sep 80	14	●	0	Archived by ESA
226–3	78°29′N. 29°05′E.	22015–10591	29 Jul 80	29	◕	10	Archived by ESA
226–4	77°33′N. 23°43′E.	22015–10594	29 Jul 80	30	●	0	Used to produce digital mosaic shown in figure 14; archived by ESA
226–5	76°31′N. 19°05′E.	21637–10543	17 Jul 79	34	●	0	Southern tip of Spitsbergen; archived by ESA
227–3	78°29′N. 27°39′E.	22016–11050	30 Jul 80	29	◑	20	Archived by ESA
227–4	77°33′N. 22°17′E.	22016–11052	30 Jul 80	30	◕	10	Archived by ESA
227–5	76°31′N. 17°39′E.	21278–10461	23 Jul 78	33	●	0	Used to produce digital mosaic shown in figure 14; archived by ESA
228–1	80°01′N. 39°39′E.	30151–11170	03 Aug 78	26	◑	20	
228–2	79°19′N. 32°28′E.	2541–11040	16 Jul 76	31	◑	60	
228–3	78°29′N. 26°13′E.	22017–11105	31 Jul 80	29	◕	10	Good image of Svenskøya; archived by ESA
228–4	77°33′N. 20°51′E.	22017–11111	31 Jul 80	30	◕	10	Archived by ESA
228–5	76°31′N. 16°13′E.	22017–11114	31 Jul 80	31	◑	20	Archived by ESA
229–1	80°01′N. 38°12′E.	30152–11224	04 Aug 78	26	●	0	Good image of eastern part Kvitøya
229–2	79°19′N. 31°02′E.	2201–11220	11 Aug 75	25	◑	70	Kvitøya
229–3	78°29′N. 24°47′E.	22018–11163	01 Aug 80	28	◑	30	Used to produce digital mosaic shown in figure 14; archived by ESA

TABLE 7.—*Optimum Landsat 1, 2, and 3 images of the glaciers of Svalbard, Norway*—Continued

Path-Row	Nominal scene center (lat-long)	Landsat identification number	Date	Solar elevation angle (in degrees)	Code	Cloud cover (in percent)	Remarks
229–4	77°33′N. 19°24′E.	22018–11170	01 Aug 80	30	◕	10	Archived by ESA
229–5	76°31′N. 14°47′E.	22018–11172	01 Aug 80	31	◑	30	Archived by ESA
230–1	80°01′N. 36°46′E.	30152–11224	04 Aug 78	25	●	0	Partial image (90%); archived by ESA
230–1	80°01′N. 36°46′E.	21641–11155	21 Jul 79	29	◑	60	Used to produce digital mosaic shown in figure 14; archived by ESA
230–2	79°19′N. 29°36′E.	2543–11153	18 Jul 76	31	●	5	
230–2	79°19′N. 29°36′E.	22055–11221	07 Sep 80	15	◑	20	Used to produce digital mosaic shown in figure 14; archived by ESA
230–3	78°29′N. 23°21′E.	2543–11155	18 Jul 76	32	◕	10	Good image of northern Edgeøya, Barentsøya, and Negribreen on Spitsbergen
230–4	77°33′N. 17°58′E.	2543–11162	18 Jul 76	33	◕	10	Good image of Spitsbergen from Billefjorden to Hornsund
230–5	76°31′N. 13°21′E.	2543–11164	18 Jul 76	34	◑	20	
231–1	80°01′N. 35°20′E.	30154–11341	01 Jul 78	31	●	0	Very good image of Kvitøya; subglacial drainage divides visible
231–2	79°19′N. 28°10′E.	22020–11274	03 Aug 80	27	◑	30	Archived by ESA
231–3	78°29′N. 21°55′E.	2077–11344	09 Apr 75	18	◑	70	
231–4	77°33′N. 16°32′E.	2472–11235	08 May 76	29	◕	10	
231–5	76°31′N. 11°55′E.	2472–11242	08 May 76	30	◑	40	
232–1	80°01′N. 33°54′E.	22021–11325	04 Aug 80	25	◑	30	
232–2	79°19′N. 26°44′E.				◔		
232–3	78°29′N. 20°29′E.	2456–11352	22 Apr 76	23	◑	50	
232–4	77°33′N. 15°06′E.	2473–11293	09 May 76	29	◑	25	
233–1	80°01′N. 32°28′E.	2528–11324	03 Jul 76	31	◑	25	
233–2	79°19′N. 25°18′E.	2528–11330	03 Jul 76	33	◑	50	
233–3	78°29′N. 19°03′E.	2528–11333	03 Jul 76	34	◑	60	
233–4	77°33′N. 13°40′E.	2474–11352	10 May 76	29	◑	30	

TABLE 7.—*Optimum Landsat 1, 2, and 3 images of the glaciers of Svalbard, Norway*—Continued

Path-Row	Nominal scene center (lat-long)	Landsat identification number	Date	Solar elevation angle (in degrees)	Code	Cloud cover (in percent)	Remarks
234–1	80°01′N. 31°02′E.	30049–11502	23 Apr 78	21	●	0	Very good image of Kvitøya; subglacial drainage divides visible
234–2	79°19′N. 23°52′E.	2529–11385	04 Jul 76	32	◑	30	Prominent ablation features, Nordaustlandet
234–2	79°19′N. 23°52′E.	22383–11413	01 Aug 81	27	◑	20	Used to produce digital mosaic shown in figure 14; archived by ESA
234–3	78°29′N. 17°37′E.	1245–11583	25 Mar 73	12	●	5	
234–3	78°29′N. 17°37′E.	22041–11453	24 Aug 80	21	◑	50	Used to produce digital mosaic shown in figure 14; archived by ESA
234–3	78°29′N. 17°37′E.	22383–11415	01 Aug 81	28	◕	10	Archived by ESA
234–4	77°33′N. 12°14′E.	21645–11400	25 Jul 79	31	◑	20	Used to produce digital mosaic shown in figure 14; archived by ESA
235–1	80°01′N. 29°36′E.	30122–11564	05 Jul 78	31	◑	50	
235–2	79°19′N. 22°26′E.	2530–11443	05 Jul 76	32	◑	15	Prominent ablation features, Nordaustlandet
235–3	78°29′N. 16°11′E.	2476-11462	12 May 76	29	◕	10	
235–4	77°33′N. 10°48′E.	2476–11464	12 May 76	30	◑	20	
236–1	80°01′N. 28°10′E.	22007–11554	21 Jul 80	29	◑	40	Archived by ESA
236–2	79°19′N. 21°00′E.	2549–11494	24 Jul 76	29	◑	30	Good image of northeastern Spitsbergen
236–3	78°29′N. 14°45′E.	2549–11501	24 Jul 76	31	◑	70	
236–4	77°33′N. 09°22′E.				◔		
237–1	80°01′N. 26°44′E.	22008–12013	22 Jul 80	28	◑	20	Archived by ESA
237–2	79°19′N. 19°34′E.	2496–11565	01 Jun 76	32	◑	40	Northeastern Spitsbergen
237–3	78°29′N. 13°19′E.	2496–11572	01 Jun 76	33	◕	10	Northwestern Spitsbergen and Prins Karls Forland
238–1	80°01′N. 25°18′E.	30161–12143	13 Aug 78	23	◑	15	Prominent ablation features, subglacial drainage divides, Nordaustlandet
238–1	80°01′N. 25°18′E.	21667–12015	16 Aug 79	22	◑	20	Used to produce digital mosaic shown in figure 14; archived by ESA
238–1	80°01′N. 25°18′E.	30736–12032	10 Mar 80	5	●	0	Subglacial drainage divides, Nordaustlandet; some line drops; archived by ESA

TABLE 7.—*Optimum Landsat 1, 2, and 3 images of the glaciers of Svalbard, Norway*—Continued

Path-Row	Nominal scene center (lat-long)	Landsat identification number	Date	Solar elevation angle (in degrees)	Code	Cloud cover (in percent)	Remarks
238–2	79°19′N. 18°08′E.	21631–12020	11 Jul 79	32	●	0	Used to produce digital mosaic shown in figure 14; archived by ESA
238–3	78°29′N. 11°53′E.	2462–12094	28 Apr 76	25	◑	20	
238–3	78°29′N. 11°53′E.	30160–12094	12 Aug 78	25	◑	30	Used to produce digital mosaic shown in figure 14; archived by ESA
238–3	78°29′N. 11°53′E.	21631–12022	11 Jul 79	33	●	0	Partial image (90%); archived by ESA
239–1	80°01′N. 23°52′E.	30036–12190	10 Apr 78	16	◕	10	
239–2	79°19′N. 16°42′E.	2534–12072	09 Jul 76	32	◑	20	Good image of northern Spitsbergen
239–3	78°29′N. 10°27′E.	2534–12074	09 Jul 76	33	●	0	Good image of western Spitsbergen-Prins Karl Forland
240–1	80°01′N. 22°26′E.	2541–12463	16 Jul 76	29	◑	20	
240–2	79°19′N. 15°16′E.	2535–12130	10 Jul 76	32	◑	30	Good image of northwestern Spitsbergen
240–3	78°29′N. 09°01′E.	2535–12133	10 Jul 76	33	●	0	
241–1	80°01′N. 21°00′E.	30164–12314	16 Aug 78	22	◑	15	Prominent ablation features; subglacial drainage divides, Nordaustlandet
241–2	79°19′N. 13°50′E.	2500–12194	05 Jun 76	32	◑	40	
241–3	78°29′N. 07°35′E.	2500–12201	05 Jun 76	33	◑	15	
242–1	80°01′N. 19°34′E.	2542–12521	17 Jul 76	29	◑	40	Northern Nordaustlandet
242–1	80°01′N. 19°34′E.	21257–12093	02 Jul 78	31	●	5	Used to produce digital mosaic shown in figure 14; partial image (75%); archived by ESA
242–2	79°19′N. 12°24′E.	2466–12320	02 May 76	25	●	5	
243–1	80°01′N. 18°08′E.	30040–12420	14 Apr 78	18	◕	10	
243–2	79°19′N. 10°57′E.	2467–12374	03 May 76	25	●	0	
244–1	80°01′N. 16°42′E.	2486–12423	22 May 76	29	●	0	
244–2	79°19′N. 09°31′E.	30868–12335	20 Jul 80	30	◑	40	Archived by ESA
245–1	80°01′N. 15°16′E.	30150–12543	02 Aug 78	26	◑	35	

TABLE 7.—*Optimum Landsat 1, 2, and 3 images of the glaciers of Svalbard, Norway*—Continued

Path-Row	Nominal scene center (lat-long)	Landsat identification number	Date	Solar elevation angle (in degrees)	Code	Cloud cover (in percent)	Remarks
245–2	79°19′N. 08°05′E.	2486–12430	22 May 76	30	◑	15	
246–1	80°01′N. 13°49′E.	30025–12590	03 Mar 78	12	◕	10	
246–2	79°19′N. 06°39′E.	2470–12545	06 May 76	26	●	5	
247–1	80°01′N. 12°23′E.	2489–12594	25 May 76	29	◑	25	
248–1	80°01′N. 10°57′E.	30027–13103	01 Apr 78	13	◕	10	
249–1	80°01′N. 09°31′E.	2473–13113	09 May 76	26	●	0	
250–1	80°01′N. 08°05′E.	2474–13172	10 May 76	26	●	0	

[1] Data archived by the Swedish Space Corporation in Kiruna, Sweden, in cooperation with the European Space Agency.

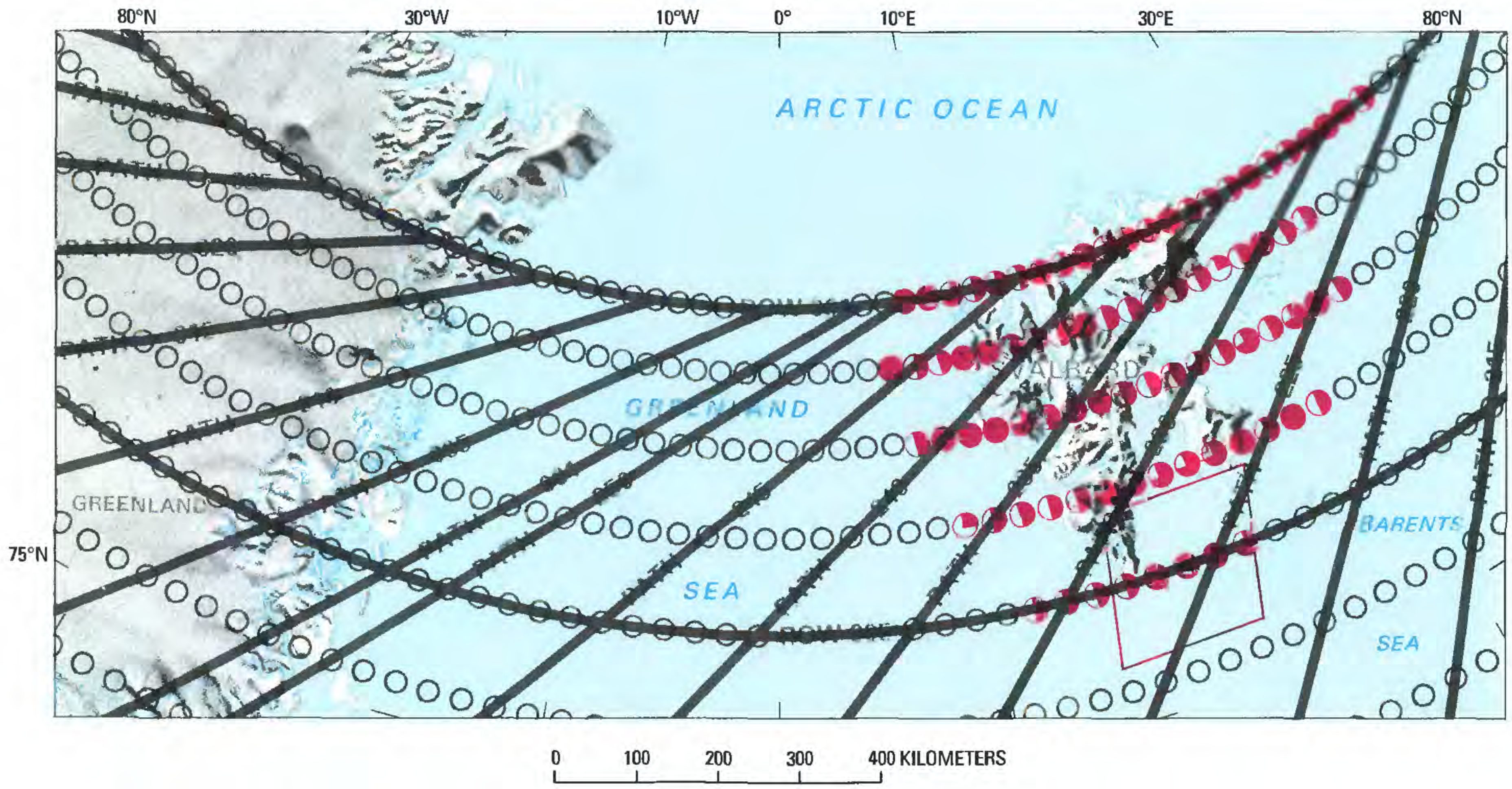

EXPLANATION OF SYMBOLS

Evaluation of image usability for glaciologic, geologic, and cartographic applications. Symbols defined as follows:

● Excellent image (0 to ≤5 percent cloud cover)

◕ Good image (>5 to ≤10 percent cloud cover)

◑ Fair to poor image (>10 to ≤100 percent cloud cover)

◔ Unusable image (100 percent cloud cover)

○ Nominal scene center for a Landsat image outside the area of glaciers

▱ Approximate size of area encompessed by nominal Landsat MSS image

Figure 18.—*Optimum Landsat 1, 2, and 3 images of the glaciers of Svalbard, Norway. The vertical lines represent nominal paths. The rows (horizontal lines) have been established to indicate the latitude at which the imagery has been acquired.*

References Cited

Ahlmann, H. W:son, 1933, Scientific results of the Swedish-Norwegian Arctic Expedition in the summer of 1931, Part VIII. Glaciology: Geografiska Annaler, v. 15, no. 4, p. 261–295.

———1948, Glaciological research on the North Atlantic coasts: Royal Geographical Society Research Series no. 1, 83 p.

Bamber, J.L., and Dowdeswell, J.A., 1990, Remote sensing studies of Kvitøyjokulen: An ice cap on Kvitøya, north-east Svalbard: Journal of Glaciology, v. 36, no. 122, p. 75–81.

Baranowski, S., 1977, The subpolar glaciers of Spitsbergen seen against the climate of this region: Wrocław Universytet, Acta Universitatis Wratislaviensis, no. 410, 94 p.

Dowdeswell, J.A., 1984, Remote sensing studies of Svalbard glaciers: Ph.D. dissertation, University of Cambridge, 250 p.

———1986, Remote sensing of ice cap outlet glacier fluctuations on Nordaustlandet, Svalbard: Polar Research, v. 4, p. 25–32.

Dowdeswell, J.A., and Collin, R.L., 1990, Fast-flowing outlet glaciers on Svalbard ice caps: Geology, v. 18, no. 8, p. 778–781.

Dowdeswell, J.A., and Cooper, A.P.R., 1986, Digital mapping in polar regions from Landsat photographic products: A case study: Annals of Glaciology, v. 8, p. 47–50.

Dowdeswell, J.A., and Drewry, D.J., 1985, Place names on the Nordaustlandet ice caps, Svalbard: Polar Record, v. 22, no. 140, p. 519–539.

———1989, The dynamics of Austfonna, Nordaustlandet, Svalbard: Surface velocities, mass balance and subglacial meltwater: Annals of Glaciology, v. 12, p. 37–45.

Dowdeswell, J.A., Drewry, D.J., Liestøl, O., and Orheim, O., 1984, Airborne radio echosounding of subpolar glaciers in Spitsbergen: Norsk Polarinstitutt Skrifter No. 182, p. 1–41.

Dowdeswell, J.A., Hamilton, G.S., and Hagen, J.O., 1991, The duration of the active phase on surge-type glaciers: Contrasts between Svalbard and other regions: Journal of Glaciology, v. 37, no. 127, p. 388–400.

Drewry, D.J., and Liestøl, O., 1985, Glaciological investigations of surging ice caps in Nordaustlandet, Svalbard, 1983: Polar Record, v. 22, no. 139, p. 357–378.

Elverhøi, A., Liestøl, O., and Nagy, J., 1980, Glacial erosion, sedimentation, and microfauna in the inner part of the Kongsfjorden, Spitsbergen: Norsk Polarinstitutt Skrifter No. 172, p. 33–61.

Gus'kov, A.S., 1983, Vodno-ledovyi balans lednikov Shpitsbergena v 1979/80 balansovom godu [Water ice balance of Spitsbergen glaciers in the 1979–80 balance year]: Akademiya nauk SSSR; Institut Geografii, Materialy Glyatsiologicheskikh Issledovaniy, Khronika Obsuzhdeniya, no. 46, p. 136–142.

Hagen, J.O., and Liestøl, O., 1990, Long term glacier mass balance investigations in Svalbard 1950–88: Annals of Glaciology, v. 14, no. 102–106.

Hagen, J.O., Liestøl, O., Roland, E., and Jørgensen, T., in press, Glacier atlas of Svalbard and Jan Mayen: Norsk Polarinstitutt, Meddeleser.

Hamberg, A., 1932, Struktur und Bewegungs-forgänge im Gletschereis nebst Beiträge zur Morphologi der arktischen Gletscher [Structure and mechanics of glacier ice including a section on the morphology of arctic glaciers]: Naturwissenschaftliche untersuchungen des Sarekgebirges in Schwedisch-Lappland v. 1, no. 3, Gletscherkunde, p. 69–124.

Hisdal, V., 1985, Geography of Svalbard: Norsk Polarinstitutt, Polarhandbok no. 2, p. 1–80.

Lefauconnier, B., and Hagen, J.O., 1990, Glaciers and climate in Svalbard. Statistical analysis and reconstruction of the Brøgger Glacier mass balance for the last 77 years: Annals of Glaciology, v. 14, p. 148–152.

Liestøl, O., 1969, Glacier surges in West Spitsbergen: Canadian Journal of Earth Sciences, v. 6, no. 4, p. 895–897.

———1974, Glaciological work in 1972: Norsk Polarinstitutt Årbok 1972, p. 125–135.

———1976, Glaciological work in 1974: Norsk Polarinstitutt Årbok 1974, p. 183–194.

Markin, V.A., 1969, Issledovaniya teplovogo balansa lednikorykh pokrovov Shpitsbergena v periody ablyatsii 1965 i 1966 gg. [The investigations of the heat balance of Spitsbergen ice covers during the ablation periods of 1965 and 1966]: Akademiya nauk SSSR, Institut Geografii, Materialy Glyatsiologicheskikh Issledovaniy, Khronika Obsuzhdeniya, no. 15, p. 124–132.

Nathorst, A.G., Anderson, G., DeGeer, G., and Hulth, J.M., 1909, The historical sketch of Swedish exploration in Spitsbergen 1758–1908: Ymer, v. 29, p. 4–22.

Norsk Polarinstitutt, 1983, Svalbard: Oslo, 1:1,000,000-scale map.

Pfirman, S.L., and Solheim, A., 1989, Subglacial meltwater discharge in the open-marine tidewater glacier environment: Observations from Nordaustlandet, Svalbard archipelago: Marine Geology, v. 86, no. 4, p. 265–281.

Pillewizer, W., 1939, Die Kartographischen und Gletscherkundlichen Ergebnisse der Deutschen Spitzbergenexpedition 1938 [The cartographic and glaciological results of the German Spitsbergen Expedition 1938]: Petermanns Geographische Mitteilungen Ergänzungsheft no. 238, p. 36–38.

Pillewizer, W., and others, 1967, Die wissenschaftlichen Ergebnisse der Deutschen Spitzbergenexpedition 1964–65 [The scientific results of the German Spitsbergen Expedition 1964–65]: Geodätische und Geophyisikalische Veröffentlichungen, v. III, no. 9, p. 1–138.

Schytt, V., 1964, Scientific results of the Swedish glaciological expedition to Nordaustlandet, Spitsbergen, 1957 and 1958: Geografiska Annaler, v. 46, no. 3, p. 243–281.

———1969, Some comments on glacier surges in eastern Svalbard: Canadian Journal of Earth Sciences, v. 6, no. 4 (pt. 2), p. 867–873.

Steffensen, E., 1969, The climate and its recent variations at the Norwegian Arctic stations: Meteorologiske Annaler, v. 5, no. 8, 349 p.

Sverdrup, H.U., 1935, Scientific results of the Norwegian-Swedish Spitsbergen Expedition in 1934. Part III: Geografiska Annaler, v. 17, no. 1–2, p. 53–88.

Troitskiy, L.S., Zinger, E.M., Koryakin, V.S., Markin, V.A., and Mikhalyev, V.I., 1975, Glaciation of the Spitsbergen (Svalbard): Moscow, The Publishing House Nauka, 276 p. (In Russian.)

Tyrrell, G.W., 1922, The glaciers of Spitsbergen: The Transactions of the Geological Society of Glascow, v. XVII, pt. 1, p. 1–49.

Voigt, U., 1967, Ergebnisse photogrammetrischen Messungen auf dem mittleren Lovengletscher in den Jahren 1962 und 1964/65, *in* Die wissenschaftlichen Ergebnisse der deutschen Spitzbergenexpedition 1964–65 [Results of the photogrammetric measuring of the average speed of the Loven Glacier in 1962 and 1964/65, *in* The scientific results of the German Spitsbergen expedition in 1964/65]: Geodätische und Geophysikalische Veröffentlichungen, v. III, no. 9, p. 101–109.

———1979, Zur Blockbewegung der Gletscher [Block movement of glaciers]: Geodätische und Geophysikalische Veröffentlichungen, v. III, no. 44, p. 1–128.

Glaciers of Europe—

GLACIERS OF JAN MAYEN, NORWAY

By OLAV ORHEIM

SATELLITE IMAGE ATLAS OF GLACIERS OF THE WORLD

Edited by RICHARD S. WILLIAMS, Jr., *and* JANE G. FERRIGNO

U.S. GEOLOGICAL SURVEY PROFESSIONAL PAPER 1386–E–6

Jan Mayen, Norway, has 113 square kilometers, or 30 percent of its area, covered by an ice cap and the 20 named outlet glaciers that surmount the active Beerenberg stratovolcano

CONTENTS

		Page
Abstract		E153
Introduction		153
FIGURE 1.	Index map of Jan Mayen	154
2.	Oblique aerial photograph of Jan Mayen viewed from the southwest on 23 August 1949	154
3.	Map showing craters, effusive lava flows, tephra deposits, and tephra fallout pattern associated with recent volcanic activity on Beerenberg	155
4.	Photograph on 7 April 1985 of steam billowing from the new vent that formed on the upper part of Weyprechtbreen on the northern part of the summit crater of Beerenberg Volcano	156
5.	Map of the glaciers on Nord-Jan, with locations of moraine stages, dead (stagnant)-ice remnants, and supraglacial material	156
Glacier distribution and mass-balance conditions		157
FIGURES 6–8.	Oblique aerial photographs of:	
	6. Sørbreen on Nord-Jan viewed from the southeast on 23 August 1949	158
	7. Sørbreen viewed from above 600 m in elevation on 24 August 1973	158
	8. Beerenberg viewed from the northwest on 23 August 1949	159
TABLE 1.	Size, elevation, and orientation of the glaciers on Jan Mayen, Norway	157
Historical variations in positions of glacier termini		159
FIGURE 9.	Sketch map of the frontal position of Sørbreen on different dates	160
10.	Length profiles of Sørbreen along section A–A'–A'' of figure 9	160
Comparison of glacier fluctuations with meteorological data		161
Use of satellite imagery in glacier monitoring		161
FIGURE 11.	Landsat 1 image (1084–12061; 15 October 1972) of Jan Mayen, Norway, the best Landsat image acquired of the island	163
12.	Index map to the optimum Landsat 1, 2, and 3 images of the glaciers of Jan Mayen, Norway	163
TABLE 2.	Optimum Landsat 1, 2, and 3 images of the glaciers of Jan Mayen, Norway	162
Acknowledgment		162
References cited		164

GLACIERS OF EUROPE—

GLACIERS OF JAN MAYEN, NORWAY

By OLAV ORHEIM[1]

Abstract

Jan Mayen, Norway, the northernmost island on the Mid-Atlantic Ridge, has 113 square kilometers covered by glaciers, about 30 percent of its total area. The northern part of the island is the active Beerenberg stratovolcano (2,277 meters high), which is surmounted by an ice cap from which 20 outlet glaciers emanate. Sørbreen is the largest (15 square kilometers) and the best studied of these outlet glaciers. The maximum postglacial expansion of the outlet glaciers occurred at the end of the "Little Ice Age" (around the year 1850), and an oscillating retreat has taken place since that time. A marked advance around 1910 and again in 1960 was separated by a recession that ended about 1950. The 1960 advance was caused by reduced summer temperatures and ablation. The earliest recorded observations of Søbreen were in 1632, but the first modern topographic map was not published until 1959. This map was compiled photogrammetrically from aerial photographs taken in 1949 and 1955. The glaciers on Jan Mayen are especially sensitive to change in climate. Satellite monitoring of the variations of glacier positions on this isolated island has the potential to be a valuable tool but has been limited because the cloud cover is persistent.

Introduction

Jan Mayen, Norway, is the most northerly island on the Mid-Atlantic Ridge. It extends from 70°50′ to 71°10′ N. lat and from 7°55′ to 9°05′ W. long (fig. 1). The island covers an area of 373 km^2 and has very different landscapes on the north (Nord-Jan) and south (Syd-Jan): Nord-Jan is dominated by the volcano Beerenberg, 2,277 m in elevation; narrow Syd-Jan, stretching southwest, has a maximum elevation of 769 m on Rudolftoppen (figs. 1 and 2). Jan Mayen lies in the boundary between the cold East Greenland Current and the warmer north flowing Atlantic currents in the Norwegian Sea. The island is surrounded by pack ice during winter and spring, although the ice retreats west of the island during the summer (Vinje, 1976). Meteorological observations, begun in 1922, show that the island has a cool oceanic climate, is generally cloud covered, has a mean (1951–80) annual temperature near sea level of −1.2 °C and a mean (1963–80) yearly precipitation at the present meteorological station on Syd-Jan southwest of Sørlaguna of 685 mm (Steffensen, 1982). Barr (1991) recently reviewed its history.

The island consists of basaltic rocks of relatively young age (Fitch and others, 1965; Imsland, 1978, 1980). Glacial geologic studies by Hisdal (oral commun., 1985) show that the island has been covered by glaciers during several phases of the Weichselian (Wisconsinan). The most recent episode probably terminated before 9,000 yr ago. Considerable volcanic activity has taken place subsequently, and nearly 20 percent of the area is covered by postglacial lavas (Noe-Nygaard, 1974; Imsland, 1978; Hisdal, oral commun., 1985). The most recent effusive eruptions

[1] Norwegian Polar Research Institute, P.O. Box 158, 1330 Oslo Lufthavn, Norway.

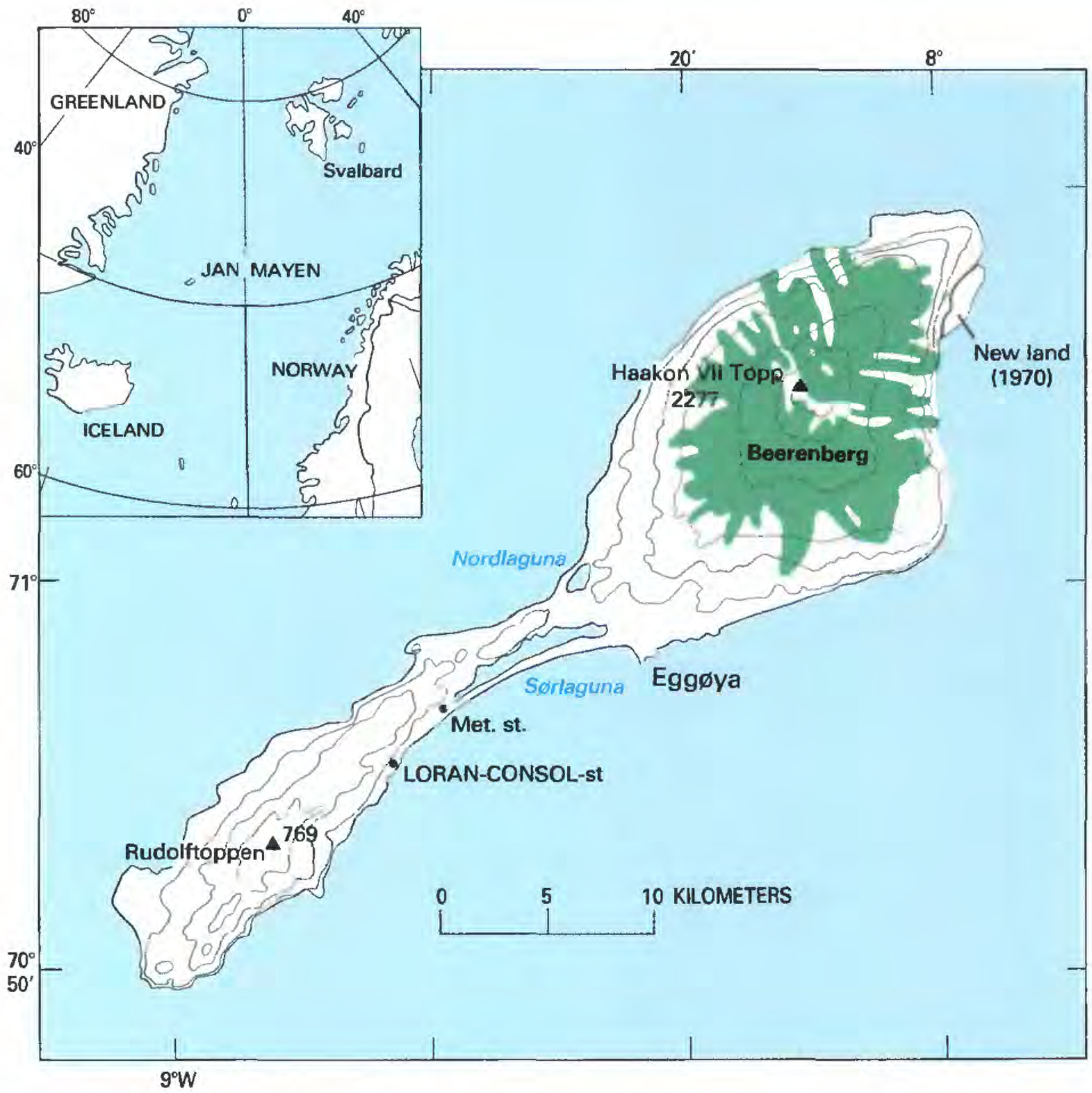

Figure 1.—*Index map of Jan Mayen. The wide, northeastern end of the island is called Nord-Jan; the narrow southeastern end is called Syd-Jan. "New land" refers to the land created by effusive volcanic activity from Beerenberg in 1970. Elevations are shown in meters (from Siggerud, 1972).*

Figure 2.—*Jan Mayen viewed from the southwest on 23 August 1949. The southernmost part (foreground) is obscured by clouds. The Beerenberg Volcano can be seen in the background. Oblique aerial photograph No. JM49 0865 from Norsk Polarinstitutt, Oslo.*

occurred in September 1970 (Siggerud, 1972; Sylvester and others, 1974; Sylvester, 1976), and on 6–9 January 1985 (Smithsonian Institution, 1984, 1985) on the northeastern side of Beerenberg (Imsland, 1985). According to Sylvester (1976), the September 1970 lava flows created about 4 km^2 of new land on the northeastern part of the island (figs. 1 and 3). Lava flows also entered the sea during the January 1985 activity (fig. 3), and a steam vent formed on the northern edge of the summit crater and produced a collapse cauldron in the upper part of Weyprechtbreen (figs. 4 and 5) (Smithsonian Institution, 1985).

Nord-Jan's glaciers, some extending to sea level, have a combined area of 113 km^2, about 30 percent of the island's area. Several of the glaciers have a very uneven surface topography. The marginal regions are often covered by supraglacial material; large parts of the ablation area are covered on some of the glaciers. There are no glaciers on Syd-Jan. Here the highest mountain (Rudolftoppen) reaches 769 m elevation, or 1,508 m less than the summit of Beerenberg (Haakon VII Topp).

There have been two postglacial periods of glacier expansion at Jan Mayen (Anda and others, 1985). The first period may have taken place around 2,500 yr ago. The glaciers had their maximum extent during the second period, around the year 1850, toward the end of the so-called "Little Ice Age." They have subsequently shown an oscillating retreat, with marked expansion around 1910, and with a minimum extent around 1950. Many glaciers advanced again about 1960, and the advance of Sørbreen probably culminated about 1965.

Anda and others (1985) concluded that the advances of the glaciers around 1960 were caused by reduced summer temperatures and ablation and *not* by increased precipitation, as reported by Lamb and others (1962), Fitch and others (1962), and Sheard (1965).

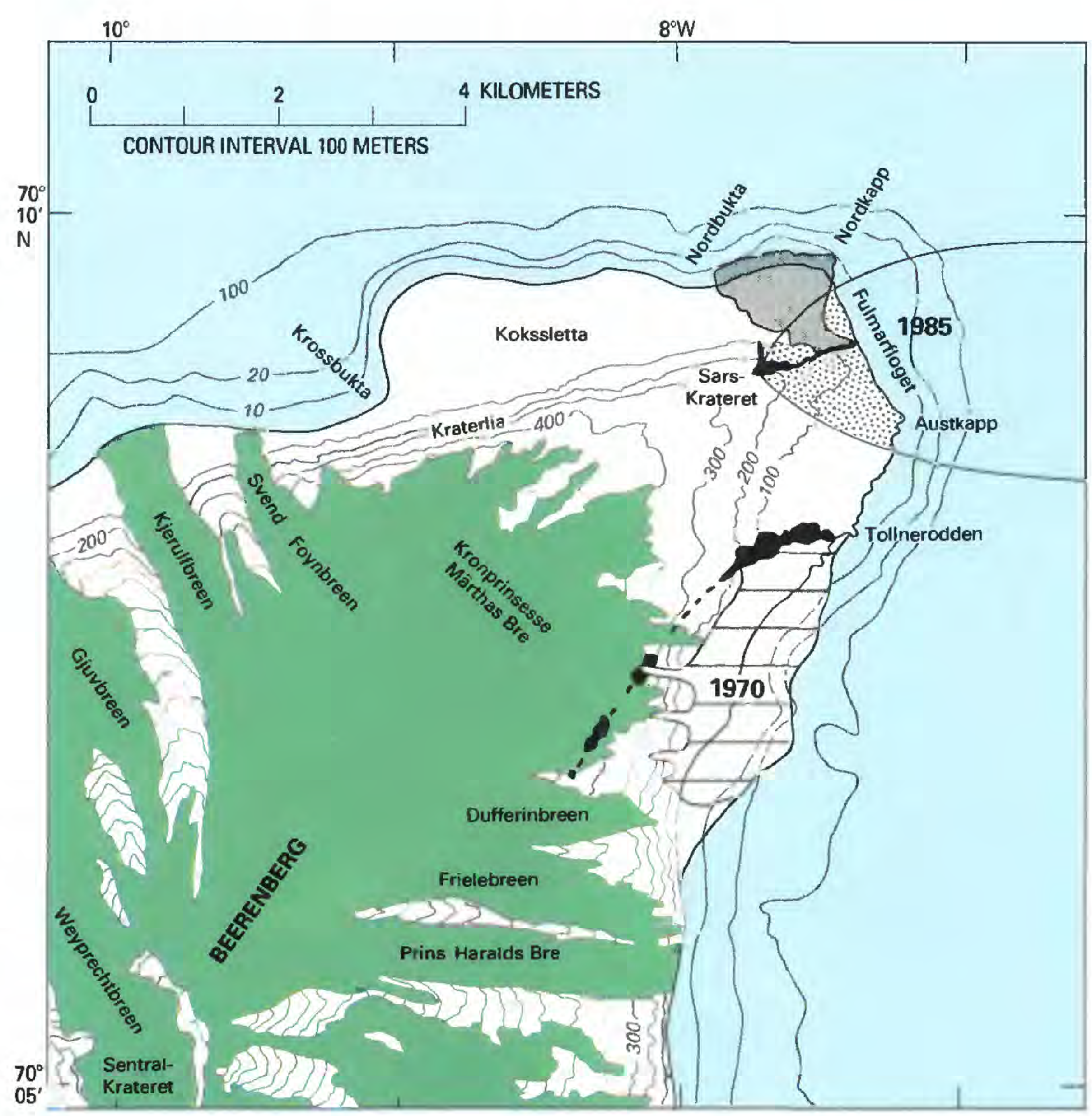

Figure 3.—Craters (solid black areas), effusive lava flows (lined, 1970; and shaded, 1985), tephra deposits (stippled, 1985), and tephra fallout pattern (parabola) associated with recent volcanic activity on Beerenberg. Note line of craters across eastern margin of Kronprinsesse Märthas Bre. Contours are in meters. Map modified from Imsland (1985).

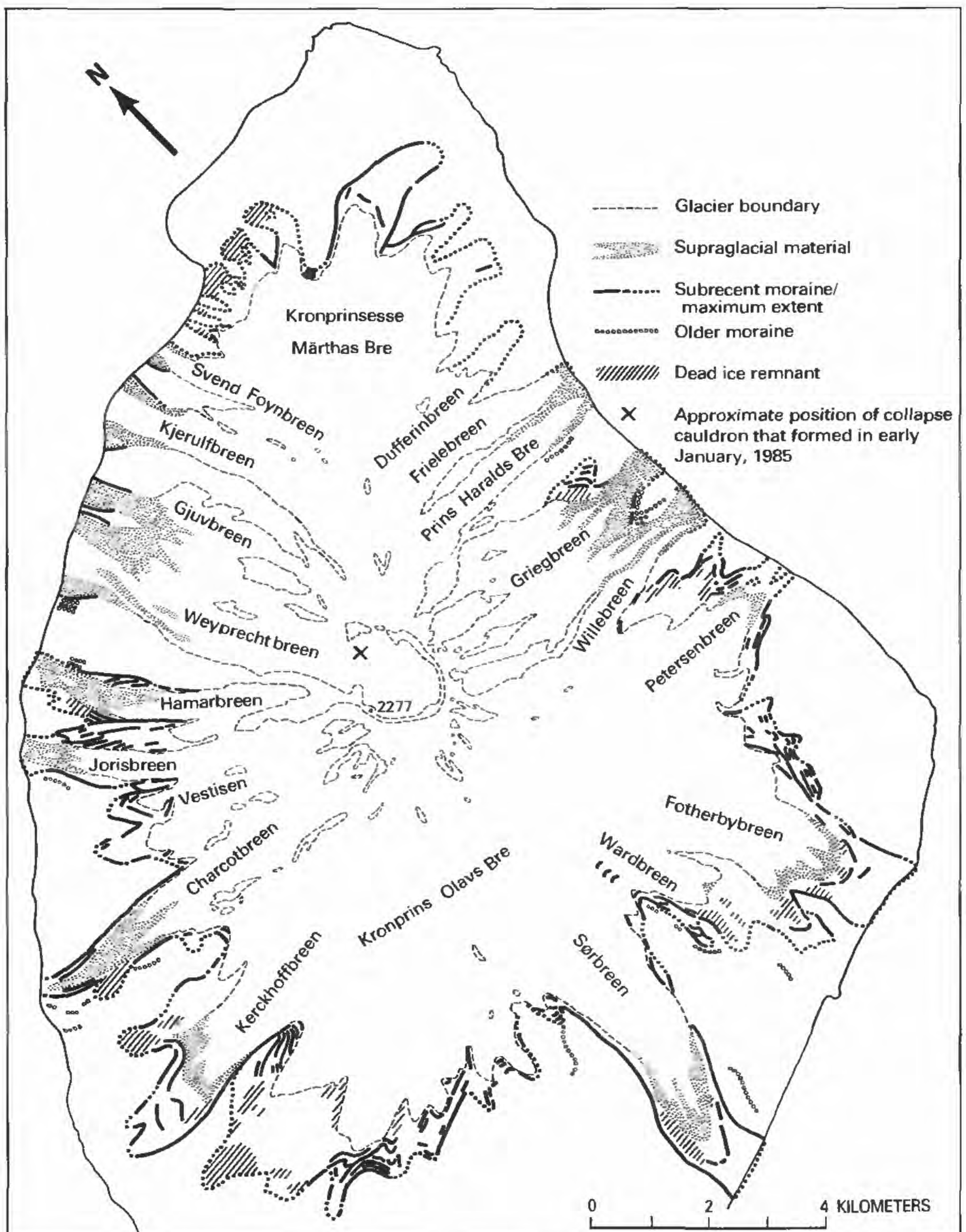

Figure 4.– *Steam billowing from the new vent (collapse cauldron) that formed on the upper part of Weyprechtbreen on the northern part of the summit crater of Beerenberg Volcano on 7 April 1985. Photograph from Norsk Polarinstitutt, courtesy of Lindsay McClelland (Smithsonian Institution, 1985).*

◀ ***Figure 5.***–*The glaciers on Nord-Jan showing locations of moraine stages, dead (stagnant)-ice remnants, and supraglacial material.*

Glacier Distribution and Mass-balance Conditions

The ice cap on Beerenberg Volcano can be divided into 20 individual outlet glaciers. These are shown in figure 5, and their individual areas, lengths, and elevations are listed in table 1. The glaciers are steep, typically covering elevation intervals of about 2,000 m over lengths of 5 to 7 km. Table 1 also shows that the elevation of the equilibrium line varies from 600 to 950 m, from the northwest-facing to the south-facing glaciers, probably caused mainly by variations in winter accumulation (Anda and others, 1985). This precipitation comes mostly from the orographic influence of north-northwesterly winds (Steffensen, 1982), giving the heaviest accumulation on the windward side of Jan Mayen.

Sørbreen (fig. 6), the largest glacier, has an area of 15 km^2 and is by far the best studied glacier on the island. Mass-balance measurements are available for the lower half of Sørbreen, up to 1,100 m (Orheim, 1976; Anda, 1984). It seems likely that the upper part of the glacier has no true summer season and that practically all precipitation here is in solid form. Over the lower part of the glacier, however, the temperature fluctuations may cause large variations in the percentage of precipitation that falls in frozen form. The studies at Sørbreen show that the winter balance is around 1 to 2 m water equivalent but that there are large local variations caused by wind drift and uneven surface topography (fig. 7). Convection and condensation account for most of the heat transfer to the surface in the ablation season, and there appears to be a good correlation between summer temperature at sea level and the ablation of the glacier. This correlation is, however, complicated by the temperature distribution over the glaciers of Jan Mayen, with frequent temperature inversions in the lower altitudes. Dibben (1965) showed that surface ablation is highest

TABLE 1.—*Size, elevation, and orientation of the glaciers on Jan Mayen, Norway*

[Eql, equilibrium line, defined as the boundary between the accumulation area (positive net mass balance) and the ablation area (negative net mass balance)]

Glacier name	Area (km^2)	Length (km)	Elevation (m)				Orientation
			Maximum	Median	Minimum	Eql	
Sørbreen	15.00	8.7	2,200	940	80	950	S.
Southwest part of Kronprins Olavs Bre	11.40	7.4	2,240	860	440	900	SW.
Kerckhoffbreen	9.00	7.3	2,200	860	280	850	W.
Charcotbreen	5.55	6.9	2,240	880	40	800	W.
Vestisen	2.30	3.4	1,500	860	540	800	W.
Jorisbreen	3.30	6.0	2,260	980	20	750	NW.
Hamarbreen	2.25	4.7	1,580	720	10	700	NW.
Weyprechtbreen	8.90	6.8	2,080	800	0	650	NW.
Gjuvbreen	2.80	5.3	2,100	660	0	600	NW.
Kjerulfbreen	5.80	6.4	2,140	900	0	650	N.
Svend Foynbreen	2.60	4.6	1,400	800	0	700	N.
Kronprinsesse Märthas Bre	9.40	4.7	1,320	710	420	750	NE.
Dufferinbreen	1.55	3.7	1,500	920	400	800	E.
Frielebreen	2.80	5.0	1,660	780	0	750	E.
Prins Haralds Bre	3.50	5.3	2,200	980	0	750	E.
Griegbreen	4.95	5.1	2,160	830	10	800	E.
Willebreen	5.50	5.9	2,160	900	0	850	E.
Petersenbreen	5.35	5.5	1,620	820	230	900	SE.
Fotherbybreen	9.00	7.2	2,140	820	300	900	SE.
Wardbreen	3.25	5.7	2,200	1,010	550	950	S.

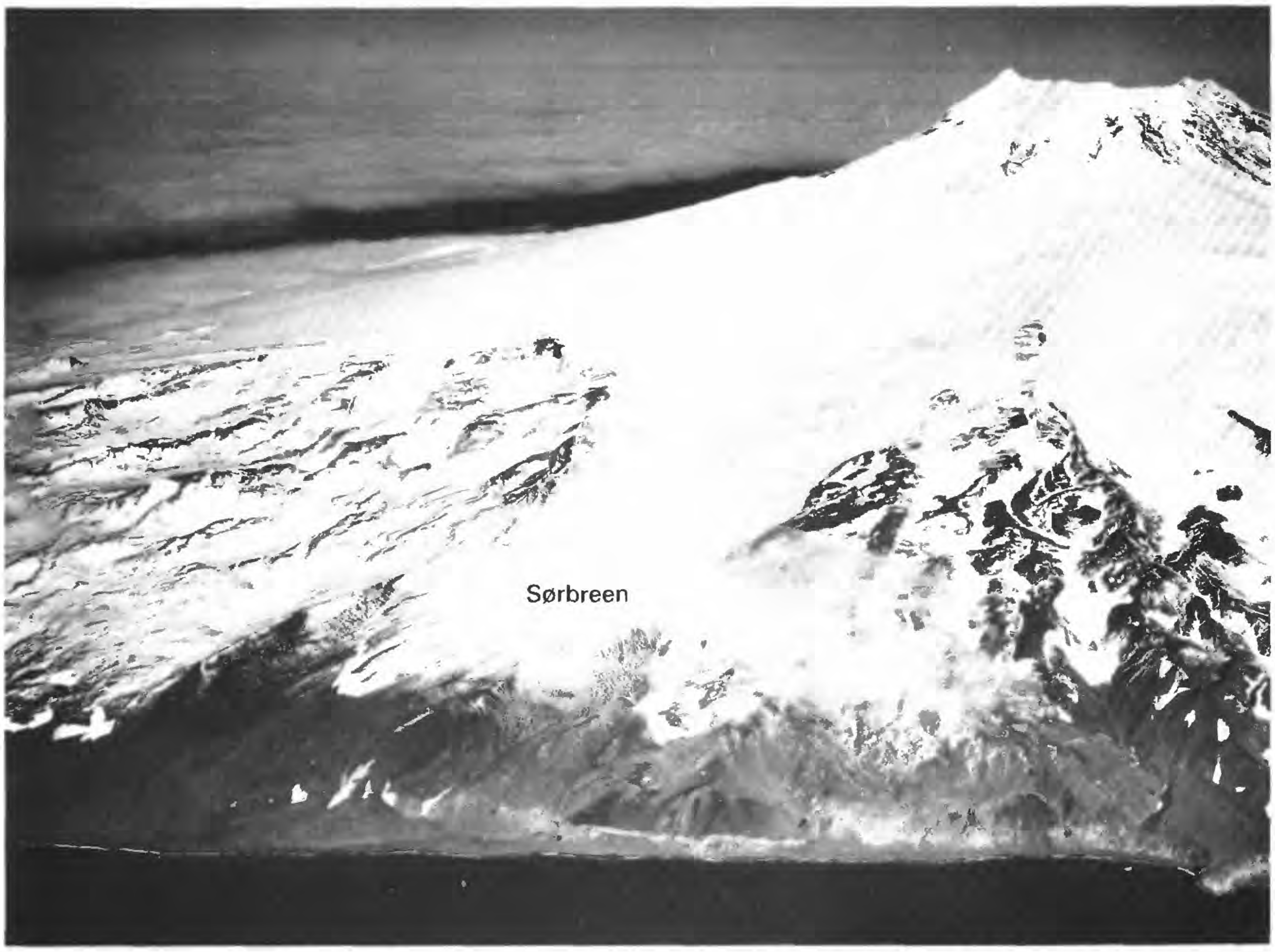

Figure 6.—Sørbreen on Nord-Jan viewed from the southeast on 23 August 1949. The summit of the Beerenberg Volcano (2,277 m) is visible on the right. Oblique aerial photograph No. JM49 0777 from Norsk Polarinstitutt, Oslo.

◀ *Figure 7.—Sørbreen viewed from above 600 m in elevation on 24 August 1973. Note the uneven topography. The summit of the Beerenberg Volcano is in the background. Oblique aerial photograph by Olav Orheim, Norsk Polarinstitutt, Oslo.*

during frontal activity (passage of warm fronts associated with low-pressure systems). Measurements by Orheim (1976) and Anda (1984) show that ablation *increases* with elevation over the lower parts of Sørbreen, because long-lasting advection fog reduces both incoming radiation and temperatures over the lowest section. This phenomenon is probably less important on the northwest glaciers. Calving is an important ablation mechanism for some of the glaciers around the northern sector of Nord-Jan (fig. 8).

Figure 8.—Beerenberg viewed from the northwest on 23 August 1949. Weyprechtbreen, the outlet glacier that emanates from a breach in the summit crater, has the largest calving front of all the Jan Mayen glaciers. Oblique aerial photograph No. JM49 0811 from Norsk Polarinstitutt, Oslo.

Historical Variations in Positions of Glacier Termini

The variations of glaciers on Jan Mayen can best be established from Sørbreen, which has been visited frequently. Maps and descriptions from 1632 (Blaeu, 1662) and from 1817–18 (Scoresby, 1820) indicate that the glacier did not reach the sea during these periods. However, these descriptions cannot be considered wholly reliable.

Sørbreen was near its maximum "Little Ice Age" extent during 1861 (Vogt, 1863). A detailed sketch shows the glacier reaching the sea; the glacier surface is depicted as nearly level with high lateral moraines. A second sketch shows that Sigurdbreen and Smithbreen also were near their maximum subrecent extents. Sørbreen also terminated in the sea in 1878 (Mohn, 1878, 1882), but the elevation of the glacier surface cannot be estimated from this source.

A map of the island and a description of several glaciers were made by the Austrian expedition in 1882–83 (Bóbrik von Boldva, 1886). The front of Sørbreen had retreated from the sea, and 80 m from the sea the glacier surface disappeared under morainal material. The glacier surface was 30 m below the uppermost level (150 m) of the lateral moraines.

Flint (1948) described Sørbreen from a brief visit in 1937. The front was then about 600 m from the sea. The following year Jennings (1939, 1948) stated that the glacier front was 960 m from the sea. Comparison of the sketch maps made by Flint and Jennings suggests that the latter misinterpreted the boundary of moraine-covered ice as the glacier front. Norsk Polarinstitutt prepared a topographic map of Jan Mayen in 1959, based on aerial photographs taken during 1949 and 1955. The glaciers were mapped photogrammetrically from the 1949 aerial photographs. Sørbreen was, at this time, 1,200 m from the sea, which is the greatest recorded retreat of the glacier. Many other glaciers also had their greatest retreats at this time.

University of London expeditions made extensive studies of Sørbreen in 1959 and 1961 (Fitch and others, 1962; Kinsman and Sheard, 1963). The glacier advanced 100 m between 1949 and 1959, and the glacier advanced an additional 124 m during the following 2 years. They also observed that several other glaciers had advanced since 1949.

Aerial photographs acquired in 1975 by the Norsk Polarinstitutt showed that Sørbreen had advanced farther since 1961. The front part of the glacier now seemed to be stagnant, and the glacier front had probably been in the same position for several years. This situation persisted until 1978. The marked advance around 1960 probably culminated by 1965.

Anda and others (1985) constructed a lichenometric growth curve for Jan Mayen and used this to obtain additional ages for the moraines of Sørbreen and neighboring glaciers.

The results of these observations are shown in figures 9 and 10. It is clear that Sørbreen is sensitive to climatic change, and the observations suggest the variations of Sørbreen will be representative of the other south- and east-facing glaciers around Nord-Jan. However, more data are needed to give more confidence to this conclusion.

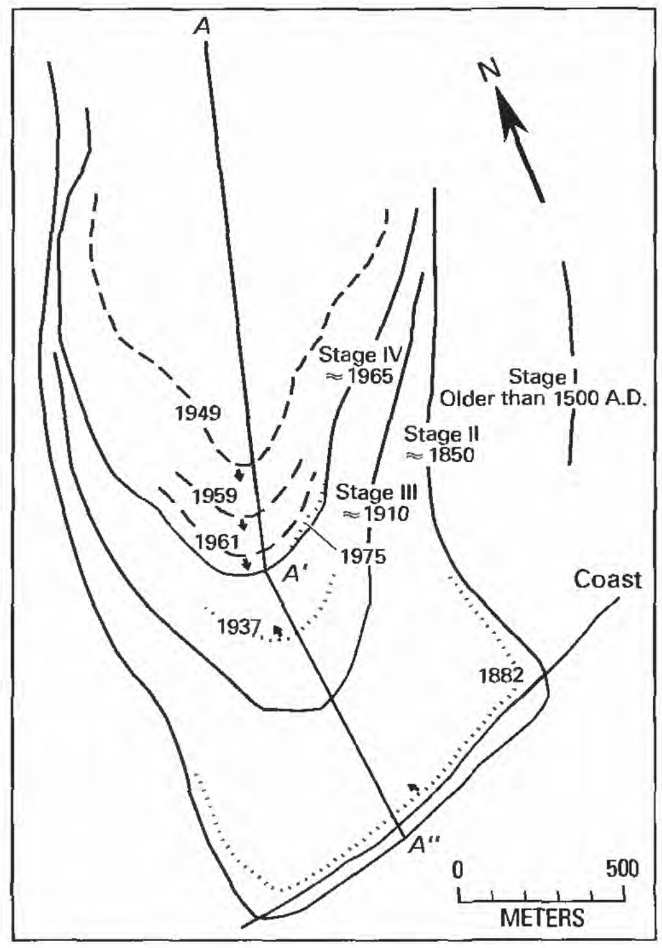

Figure 9.—*The frontal position of Sørbreen on different dates. The solid lines indicate culmination of advances, dashed lines an intermediate position during an advance, and dotted lines an intermediate position during retreat. The arrows indicate whether the glacier is advancing or retreating. Section A–A′–A″ is shown in figure 10.*

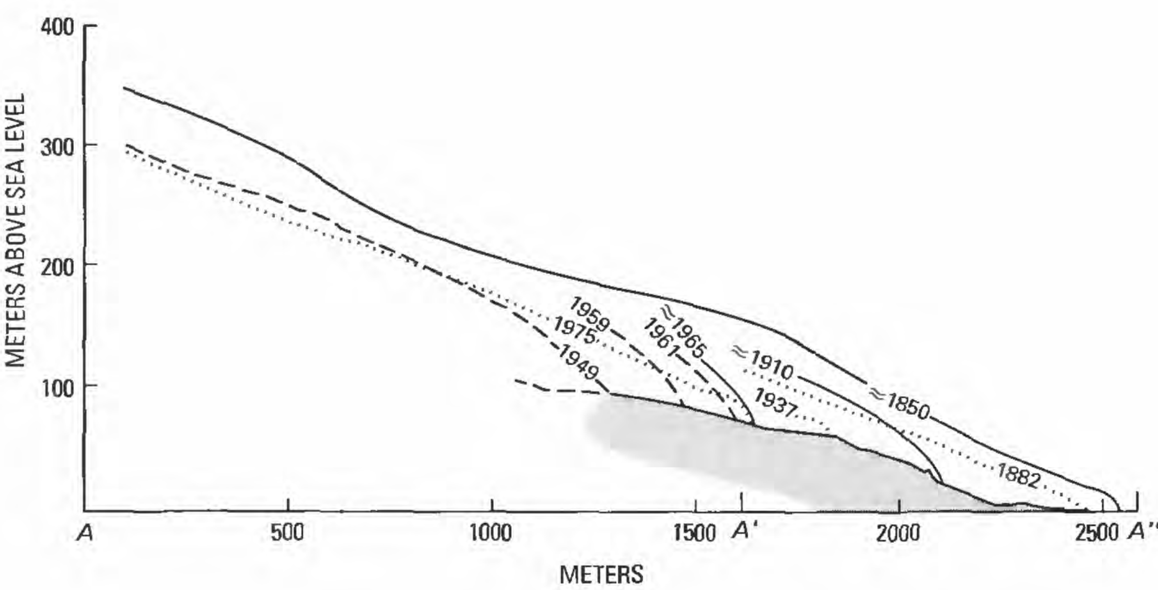

Figure 10.—*Length profiles of Sørbreen along section A–A′–A″ (see fig. 9) at various times. Vertical exaggeration 3 times. The shaded area represents the subglacial land surface.*

Comparison of Glacier Fluctuations with Meteorological Data

A meteorological station has been operated continuously on Jan Mayen since 1922, with the exception of short periods during World War II. The station has, however, been relocated several times. Parallel temperature measurements show that a continuous temperature curve can be constructed, whereas this cannot be done for the precipitation (Steffensen, 1982).

Lamb and others (1962), Fitch and others (1962), and Sheard (1965) claim that the glacier advances around 1960 were caused by increased precipitation from 1947 through the 1950's. Anda and others (1985) show that this period coincides with the period when the station was located on the western side of the island, where precipitation is highest. Thus, the recorded precipitation values during this period would not necessarily represent higher values on a continuous curve. Lamb and others (1962) also suggest that low temperatures in the 1940's may have contributed to the glacier expansion, and they refer to low mean annual temperatures. However, the records show that the summer temperatures, and thus the ablation, were not especially low at this time. Anda and others (1985) show that the summer temperatures were very high during the 1930's, which may have caused the glacier retreat from the period 1910–20 to about 1950. The marked reduction in summer temperatures from around 1940 to the mid-1960's is the most probable cause for the glacier expansion around 1960.

Use of Satellite Imagery in Glacier Monitoring

Jan Mayen is characterized by a very persistent cloud cover. On the average, only 4.4 days during the entire year are completely clear, and only 0.2 clear day occurs per month from June to September. More than 20 days are completely cloud covered during each of the summer months, and autumn shows the highest cloud-cover percentage during the year (Steffensen, 1982). Thus, it is difficult to obtain cloud-free satellite images of the island. When satellite images of the glaciers are most desired, at time of maximum ablation, the likelihood of obtaining them is the lowest.

Indeed, few glaciologically usable Landsat images have yet been obtained of Jan Mayen (table 2). The best available in the U.S. archive, 1084–12061, was acquired on 15 October 1972, but even this shows clouds over most of the island (figs. 11 and 12). The lack of recent Landsat imagery is especially unfortunate, because the glaciers on Jan Mayen are especially sensitive to climatic change, as is demonstrated by the numerous frontal variations of Sørbreen. It would therefore be particularly valuable to monitor glacier frontal variations by satellite imagery. This technique would be exceptionally useful here on this isolated island. It is also the only practical way to clarify whether all the glaciers of different aspects respond in parallel, because it is difficult to gain access to several of the glaciers.

Even with the recognition of the difficulties posed by the high cloud cover, it is still recommended that efforts be made to obtain satellite

TABLE 2.—*Optimum Landsat 1, 2, and 3 images of the glaciers of Jan Mayen, Norway*

[See figure 12 for explanation of symbols used in the "Code" column]

Path-Row	Nominal scene center (lat-long)	Landsat identification number	Date	Solar elevation angle (in degrees)	Code	Cloud cover (in percent)	Remarks
233–10	70°35'N. 06°13'W.	No usable data			◔		
234–10	70°35'N. 07°39'W.	22077–11483	29 Sep 80	16	◑	20	Archived by ESA.
235–09	71°50'N. 06°48'W.	22060–11535	12 Sep 80	21	◑	20	Covers north end of island; archived by ESA[1].
235–10	70°35'N. 09°05'W.	1084–12061	15 Oct 72	10	◑	60	Only image available from EDC[2].
236–09	71°50'N. 08°14'W.	No usable data			◔		
236–10	70°35'N. 10°31'W.	22403–11561	21 Aug 81	30	◑	10	Covers south end of island; archived by ESA.

[1] ESA archive located at Kiruna, Sweden.

[2] U.S. Geological Survey EROS Data Center (EDC) archive located at Sioux Falls, S. Dak.

imagery of Jan Mayen. Imagery with good resolution (25 m or better) obtained in late summer or autumn at regular intervals (every few years) would satisfy the monitoring requirements. Data of this kind would, with the field data now available, allow sophisticated studies of the relationship between glacier fluctuations and the observed climatic variations. It would be particularly interesting to investigate models showing how these glaciers respond to changes in mass balance. Short glaciers covering large elevation intervals likely will respond much more quickly to changes in summer temperatures and net ablation than to changes in precipitation (Anda and others, 1985). The reason is that the temperature variations influence mostly the lower reaches of the glaciers, whereas precipitation variations probably are most important around the central and upper half of the glaciers. Thus, such a model could be tested by monitoring glacier variations on Nord-Jan and combining this information with analysis of the regularly obtained meteorological data.

Acknowledgment

The editors thank Dr. Gunnar Østrem, Nores Vassdrags-og Energiverk, who read the manuscript and made helpful comments.

Figure 11.—Landsat 1 image (1084–12061; 15 October 1972) of Jan Mayen, Norway, the best Landsat image acquired (in the U.S. archive) of the island. Clouds obscure most of the coastline of both Nord-Jan and Syd-Jan, making the image unusable for determining positions of the termini of any of the 20 outlet glaciers emanating from the ice cap on Beerenberg Volcano, Nord-Jan.

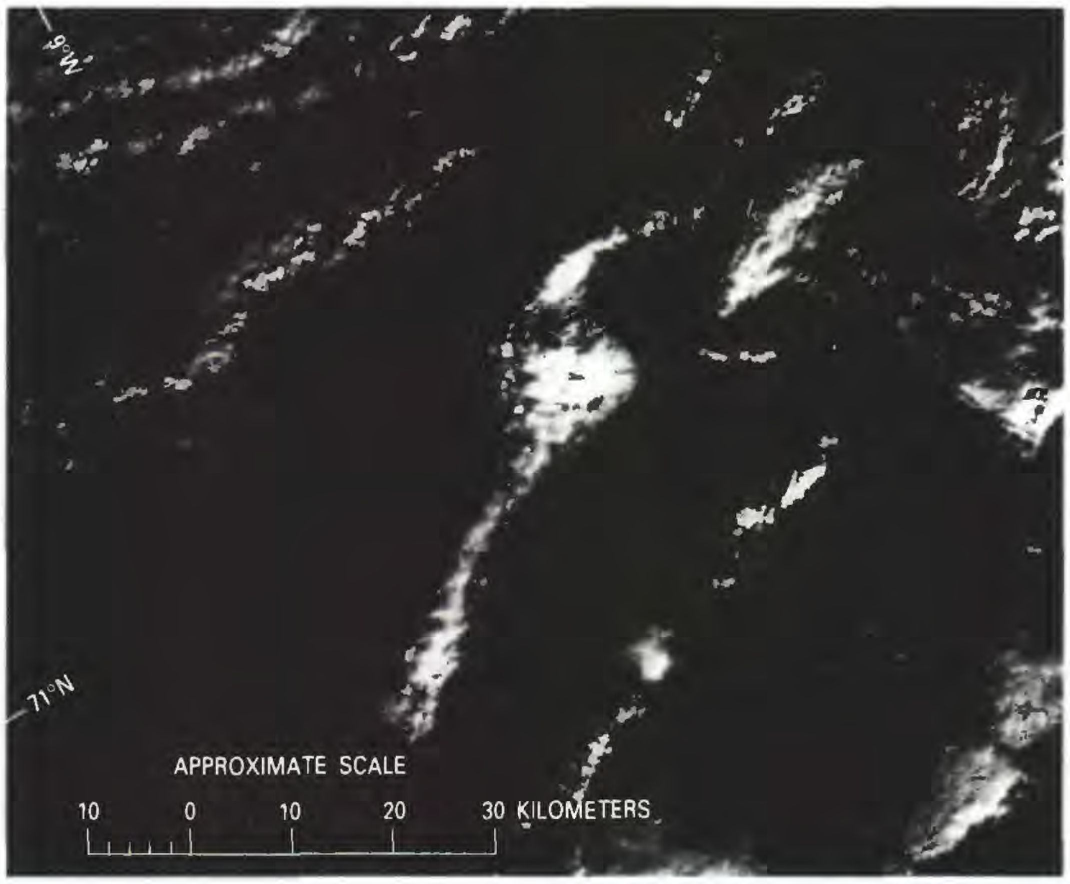

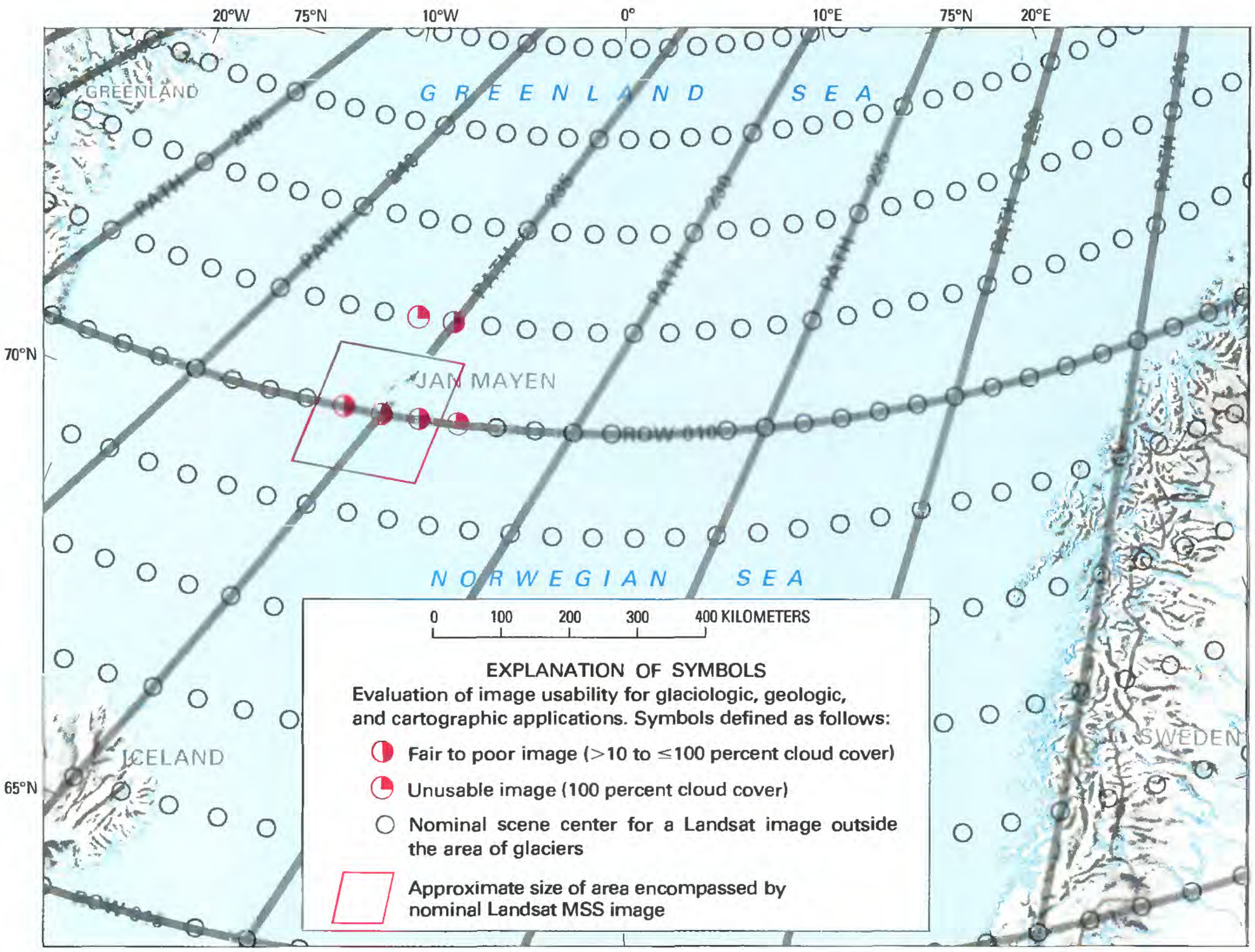

Figure 12.—Optimum Landsat 1, 2, and 3 images of the glaciers of Jan Mayen, Norway. (See also table 2.) The vertical lines represent nominal paths. The rows (horizontal lines) have been established to indicate the latitude at which the imagery has been acquired.

References Cited

Anda, E., 1984, En glasiologisk og glasialgeologisk undersøkelse på Jan Mayen [A glaciological and glacial geological study of Jan Mayen]: Cand. real. dissertation, University of Bergen, Norway, 130 p.

Anda, E., Orheim, O., and Mangerud, J., 1985, Late Holocene glacier variations and climate at Jan Mayen: Polar Research, v. 3, no. 2, p. 129–140.

Barr, S., 1991, Jan Mayen—Øyas historie gjennom 1500 år [Jan Mayen—The island's history during 1,500 years]: Oslo, Chr. Schibsteds Forlag, 264 p.

Blaeu, J., 1662, Insvla quae a Ioanne Mayen. Nomen Scripto [An island which is known as Jan Mayen], *in* Atlas maior sive Cosmographiae Blaviana, qva solum, salum, coelvm, accvratissime describvntvr: Amstelaedami, Joannis Blaev, v. 1, p. 19–21.

Bóbrik von Boldva, A.A., 1886, ...Aufnahme und Beschreibung der Insel Jan Mayen und Beobachtungen über Gletscherbewegung ...., *in* Die Österreichische Polarstation Jan Mayen, v. 1, pt. 2, (Kaiserlichen Akademie der Wissenschaften): Vienna, K. Gerold's Sohn, 50 p.

Dibben, P.C., 1965, A heat-balance study on Sørbreen, Jan Mayen: Journal of Glaciology, v. 5, no. 42, p. 793–803.

Fitch, F.J., Kinsman, D.J.J., Sheard, J.W., and Thomas, D., 1962, Glacier readvance on Jan Mayen: IUGG/IASH, Symposium of Obergurgl: International Association of Scientific Hydrology Publication No. 58, p. 201–211.

Fitch, F.J., Nairn, A.E.M., and Talbot, G.J., 1965, Paleomagnetic studies on rocks from North Jan Mayen: Norsk Polarinstitutt Årbok 1973, p. 49–60.

Flint, R.F., 1948, Glacial geology and geomorphology. The coast of Northeast Greenland. With hydrographic studies in the Greenland Sea: The Louise A. Boyd Arctic Expedition of 1937 and 1938 (Boyd, L.A., ed.), American Geographical Society Publication No. 30, p. 91–210.

Imsland, P., 1978, The geology of the volcanic island Jan Mayen, Arctic Ocean: Nordic Volcanological Institute Report No. 78–13, October 1978, Reykjavík, 74 p.

———1980, The petrology of the volcanic island Jan Mayen, Arctic Ocean: Nordic Volcanological Institute Report No. 80–03, August 1980, Reykjavík, 501 p.

———1985, Eldgosið á Jan Mayen í Janúar 1985 [Volcanic eruption on Jan Mayen in January 1985]: Jökull, v. 35, p. 97–102.

Jennings, J.N., 1939, The glaciers of Jan Mayen; Appendix II of the Imperial College Expedition to Jan Mayen Island (King, Alexander): The Geographical Journal, v. 94, no. 2, p. 128–131.

———1948, Glacier retreat in Jan Mayen: Journal of Glaciology, v. 1, no. 4, p. 167–181.

Kinsman, D.J.J., and Sheard, J.W., 1963, The glaciers of Jan Mayen: Journal of Glaciology, v.4, no. 34, p. 439–448.

Lamb, H.H., Probert-Jones, J.R., and Sheard, J.W., 1962, A new advance of the Jan Mayen glaciers and a remarkable increase of precipitation: Journal of Glaciology, v. 4, no. 33, p. 355–365.

Mohn, H., 1878, Den norske Nordhavsexpeditions Reise til Jan Mayen [The Norwegian North Sea Expedition's voyage to Jan Mayen]: Naturen, v. 2, p. 153–157.

———1882, Geografi og naturhistorie [Geography and natural history]: Den Norske Nordhavsexpedition 1876–1878, Christiania, p. 3–29.

Noe-Nygaard, A., 1974, Cenozoic to Recent volcanism in and around the North Atlantic basin, *in* Nairn, A.E.M., and Stehli, F.G., eds., The ocean basins and margins: New York, Plenum Publishing Corporation, v. 2, p. 391–443.

Orheim, O., 1976, Bremålinger på Jan Mayen [Glacier surveys in Jan Mayen]: Norsk Polarinstitutt Årbok 1974, p. 249–252.

Scoresby, W., Jr., 1820, An account of the Arctic regions, with a history and description of the northern whale-fishery: Edinburgh, A. Constable and Co., v. 1, 653 p. and v. 2, 582 p.

Sheard, J.W., 1965, Seasonal weather trends in relation to fluctuations of the Jan Mayen glaciers since 1920: Journal of Glaciology, v. 5, no. 42, p. 805–811.

Siggerud, T., 1972, The volcanic eruption on Jan Mayen, 1970: Norsk Polarinstitutt Årbok 1970, p. 5–18.

Smithsonian Institution, 1984, Volcanic events: SEAN (Scientific Event Alert Network) Bulletin, v. 9, no. 12, p. 2–3.

———1985, Volcanic events: SEAN (Scientific Event Alert Network) Bulletin, v. 10, no. 3, p. 5–7.

Steffensen, E., 1982, The climate at Norwegian arctic stations: Klima, v. 5, p. 3–44.

Sylvester, A.G., 1976, History and surveillance of volcanic activity on Jan Mayen Island: Bulletin Volcanologique, v. 39 (1975), no. 2, p. 313–335.

Sylvester, A.G., Sørnes, A., and Siggerud, T., 1974, History and surveillance of volcanic activity of Jan Mayen Island: Discussion paper distributed at the NATO Advanced Study Institute, Geodynamics of Iceland and the North Atlantic Area, Reykjavík (1–7 July 1974), 3 p.

Vinje, T., 1976, Sea ice conditions in the European sector of the marginal seas of the Arctic, 1965–1975: Norsk Polarinstitutt Årbok 1975, p. 163–174.

Vogt, K.C., 1863, Nord-fahrt entlang der norwegischen Küste, nach dem Nordkap, den Inseln Jan Mayen und Island, auf dem schooner Joachim Hinrich unternommen wahrend der Monate mai bis oktober 1861 von dr. Georg Berna, *in* Begleitung von Vogt, C., Hasselhorst, H., Gressly, A., und Herzen, A., Erzählt von Carl Vogt, mit einem wissenschaftlichen Anhang, drei Karten und fünfzig teils in Farben gedruckten, teils in Holz geschnitten Illustrationen nach original Zeichnungen von Hasselhorst: Frankfurt am Main, in Commission bei C. Jügel, 429 p.